Examining the Role of Canonical Wnt Signalling during Developmental Vascular Patterning

A Thesis Submitted for the Degree of Doctor of Philosophy in Cardiovascular Science

Mary A. A. Strevens

University of Oxford

Magdalen College

Trinity 2025

This thesis is dedicated to my parents,
Andrew and Alison

Abstract

The vascular system is composed of heterogeneous endothelial cell (EC) subtypes, each with distinct characteristics and functions. This heterogeneity is shaped, in part, by enhancer-mediated transcriptional regulation. Mapping how enhancers drive gene expression in specific EC subsets is central to understanding the upstream signalling pathways that govern vascular development; however, functional enhancer discovery has proved challenging. The identification of a novel enhancer specifically active in angiogenic ECs therefore provided a powerful tool to investigate the transcriptional networks orchestrating angiogenesis. This enhancer, located 58 kilobases downstream of the *SOX7* gene, was termed SOX7-58.

In this thesis, I identify and characterise the transcriptional regulators of the SOX7-58 angiogenic enhancer, combining validated phylogenetic foot-printing with mutational analysis in F0 zebrafish assays. These analyses indicated a potential requirement for T-cell factor/lymphoid enhancer-binding factor (TCF/LEF) binding sites in maintaining the angiogenic specificity of the enhancer. Further *in silico* analysis suggested similar regulatory logic in another angiogenic enhancer, DLL4in3, where TCF/LEF motifs were likewise essential for correct enhancer activity. Given that TCF/LEF transcription factors act as nuclear effectors of canonical Wnt signalling, I next assessed the role of canonical Wnt in vascular development *in vivo* using EC-specific *Ctnnb1* ablation. Combining immunohistochemistry with a panel of enhancer:*LacZ* transgenes, I analysed the consequences of disrupted Wnt signalling on EC subpopulations. Arterial EC identity remained intact in the absence of Wnt signalling, whereas angiogenic and venous EC enhancers displayed expanded or ectopic activity, without changes in overall vascular density.

Further, EC-specific *Ctnnb1* ablation during coronary vascular development, where VEGFA- and VEGFC-driven angiogenesis are uncoupled, produced no significant phenotypic effects. In contrast, postnatal retinal EC deletion of *Ctnnb1* caused both expanded angiogenic enhancer activity and impaired angiogenesis. Collectively, these findings suggest that canonical Wnt signalling may function as a negative regulator of angiogenesis by constraining gene expression in a spatially specific manner.

Acknowledgements

This thesis would not have been realised without the support of many individuals, but none more so than that of my supervisor, Professor Sarah De Val. Throughout, Sarah has provided sharp scientific clarity as well as valuable lessons in tenacity and integrity.

I am also greatly indebted to the De Val group, both past and present. In particular, Dr Dorota Szumska-Bilska, Dr Sophie Payne and Dr Susann Bruche, all of whom have been in the group throughout my time there. I could not have asked to work in a more supportive group, both professionally and personally, and I will cherish our time together. I would like to pay particular acknowledgement to Dr Svanhild Nornes, whose expertise in zebrafish were invaluable for the first part of my project, and to Dr Susann Bruche, who worked tirelessly to optimise the CUT&RUN.

Moreover, this project would not have been completed without the support of the BMS staff, most notably, Daniel Andrews, Matthew Honey, Clare Allen, and Rebecca Cuddon. I would also like to acknowledge Robert Crickley at the Ludwig Institute, University of Oxford, for his guidance with the microscopy work, and Indrika Ratnayaka, for her cryo-sectioning skills.

To have completed my DPhil at the Institute for Developmental and Regenerative Medicine was incredibly fortunate. It has been a privilege be part of the institute during its formative years, and I am very grateful to Professor Paul Riley for building such a wonderful and collaborative community. On the cardiac floor I have too many peers to thank individually, and so I will simply express my appreciation to everyone collectively. I have learnt such a great deal and had fun whilst doing so; I count myself very lucky to have worked alongside such brilliant colleagues. With that said, I would particularly like to thank Ben Chapman for his calm and steady support during the final stages of the writing process.

This project would not have been possible without the award of a British Heart Foundation Studentship. I owe particular thanks to Robert Easton and Andrew Spokes for their generous donations and support throughout my research. I would also like to acknowledge the British Microcirculation and Vascular Biology Society, the Department

of Physiology, Anatomy and Genetics (University of Oxford) and Magdalen College (University of Oxford) for supporting my attendance at national and international conferences.

Finally, I would like to express my appreciation to all the friends and family who have supported me throughout my DPhil. Whether friendships forged in my undergraduate, or newly made in the final year of the DPhil, each relationship has enriched my time in Oxford. I would like to especially thank my close family – Alison, Andrew and Will – as well as my partner, Peter Bristow. Your steadfast encouragement has made it all possible.

Summary of DPhil Activity:

I. Meetings attended

a. Oral Presentations

London Vascular Biology Forum | *Imperial University, United Kingdom, October 2024*

74th Annual Meeting of the British Microcirculation and Vascular Biology Society | *University of Bristol, United Kingdom, July 2024*

British Heart Foundation National Student Conference | *University of Bristol, United Kingdom, June 2024*

Institute of Developmental and Regenerative Medicine Seminar | *University of Oxford, United Kingdom, April 2024*

b. Poster Presentations

Gordon Conference: Angiogenesis and Social Interactions with Neighbouring Cells and Tissues in Health and Disease | *Salve Regina University, United States of America, July 2025*

16th Young Embryologist Network Meeting | *Francis Crick, United Kingdom, May 2024*

Oxford Medical Sciences Division Scientific Symposium | *University of Oxford, United Kingdom, July 2024*

British Society for Cardiovascular Research Early Career Researcher Symposium | *University of Sheffield, United Kingdom, April 2024*

Department of Physiology, Anatomy and Genetics Graduate Poster Day | *University of Oxford, United Kingdom, November 2023*

II. Prizes

a. Presentation Prizes

British Society for Cardiovascular Research Early Career Researcher Symposium | *University of Sheffield, United Kingdom, April 2024* | **Best Poster Prize**

16th Young Embryologist Network Meeting | *Francis Crick, United Kingdom, May 2024* | **Best Poster Prize**

74th Annual Meeting of the British Microcirculation and Vascular Biology Society | *University of Bristol, United Kingdom, July 2024* |**Best Oral Presentation**

b. Travel Awards

Student Assistance Scheme, British Microcirculation and Vascular Biology Society 2024

Terence Ryan Conference Grant, British Microcirculation and Vascular Biology Society 2025

Travel Grant, Department of Physiology, Anatomy and Genetics, University of Oxford 2025

Travel Grant, Magdalen College, University of Oxford 2025

III. Teaching

a. Tutor in Cells and Systems Biology

Oriel College, University of Oxford, 2022 – 2023

Both students achieved high distinctions in their preliminary examinations

IV. Funding

This research was funded by the 4-year British Heart Foundation PhD studentship as part of The McKie McLean Class of 2021.

Abbreviations

There are a few examples where the same abbreviation is used to mean two different terms. These abbreviations are only used in figures, and the full term is clearly stated in the figure legend.

A Aorta
A Artery
AP1 Activator protein 1
APC Adenomatous polyposis coli
ATAC-seq Assay for transposase-accessible chromatin sequencing
ATP Adenosine triphosphate
AXIN Axis inhibition protein
BBB Blood brain barrier
C/EBP CCAAT/enhancer-binding proteins
ChIP-seq Chromatin immunoprecipitation sequencing
CK1 Casein kinase 1
CNS Central nervous system
COUP-TFII Chicken ovalbumin upstream promoter transcription factor II
CV Cardinal vein
DA Dorsal aorta
DAPI 4′,6-diamidino-2-phenylindole
DBD Deoxyribonucleic acid binding domain
DLAV Dorsal longitudinal anastomosing vessel
DLL4 Delta-like protein 4
DNA Deoxyribonucleic acid
DPF Days post fertilisation
DVL Dishevelled
E Embryonic day
EC Endothelial cell
ECM Extracellular matrix
EDTA Ethylenediaminetetraacetic acid
EMCN Endomucin
EGF Epidermal growth factor
EMSA Electrophoretic mobility shift assay
ENCODE Encyclopaedia of deoxyribonucleic acid elements
EPC Endothelial precursor cell
ERG Ets-related gene
ETS E26 transformation-specific
ETV2 ETS variant transcription factor 2
FGF Fibroblast growth factor
FLI1 Friend leukaemia integration 1
FLK Foetal liver kinase
FOX Forkhead box
FZD Frizzled
GFP Green fluorescent protein
GO Gene ontology
GR Glucocorticoid receptor
GSK3β Glycogen synthase kinase 3 beta
GTF General transcription factor
H Histone
HAT Histone acetyltransferase
HDAC Histone deacetylase
HIF1 Hypoxia-inducible factor 1
HLX H2.0-like homeobox transcription factor
HP Hepatic primordia
HPF Hours post fertilisation
HUVEC Human umbilical vein endothelial cells
IB4 Isolectin B4
Inr Initiator
ISV Intersegmental vessel
KLF Krüppel-like factor
KDR Kinase insert domain receptor
L Lung
LB Luria-Bertani
LB Limb bud
LEF Lymphoid enhancer factor
LGR4/5/6 Leucine-rich repeat-containing G-protein coupled receptor 4/5/6
LRP5/6 Low-density lipoprotein receptor-related protein 5/6
MEF2 Myocyte enhancer factor-2
MMP Matrix metalloprotease
mRNA messenger ribonucleic acid
NFAT Nuclear factor of activated T-cells
NICD Notch intracellular domain
nm Nanometre
NR2F2 Nuclear receptor subfamily 2 group F member 2

NT Neural tube
NTP Nucleoside triphosphate
P Post-natal day
p Probability
PBS Phosphate-buffered saline
PCR Polymerase chain reaction
PCV Posterior cardinal vein
PDGF Platelet-derived growth factor
PECAM Platelet endothelial cell adhesion molecule
PFA Paraformaldehyde
Pol II RNA Polymerase II
RNA Ribonucleic acid
RPBJ Recombination signal binding protein for immunoglobulin kappa J region
RT Room temperature
RUNX Runt-related transcription factor
S Stalk
scRNA single-cell ribonucleic acid sequencing
SMAD Suppressor of mothers against decapentaplegic
SMC Smooth muscle cell
SOX SRY-related HMG-box
SP Sum-of-pairs
SV Sinus venosus
T Tip
TAD Topologically-associated domain
TAG Transcription factor activity gradient
TAL1 T-cell acute lymphocytic leukaemia protein 1
TBP TATA-binding protein
TCF T-cell factor
TEAD TEA domain
TEK Tunica interna endothelial cell kinase
TF Transcription factor
TG Transgenic
TGF Transforming growth factor
TNF Tumour necrosis factor
TSS Transcription start site
TSPAN Tetraspanin
Ub Ubiquitin
µl Microlitres
UCSC University of California, Santa Cruz
V Vein
V Ventricle
VEGF Vascular endothelial growth factor
VEGFR Vascular endothelial growth factor receptor
WNT Wingless-related integration site
WT Wild-type

Declarations

This dissertation is submitted to the Medical Sciences Division, University of Oxford, in fulfilment of the requirements for the degree of Doctor of Philosophy. This thesis is entirely my own work and describes my own research, except where otherwise stated. Where information has been derived from other sources, I confirm that this has been indicated in the dissertation. Any data that are not my own work are acknowledged and referenced appropriately. This work has not been submitted for a degree in this or any other University.

Mary A. A. Strevens

Contributions from other individuals in the main thesis:

1. Dr Svanhild Nornes (Institute for Developmental and Regenerative Medicine, University of Oxford) performed the zebrafish embryo microinjections

2. Indrika Ratnayaka (Ludwig Institute of Cancer Research, University of Oxford) performed the cryo-sectioning of mouse embryos

3. Professor Sarah De Val (Institute for Developmental and Regenerative Medicine, University of Oxford) dissected the retinae from the eyeballs, and for the last few samples, finished the collection and processing of retinae

Table of Contents

Contents of Figures

Contents of Tables

Contents of Equations

Chapter 1: Introduction

1.1 Development of the Vasculature

The vasculature, derived from the Latin word 'vascula' meaning small vessels, refers to a highly-branched hierarchical network of tubular structures connecting the heart to every organ and tissue in the body.[1-6] It is the first organ system to become functional during vertebrate development, marking a critical milestone and rate-limiting step in embryogenesis.[5] Since William Harvey first described the principle of blood circulation, the vascular system has been realised as both remarkably dynamic and multifaceted: it facilitates the transportation of oxygen and nutrients; regulates blood volume and pressure control; supports immune and paracrine signalling; and maintains tissue homeostasis.[4,6] On the other hand, aberrant vasculature can significantly advance chronic disease, such as ischaemic heart disease and stroke, as well as tumour progression.[2,4,7] The importance of studying the formation of new blood vessels is thus two-fold: not only can it inform on potential regenerative strategies, it can also provide the mechanistic insights needed to develop targeted therapies for the inhibition of pathological growth.[3]

Blood vessels comprise three primary layers: the tunica intima, a single layer of endothelial cells (ECs) supported by a thin basal lamina (or basement membrane); the tunica media, which contains smooth muscle cells and elastic fibres; and the tunica adventitia, which is composed of connective tissue, collagen, and in larger blood vessels, a vasa vasorum.[6,8] In combination, these layers provide both the mechanical support needed to anchor the vessel to its surrounding tissues, but also the ability to effectively regulate blood flow and pressure through changes in vascular tone.[5]

The vascular system develops via two sequential mechanisms: vasculogenesis and angiogenesis.[5,9,10] Vasculogenesis is defined as the *de novo* formation of blood vessels from aggregated mesoderm-derived EC progenitors; angiogenesis instead describes the generation of neovessels from pre-existing vascular structures.[5,9] In the murine embryo, vasculogenesis is initiated around embryonic (E) day 6.5-7 and angiogenesis around E8.5 (Table 1).[11] In comparison, vasculogenesis begins at approximately 18-21 days post-fertilisation (dpf) in the human embryo, with angiogenesis following around 21-25 dpf (Table 1).[12]

Table 1: Timeline for the initiation of vasculogenesis and angiogenesis in humans (*Homo sapiens*) and mice (*Mus musculus*)

Species	Vasculogenesis Initiation	Angiogenesis Initiation
Human (*Homo sapiens*)	18-21 dpf	21-25 dpf
Mouse (*Mus musculus*)	E6.5 - 7	E8.5

As embryogenesis progresses, the emerging nascent vessels form a primitive plexus. This plexus then gradually matures and remodels, while at the same time differentiating into arteries, veins, and capillaries.[5] Whilst the acquisition of subtype-specific EC identity is governed by differential gene expression, which can be observed prior to heartbeat, the onset of haemodynamic force further regulates EC phenotype.[13] As the embryo grows, the mature vascular network expands concomitantly to sufficiently meet the increasing metabolic demands of development.

1.1.1 Vasculogenesis

In both the human and murine embryo, vasculogenesis occurs prior to the onset of blood flow (Figure 1).[14] In the mouse embryo, gastrulation occurs on E6.5, inducing the differentiation of mesodermal progenitors into haemangioblasts.[15,16] This effectively marks the initiation of vasculogenesis. It should be noted that the hypothesis of a shared progenitor population for haematopoietic and endothelial lineages remains contentious and not wholly accepted.[17]

The haemangioblasts then cluster into spatially organised blood islands: cells on the periphery differentiate into angioblasts whilst the cells in the centre form haematopoietic progenitor cells.[11,18,19] Haemangioblasts are thus described as bipotent progenitors, and to some extent, these two lineages retain a degree of interchangeable multipotency.[15] For example, the haemogenic endothelium (a differentiated subpopulation of CD32-positive ECs) has the capacity to develop into multilineage haematopoietic stem cells during a short developmental period.[2,20,21,22]

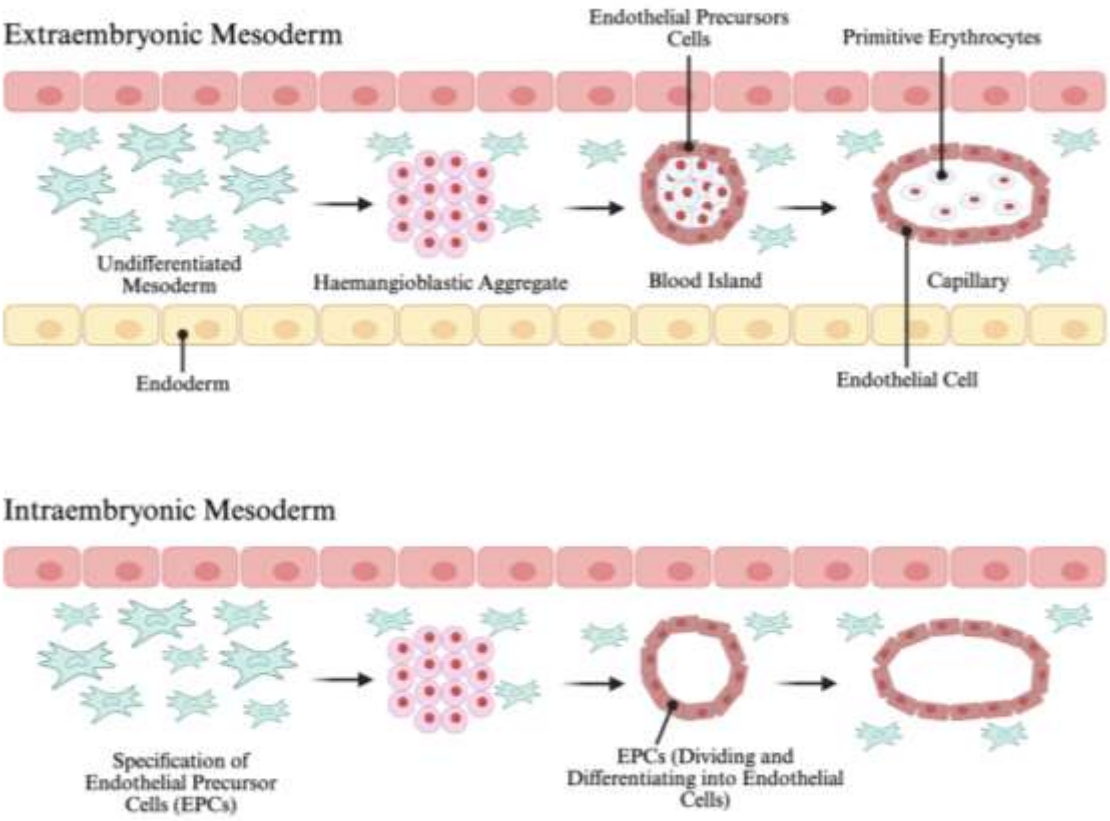

Figure 1: Vasculogenesis initiates from E6.5. In the extraembryonic mesoderm, undifferentiated mesoderm cells aggregate into blood islands throughout the yolk sac wall. Whilst cells in the periphery differentiate into ECs, the cells in the middle differentiate into primitive erythrocytes. In contrast, in the embryo proper, the aggregates of mesodermal cells only differentiate into ECs: this process does not form primitive blood cells. As the embryo develops, these capillaries merge to form a vascular network. Figure is replicated from DeSesso *et al* (2017).

Initially, at E6.5, haemangioblasts are marked by the expression of T-cell acute lymphocytic leukaemia protein 1 (TAL1, encoded by *Tal1*) or Vascular Endothelial Growth Factor Receptor 2 (VEGFR2, encoded by *Vegfr2*, also known as Kinase Insert Domain Receptor, KDR, encoded by *Kdr*, or Foetal Liver Kinase 1, FLK1, encoded by *Flk1*), but after E7.5, the developing ECs upregulate Platelet Endothelial Cell Adhesion Molecule 1 (PECAM, encoded by *Pecam1*), Tunica interna endothelial cell kinase (TEK, encoded by *Tek*, also known as TIE2), and Laminin. One of the most important transcription factors (TF) involved in the differentiation of angioblasts is ETS variant transcription factor 2 (ETV2).[23] In mice, EC-specific *Etv2* null embryos die at E9 and develop no EC lineages.[24]

Eventually the blood islands conjoin to form a primitive reticulate of nascent blood vessels.[22] Not all vessels are formed by the same mechanism: for example, the dorsal aorta is formed by the direct coalescence of angioblasts, whilst the ventral aorta and cardinal veins are formed by the migration of angioblasts from distant locations.[11] As angioblasts differentiate into ECs, they establish luminised tubular structures, deposit a basal lamina, and form the primary vascular plexus. Stabilisation follows, with tight junctions, adherens junctions, and gap junctions restricting further angioblast migration.[9]

By the two-somite stage, the extra-embryonic vasculature anastomoses with the intra-embryonic vasculature.[11,25] This allows the developing heart tube to be connected to the primary vascular plexus prior to the onset of cardiac contractions.[11]

There remains some controversy in the literature as to whether vasculogenesis is restricted to embryogenesis, or whether it can also occur in the adult context.[2] Indeed, whilst some experiments appear to show that bone-marrow-derived EPCs contribute to adult vascularisation in significantly damaged regions of the vasculature, other studies show no incorporation of the EPCs into the growing EC layer, instead suggesting that they contribute to vascularisation through the secretion of pro-angiogenic factors.[26,27]

1.1.2 Angiogenesis

After its initial formation, the primitive vascular plexus undergoes a period of rapid expansion and extensive remodelling. Angiogenesis, the process of forming new blood vessels from pre-existing vasculature, plays a pivotal role in this transformation (Figure 2).[5,9,11]

The term ‘angiogenesis’ was first coined by Dr John Hunter in 1787 to describe blood vessel growth in the reindeer antler.[28] It is derived from Greek, combining ‘angio-’ meaning vessel with ‘-genesis’ meaning birth or creation. However, it should be emphasised that not all angiogenesis occurs in physiological contexts; dysregulated angiogenesis can be a hallmark of cancer where it facilitates tumour metastasis.[29]

Angiogenesis is initiated by pro-angiogenic signals induced by local tissue hypoxia (Table 2).[30] There are several different types of angiogenesis but I will focus on describing the two most common, and perhaps consequently the two most studied, in detail. These are: sprouting angiogenesis, where endothelial cells migrate to form new

vessels; and intussusceptive angiogenesis, characterised by the insertion of tissue pillars within pre-existing capillaries to generate new vessels.[5,9,11,31-33]

Table 2: Pro-angiogenic factors and their receptors

Vascular Endothelial Growth Factor (VEGF); Platelet Derived Growth Factor (PDGF); Fibroblast Growth Factor (FGF); Epidermal Growth Factor (EGF); Transforming Growth Factor (TGF); Matrix metalloproteinases (MMPs); Tumor Necrosis Factor (TNF) and Angiopoietins

Pro-Angiogenic Factor	Receptors
VEGF (VEGF-A and VEGF-C)	Tyrosine kinase receptors (VEGFR1, VEGFR2 and VEGFR3)
PDGF (PDGF-BB and PDGF-AB)	Tyrosine kinase receptors (PDGFRRα and β)
FGF (FGF-2 and FGF-1)	Tyrosine kinase receptors (FGFR1, FGFR2, FGFR3, and FGFR4)
EGF (EGF and TGF-α)	Tyrosine kinase receptors: EGFR (ErbB1, HER1), ErbB2 (HER2), ErB3 (HER3), and ErbB4 (HER4)
TGF (TFG-β1 and TGF-β2)	Serine/threonine kinase receptors (type I and type II)
MMPs (MMP-2 and MMP-9)	Low-density lipoprotein receptor-related protein (LRP)
TNF (TNF-α and TNF-β)	Tyrosine kinase receptors (TNFRI, and TNFRII)
Angiopoietin (Ang-1 and Ang-2)	Tyrosine kinase receptors (Tie-1 and Tie-2)

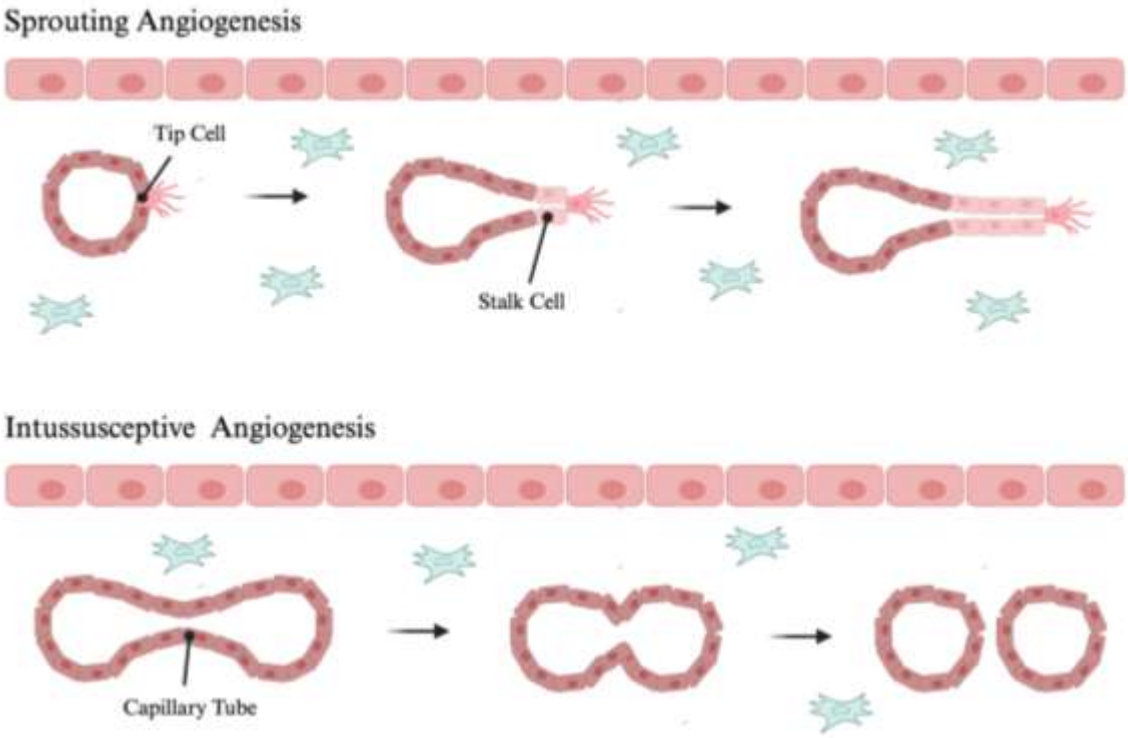

Figure 2: There are two main types of angiogenesis: sprouting and intussusceptive angiogenesis. In sprouting angiogenesis, one of the ECs differentiates into a tip EC. This tip EC migrates into the surrounding mesenchyme, with the adjacent ECs adopting a stalk EC identity. This allows the new sprout to elongate. In contrast, intussusceptive angiogenesis involves the longitudinal splitting of a blood vessel to form two new vessels, each with a lumen. Figure is replicated from DeSesso et al (2017).

1.1.2.1 Sprouting Angiogenesis

Sprouting angiogenesis is primarily driven by a gradient of pro-angiogenic factors released from oxygen- and nutrient-deprived tissues.[3,10,34] These pro-angiogenic factors bind to receptors on the membrane of quiescent ECs, activating the ECs, and leading to the release of proteases. These proteases degrade both the basement membrane and the extracellular matrix (ECM), helping to establish a permissive environment for EC proliferation and migration.[35,36] Moreover, this degradation leads to the release of ECM-bound growth factors, amplifying the pro-angiogenic signal further.[37]

The developing angiogenic sprout is comprised of two distinct types of EC: tip ECs and stalk ECs.[38,39] The identity of either is not pre-determined, but instead results from a

tightly regulated tip selection process driven by VEGF-Notch signalling interactions between neighbouring ECs (Figure 3).[38]

VEGFA, one of the most potent pro-angiogenic factors, initiates tip cell selection by binding to VEGFR2 receptors on the EC membrane.[34,38-40] This binding event triggers internal VEGF-VEGFR2 signalling and the downstream upregulation of Delta-like ligand 4 (DLL4).[41-46] Ruhrberg *et al* (2002) demonstrated that extracellular VEGFA gradients regulate vascular branching by generating mice expressing only the diffusible VEFG120 isoform, which lacks heparin-binding domains and therefore cannot bind the ECM. These embryos exhibited reduced capillary branching and impaired endothelial filopodia guidance despite normal endothelial proliferation. This effectively indicated that matrix-bound VEGF isoforms normally establish localised gradients that polarise ECs and guide angiogenic sprouting.[47]

Importantly, DLL4 is a membrane-bound ligand, meaning that signalling occurs only through direct cell-contact between adjacent EC. ECs exposed to higher local concentrations of VEGFA therefore upregulate DLL4 and adopt a prospective tip-cell phenotype characterised by increased VEGF2 signalling and the extension of numerous filopodia that guide the sprout along the VEGF gradient.

DLL4 expressed on the surface of these prospective tip cells binds to Notch receptors (primarily Notch1) on neighbouring ECs. This interaction activates Notch signalling in adjacent cells through a sequence of proteolytic cleavages mediated by ADAM metalloproteases and the γ-secretase complex. The released Notch intracellular domain (NICD) then translocates to the nucleus, where it regulates transcription of Notch target genes that alter EC responsiveness to VEGF. One key consequence is the suppression of VEGF2 expression alongside the upregulation of VEGFFR (Flt-1).[45] Hellström *et al* (2007) demonstrated that DLL4-Notch signalling regulates tip cell selection in the developing mouse retina, as inhibition of Notch with γ-secretase inhibitors or Dll4 haploinsufficiency caused excessive tip cell formation and hypersprouting.[41] Siekmann and Lawson (2007) similarly showed that loss of the Notch mediator Rbpsuh in zebrafish embryos led to excessive sprouting, with ECs lacking Notch preferentially adopting a tip cell position. They further demonstrated that Notch limits VEGF signalling; the VEGF receptor FLT4 became ectopically expressed in sprouts lacking Notch, and loss of DLL4

increased EC numbers, indicating the Dll4-Notch signalling constrains VEGF-driven angiogenic sprouting.[44]

VEGFR1 acts primarily as a decoy receptor with high affinity for VEGFA but weak signalling capacity (Figure 3). In addition to its membrane-bound form, VEGFR1 can be produced as a soluble form (sVEGFR1) through alternative splicing or proteolytic cleavage of the receptor ectodomain. When sVEGFR1 is secreted into the extracellular environment, it binds VEGFA, thereby preventing VEGFA from binding to VEGF2. This creates an effective VEGF trap which dampens the VEGF signalling in neighbouring ECs. By reducing VEGF2 activation and VEGF availability, Notch-induced VEGF1 expression reinforces the suppression of the tip cell phenotype in adjacent cells and promotes adoption of the stalk cell fate. Fong *et al* (1995) found that VEGFR1 is essential for proper vascular organisation as murine embryos lacking VEGFR1 formed ECs normally but assembled them into abnormal vascular channels and died *in utero*.[48] Work by Kearney *et al* (2002) further supported this decoy role by showing that loss of VEGFR1 increases VEGFR2 phosphorylation and EC proliferation during development, demonstrating that VEGFR1 modulates VEGF-induced angiogenesis by reducing VEGF availability for VEGFR2 signalling.[49]

In this way, a lateral inhibition mechanism is established: the first EC to upregulate high levels of DLL4 in response to VEGFA assumes the tip cell phenotype, while activation of Notch signalling in neighbouring cells suppresses their VEGF responsiveness and drives them toward a stalk cell identity. This VEGF-DLL4-Notch feedback loop therefore ensures that only a limited number of ECs adopt the migratory tip cell phenotype while surrounding cells contribute to sprout elongation.

The dynamic competition between ECs for the tip cell position ensures optimal sprout progression, with cells able to switch roles as environmental cues change.[38] This plasticity allows the vascular network to adapt and grow in response to angiogenic signals. Tip ECs extend filopodia and lamellipodia to guide the sprout, whilst stalk cells elongate and proliferate, providing structural support to the developing sprout.[38,50] When tip cells from adjacent sprouts meet, they anastomose, creating a continuous, perfused vessel.

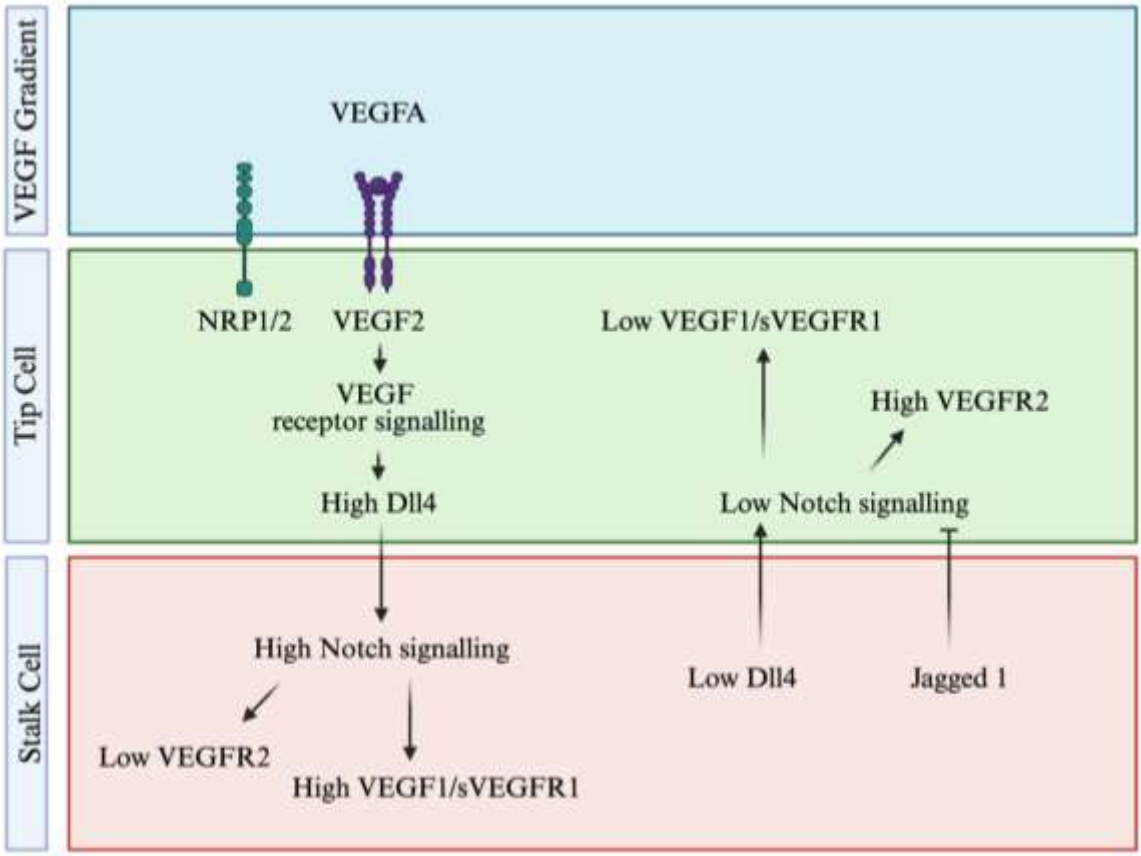

Figure 3: Tip EC selection during sprouting angiogenesis. VEGFA binds to VEGF2, triggering an upregulation of *Dll4* expression in tip ECs. This high level of *Dll4* expression activates Notch signalling in the neighbouring stalk EC, leading to a reduction of VEGF2 expression whilst increasing the VEGF1/sVEGF1 expression levels. This establishes a scenario in which the tip EC receives low Notch signalling, allowing a high expression level of VEGF2. Figure replicated from Blanco and Gerhardt (2013).

1.1.2.2 Intussusceptive Angiogenesis

Intussusceptive angiogenesis involves the longitudinal division of pre-existing blood vessels, enabling the expansion and reorganisation of an immature capillary plexus.[3,9,31-33] This process begins when ECs from opposing vessel walls make contact, forming a transluminal bridge that reorganises the endothelial bilayer and creates an interstitial pillar core. Myofibroblasts and pericytes then infiltrate the pillar, increasing its diameter and promoting fusion with neighbouring pillars. This results in the bifurcation of a single vessel into two parallel capillaries.[31,51]

Compared to sprouting angiogenesis, intussusceptive angiogenesis is a more rapid and energetically efficient mechanism, requiring minimal EC migration and proliferation.[32] It occurs in distinct forms: intussusceptive microvascular growth, which rapidly expands the vascular network; intussusceptive arborisation, which structures the network into a hierarchical vascular tree; and intussusceptive branching remodelling, which refines the vessel architecture to optimise vascular function.[33]

1.1.3 Vascular Remodelling

Intra-embryonic and extra-embryonic primitive vascular networks anastomose at the two-somite stage, prior to the onset of blood circulation.[11] By the three-somite stage, the heart tube becomes functional, and by the five-somite stage, the vascular network first experiences haemodynamic force exerted by the circulating blood cells.[5,52,53] It is this mechanical force which is so important in the ensuing remodelling process. As reported in his seminal paper, William Chapman used a chick embryo to demonstrate that an abnormal peripheral vascular system forms if the embryonic heart is surgically ablated.[54] Recent advances in genetically modified animal organisms now allow for more elegant experimentation. For example, murine embryos deficient in *Nkx2.5*, and therefore without heartbeat, have attenuated blood vessel remodelling.[55]

Using mechanosensors on their membrane, ECs are able to detect the mechanical stimuli generated by blood flow, and in response, activate very specific downstream gene expression programmes.[56] This is referred to as mechanotransduction.[56] Piezo1, an ion channel activated by shear stress, is known to be particularly important for embryonic vascular development.[57] Subsequent changes include modifications in vessel diameter, branching, or wall thickness. Remodelling is not just physiologically important; it is

critical for embryonic survival. This is reflected in the frequent embryonic lethality associated vascular patterning defects.[58]

1.1.4 Arterial and Venous Specification

A mature vascular network is comprised of heterogenous EC subpopulations.[1,4,59] This heterogeneity enables the vascular system to efficiently transport oxygen by forming distinct vessel types – arteries, capillaries, and veins. These vessels are exposed to different haemodynamic environments, leading to their ECs acquiring further specialisations. At the most fundamental level, this involves the establishment of specific arterial and venous EC identities. This process is known as arterial and venous specification (Figure 4).[60-63]

Arterial and venous specification was initially thought to be driven by the onset of blood flow, with ECs prior to this event being homogeneous with no pre-defined identity. However, this dogma has been challenged in recent years by studies showing selective expression of arterial and venous markers prior to circulation.[61,62] Indeed, it is now thought that early arterial and venous ECs emerge from distinct angioblast subpopulations. This suggests a degree of genetic pre-determination from as early as vasculogenesis. Nevertheless, hemodynamic forces are still important: whilst blood flow is not required for the initial establishment of identity, it is essential for its maintenance. Indeed, early vessel identity exhibits a degree of plasticity, with arterial or veins fates reversibly determined upon blood flow reversal. Furthermore, complete arterial differentiation does not occur in murine embryos lacking circulation, highlighting the necessity of blood flow-induced shear stress in both the establishment and maintenance of arterial identity.[61,62,64]

The formation of arteries and veins later in development has also been a source of much discussion. The initial hypotheses often centred around the idea of outward budding from existing defined blood vessels.[62] Advancements in fate-mapping and single-cell RNA sequencing (scRNA-seq) technology has now enabled more robust analysis, resulting in a revised hypothesis that venous ECs act as the primary source of both angiogenic and arterial ECs.[4,60]

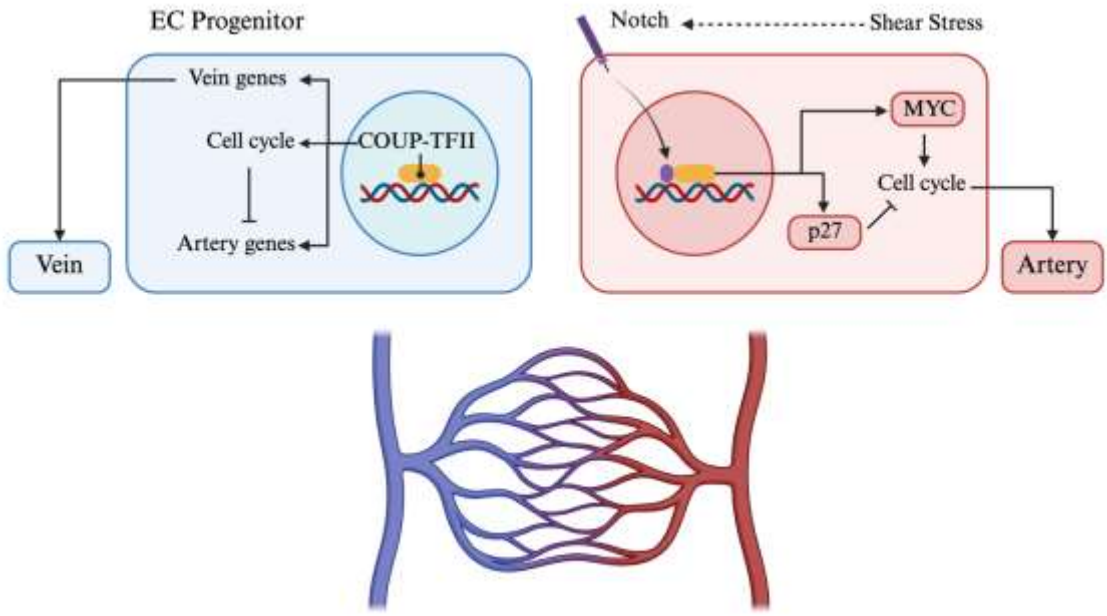

Figure 4: Arterial and Venous Specification. The differentiation of arterial ECs is coupled to reduced cell cycling frequency. Shear stress activates Notch signalling, leading to the upregulation of p27 expression. p27 inhibits MYC-induced transcription of cycle cell genes. Figure replicated from Trimm *et al* (2023)

One of the most important determinants of arterial/venous EC identity that has emerged is cell cycling.[4,65,66] Whilst high levels of cell cycling appears to favour venous EC identity, a reduced cell frequency cycling instead promotes arterial EC identity. This is seen in the postnatal retina vasculature where shear stress arrests the cell cycle and promotes arterial gene expression.[65] Moreover, enhanced VEGFA and Notch signalling in the capillaries pushes the ECs towards an arterial identity by supressing MYC-dependent cell cycle progression.[67] In contrast, overexpression of *NR2F2* (*COUP-TFII*) facilitates cell cycle progression, inhibiting arterial differentiation, and thereby maintaining venous identity.[66-68] Thus, proliferating ECs appear to be predisposed to a venous fate, while arterial differentiation is linked to cell cycle arrest.[4]

Since reduced cell cycling is a pre-requisite of arterial EC identity, the arterial network cannot expand via intrinsic proliferation. Therefore, it must instead recruit ECs from veins and capillaries.[4] This has been demonstrated in lineage-tracing studies in the mouse heart, which found that *Apj*-expressing capillary EC cells undergo arterial specification during specific developmental windows.[66] Similarly, in postnatal mouse retinas, lineage-tracing

experiments have shown that ECs migrate from veins to capillaries and subsequently to arteries during vascular maturation.[69-71]

VEGF-VEGFR signalling is also heavily implicated in arterial/venous specification.[4,72,73] Whilst low levels of VEGFA are associated with venous identity, high VEGFA concentrations are thought to promote arterial differentiation via Notch-RBPJ signalling activation.[67,74] The precise transcriptional regulation of arterial and venous specification will be explained in more detail later on.

1.1.5 Vessel Maturation

Upon the formation of a morphologically and genetically distinct vascular network, the vessels mature and stabilise.[4,5] One way this is achieved is via the deposition of extracellular matrix proteins to form a basement membrane.[75,76] Further structural support is then provided by the recruitment of smooth muscle cells and pericytes, collectively known as mural cells, to the maturing vessel wall. This recruitment involves reciprocal paracrine signalling between ECs and the mural precursor cells; ECs secrete PDGFB to interact with PDGFRB on mural cell precursors, whilst the precursors release angiopoietin-1 (ANGPT1) to bind with the TEK receptor on ECs.[5,76-79]

After contact with ECs, the mural cell precursors undergo differentiation, driven in part by the TGFB1 signalling pathway.[5] This pathway promotes the expression of mural cell markers, suppresses EC and mural cell proliferation, and stimulates elastin secretion by smooth muscle cells (SMCs) and fibroblasts.[5,80-83] Disruption of either the TGFB or PDGFB signalling pathway impairs pericyte recruitment, leading to vascular defects. The interaction between differentiated mural cells and ECs stabilises the vessel wall, establishing a quiescent vessel bed.[84] Notably, this stabilisation is reversible.[5] ANGPT2, an antagonist of ANGPT1/TEK signaling, plays a key role in facilitating vessel destabilisation in regions undergoing active remodelling.[84]

1.1.6 Coronary Vasculature Development

The coronary vasculature is the network of blood vessels that supplies the myocardium.[85-89] In mammals, the coronary vasculature includes the coronary arteries, which deliver oxygenated blood from the aorta; coronary veins, which return deoxygenated blood to the right atrium via the coronary sinus; and capillaries, which enable the exchange between

blood and cardiomyocytes.[86] Any disruption in coronary blood flow can have severe, and sometimes fatal, consequences. For example, myocardial ischaemia can lead to a wide array of pathophysiological conditions such as myocardial infarction, arrhythmias and sudden cardiac death.[90]

One long-standing hypothesis in the field posited that the coronary network developed as the angiogenic outgrowth of the aorta.[85] However, this was eventually disproven by detailed histological studies in quail-chick transplantations observing that the fully assembled capillary plexus had no connection to the aorta until 8 dpf.[91] More recently, mouse genetic cell lineage experiments have led to wide acceptance that the coronary vasculature has two primary progenitor sources - the sinus venosus (SV) and the endocardium - which predominantly localise to distinct, yet partially overlapping, regions of the heart.[4,92-97] Broadly speaking, coronary ECs derived from the SV contribute to the outer ventricular wall vessels, whilst endocardium-derived coronary ECs form vessels in the septum and inner ventricular walls.[85,86,88,98] Despite significant advancements in the genetic lineage tracing tools available, controversy persists as to their precise contributions.

In mice, whilst both progenitor sources initiate sprouting between E11.5-12.5, they are induced to do so by disparate molecular signals.[93] Indeed, sprouting from the SV is mediated by epicardial secretions of VEGFC binding to the VEGFR3-expressing endothelium, whilst endocardium-derived sprouting is driven by VEGFA binding to endocardial VEGFR2 receptors.[85,86] Upon sprouting onto the developing heart, the newly forming vessels undergo phenotypic change within the coronary plexus before extensive remodelling to form mature coronary arteries, capillaries and veins.[95]

Whilst the endocardium progenitor pool is considered the dominant contributor to coronary ECs, it has been hypothesised that this contribution predominantly occurs in the neonatal, rather than embryonic, stage. Certainly, the neonatal heart undergoes rapid vascularisation; the compaction of previously non-vascular trabecular myocardium causes the expansion of endocardium-derived vessels into this region.[99] However, whilst initial studies reported lineage conversion of neonatal endocardial cells, more recent examinations have shown that the endocardial to coronary EC transition is restricted to the embryonic heart.[92,100] This incongruity can be accounted for by the use of different endocardial markers: *Npr3* is a far more specific endocardial marker than *Nfact1*.[96]

1.2 Transcriptional Regulation of Gene Expression

There are approximately 20,000 protein coding genes within human genome, with almost every cell carrying an identical copy of this genome.[101-103] Notable exceptions to this include erythrocytes and thrombocytes, which are anucleate, and gametes, which are haploid.[103] However, with the vast majority of cells containing the exact same underlying genetic information, a mechanism must exist to enable the emergence of heterogeneous cellular morphology and function.

For a significant time, the field grappled with this conundrum, until in 1961, Francois Jacob and Jacques Monod proposed the operon model in a seminal paper.[104] This model demonstrated how a collection of genes could be co-ordinately controlled by a repressor protein and thereby serve as the foundational basis for gene regulation.[104] The significance of this finding, in combination with work from Andre Lwoff on lysogeny, was recognised with the 1965 Nobel Prize in Physiology or Medicine.[105,106] It has since been confirmed that, in both prokaryotes and eukaryotes, cellular heterogeneity is primarily achieved through the tight regulation of gene expression. Indeed, whilst each cell contains the entire human genome, and between 10% to 20% of genes are ubiquitously expressed, each individual cell has a unique gene expression profile.[107] Moreover, within each cell there is also temporal variation: whilst some genes have ubiquitous expression at relatively consistent levels, other genes have considerable variation in their expression levels. This variation is vital to ensure cells can respond appropriately to both internal and environmental signals, maintain homeostasis, and differentiate during development.

In 1957, Francis Crick coined the ‘central dogma’ of molecular biology, which refers to the transfer of genetic information from deoxynucleic acid (DNA) to functional proteins, via a ribonucleic acid (RNA) intermediary.[103,108] Simply put, this process can be regulated at many levels: (1) the transcription of DNA to messenger RNA (mRNA), (2) the translation of mRNA to an amino acid sequence, (3) and the post-translational modifications of this initial amino acid sequence to synthesis a functional protein. Crucially, from one gene, many copies of mRNA can be transcribed, and from one mRNA molecule, many amino acid sequences can be transcribed. Ultimately, this allows a large quantity of protein to be synthesised from a single gene.[108]

1.2.1 Organisation of Genetic Information

The length of the DNA encoded within the human genome is roughly 3.2 x 10^9 nucleotide pairs, and yet, apart from a small amount contained within the mitochondria, the vast majority of eukaryotic DNA resides inside the nucleus of the cell.[103,109] Here it is highly condensed into dynamic chromatin structures (Figure 5).[110,111]

Chromatin refers to the complex formed between nuclear DNA, histones, and non-histone chromosomal proteins.[112-114] At the most basic level, DNA is packed into nucleosomes where 147 nucleotides are tightly wound around an octameric core of histone proteins in 1.65 left-handed superhelical turns.[114-116] As a tripartite complex, the histone octamer comprises an inner core tetramer of histones H3 and H4, and two outer histone H2A/H2B dimers.[117] All four histone proteins are relatively small (102-135 amino acids), share a histone fold structural motif, and have a N-terminal amino acid which can be covalently modified.[103] Each nucleosome core is connected by linker DNA, which on average is 200 nucleotide pairs in length.[114,118] Nucleosomes are further organised into solenoids, helical arrays with a diameter of 30nm, which are then arranged around a central scaffold protein.[119] Chromatin then undergoes three-dimensional to form a chromosome.[114]

Within the eukaryotic nucleus, there are two main types of chromatin.[111] Euchromatin is more predominant in transcriptionally active gene bodies and regulatory elements.[111,114] Structurally, it has a less condensed arrangement of nucleosomes which exposes the DNA more readily to the transcriptional machinery. In contrast, heterochromatin is highly condensed and more associated with transcriptionally inactive regions of the genome.[111,114] Heterochromatin can be further subdivided into constitutive and facultative subtypes.[120,121] Constitutive heterochromatin refers to permanently condensed chromatin, whilst facultative heterochromatin retains the ability to switch between condensed and open states in response to external cues. In this way, heterochromatin plays a key role in maintaining genome stability, regulating gene expression, and ensuring proper chromosome segregation during cell division. Spatially, heterochromatin is segregated from euchromatin in the nucleus, preferentially localising toward the nuclear periphery and regions surrounding the nucleolus.[111,121]

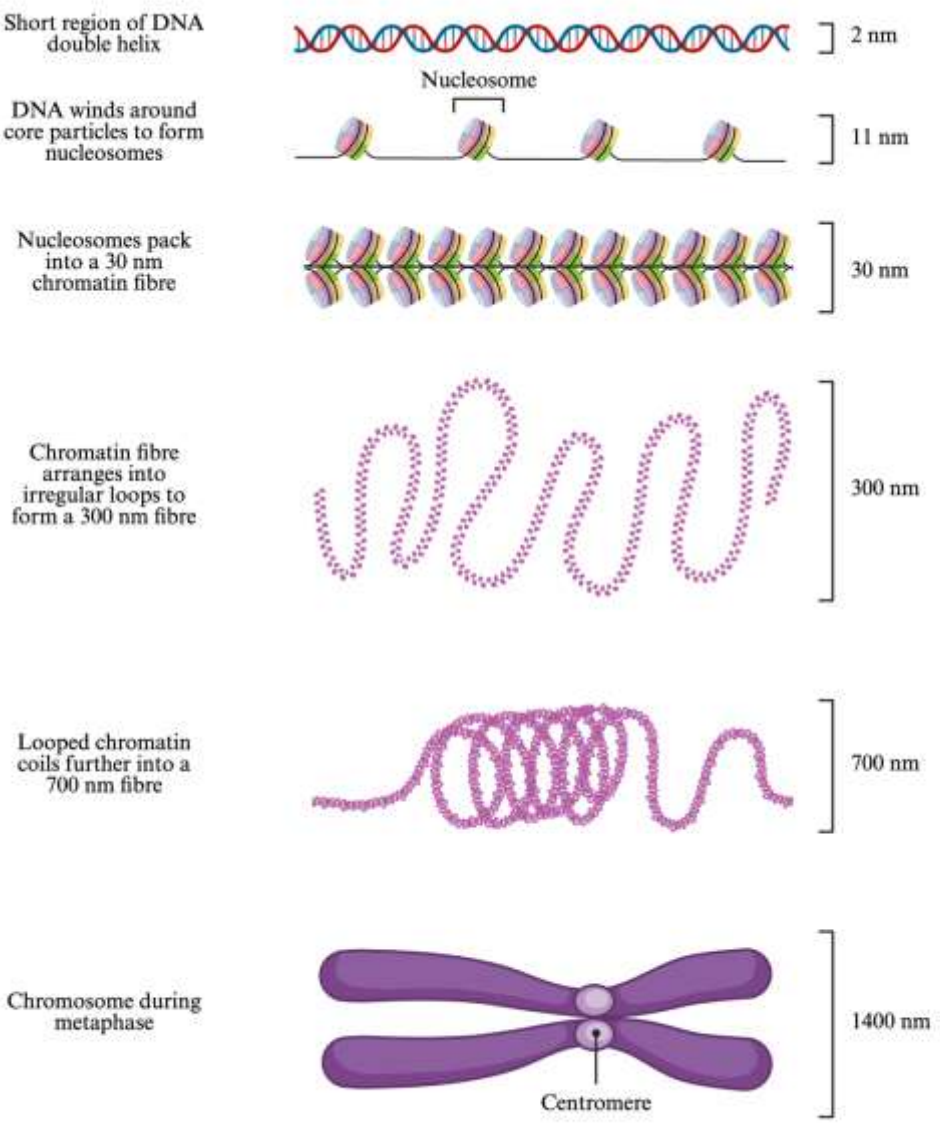

Figure 5: Organisation of Genetic Material. DNA is wound around histone octamer to form nucleosomes, with the nucleosomes then packed into a 30 nm chromatin fibre. This chromatin fibre is then arranged into irregular loops to form a 300 nm fibre, which is itself looped into a 700 nm fibre. In metaphase, these structures are then stored as chromosome. Figure replicated from Jansen *et al* (2011) using the 'Chromatin Organization' template in by BioRender.com

1.2.2 Histone Modifications

One way that gene expression can be regulated is through chromatin modifications (Table 3).[114,122] These include the methylation, acetylation, phosphorylation and ubiquitylation of the histone proteins in the nucleosome core (Figure 6).[123] Collectively, these modifications fall under the umbrella of epigenetics.[124] Epigenetics, derived from the Greek prefix 'epi-' meaning 'on' and 'genesis' meaning 'origin, source' was first used by Conrad Waddington in 1942 to describe modifications which alter DNA accessibility and chromatin structure without changing the underlying DNA sequence.[125] These changes can be heritable.

As previously explained, chromatin exists in a dynamic equilibrium between a condensed, transcriptionally repressive state (heterochromatin) and a more open, transcriptionally permissive state (euchromatin). Histone modifications alter the physical interaction between DNA and histones, as well as recruit effector proteins that influence chromatin compaction (Figure 7). For example, histone acetylation is generally associated with transcriptional activation. This process is catalysed by histone acetyltransferases (HATs), which transfer acetyl groups to lysine residues on histone tails, neutralising their positive charge and weakening their interaction with negatively charged DNA.[126] This results in a more open chromatin conformation that facilitates transcription factor binding. Conversely, histone deacetylases (HDACs) remove these acetyl groups, restoring positive charge, promoting chromatin condensation, and typically repressing gene expression.[126]

Certain histone modifications are associated with particular regions of the genome: tri-methylation of histone H3 at lysine 4 (H3K4me3) is often found in promoter regions near the transcriptional start site (TSS); the acetylation of histone H3 at lysine 27 (H3K27ac) is a well-recognised marker for active enhancers; and the methylation of histone H3 at lysine 36 (H3K36me) is associated with gene bodies of transcriptionally active genes (Table 3).[127-130] These covalent modifications control critical aspects of the chromatin landscape and increase the binding affinity of chromatin remodelling factors.

Figure 6: Post-translation Modifications of Histones Tails within the Nucleosome Core. Schematic representation of the histone octamer with H2A, H2B, H3, and H4 at the nucleosome core, with their N-terminal tails extending outward. The labelled residues indicate known sites of post-translational modifications: methylation (Me), acetylation (Ac), ubiquitination (Ub), and phosphorylation (P).

Table 3: A Summary Table of Common Histone Modifications

Histone Modification	General Effect on Gene Expression	Common Genomic Location
H3K4me3	Activator	Active promoters (near transcription sites)
H3K4me1	Activator (poised/active)	Enhancers
H3K27ac	Activator	Active promoters and enhancers
H3K9ac	Activator	Active promoters
H3K36me3	Activator	Gene bodies
H3K27me3	Repressor	Silenced promoters, developmental genes
H3K9me3	Repressor	Constitutive heterochromatin
H4K16ac	Activator	Active chromatin regions

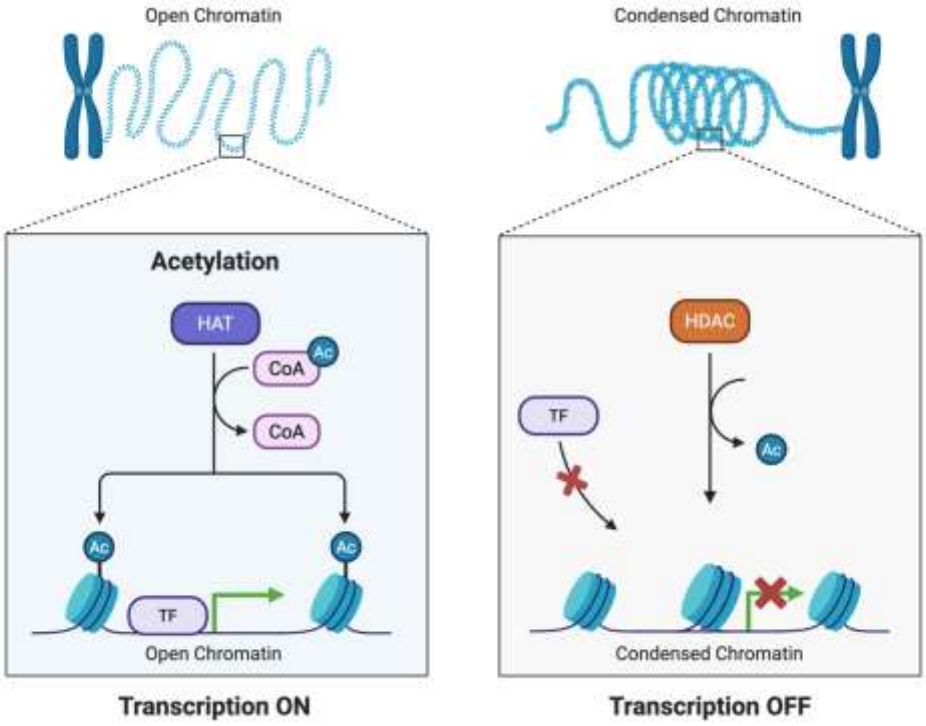

Figure 7: Histone acetylation regulates chromatin accessibility and transcriptional activity. Schematic representation of the opposing roles of HATs and HDACs in controlling chromatin structure. In the left panel, HAT enzymes transfer acetyl groups (Ac) from acetyl-CoA to lysine residues on histone tails, neutralising their positive charge and weakening histone–DNA interactions. This results in an open chromatin conformation that permits TF binding and actives gene transcription. In the right panel, HDACs remove acetyl groups, restoring positive charge to histones and promoting tighter DNA wrapping and chromatin condensation. This compact structure restricts TF access and leads to transcriptional repression.

In addition to histone modifications, DNA methylation represents another key epigenetic regulatory mechanism.[131] DNA methylation typically occurs at cytosine residues within CpG dinucleotides and is catalysed by DNA methyltransferases (DNMTs).[132] In promoter regions, particularly within CpG islands, DNA methylation is generally associated with transcriptional repression. Methylated DNA can directly inhibit transcription factor binding or recruit methyl-CpG-binding domain proteins, which in turn attract repressive chromatin-modifying complexes, including HDACs.

In the last few decades there has been a great advancement in the techniques used to study the epigenome. Chromatin immunoprecipitation sequencing (ChIP-seq), assay for transposase-accessible chromatin sequencing (ATAC-seq), and cleavage under targets and release using nuclease (CUT&RUN) have all enabled the complete genome mapping of histone marks and chromatin accessibility.[133,134] Datasets across different species have

been compiled and made publically available, thereby serving as a useful platform to investigate gene regulation.

1.2.3 Transcription: Components of Transcriptional Regulation

Transcription refers to the process by which the genetic information encoded in DNA is converted into a mRNA molecule.[103] This is a very complex process involving the orchestration of multiple proteins and regulatory elements. Epigenetic mechanisms, already discussed, form one important layer of regulation by altering the chromatin architecture and DNA accessibility.[124,125] Another important layer involves the binding of specific TFs to regulatory elements (promoters, enhancers and silencers).[24,62,103,135-137] These factors recruit coactivators or corepressors, which interact with the basal transcription machinery to activate or repress transcription.

1.2.3.1 Promoters

Eukaryotic core promoters play an important role in governing transcription initiation and direction by acting as a binding platform on which the pre-initiation complex (PIC) can assemble.[103,138] Core promoters are typically 50 to 100 base pairs in length and encompass the transcription start site.[138,139] However, not all core promoters are the same, and it is becoming increasingly apparent that great diversity exists with regard to both their sequence and architecture.[140] It has been proposed that metazoan promoters can be categorised into three distinct types: promoters with sharp initiation patterns; promoters with dispersed initiation patterns for broadly expressed housekeeping genes; and promoters of key developmental TFs implicated in morphogenesis.[138,141,142]

To allow the general TFs (GTFs) to bind, the core promoter is densely packed with core promoter motifs.[143] Particularly well-documented is the TATA box; a high density adenine and thymine sequence typically found 25-30 base pairs upstream of the TSS.[144] This is recognised by the TATA-binding protein (TBP).[145] However, more recent genome-wide analysis studies have demonstrated that most mammalian core promoters do not have a consensus TATA box, positing a more flexible model of promoter recognition.[144,146]

The initiator (Inr) motif is another well-characterised promoter element.[147] Despite being more abundant than the TATA box, it is not found in all species and there can be considerable variability in the consensus sequence.[138] In the absence of a TATA box, the Inr is often found alongside the downstream promoter element, which is able to bind TFIID.[147] In humans, other core promoter motifs of note include the TFIIB recognition elements and then downstream core element.[138] Moreover, core promoters associated with housekeeping genes have a propensity to overlap with regions of increased GC content and high density of CpG dinucleotides, termed CpG islands.[148]

Although core promoters can initiate transcription on their own, they have low basal activity.[138] To overcome this problem, a proximal promoter is located upstream of the core promoter, containing many primary regulatory elements to increase transcriptional activity.[138]

1.2.3.2 Enhancers

Enhancers are *cis*-regulatory element which operate in the genome as non-coding regulators of gene expression.[149-151] This regulation can occur regardless of their orientation and despite them often being located hundreds of kilobases away from the TSS of their target gene.[152,153] Whilst enhancers can vary considerably in length, often from 200 to 2000 base pairs, their sequences are highly enriched in TF binding motifs. It is these motifs that allow the binding of sequence-specific TFs which direct the very precise spatiotemporal patterns of gene expression.[154] Enhancers can either be silenced, poised, or in active state depending upon their accessibility for TF binding. These states are heavily influenced by the histone modifications on surrounding nucleosomes, as for example, in order for an enhancer to be active, it must be positioned in an open chromatin region with H3K27ac and H3K4me1 marked histones.[127,129] Upon binding to the enhancer sequence, tissue-specific TFs actively recruit additional coregulators to modify the chromatin landscape and bring the enhancer within close proximity of its cognate promoter.[137] Examples of coregulators include histone acetyltransferases, histone methyltransferases, chromatin remodelling factors and the Mediator complex. A single gene is often regulated multiple enhancers, expressed in an overlapping pattern.

Enhancers can be classified into subtypes based on their activity and distance from target genes.[149] One group are called constitutive enhancers. These are active in many cell

types, regulating housekeeping genes. On the other hand, tissue-specific enhancers function only in specific cell types or developmental stages, ensuring genes are expressed only when and where they are needed. Super-enhancers are clusters of enhancers that drive exceptionally high levels of transcription, often associated with genes controlling cell identity, such as in stem cells or cancer cells.[155]

In the human genome more than two million enhancers have been identified, however it has proven challenging to properly validate them.[156-158] This is in part because biochemical assays sometimes provide conflicting results but also because the scale of enhancers to functionally test is immense.[158]

1.2.4 Enhancer-Promoter Interactions

Since enhancers can reside a substantial distance from their cognate promoters, and indeed can skip promoters, a mechanism must exist to selectively mediate gene expression.[151,153] The stable contact model, involving chromatin looping to bring the two into close spatial proximity, is perhaps the classical model, but more recently, an 'action-at-a-distance' model has also been posited.[153] This instead suggests that enhancer-promoter interactions can occur without the need for physical closeness: mediation is achieved either by liquid-liquid phase condensates of TFs, co-activators, and Pol II; or it can be attained by a TF activity (TAG) gradient.[159,160] In the TAG model, co-activators which are bound to the enhancer facilitate a concentration gradient of acetylated TFs. Consequently, nearby promoters have a higher probability of interacting with acetylated TFs which have diffused away from the enhancer. This would provide an interesting explanation for the weak correlation observed between enhancer-promoter 3D distance and transcription.

Although the 'action-at-a-distance' model would enable enhancer-promoter interactions outside of topologically associated domains (TADs), most interactions are contained within the TAD boundaries.[161] The TADs themselves, which can range from 100 kilobases to 1 million bases, are then organised into smaller subTADs, affording even more precise regulatory control over transcription.[162] Whilst TAD boundaries are conserved between cell types, subTADs exhibit considerable variability. The importance of TAD boundaries is highlighted in their absence, with aberrant gene expression resulting in a range of severe developmental disorders.[163]

The way in which TADs facilitate high frequency enhancer-promoter interaction is through a combination of convergent CCCTC-binding factor (CTCF) binding and cohesion. This is referred to as the 'loop extrusion' model.[162] Cohesin, a structural maintenance of chromosome complex, stochastically binds to the chromatin, extruding the chromatin in loops until it reaches a CTCF-bound boundary element on both strands. The stalling of cohesin at this point creates a tight spatial domain for enhancer and promoter interactions.

1.2.5 Transcription Factors

TFs are defined as DNA-binding proteins which help regulate the transcription of genes into mRNA molecules.[103,138] By influencing the recruitment and activity of RNA Polymerase II (Pol II) and the associated transcriptional machinery, TFs can control the spatiotemporal pattern of gene transcription as well as the level of gene expression. Moreover, by creating either negative or positive feedback loops, TFs can effectively self-regulate their own expression by activating or repressing downstream signalling pathways.[164] In the Gene Ontology (GO) database, the human genome is predicted to encode over 1,400 TFs.[165]

Each TF is comprised of a DNA-binding domain (DBD) and a transcriptional activation or repression domain. Using the DBD, a TF is able to recognise specific 6-12 base pair degenerate DNA sequences known as response elements, usually found in the promoter or enhancer regions of target genes.[166] These sequences are often palindromic, allowing for the binding of dimeric TFs.

Considering that the DBD recognises such a short sequence, a single TF has the potential to bind to thousands of different sites in the genome, and yet the specificity of the TF-DNA interaction is absolutely critical for accurate gene regulation. In order to resolve this apparent conflict, regulatory elements often require the coordinated action of multiple TF binding events, either through homotypic or heterotypic interactions.[166] This combinatorial binding can either be additive (individual TF concentration is proportional to enhancer activation) or cooperative (individual TF concentration has a non-linear relationship with enhancer activation).[166]

Different enhancer activity models have been proposed: the enhanceosome model, the billboard model and the TF collective model.[149,166] In the enhanceosome model, enhancers only permit cooperative TF binding in a precise, specific arrangement manner. These binding events are interdependent, promoting all-or-none gene expression. The interferon-β enhancer is one such example: precise combination of TFs must bind in a coordinated and sequential manner to form a functional enhanceosome.[166,167] In contrast, the billboard model proposes that TFs can bind independently, and therefore the precise positioning of TF binding sites is not essential provided all TFs are bound. The activity of the enhancer is thus determined by the cumulative effects of multiple TFs.[168] Finally, the TF collective model presents a hybrid between the rigidity of the enhanceosome model and the flexibility of the billboard model: different combinations of TFs bind cooperatively to the enhancer, and the collective action of these factors ultimately drives gene expression.[169]

1.3 Transcriptional Regulation of Vascular Development

As discussed earlier, despite all originating from angioblasts, ECs are remarkably heterogenous in both their structural characteristics, and their functional responses to physiological and pathological stimuli.[1,4,59] This heterogeneity is paramount to organotypic specialisation during development. At the most basic level, heterogeneity is observed in the different vessel types, whether they are arteries, veins or capillaries.[61] This is achieved by tight and dynamic regulation of gene expression, with each EC subtype expressing a unique combination of genes (Figure 9). At the transcriptional level, this is in part controlled by TFs either activating or repressing target gene expression (Figure 8).

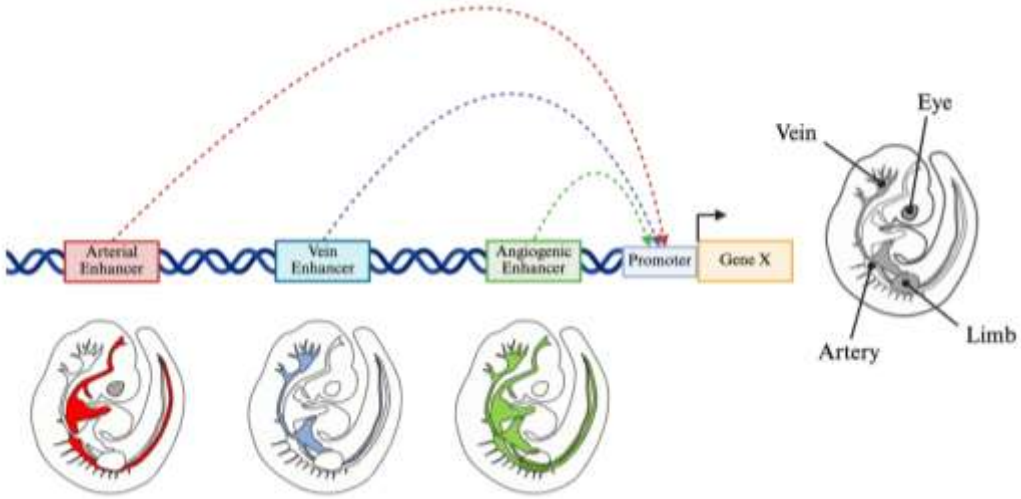

Figure 8: Multiple enhancers can regulate a single gene. Mammalian gene expression is primarily regulated by enhancers, with multiple enhancers able to regulate a single gene. Therefore, the spatiotemporal specificity of gene expression is dependent on TFs assembling at the relevant enhancer. Figure adapted from McCracken *et al* (2023), which itself is adapted from Oudelaar and Higgs (2021) and Shlyueva, Stampfel and Stark (2014).

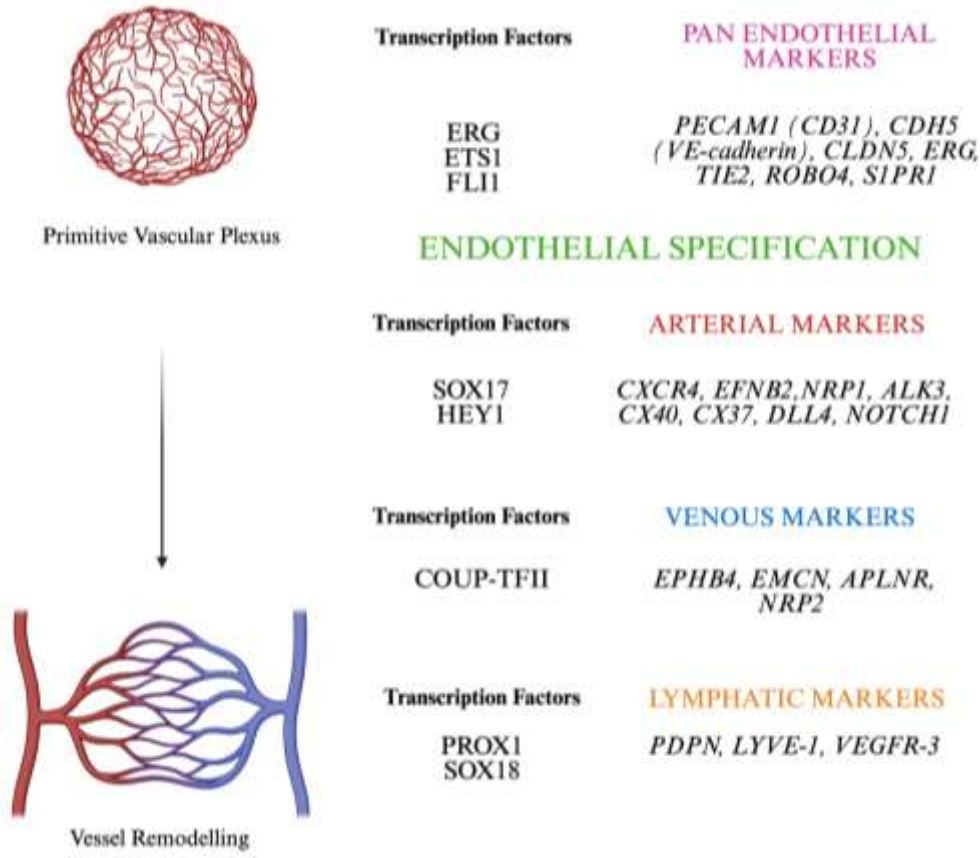

Figure 9: Important TFs involved in vascular development at different stages, including arteriovenous specification. Figure has been adapted from Dejana (2010), but with updated information from Payne et al (2023) and McCracken et al (2023)

1.3.1 ETS Transcription Factors

ETS (E26 transformation-specific) TFs are considered one of the most important TF families underpinning vascular development (Table 4).[135,170-173] For example, morpholino-mediated knock-down of four *Ets* genes in developing zebrafish embryos results in almost complete loss of endothelial differentiation.[174] There are at least 19 known ETS factors expressed in human ECs, all with a highly conserved 85 amino acid ETS DNA-binding domain.[136,175] This domain comprises a winged helix-turn-helix motif which mediates binding to a consensus DNA sequence GGA(A/T).[176,177] To date, every EC-specific promoter or enhancer region identified has an essential ETS binding motif.[136,172] However, the functional significance of individual ETS factors has proved hard to untangle: multiple ETS factors are expressed in ECs, their binding domains are highly conserved, and there is a high degree of redundancy between many of the factors.[135] Whilst most ETS proteins activate gene transcription, a few transcriptional repressors have been identified, and some have been found to display both activating and repressing functions.[177]

ETV2, expressed in EC progenitors from E6.5, has emerged as having notable importance in early vascular development and is widely regarded as a master regulator of endothelial lineage commitment during vasculogenesis.[171,178,179] Indeed, some in the field claim that it should be considered a 'pioneer factor' due to its ability to bind nucleosomal DNA and initiate chromatin remodelling at otherwise inaccessible genomic regions. In engineered embryonic stem differentiation and reprogramming models, Gong *et al* (2022) demonstrated that ETV2 recruits the ATP-dependent remodeller BRG1 to closed chromatin, thereby promoting chromatin opening.[180] This process increases the enrichment of active histone marks, including H3K27ac, at endothelial gene loci. Together, these effects establish a permissive epigenetic landscape that activates endothelial gene programmes and supports lineage reprogramming.

Whilst overexpression of *Etv2* triggers upregulation of vascular markers and an absence of haematopoietic cell differentiation, its knockdown instead leads to embryonic lethality between E9 and E10 coupled with a complete loss of EC lineage.[135,181] ETV2 can also act redundantly with Friend leukaemia integration 1b (Fli-1b) during early embryonic angiogenesis; zebrafish embryos lacking both *Etv2* and *fli1b* fail to form angiogenic sprouts.[178] Both TFs target many similar transcriptional targets during developmental

angiogenesis, such as VEGFR and TIE2. For example, ETV2 is known to bind to an enhancer sequence within the region of the 10th intron of the *Flk1* gene which encodes for VEGF2.[182]

Although ETS factors are required for EC identity, they are not sufficient to direct specific EC-subtype gene expression patterns.[183] Therefore, they must work in combination with other TFs in complex regulatory networks.

Table 4: Consensus binding motifs for ETS TFs: ETV2, FLI1, ERG, ETS1 and ELK3. Figure replicated from Payne *et al* (2023)

TF	Sequence logo	Data Type (Species/cell type)
ETV2		HT-Selex (Human Transfected LoVo/Hek293)
FLI1		ChIP-seq (Human)
ERG		ChIP-seq (Human)
ETS1		ChIP-seq (Mouse)
ELK3		HT-Selex (Human Transfected LoVo/Hek293)

1.3.2 FOX Transcription Factors

Another important TF family for directing vascular development is the Forkhead box (FOX) family (Table 5).[24,62] In humans and mice, 44 FOX proteins have been identified, which can be further classified into 22 subfamilies (FOXA–FOXS).[24,184] Of these, the FOXC and FOXO subfamilies have been associated with vasculogenesis and angiogenesis.[62]

In humans, the FOXO subfamily consists of four members: FOXO1, FOXO3, FOXO4, and FOXO6.[24] FOXO1 is most strongly expressed in ECs, where it is first detected from E7.75.[24] It has a role in vascular development during embryogenesis and postnatally.[185-187] For example, constitutive *Foxo1* deletion in murine embryos results in severe vascular defects and lethality at E11.[186] Likewise, in the postnatal retina, induced EC deletion of *Foxo1* yielded fewer angiogenic sprouts and a denser, more hyperplastic vasculature.[185]

The other important subfamily is FOXC, comprised of FOXC1 and FOXC2.[24] First detected from E8, they have a very similar binding specificity and expression patterns, suggesting a degree of redundancy between the two.[188] Indeed, both *Foxc1* and *Foxc2* null mutants die early and have similar cardiovascular defects, whilst compound homozygous embryos exhibit a far more severe phenotype.[189,190] FOXC factors have also been implicated in the acquisition of arterial identity; compound global deletion of the *Foxc1* and *Foxc2* causes severe arterial and venous malformations and significantly reduced arterial gene expression.[191] Moreover, EC enhancer analysis has proffered a role for the combinatorial binding of FOXC and ETS factors at compound FOX:ETS motifs.[23]

Table 5: Consensus binding motifs for FOX TFs: FOXC1, FOXC2 and FOXO1.
Figure replicated from Payne et al (2023)

TF	Sequence logo	Data Type (Species/cell type)
FOXC1		HT-Selex (Human Transfected LoVo/Hek293)
FOXC2		HT-Selex (Human Transfected LoVo/Hek293)
FOXO1		ChIP-seq (Mouse)

1.3.3 SOX Transcription Factors

The SOX (SRY-related HMG-box) TF family consists of 20 members classified into subgroups (SOX A– H).[62] For vascular development, the most notable subgroup is SOXF, comprising SOX7, SOX17, and SOX18 (Table 6).[24,62] These are all expressed in the EC

progenitors from E7.75 and are considered key regulators of EC specification: SOX17 is essential for arterial differentiation; SOX7 functions alongside SOX17 to promote EC proliferation and angiogenesis; and SOX18 is particularly important in lymphatic vessel development.[24,57,192,193]

Severe vascular defects are observed with EC-specific deletion of any SOXF factor. *Sox7* EC-specific deletion was shown to result in embryos with significant growth retardation and a disorganised vascular network, whilst *Sox17* deletion caused a comparable reduction in angiogenic sprouting.[194,195] More recently, SOX17 has been linked to arterial differentiation through the regulation of the Notch pathway.[192,196] Analysis of two arterial EC-specific enhancers for *Dll4* (the Notch ligand) also revealed a requirement for direct SOX17 binding.[197] A key role in arterial development has been further supported by mutant SOX17 embryos, which lack proper arterial differentiation alongside an increase in venous markers.[192]

Table 6: Consensus binding motifs for SOXF TFs: SOX7, SOX17 and SOX18.
Figure replicated from Payne et al (2023)

TF	Sequence logo	Data Type (Species/cell type)
SOX7		ChIP-seq (Mouse)
SOX17		ChIP-seq (Mouse)
SOX18		ChIP-seq (Human)

1.3.4 TCF/LEF Transcription Factors

The TCF/LEF (T-cell factor/lymphoid enhancer-binding factor) family of transcription factors act as nuclear effectors of the canonical Wnt signalling pathway (Figure 10).[18,62,198,199] The naming of the TCF and LEF proteins is somewhat confusing. In vertebrate there are four TCF/LEF proteins present: TCF7 (also called TCF1), TCF7L1 (TCF3), TCFL2 (TCF4) and LEF1 (TCF1α) (Table 7).[200]

Wnt signalling is an evolutionarily conserved signal transduction cascade that regulates cell proliferation, differentiation, and fate determination.[201] Canonical Wnt signalling exerts its signalling via the intracellular protein β-Catenin, which is encoded by the *Ctnnb1* gene. Wnt signalling is highly complex: there are 19 different Wnt ligands that can potentially bind and signal via 10 members of the Frizzled (FZD) family.[198] It should be noted that β-Catenin also binds to cadherins (VE- and N-cadherin in ECs) at cell-cell adherens junctions, stabilising their interaction with the cytoskeleton.[202] In the absence of a Wnt ligand, β-Catenin is bound by the β-Catenin destruction complex which comprises Axin, adenomatous polyposis coli (APC), and glycogen synthase kinase 3β (GSK-3β). This promotes the continuous phosphorylation of β-Catenin, leading to its subsequent degradation by the ubiquitin-proteasome system.[199,203] In the presence of a Wnt ligand, the Wnt ligand binds to a cell surface receptor complex consisting of FZD and low-density lipoprotein receptor related protein 5 or 6 (LRP5/6). This binding activates Dishevelled (DVL) proteins which then inhibits the β-Catenin destruction complex. This allows cytoplasmic β-Catenin to stabilise, accumulate, and translocate to the nucleus where associates with transcriptional effectors – such as TCF and LEF family member – to stimulate the transcription of WNT-responsive genes.[203]

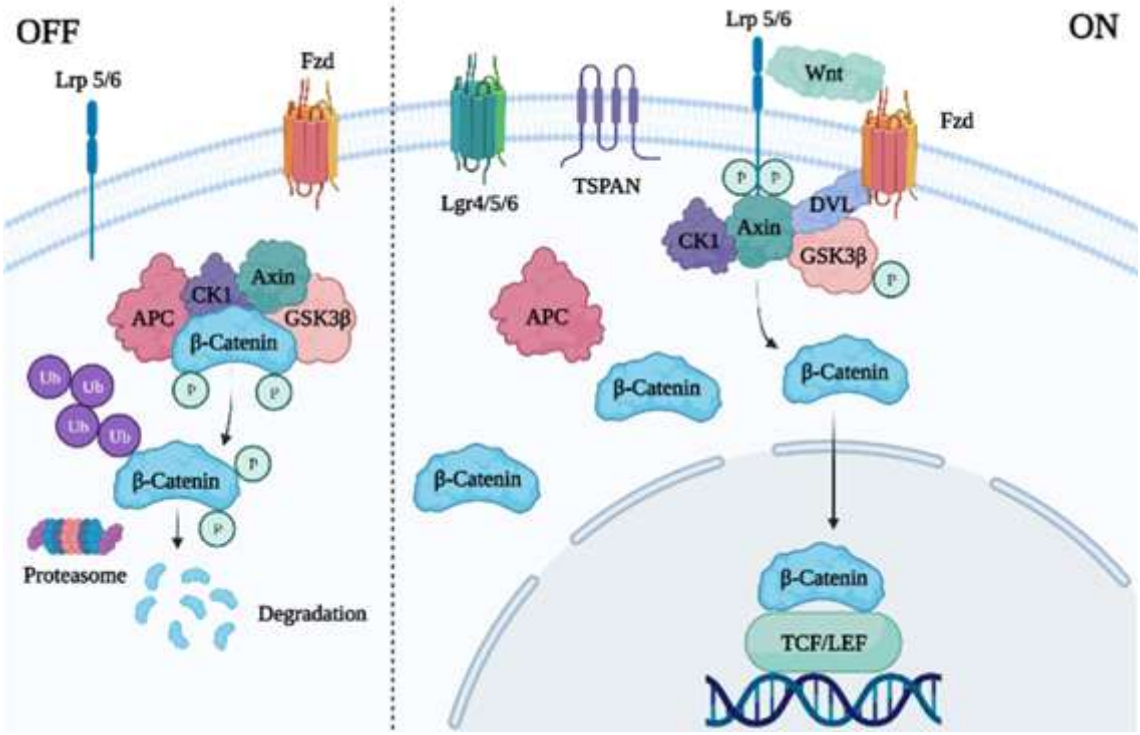

Figure 10: Schematic of the canonical Wnt signalling pathway. Figure is replicated from Schunk *et al* (2021).

It is already clear that canonical Wnt signalling is important during embryogenesis. This has been well-established across a wide-range of model organisms.[73,199,204-212] For example, global murine *Ctnnb1* knockout models embryonically lethal between E6.5 and E7.5.[213-219] Whilst different floxed *Ctnnb1* alleles can be used to generate *Ctnnb1* knockout models, the most common allele is the Ctnnb^{tm2Kem} allele.[220] This allele has one *loxP* site in intron 1, and one *loxP* in intron 6 of the *Ctnnb1* gene. Upon recombination, this effectively deletes exons 2 to 6. Since exon 2 contains the start codon, and exons 3 to 6 encode part of the Armadillo repeat domain, this recombination produces a robust loss-of-function phenotype.[221]

In the context of the vasculature, canonical Wnt signalling has been implicated in both physiological and pathological vascular morphogenesis.[198,199,222] One of the earliest indications linking Wnt signalling and vascular development came from *in vitro* studies of cultured ECs, demonstrating that ECs express multiple Wnt pathway components.[199,223] Thereafter, *in vivo* murine studies have confirmed a critical role for canonical Wnt signalling in vascular development.[73,199,204-212]

Whilst EC-specific deletion of *Ctnnb1* in mice has generally been concluded not to affect vasculogenesis, debate remains about angiogenesis and later vascular development.[31] In particular, CNS vasculature has emerged as vulnerable to perturbation in EC canonical Wnt signalling. Following EC-specific *Ctnnb1* ablation, Daneman *et al* (2009) reported defects in vessel number and the formation of haemorrhagic vascular malformations, Corada *et al* (2010) observed severe hypovascularisation and bleeding within the spinal cord of E11.5 embryos, and Stenman *et al* (2008) found CNS-specific defects such as haemorrhage and disorganisation of the neural tissue.[18,211,212] Intriguingly, Daneman *et al* did not report any vascular defects in non-CNS tissue, with Wythe *et al* (2013) also noting morphologically normal vasculature.[73,211] In contrast, Cattelino *et al* (2003) reported that EC-specific *Ctnnb1* ablation caused significant defects in all vessel lumen morphology and vascular patterning, diffuse haemorrhages in different regions of the vascular tree, and early lethality at E11.5-13.5.[209] Whilst there could be many explanations for this discrepancy, one important difference in the experimental setup is the choice of EC-*Cre* driver. Indeed, rather than using a *Tek-Cre* driver, as is more common, some studies used a *Flk1-Cre* driver.[212] This is an atypical selection, especially as *Flk1-Cre* expression is

far more pronounced in the CNS region before E11.5. This could have resulted in the more severe CNS vascular phenotypes.

As well as loss-of-function studies, *Ctnnb1* overexpression has also been investigated.[210] To achieve this, the Ctnnb1^{tm1Mmt} allele was designed to specifically excise exon 3 upon recombination, thereby removing the phosphorylation sites.[224] Since the β-catenin protein produced can no longer be degraded, Wnt responsive genes are continuously activated, independent of upstream Wnt ligand stimulation. Using this model, Corada *et al* (2010) reported embryonic lethality by E12.5, with major perturbations to vascular development and defects in arterial-venous specification.[210] In particular, it was noted that overexpression of β-Catenin induced an upregulation of *Dll4* expression in normally venous compartments.[210] However, when ablating *Ctnnb1* specifically in the endothelium, Wythe *et al* reported no changes in expression of *Dll4* mRNA at E9.5, with no arteriovenous malformations.[73]

These contradictory results have led to some debate in the field: is canonical Wnt signalling only important in CNS angiogenesis, or does it also play an important role in arterial-venous patterning? Some of the inconsistencies in the literature likely reflect the well-documented differences observed between mouse background, the different EC-*Cre* drivers used, and the potential leakiness of Cre expression.[219] Adding complexity to the analysis is the fact that there are at least three different *Tek-Cre* mouse models in circulation, all with differing levels of expression in ECs, and until recently, the inclusion of a *Cre*-reporter allele has not been common.[19] In addition, many of these studies strongly rely on Wnt 'reporters' as a proxy for Wnt signaling activity.[25,26,29,35] This is a flawed approach since these are merely multimerized TCF sites lacking any co-factors relevant for required for EC activity.

Table 7: Consensus binding motifs for TCF/LEF TFs: TCF4 and LEF1.

TF	Sequence logo	Data Type (Species/cell type)
TCF4		ChIP-seq (Human)
LEF1		HT-Selex (Human Transfected LoVo/Hek293)

Thesis Aims

The overarching hypothesis is that through understanding the transcriptional regulation of endothelial-specific enhancers, important upstream and downstream signalling pathways in vascular development can be elucidated.

This thesis contains two sequential investigations. First, I examined upstream regulators of a novel angiogenic enhancer, identifying a potential role for TCF/LEF TFs in the regulation of angiogenic gene expression. Second, I determined the endothelial developmental consequences of disrupted canonical Wnt signalling.

The primary aims of this thesis were:

1. To identify functional TF binding motifs in the SOX7-58 enhancer sequence
2. To investigate the vascular consequences of perturbing canonical Wnt signalling in ECs
3. To assess changes in different EC subpopulations in the absence of canonical Wnt signalling

These are achieved in the following ways:

1. Phylogenetic foot-printing of the SOX7-58 and mutagenic analysis in F0 transgenic zebrafish embryos (**Chapter 3**). This is used to identify functional TF binding sites which drive the precise spatiotemporal enhancer activity pattern of SOX7-58.
2. Generation of Cre models for *Ctnnb1* EC ablation and assessments of embryonic lethality, crown-to-rump length, and vascular density and localisation (**Chapter 4**).
3. Assessment of the activity of EC subtype-specific enhancer:*LacZ* transgenes after different types of *Ctnnb1* EC ablation (**Chapter 4**). This enables different stages in vascular development to be probed, including arteriovenous specification, and sprouting angiogenesis.

Chapter 2: Materials and Methods

2.1 Animal husbandry

All animal experiments were compliant with the United Kingdom Animal (Scientific Procedures) Act 1986, approved by the Clinical Medicine Local Ethical Review Committee, University Oxford, and licensed by United Kingdom Home Office.

Both zebrafish and mice were maintained within appropriate facilities at the University of Oxford. Adult zebrafish were maintained at 28.5°C in system water.

2.2 Transgenic zebrafish

2.2.1 Cloning of enhancer constructs

Putative enhancer sequences were generated as custom-made double-stranded linear DNA fragments (GeneArt®Strings™, Life Technologies). Prior to cloning, 3' adenosine overhangs were added via an A-tailing reaction (Table 8), and incubated at 72°C for 20 minutes. A-tailed products were stored at 4°C and used the same day.

Table 8: Protocol for A-tailing reaction of double-stranded linear DNA fragment

Reagent	Volume (µL)
Enhancer DNA	16.2
10 X PCR buffer	2
50 mM $MgCl_2$	0.7
dNTP mix	0.6
Taq DNA polymerase	0.5

Upon addition of an A-tail, the putative enhancer fragments were cloned into a pCR8/GW/TOPO entry vector using the TOPO™ TA Cloning™ Kit (Invitrogen™, Thermo Fisher Scientific). The ligation reaction contained 4.5 µL of A-tailed DNA, 1 µL of salt solution, and 1 µL of the pCR8 vector (Table 9). This reaction was gently mixed, centrifuged, and incubated at room temperature (RT) for 30 minutes.

Table 9: Protocol for ligation reaction

Reagent	Volume (µL)
A-tailed enhancer DNA	4.5
Salt solution	1
PCR8 vector	1

2 µL of the ligation reaction was added to chemically competent *E. coli*. After a 10 minute incubation on ice, the cells were heat shocked for 2 minutes at 37°C. The cells were then returned to ice for 1 – 2 minutes on ice, and then placed in 250 µL Luria-Bertani (LB) broth at 37°C for 25 - 45 minutes. Following recovery, 20 µL of 50 mg/mL spectinomycin was added, and the cells were plated on LB agar. Plates were incubated overnight at 37°C. For each plate, six colonies were picked into 3 mL LB broth with spectinomycin (final concentration: 0.1 mg/mL). These were grown overnight at 37°C in a shaking incubator.

Plasmids were extracted using a standard alkaline lysis miniprep protocol (Qiagen). Briefly, 1.5 mL of culture was pelleted and resuspended in 100 µL P1 buffer, lysed with 100 µL P2 buffer, and neutralised with 100 µL P3 buffer. After centrifugation at 16,000 rpm for 10 minutes, the supernatant was precipitated with 600 µL ice-cold ethanol, centrifuged at 16,000 rpm for another 10 minutes, aspirated dry, and then resuspended in 20 µL sterile water.

To verify insert presence and orientation, miniprepped plasmids were subjected to restriction digest. Digestion reactions contained 2 µL of plasmid DNA, 15 µL of sterile water, 2 µL of CutSmart buffer, and 1 µL of restriction enzyme (Table 10). Reactions were incubated at 37°C for up to 1 hour, and digestion products were analysed on a 1% agarose gel (25 minutes at 180 volts).

Table 10: Protocol for restriction enzyme reaction

Reagent	Volume (µL)
Sterile water	15
CutSmart Buffer	2
Plasmid DNA	2
Restriction Enzyme	1

Successfully digested constructs were purified using column purification. 250 µL binding buffer was added to each 50 µL digest, and then the reaction mixture was transferred to a spin column and centrifuged at 11,000 rpm for 30 seconds. The column was washed with 750 µL wash buffer, centrifuged for 1 minute, then spun dry for 2 minutes. The DNA was then eluted in 30 µL sterile water, incubated on the column for 1 - 4 minutes, and centrifuged for 1 minute. A NanoDrop spectrophotometer (ThermoFisher) was used to quantify the final DNA concentration.

Samples were submitted for Sanger sequencing (Eurofins Genomics). Sequencing reactions contained 15 - 20 µL of plasmid DNA at 50 -100 ng/µL. The T7 primer, provided by the sequencing company, was used for reads.

If the sample contained the correct sequence, the enhancer insert was then transferred into the destination vector, pE1b:GFP. LR recombination was performed using Gateway^{TM} LR Clonase^{TM} II Enzyme mix (ThermoFisher). The reaction contained 1 µL of entry vector (37.5 ng/µL), 1 µL of destination vector (37.5 ng/µL), and 0.5 µL of LR recombinase (Table 11). The reaction was incubated at room temperature (RT) for an hour, followed by the addition of 0.25 µL Proteinase K and incubation at 37°C for 15 minutes. The resulting product was transformed into competent *E. coli* as described above and selected on LB agar plates containing ampicillin. Colonies were grown, miniprepped, and validated via digestion and sequencing as before.

Table 11: Protocol for the LR reaction

Reagent	Volume (µL)
37.5ng/µl entry vector (insert-containing PCR8)	1
37.5ng/µl destination vector (pE1B:GFP)	1
LR recombinase	0.5

2.2.2 Tol2-mediated transgenesis

F0 mosaic transgenic zebrafish embryos were generated via Tol2-mediated integration. Breeding pairs were set up overnight in tanks, with wildtype male and female fish separated by plastic dividers. The following morning the dividers were released to allow the production of fertilised oocytes. Whilst still at the 1-cell stage, the oocytes were injected with 0.5 nl of 50ng/µL Tol2 transposase and 60 ng/µL pE1b-enhancer-GFP

expression vector using the FemtoJet® microinjector (Eppendorf). This was performed by Dr Svanhild Nornes. Embryos were maintained in E3 medium (5 mM NaCl; 0.17 mM KCl; 0.33 mM $CaCl_2$; 0.33 mM $MgSO_4$ and 0.00001% Methylene Blue) at 28.5°C.

2.2.3 Expression screens and quantification

At pre-determined timepoints – ranging between 24 hours and 72 hours – embryos were dechorionated with forceps, and anaesthetised with 0.01% tricaine methanesulfonate (A5040, Merck). Using the MVX10 microscope (Olympus Corporation), the expression of the fluorescent reporter protein was scored either by location (intersegmental vessel, artery or vein) or in a binary manner (EC expression vs no EC expression). For each putative enhancer sequence, or mutated enhancer sequence, the percentage of injected fish showing reporter gene expression in ECs was recorded.

Representative fish were then selected for further imaging on the Zeiss LSM 710 confocal microscope.

2.2.4 Image acquisition

In a flat-bottom 96-well plate, representative fish embryos were embedded in 0.1% TopVision low melting agarose (R0801, Thermo) in E3 medium with tricaine methanesulfonate. GFP reporter gene expression was detected using a Zeiss LSM 710 confocal microscope. To image the entire fish, the tile scan command was combined with Z-stack collection at 488 nm excitation and 509 nm emission.

2.2.5 Sequences of enhancers tested in transgenic zebrafish

2.2.5.1 ClustalW and sequence motif analysis

Human, mouse and opossum sequences of angiogenic enhancers (SOX7-58, DLL4in3, HLX-3 and ETS1+195) were aligned using ClustalW. For hand annotation, putative TF binding motifs were assessed via a resource generated from JASPAR (https://jaspar.elixir.no). Otherwise, putative TF binding motifs were assessed via TRANSFAC™, or FIMO (MEME SUTIE) (https://meme-suite.org/meme/doc/fimo.html) using the JASPAR2024_vertebrate_non-redundant_pfms dataset.

2.2.5.2 SOX7-58 enhancer sequences

Human sequence:

AATCATCGTGGACTCTTGCAGAAAAACAAGGCTGAGAGGAAGCCAACCAA
GGCAGAAAGGTGACCCCATCTGTGCGCTGACTCAGACAGCAAAGCGGTGGG
TTTCCCTTATGAGATCATGGATTGGCCGCCAGAGACCGCTACTAATGTTAGA
ACAGGGTTTTTCCCTGAAAGAGTCACAATTCCTCTCCCTGGCAAAACAGGA
ACTGGTCCTAACAGGAATATTATGTAATACCAGAACTGAGGAGCTCAGGAA
AAGCAGGATGAGGGTGGGGGTGGGGATTGAAGAGCAGAGCCCTTTGTGGG
AGCGTGAAAGGGACAAGCCCAGTACCGGCTTCCTGCCAGCCTCCCCTTCCCT
CCTGCTGCAGCGCCTTCCCTCACGGGATGAGCAGGCATCTCATAGGCAGAC
AGAACATGGAGCAGGAATAAAAGACTCCCA

Mouse sequence:

GAGGAGTACAGACTAGTACATACACAGAAGAAAGAAGGCCTCTGGAGCCA
CCGGCACAAGTGGCCCCATCTGTGCGCTGACTCAGACAGGAACAGCAAGGC
CGGTGGAGGACGACATTTCCGTTATGAGATCATGCGCTGGCCACTGTAGCTT
CAACTGAAGCCAGCCCAGGGGTTTTCCCTGAAAGAGTCACAATTCCTCTCCC
CAGCAAAACAGGAACTGATCCTAACAGGAATATTATGTAATGCCAGGGAAC
CAGGAGAGTGGGAAAAGCAGGGTTGGGGGAGAAGCACCACAGGATGAAGG
CAGAGATGGGGTAGAAAAGCAGAGCCACTCTGAGCAGCTTTTGGACATGGG
ACAGGCCCAGTAGCCACTCAGCCCCTTCCAGCTCCCTGGAGTTACTTTCCAG
GGGTAACCAGGTATCCTTCAGGCAGGCATCACCTCCCCATCTGAGAGAGGA
ACTGCAAGGACCTGAATACAGAGAAGAAAGCTGACA

Opossum sequence:

GGAAAAATTGTACTAAAAATAGCAAACAATGTATATATATGAGAAGAAAA
AAAGGCTGAAGAGAATCTGATTAAGGCCGAGTCAAATAGGAAAAGAAAAG
TTTGTAAAGTGCTGTATTTCCCATATGAGGTAATGTACTGAACCCACTACCA
CTACTAATGTTAGAACAGGGTTTTTCCCTGAAAGAGTCATAATTCCTTTCTC
CGGCAAAACAGGAACTGATCATAACAGGAATATTATGTAATTGCAGGGAAC

AGAGAAGACTGGGGAAATTAAGATAGGAGGCAAGAGTGACAGGATAAAGG
TGGAGGCAGGGAATGGAAAAGCAGTCAGGGACCATTAAGAGAGTCAACAA
AGGACAAATTCCTTCTTGTTTCACTGTCTCAATGGTCCATTCTTTCTCCCCAC
CCTCCTTTTTTTTTTTTAAACTCTCTTGAGTTATGGATTGGGGCACTGGGTCT
AGACTTTAATAACAGAAAGATTTCTGGAA

2.2.5.3 Mutated SOX7-58 Sequences

mutFOS:JUN *SOX7-58:*

GGTGGAGGGTGCAGTGAGCCAAGATCGTGCCACTGCACTCTACCTTGGAAG
ACAGAGCAAGACACTGTCTCAAAAAAAAAACAGGAAAAAAAAGTGAATGT
ATATCTATTGGTATAATATCATTAGAGTTCTTCCTGGAGTACAGTAAGTAAC
CTAAGGCATCTGTGTCTAAGTGAAAGTGGTCACAGAAAGTGGCCTACCTGA
AGCCTGGCAGTTCCATTATCCTAGGAGAAATCATCGTGGACTCTTGCAGAA
AAACAAGGCTGAGAGGAAGCCAACCAAGGCAGAAAGGTGACCCCATCTGT
GCGCTGACTCAGACAGCAAAGCGGTGGGTTTCCCTTATGAGATCATGGATT
GGCCGCCAGAGACCGCTACTAATGTTAGAACAGGGTTTTTCCCTGAA**cccaa**C
ACAATTCCTCTCCCTGGCAAAACAGGAACTGGTCCTAACAGGAATATTATGT
AATACCAGAACTGAGGAGCTCAGGAAAAGCAGGATGAGGGTGGGGGTGGG
GATTGAAGAGCAGAGCCCTTTGTGGGAGCGTGAAAGGGACAAGCCCAGTAC
CGGCTTCCTGCCAGCCTCCCCTTCCCTCCTGCTGCAGCGCCTTCCCTCACGG
GATGAGCAGGCATCTCATAGGCAGACAGAACATGGAGCAGGAATAAAAGA
CTCCCACCTTCTCCAAGGCTGACGGTAACTGACCATGTAACTACAGTGTAAC
TGAGGGGACCCTGCATAGACAGAAGATGGGCCAGCGAGATGAGGAGCCAT
GCTGGACGAGCATCCTTTTTTTCCAGATGTATAAGGTATAAGTGACAGAGG
AAGACTCTATGTTTAAGGTGTGCCATGTGATGTTTTGACCTACATATACATA
GCAAAATGATCCCCACAGTCAAGCTAATTAA

mutC/EBP *SOX7-58:*

GGTGGAGGGTGCAGTGAGCCAAGATCGTGCCACTGCACTCTACCTTGGAAG
ACAGAGCAAGACACTGTCTCAAAAAAAAAACAGGAAAAAAAAGTGAATGT
ATATCTATTGGTATAATATCATTAGAGTTCTTCCTGGAGTACAGTAAGTAAC

CTAAGGCATCTGTGTCTAAGTGAAAGTGGTCACAGAAAGTGGCCTACCTGA
AGCCTGGCAGTTCCATTATCCTAGGAGAAATCATCGTGGACTCTTGCAGAA
AAACAAGGCTGAGAGGAAGCCAACCAAGGCAGAAAGGTGACCCCATCTGT
GCGCTGACTCAGACAGCAAAGCGGTGGGTTTCCCTTATGAGATCATGGATT
GGCCGCCAGAGACCGCTACTAATGTTAGAACAGGGTTTTTCCCTGAAAGAG
TCACAATTCCTCTCCCTGGCAAAACAGGAACTGGTCCTAACAGGAATATTA**g**
G**gc**ATACCAGAACTGAGGAGCTCAGGAAAAGCAGGATGAGGGTGGGGGTGG
GGATTGAAGAGCAGAGCCCTTTGTGGGAGCGTGAAAGGGACAAGCCCAGT
ACCGGCTTCCTGCCAGCCTCCCCTTCCCTCCTGCTGCAGCGCCTTCCCTCACG
GGATGAGCAGGCATCTCATAGGCAGACAGAACATGGAGCAGGAATAAAAG
ACTCCCACCTTCTCCAAGGCTGACGGTAACTGACCATGTAACTACAGTGTAA
CTGAGGGGACCCTGCATAGACAGAAGATGGGCCAGCGAGATGAGGAGCCA
TGCTGGACGAGCATCCTTTTTTTCCAGATGTAATAAGGTATAAGTGACAGAG
GAAGACTCTATGTTTAAGGTGTGCCATGTGATGTTTTGACCTACATATACAT
AGCAAAATGATCCCCACAGTCAAGCTAATTAA

mutTCF/LEF *SOX7-58:*

GGTGGAGGGTGCAGTGAGCCAAGATCGTGCCACTGCACTCTACCTTGGAAG
ACAGAGCAAGACACTGTCTCAAAAAAAAAACAGGAAAAAAAAGTGAATGT
ATATCTATTGGTATAATATCATTAGAGTTCTTCCTGGAGTACAGTAAGTAAC
CTAAGGCATCTGTGTCTAAGTGAAAGTGGTCACAGAAAGTGGCCTACCTGA
AGCCTGGCAGTTCCATTATCCTAGGAGAAATCATCGTGGACTCTTGCAGAA
AAACAAGGCTGAGAGGAAGCCAACCAAGGCAGAAAGGTGACCCCATCTGT
GCGCTGACTCAGACAGCAAAGCGGTGGGTTTCCCTTATGAGATCATGGATT
GGCCGCCAGAGACCGCTACTAATGTTAGAACAGGGTTTTTCCCTGA**tc**GGAG
TCACAATTCCTCTCCCTGGCAAAACAGGAACTGGTCCTAACAGGAATATTA**g**
G**gc**ATACCAGAACTGAGGAGCTCAGGAAAAGCAGGATGAGGGTGGGGGTGG
GGATTGAAGAGCAGAGCCCTTTGTGGGAGCGTGAAAGGGACAAGCCCAGT
ACCGGCTTCCTGCCAGCCTCCCCTTCCCTCCTGCTGCAGCGCCTTCCCTCACG
GGATGAGCAGGCATCTCATAGGCAGACAGAACATGGAGCAGGAATAAAAG
ACTCCCACCTTCTCCAAGGCTGACGGTAACTGACCATGTAACTACAGTGTAA
CTGAGGGGACCCTGCATAGACAGAAGATGGGCCAGCGAGATGAGGAGCCA
TGCTGGACGAGCATCCTTTTTTTCCAGATGTAATAAGGTATAAGTGACAGAG

GAAGACTCTATGTTTAAGGTGTGCCATGTGATGTTTTGACCTACATATACAT
AGCAAAATGATCCCCACAGTCAAGCTAATTAA

mutFOX:ETS *SOX7-58:*

GGTGGAGGGTGCAGTGAGCCAAGATCGTGCCACTGCACTCTACCTTGGAAG
ACAGAGCAAGACACTGTCTCAAAAAAAAAACAGGAAAAAAAAGTGAATGT
ATATCTATTGGTATAATATCATTAGAGTTCTTCCTGGAGTACAGTAAGTAAC
CTAAGGCATCTGTGTCTAAGTGAAAGTGGTCACAGAAAGTGGCCTACCTGA
AGCCTGGCAGTTCCATTATCCTAGGAGAAATCATCGTGGACTCTTGCAGAA
AAACAAGGCTGAGAGGAAGCCAACCAAGGCAGAAAGGTGACCCCATCTGT
GCGCTGACTCAGACAGCAAAGCGGTGGGTTTCCCTTATGAGATCATGGATT
GGCCGCCAGAGACCGCTACTAATGTTAGAACAGGGTTTTTCCCTGAAAGAG
TCACAATTCCTCTCCCTGGCAAA**t**C**ta**GAACTGGTCCTA**t**C**ta**GAATATTATGTA
ATACCAGAACTGAGGAGCTCAGGAAAAGCAGGATGAGGGTGGGGGTGGGG
ATTGAAGAGCAGAGCCCTTTGTGGGAGCGTGAAAGGGACAAGCCCAGTACC
GGCTTCCTGCCAGCCTCCCCTTCCCTCCTGCTGCAGCGCCTTCCCTCACGGG
ATGAGCAGGCATCTCATAGGCAGACAGAACATGGAGCAGGAATAAAAGAC
TCCCACCTTCTCCAAGGCTGACGGTAACTGACCATGTAACTACAGTGTAACT
GAGGGGACCCTGCATAGACAGAAGATGGGCCAGCGAGATGAGGAGCCATG
CTGGACGAGCATCCTTTTTTTCCAGATGTAATAAGGTATAAGTGACAGAGG
AAGACTCTATGTTTAAGGTGTGCCATGTGATGTTTTGACCTACATATACATA
GCAAAATGATCCCCACAGTCAAGCTAATTAA

mut[FOX, FOS:JUN, C/EBP, TCF/LEF] *SOX7-58:*

GGTGGAGGGTGCAGTGAGCCAAGATCGTGCCACTGCACTCTACCTTGGAAG
ACAGAGCAAGACACTGTCTCAAAAAAAAAACAGGAAAAAAAAGTGAATGT
ATATCTATTGGTATAATATCATTAGAGTTCTTCCTGGAGTACAGTAAGTAAC
CTAAGGCATCTGTGTCTAAGTGAAAGTGGTCACAGAAAGTGGCCTACCTGA
AGCCTGGCAGTTCCATTATCCTAGGAGAAATCATCGTGGACTCTTGCAGAA
AAACAAGGCTGAGAGGAAGCCAACCAAGGCAGAAAGGTGACCCCATCTGT
GCGCTGACTCAGACAGCAAAGCGGTGGG**c**TTCCCTTATGAGATCATGGATTG
GCCGCCAGAGACCGCTACTAATGTTAGAACAGGGTT**c**TTCCCTGA**tcccaa**CAC

AATTCCTCTCCCTGGCAAAACAGGAACTGGTCCTAACAGGAATATTA**g**G**g**cA
TACCAGAACTGAGGAGCTCAGGAAAAGCAGGATGAGGGTGGGGGTGGGGA
TTGAAGAGCAGAGCCCTTTGTGGGAGCGTGAAAGGGACAAGCCCAGTACCG
GCTTCCTGCCAGCCTCCCCTTCCCTCCTGCTGCAGCGCCTTCCCTCACGGGAT
GAGCAGGCATCTCATAGGCAGACAGAACATGGAGCAGGAATAAAAGACTC
CCACCTTCTCCAAGGCTGACGGTAACTGACCATGTAACTACAGTGTAACTGA
GGGGACCCTGCATAGACAGAAGATGGGCCAGCGAGATGAGGAGCCATGCT
GGACGAGCATCCTTTTTTTCCAGATGTAATAAGGTATAAGTGACAGAGGAA
GACTCTATGTTTAAGGTGTGCCATGTGATGTTTTGACCTACATATACATAGC
AAAATGATCCCCACAGTCAAGCTAATTAA

2.2.5.4 DLL4in3 sequence

AGAGTTTCCTGGCGAAGTCTCTGCAGAAAGAGGCTTTGGTCAGAGAACCTG
ATTCAGAAAGCCAACCTGATTCAGAGAGAGTTGACTGCTGCCAACTCTCTCT
TTAGTTGTGACTATGGTGGTCAGTTCACACTCTAATTATCTAGATTAACTCT
ACCTGCAAGTAAGCACAGGCCAGAGGGTCCCAGAATCTTGCTACTTAGTCT
CCCTGGGTGTGTGCATGTGCAGGGGGCTTGATAGCATTCAAAAAAGGGTAC
AATGGACGGATGTTAAGATATCCTAGGGTTGTGGAGGCAGATACGGAGGGG
AAAGAGGAAAAGAGGTCAAAATGGAAAAAAAGAAAAAATTTAAAGGGGG
AAGTTTTCTGGTTCGAGAACTGGGAGCAAGGGGTTCTGTTCTAGACGTAGGT
AATGGTTTTTCTTTTTCCTTTTCAAAGTGAGAATTGTTGTGCTGGTGAAATAT
CCTTTTCCTCTGTGTCAGAACAACATCCCAAAGCCATTATTCCCTTTCCAAA
GGAGCGGAATTCGCAAAAGGTGTAAAATACAGGAAGAGGCCCGTCAGCGG
CGCTGGCAGCCTCGGCCTTTCTCACCGCCGTGCTCCCCGCGTTCCCACGCCA
AAAATAACCCGCAGGAAACGCAATTGTGCTCTGAGTCCAGGCAGCGAGCGG
AATCCGAGCGTCCAGCGCGGGGCGCAGCTCCGGCCAAGCTAAGCGTCCTGG
CCCCCACCCCCCAAGCCTGCGTCCCCAACCCCCACCCCCGCCTATAACTGGT
TAACTCTTTCGGCGCTGTGTGATGTCGCCCCCCTGTGGCCGAGAAGTTAGAT
ACTCACCTGGCCGCAGGTCGTCTCCCGGTGTGTGCCAAGCTTGGATGTTGAG
TGAGAAGGTTCCCTGGGAAGCAAAAGGGGGGGTGGGGGACATTAGAGATA
GCGATATCAGCAG

2.2.5.5 Mutated DLL4in3 sequence

AGAGTTTCCTGGCGAAGTCTCTGCAGAAAGAGGCTTTGGTCAGAGAACCTG
ATTCAGAAAGCCAACCTGATTCAGAGAGAGTTGACTGCTGCCAACTCTCTCT
TTAGTTGTGACTATGGTGGTCAGTTCACACTCTAATTATCTAGATTAACTCT
ACCTGCAAGTAAGCACAGGCCAGAGGGTCCCAGAATCTTGCTACTTAGTCT
CCCTGGGTGTGTGCATGTGCAGGGGGCTTGATAGCATTCAAAAAAGGGTAC
AATGGACGGATGTTAAGATATCCTAGGGTTGTGGAGGCAGATACGGAGGGG
AAAGAGGAAAAGAGGTCAAAATGGAAAAAAAGAAAAAATTTAAAGGGGG
AAGTTTTCTGGTTCGAGAACTGGGAGCAAGGGGTTCTGTTCTAGACGTAGGT
AATGGTTTTTCTTTTTCCTTTTaAAAGTGAGAATTGTTGTGCTGGTGAAATAT
CCTTTTCCTCTGTGTCAGAACAACATCaaAAAGCCATTATTCCCTTTCaAAAG
GAGCGGAATTCGCAAAAGGTGTAAAATACAGGAAGAGGCCCGTCAGCGGC
GCTGGCAGCCTCGGCCTTTCTCACCGCCGTGCTCCCCGCGTTCCCACGCCAA
AAATAACCCGCAGGAAACGCAATTGTGCTCTGAGTCCAGGCAGCGAGCGGA
ATCCGAGCGTCCAGCGCGGGGCGCAGCTCCGGCCAAGCTAAGCGTCCTGGC
CCCCACCCCCCAAGCCTGCGTCCCCAACCCCCACCCCCGCCTATAACTGGTT
AACTCTTTCGGCGCTGTGTGATGTCGCCCCCCTGTGGCCGAGAAGTTAGATA
CTCACCTGGCCGCAGGTCGTCTCCCGGTGTGTGCCAAGCTTGGATGTTGAGT
GAGAAGGTTCCCTGGGAAGCAAAAGGGGGGGTGGGGGACATTAGAGATAG
CGATATCAGCAG

2.3 Stable transgenic mice

Stable transgenic mouse lines were originally generated on a C57BL/6J background via pro-nuclear injection into fertilised mouse oocytes. Enhancer:*LacZ* transgenic murine lines used in this doctoral project are: *Tg*(*CoupTFII-965:LacZ*), *Tg(Dll4-12:LacZ*), *Tg(DLL4in3:LacZ*), *Tg(NOTCH1+16:LacZ*), and *Tg(SOX7-58:LacZ*). *Tg(Tek-Cre)*1*2Flv* mice were originally purchased from JAX (stock number 004128), whilst *Tg*(*Etv2-Cre*)*1Blk* mice came from Materna *et al* (2020), and were kindly donated by Prof Catherine Porcher.[225] *Tg*(*Cdh5-CreERT2*^{1Rha}) mice were originally made by Dr Ralf Adams, whilst *Tg*(*iSuRe-Cre*) mice were originally made by Dr Rui Benedito. *Tg*(*Ctnnb1*^{tm2Kem}) mice were available in house.

2.3.1 Tamoxifen administration for embryonic and neonatal samples

To study the development of coronary vasculature, 100 µl of 10mg/ml tamoxifen was administrated to the pregnant mothers on two consecutive days, either at E9.5 and E10.5, or at E11.5 and E12.5. This administration was conducted via oral gavage. Embryos were then taken either at E12.5 – 13.5, or E14.5 – E16.5, respectively.

To study the development of the postnatal retinal vasculature, pups were orally fed either 2 µl of 25mg/ml tamoxifen on P1 and P2, or orally fed 2 µl of 2.5mg/ml tamoxifen on P1. To orally feed, tamoxifen in corn oil was placed on the tongues of pups.

2.3.2 Embryo collection

Matings were set up between male and female mice, with vaginal plugs used as an estimate for the onset of gestation. Coitus was assumed to occur at midnight the night before the plug was found. Following sacrifice of the mother, embryos were dissected from the uteri and dropped in ice-cold phosphate-buffered saline (PBS). Whole embryos were harvested between E9.5 and E13.5, and embryonic hearts from E12.5 to E16.5. In both instances, their yolk sacs were collected for genotype analysis. Throughout, dissection occurred in ice-cold PBS. Both sexes were used in embryonic experiments.

2.3.3 Pup collection for retina studies

The day on which pups were born was designated P0. At P5, pups were sacrificed, eyeballs were removed with fine forceps and fixed in 4% paraformaldehyde (PFA) for an hour at 4ºC. Post-fixation, the eyeballs were quickly rinsed in PBS twice, then left to further rinse in PBS for 30 minutes at 4ºC on a rocker. The retinas were then dissected out and processed intact (without making radial cuts) to preserve morphology until staining. Both sexes were used in neonatal experiments.

2.3.4 Genotyping

Tissue samples were collected as ear biopsies from adults, yolk sacs from embryos, and tail tips from neonates.

Tissue samples were incubated in 100 µL of 25 mM NaOH/0.2 Mm EDTA lysis buffer at 98ºC for 60 - 80 minutes, then neutralised with 100µL of 40 mM Tris-HCl (pH 5.5)

and vortexed. For each polymerase chain reaction (PCR), 0.2 µl of supernatant was added to GoTaq Green master mix (Promega, M7122), nuclease-free H_2O and the relevant PCR primers (Table 12 and Table 14). PCR products were separated using agarose gel electrophoresis, with 15 µl loaded onto a 1 - 2% agarose gel at 180V for 25 minutes.

Table 12: Protocol for PCR reaction

Reagent	Volume (µL)
GoTaq Green Mix	10
Nuclear-free H_2O	6
Primer (Forward)	1
Primer (Reverse)	1
DNA lysate	2
Total Volume	20

Table 13: Programmes for PCR reactions

Gene	ID (ºC/min)	No. of Cycles	D (ºC/sec)	A (ºC/sec)	E (ºC/sec)	FE (ºC/sec)
LacZ	95/3	30	95/30	63/30	72/30	72/5
Ctnnb1	94/3	30	94/30	60/30	72/30	72/5
Cre	94/3	30	94/30	62/30	72/30	72/5
Tek-Cre	94/3	30	94/40	56/30	72/40	72/5
Etv2-Cre	95/10	35	95/30	59/30	72/30	72/7
iSuRe-Cre	94/3	35	94/30	60/30	72/30	72/5
Cdh5CreERT	94/3	30	94/30	60/45	72/45	72/5

Table 14: Primers for PCR reactions

Primer Name	Sequence
LacZ_F	GTCGTTTTACAACGTCGTGAC
LacZ_R	GATGGGCGCATCGTAACCGTG
Ctnnb1_F	AAGGTAGAGTGATGAAAGTTGTT
Ctnnb1_R	CACCATGTCCTCTGTCTATTC
Cre_F	CATTTGGGCCAGCTAAACAT
Cre_R	ATTCTCCCACCGTCAGTACG
Tie2-*Cre*_F	GGCTAATGGCTGTGGAATCTGG
*Etv2-Cre*_F	TGTCACACCACCAAATCCTCA
*Etv2-Cre*_R	TCTTGCGAACCTCATCACTCG
iSURE_Sv40pA_F	CCCCCTGAACCTGAAACATA
iSURE_AVT-Mtom_R	CCTTGCTCACCATGGTCTTG
Chr17_F (iSURE control)	GCTCTGCATGTTGCAAGAAA
Chr17_R (iSURE control)	GTGTCTGTACCAGGTTGGTTTG
Cdh5CreM_F	GGAGGCTGGAAAGTAGAGCA
Cdh5CreM_R	TCCCTGAACATGTCCATCAG

2.4 Histology

2.4.1 Whole mount X-Gal staining

2.4.1.1 Whole mount X-Gal staining for whole embryos and embryonic hearts

After dissection from the uteri, embryos were fixed in a solution of 2% PFA and 0.2% glutaraldehyde dissolved in 1xPBS. E9.5 embryos were fixed at 4°C for 30 minutes; E10.5 and E11.5 embryos at 4°C for 60 minutes; and E12.5 at 4°C for 120 minutes. After fixation, E9.5 - E11.5 whole embryos and E12.5 - E13.5 hearts were rinsed in 1xPBS for 30 minutes at 4°C. Whole embryos aged E12.5 or older were rinsed twice for 30 minutes in Rinse solution (0.1% sodium deoxycholate 0.2% Nonidet P-40, 2 mM magnesium chloride dissolved in 1xPBS) at 4°C.

Embryos were then stained in 1 mg/mL X-GAL in dimethylformamide dissolved in stain solution (5 mM potassium ferrocyanide, 5 mM ferricyanide, 0.1% sodium deoxycholate, 0.2% Nonidet P-40 and 2 mM magnesium chloride). Whole embryos were stained for 3

hours at RT, whilst embryonic hearts were stained overnight at RT. Subsequently, the embryonic tissue was briefly rinsed twice in PBS and fixed overnight in 4% PFA at 4ºC.

Images were captured using a Leica M165C binocular dissecting stereo microscope equipped with a ProgRes CF Scan camera and CapturePro software (Jenoptik).

2.4.1.2 Whole mount X-Gal staining on postnatal retinae

After dissection, post-natal retinae were incubated in Rinse solution (0.1 M Phosphate buffer, 2 mM $MgCl_2$, 0.01% sodium deoxycholate, and 0.02% Nonidet P-40) for two washes of 20 minutes at 4ºC. They were then transferred to a retina staining solution (5mM potassium ferricyanide and 5mM potassium ferrocyanide, 0.01% sodium deoxycholate, 0.02% Nonidet P-40, 2 mM magnesium chloride and 0.1 M Phosphate buffer) containing 1 mg/mL X-GAL for incubation overnight at 4ºC.

After incubation, samples were rinsed twice in detergent rinse for 20 minutes at RT, and then washed in 1xPBS. They were then briefly fixed in 4% PFA in PBS for 10 minutes at RT.

2.4.2 Paraffin embedding and sectioning

After whole mount X-Gal staining and imaging, select embryos were embedded in wax prior to sectioning. This procedure utilized a tissue processor (Excelsior AS, Cat.# A82300001, Thermo Scientific). Embryos were dehydrated through a series of ethanol washes, cleared with xylene, and then infiltrated with liquid paraffin (Table 15). Embryos were then placed into moulds using a HistoStar Embedding Workstation, orientated as appropriate (Cat.# A81000002, Thermo Scientific). Embedded embryos were sectioned at a thickness of 6-8µm using the HM 353S Automatic Microtome (Cat.# 905200, Thermo Scientific). These sections were mounted onto glass slides using a heat bath and left to dry for 24 hours at RT.

Table 15: Protocol for tissue processing

Reagent	Time (minutes)	Pressure
70% EtOH	30	Atmospheric pressure
90% EtOH	30	Atmospheric pressure
96% EtOH I	60	Atmospheric pressure
96% EtOH II	30	Atmospheric pressure
100% EtOH I	60	Atmospheric pressure
100% EtOH II	30	Atmospheric pressure
Histoclear	60	Atmospheric pressure
Histoclear	60	Atmospheric pressure
Histoclear: Wax (1:1)	60	Pressure-assisted
Wax I	60	Pressure-assisted
Wax II	60	Pressure-assisted
Wax III	60	Pressure-assisted

2.4.3 Nuclear Fast Red staining

After sectioning, slides with embryonic tissue were de-waxed through a series of Histoclear, rehydrated into tap water; counterstained with Nuclear Fast Red; and then dehydrated again through a series of ethanol dilutions and incubated in Histoclear (Table 16). VectaMount permanent mounting medium (Vector Labs) was then used to mount the slides. Slides were left to dry before being imaged with the slide scanner (Hamamatsu NanoZoomer S210, C13239 series).

Table 16: Protocol for Nuclear Fast Red staining

Reagent	Time (minutes)
Histoclear	2
Histoclear II	2
100% EtOH I	1
100% EtOH II	1
90% EtOH	1
70% EtOH	1
Tap Water	1
Nuclear Fast Red Stain	1
Tap Water	1-2, replace until clear
70% EtOH	1
90% EtOH	1
100% EtOH I	2
100% EtOH II	1
Histoclear	2
Histoclear II	2
Air Dry	1

2.4.4 Immunofluorescence (IF)

Embryos for immunofluorescence were frozen in place of paraffin embedding. First, they were fixed in 4% PFA for 30 minutes at 4ºC. They were taken through a methanol series (Table 17) to facilitate long-term storage.

Table 17: Protocol for methanol de-hydration

Reagent	Time (minutes)
4% PFA	30
PBS I	5
PBS II	5
50:50 PBS: CH_3OH	5
25:75 PBS: CH_3OH	5
100% CH_3OH	5
100% CH_3OH	5
100% CH_3OH	Long-term storage

2.4.4.1 Cryo-embedding and sectioning

Embryos selected for IF analysis were taken through a methanol re-hydration series (Table 18). The embryos were then rinsed twice in 1xPBS, before being placed in a 70:30 1xPBS: sucrose solution overnight at 4ºC. Tissues were then embedded in a mixture of equal parts 70:30 1xPBS: sucrose and Tissue-*Tek* OCT. Excess sucrose was then removed by passing the embryos through a small bath of 100% Tissue-*Tek* OCT. Embryos were orientated vertically, with the head positioned inferiorly, and embedded in a mould with fresh OCT over dry ice and stored at -80ºC.

Table 18: Protocol for methanol re-hydration series

Reagent	Time (minutes)
25:75 PBS: EtOH	15
50:50 PBS: EtOH	15
PBS I	5
PBS II	5
4% PFA	60

Cryosections were cut at a thickness 10 µm using a CM-3050-S Cryostat (Leica Biosystems).

2.4.4.2 Immunofluorescence staining on embryonic cryo-sections

Cryosections were air-dried at RT for 15 minutes, then re-hydrated for 15 minutes in 1xPBS containing 0.1% Tween-20 (PBS-T). Slides were then incubated in 0.5% Triton X-100 in 1xPBS for 10 minutes at RT to permeabilise the tissue. This was followed by two rinses in 1xPBS, 5 minutes each. Sections were then incubated with blocking solution Sections were then incubated with Blocking solution (4% FBS; 10% donkey serum; 0.2% Triton X-100 in PBS) for 1 hour at RT, before being incubated overnight at 4°C with primary antibodies diluted in the blocking solution (Table 19).

Table 19: Primary antibodies

Primary Antibody	Species	Dilution
hSox17 (R&D Systems, Catalog #AF1924)	Goat	1 in 500
Endomucin (Thermo Fisher Scientific, Catalog #14-5851-82)	Rat	1 in 50
NR2F2 (Sigma-Aldrich, Catalog #AV100816)	Rabbit	1 in 100

Following overnight incubation, slides were rinsed twice with 1xPBS and washed three times for 15 minutes each in PBS-T on a rocker. Sections were incubated for 1 hour at RT with secondary antibodies diluted in PBS containing 0.1% Triton X-100 (Table 20).

Table 20: Secondary antibodies

Secondary Antibody	Species	Dilution
AlexaFluor 488 (Thermo Fisher Scientific, Catalog #A-21208)	Donkey anti-rat	1 in 500
AlexaFluor 546 (Thermo Fisher Scientific, Catalog #A-11056)	Donkey anti-goat	1 in 500
AlexaFluor 647 (Thermo Fisher Scientific, Catalog #A-31573)	Donkey anti-rabbit	1 in 500

After secondary incubation, slides were rinsed twice with 1xPBS and washed three times for 10 minutes each in PBS-T. Nuclei were counterstained by incubating the slides in DAPI solution for 10 minutes at RT. This was followed by three washes in 1xPBS for 5 minutes each. Finally, slides were mounted using Fluoromount mounting medium. Slides were stored in the dark at 4°C until imaging.

2.4.4.3 Image acquisition and analysis

Cryosection slides were imaged on the Zeiss LSM 710 confocal microscope using four lasers: 405 nm diode, 488 nm Argon, 561 nm DPSS, 633 nm HeNe. Sections were imaged using the tile scan command, with the images analysed on Quantitative Pathology (QuPath) Analysis, an open source software.

Table 21: Lasers used on the Zeiss LSM 710 confocal microscope

Fluorophore	Excitation Peak (nm)	Emission Peak (nm)	Zeiss LSM 710 Laser Line
DAPI	358	461	405 nm diode
Alexa Fluor 488	495	519	488 nm Argon
Alexa Fluor 546	556	573	561 nm DPSS
Alexa Fluor 647	650	668	633 nm HeNe

2.4.4.4 Immunofluorescence staining for postnatal retinae

After X-gal staining and post-fixation, retinae were washed twice with 1xPBS (5 minutes each) to remove residual fixative. The retinae were then blocked in 10% donkey serum in PBS for 1 hour at 4°C, and incubated overnight at 4°C in a solution of isolectin B4 conjugated to Alexa Fluor 488, diluted 1:50 in blocking buffer (10% donkey serum in PBS).

The following day, retinae were washed twice in 1xPBS (10 minutes each) at RT before being flattened into a petal shape via four radial incisions. Retinae were mounted in fluorescent mounting medium on slides.

2.4.4.5 Image acquisition and analysis

The retinae were imaged on the Zeiss LSM 710 confocal microscope using the tile scan command in combination with Z-stack collection. This was done at 488 nm excitation and 510 nm emission, and at 561 nm excitation and 610 nm emission. This enabled both the Alexa Fluor 488 and MbTomato to be visualised. Analysis was performed in both FIJI/ImageJ and QuPath Analysis.

2.5 Statistical analysis

Statistical analyses were performed using GraphPad Prism software. Data was first assessed for normality using the Shapiro-Wilk test to determine whether the distributions were parametric or non-parametric. For datasets that were normally distributed, comparisons between two groups were carried out using an unpaired, two-tailed Student's *t*-test. Although data in this thesis was all parametric, for non-normally distributed data, the Mann-Whitney U test would have been used for two group comparisons. Categorical data was analysed using Fisher's Exact Test, or a Chi-squared Test, as appropriate. Statistical significance was defined as $P < 0.05$ ($^{*}P < 0.05$, $^{**}P < 0.01$, $^{***}P < 0.001$, $^{****}P < 0.001$).

Chapter 3: Delineating direct transcriptional regulators of SOX7-58

3.1 Background

3.1.1 Using enhancers as a tool to understand gene regulation

Enhancers play a critical role in the spatial and temporal regulation of gene expression.[24,157,226] Each enhancer contains multiple TF binding motifs which facilitate the recruitment of specific TFs. By establishing which individual TFs, or cohorts of TFs, are required for enhancer activation, and thus a particular gene expression pattern, important upstream signalling and transcriptional regulatory cascades can be investigated.[226] For instance, analysis of two enhancers - DLL4in3 and HLX-3 - has revealed a previously unrecognised role for MEF2 TFs in driving sprouting angiogenic gene expression downstream of VEGFA.[227]

EC-expressed genes are frequently regulated by multiple enhancers.[24,228] These enhancers often drive distinct yet overlapping patterns of gene expression, contributing to the fine-tuned control of EC function.[182,183,227,229,230] By systematically mapping enhancer activity across EC subpopulations, and identifying the TFs critical for their activation, it is possible to uncover key regulatory pathways that define EC subtype-specific identity and function.[183,197,226,227,229,230]

3.1.2 *In silico* identification of a novel enhancer for SOX7

In the vasculature, the SOX7 TF is thought to play a role in both arterial specification and angiogenesis.[57,194,197,231,232] One previous enhancer has been identified for *SOX7*, located 14 kilobases downstream of the SOX7 TSS and named SOX7+14.[233,234] This enhancer has been shown to direct arterial EC expression.[229,234] Recently, the De Val group identified a second SOX7 enhancer, located 58 kilobases upstream of the *SOX7* gene and termed SOX7-58 (Figure 11 and Figure 12).

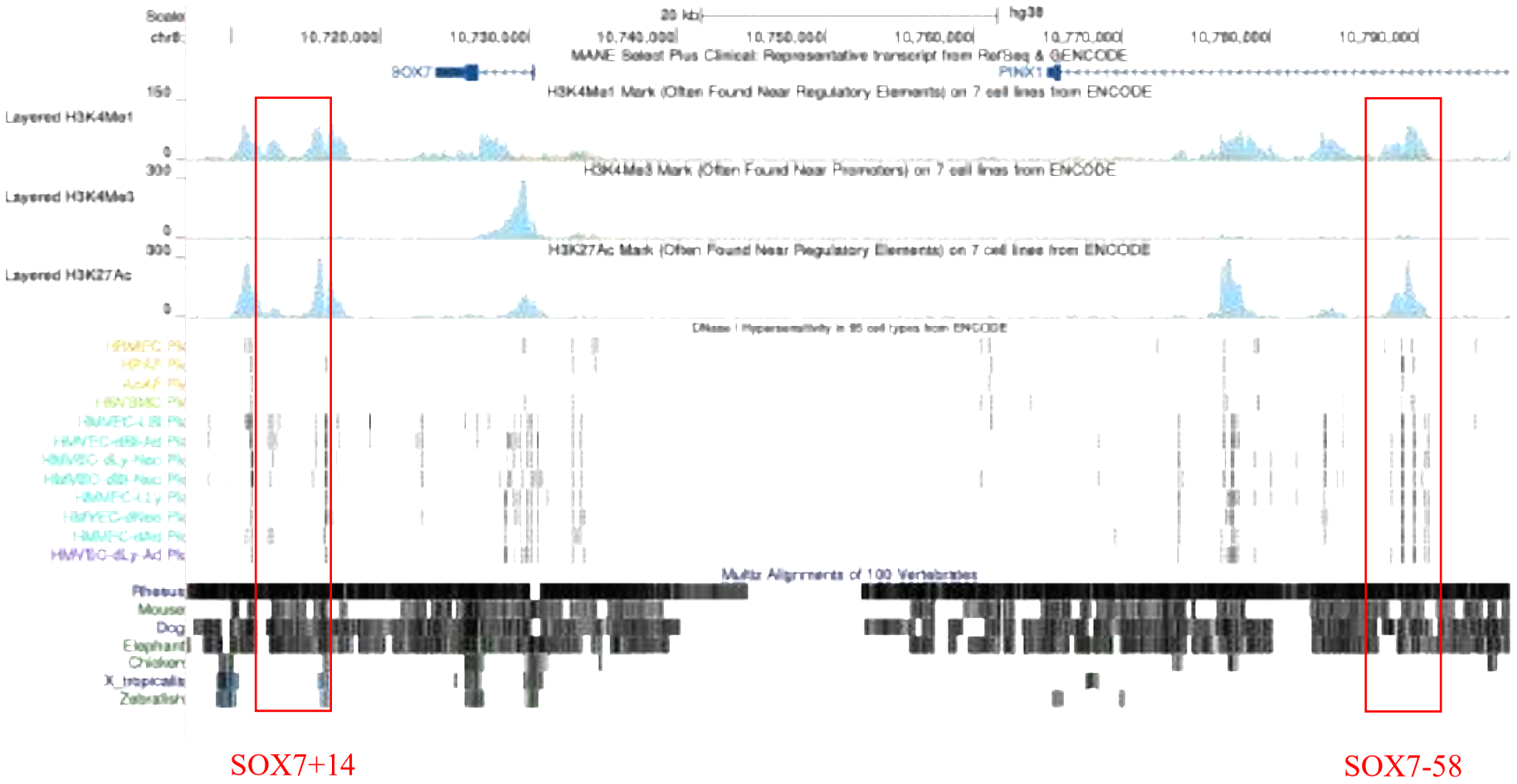

Figure 11: An *in silico* enhancer screen of the human *SOX7* gene locus predicts previously undiscovered putative enhancer sequence. The putative enhancer region was denoted according to its distance from the TSS in kilobases. In the putative SOX7-58 enhancer region, there were histone marks characteristic of enhancer (H3K4Me1 and H3K27Ac) but not promoter (H3K4Me3) elements. Moreover, it resides within an area of DNaseI hypersensitivity reflective of open chromatin in ECs, and is conserved from human to elephant.

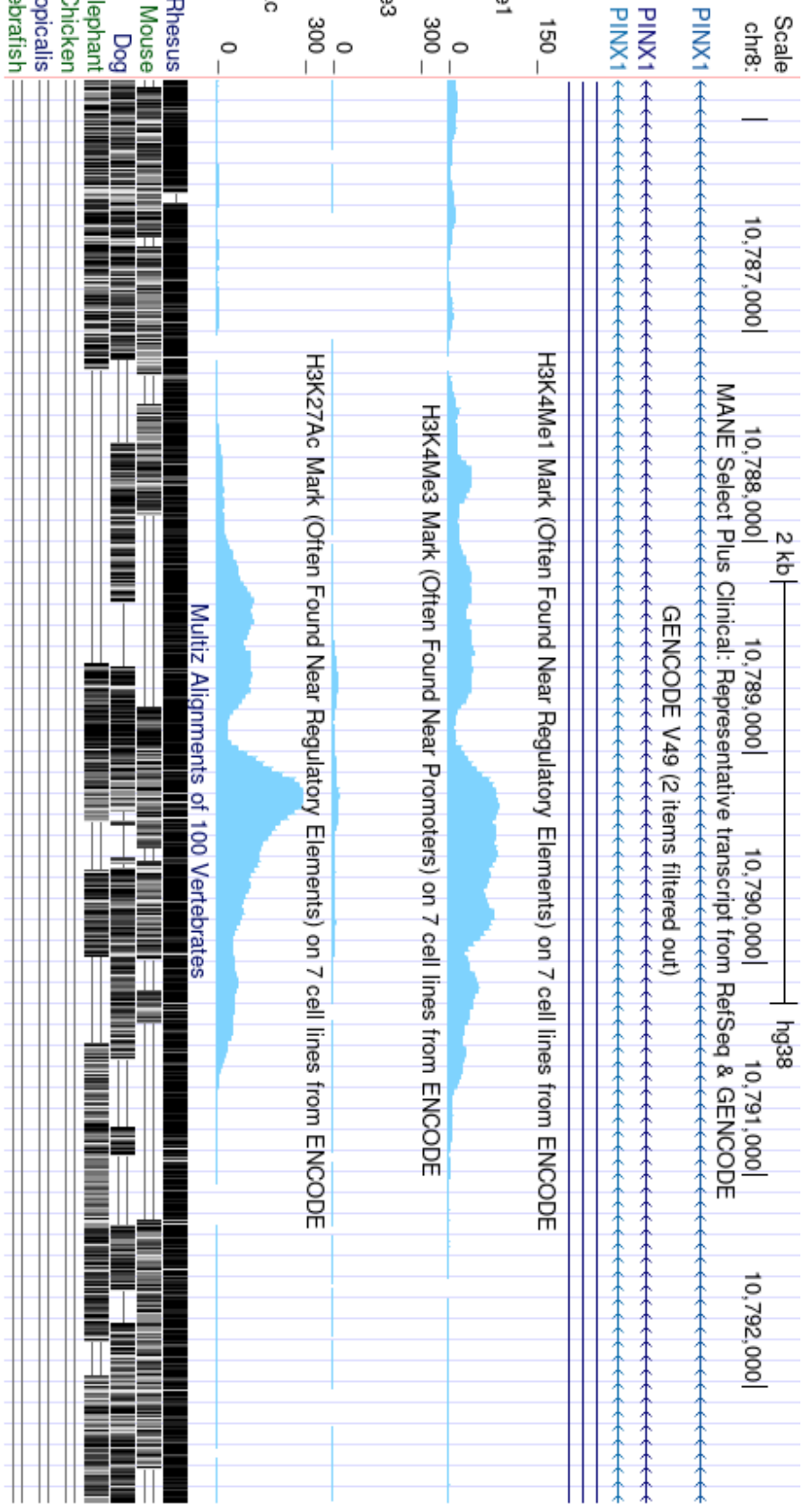

Figure 12: A putative enhancer sequence has been identified 58 kilobases from the TSS of SOX7.

The identification of this enhancer used a multi-step *in silico* approach.[226] Although enhancers can regulate their cognate genes regardless of orientation, and sometimes from a considerable distance, most are found within 100kb of the promoter. Thus, this region was prioritised in the search for novel enhancers regulating *SOX7*. On the UCSC Genome Browser (https://genome.ucsc.edu) on the Human (GRCh38/hg38), the *SOX7* locus was mapped to Chromosome 8 (chr8:106,481,882 – 106,502,574).

Putative enhancers are often predicted by their epigenetic signature.[226] To this end, the Encyclopaedia of DNA Elements (ENCODE) project provides a valuable resource: over 1,640 datasets from sequence-based studies, integrated across 147 different human cell types.[235] The *SOX7* locus was initially screened for regions enriched for H3K27ac (active enhancers) and H3K4me1 (both poised and active enhancers), but lacking H3K4me3 (promoter-associated) peaks. To ensure functional relevance, DNase I hypersensitivity heat maps from 12 EC lines were used to pinpoint regions of open chromatin. Finally, the sequence was phylogenetically foot-printed across species (from human to zebrafish) to infer conservation. Whilst other putative enhancers were also identified, SOX7-58 satisfied these initial requirements: it had peaks for H3K27Ac and H3K4Me1 but not H3K4Me3; it had open chromatin in all 12 of the EC lines; and it was conserved from the human to elephant genome (Figure 11 and Figure 12).

3.1.3 Functional analysis of the human SOX7-58 enhancer sequence *in vivo*

To functionally validate SOX7-58 as an EC enhancer, *in vivo* transgenic enhancer:reporter assays were performed in both zebrafish and mouse models. In these assays, SOX7-58 was cloned upstream of a minimal promoter driving a reporter gene. The resulting transgenes were then introduced into embryos: zebrafish embryos via mosaic Tol2-mediated transgenesis, and mouse embryos via pronuclear injection. Given that the minimal promoters selected have very weak basal transcriptional activity, with no intrinsic regulatory sequences, the spatiotemporal activity of the reporter gene reflects the activity of SOX7-58.[151,236]

3.1.3.1 Functional analysis of human SOX7-58 enhancer sequence in transient (F0) mosaic transgenic zebrafish embryos

For *in vivo* transgenic enhancer:reporter expression screens, zebrafish are a highly efficient and cost-effective platform: a single breeding produce a large number of embryos in a single clutch, the embryos themselves develop rapidly, and for an animal model, are inexpensive to maintain.[236,237] Furthermore, zebrafish embryos are optically transparent, enabling non-invasive imaging of fluorescent reporter activity.[238] Although murine models offer closer physiological relevance to humans, zebrafish still maintain a relatively high genetic similarity; around 70% of human genes have a recognised zebrafish orthologue.[239] Moreover, it has been repeatedly demonstrated that enhancers derived from other species can direct conserved expression patterns in zebrafish.[236,240-242]

Tol2-mediated transgenesis was used to introduce SOX7-58 into the zebrafish genome (Figure 13). Derived from a medaka fish transposable element, this approach uses a non-autonomous Tol2 vector containing inverted terminal repeats and a transgene cassette.[243,244] In this instance, the transgene cassette contained the SOX7-58 sequence upstream of an E1B minimal promoter and a GFP reporter gene.[243] To ensure its stable genomic integration, 60ng/µl of SOX7-58-containing Tol2 destination vector was co-injected with 0.5nl of 50ng/µl of Tol2 transposase mRNA into one-cell stage zebrafish embryos. Compared with injection of naked DNA, which has very low germline transmission, Tol2 transgenesis can yield transgenic F1 offspring from 50-70% of injected zebrafish.[237,243]

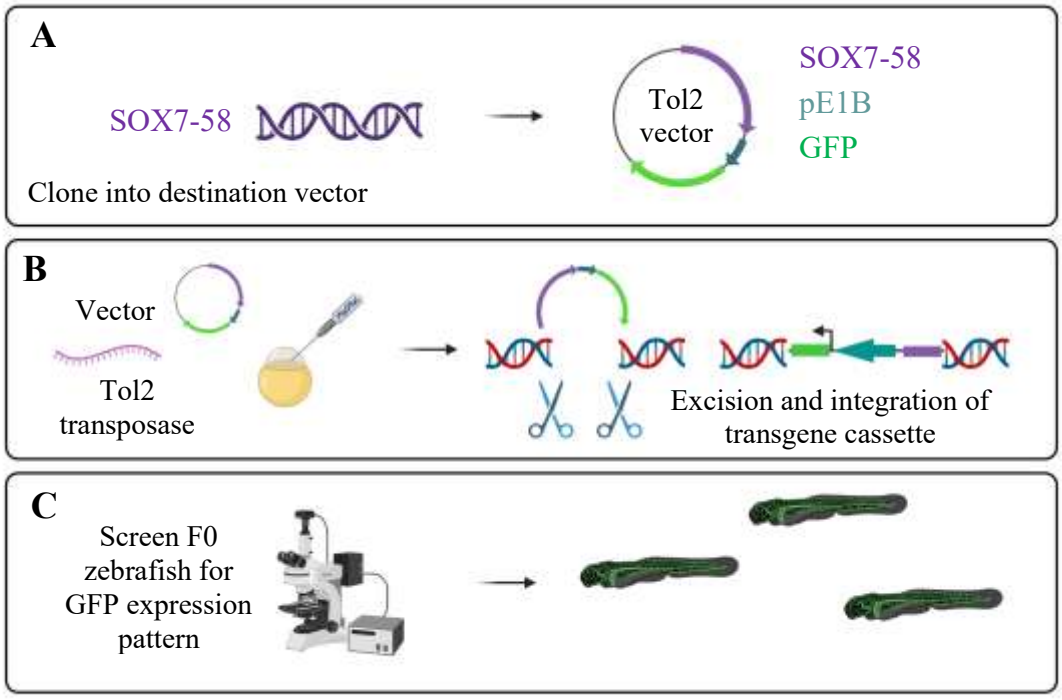

Figure 13: A schematic to show the Tol2 transgenesis reporter assay strategy in zebrafish. (A) SOX7-58 is cloned into the Tol2 destination vector, upstream of the E1B minimal promoter, and the GFP reporter gene. (B) The Tol2 destination vector is then injected into fertilised one-cell stage zebrafish embryo, alongside Tol2 transposase. This allows the transgene to be excised from the donor plasmid vector and integrated into the zebrafish genome. (C) The injected zebrafish are then screened at 28hpf and 48hpf for GFP expression in the developing vasculature.

At two timepoints – 28 hours post fertilisation (hpf) and 48 hpf – *SOX7-58:*GFP expression was analysed. This was assessed qualitatively: *SOX7-58:*GFP expression was noted as either being present only in ECs, present only in non-ECs, present in both ECs and non-ECs, or completely absent.

At 28 hpf, the *SOX7-58:*GFP transgene was predominantly active in intersegmental vessels (ISVs), with weaker expression also observed in the DA (dorsal aorta) (Figure 14: Panel B). However, there was also significant non-EC GFP expression, perhaps indicating that SOX7-58 activity is not spatially restricted to ECs. One major caveat of Tol2 transgenesis is the random integration of the transgene, which can lead to position effects.[245,246] For example, random genomic insertion can expose the *SOX7-58:*GFP transgene to nearby regulatory elements, producing artefactual GFP signals.[244]

At 48 hpf, the *SOX7-58:*GFP activity had expanded to both the dorsal longitudinal anastomosing vessel (DLAV) and the posterior cardinal vein (PCV) (Figure 14: Panel C). Given that tip ECs from the ISVs migrate dorsally toward the DLAV between 28hpf and 48 hpf, and the half-life of GFP is approximately 24 hours, this could suggest that *SOX7-58:*GFP expression in the DLAV at 48 hpf reflects earlier activity in tip ECs from ISVs.

HLX-3 has previously been identified as an enhancer specifically active in angiogenic ECs.[227,247] In transient transgenic *HLX-3:*GFP zebrafish embryos, GFP expression was first detected at 26 hpf in sprouting ISVs, marking both tip and stalk ECs.[247] By 29–31 hpf, activity intensified and remained restricted to sprouting ECs, and by 48 hpf, expression was observed in the DLAV and, in around 13% of cases, in venous ISVs from the PCV.[247] Expression was strongest at the root of venous sprouts, indicating activity during their connection to intersegmental arteries.[247] Although by no means identical, this expression pattern appears similar to that of the *SOX7-58:*GFP transgene (Figure 14).

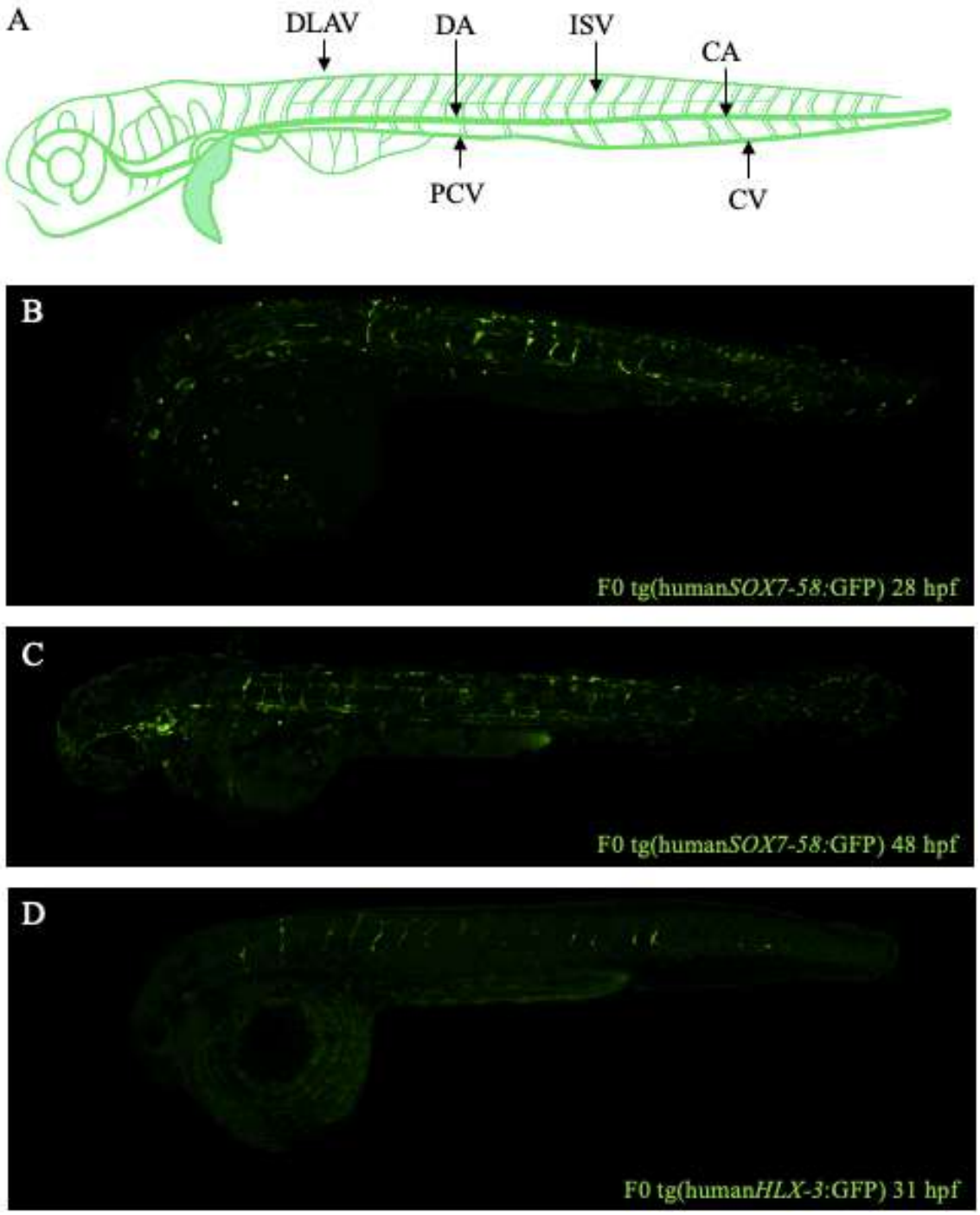

Figure 14: At both 28 hpf and 48 hpf, the human SOX7-58 enhancer was able to drive GFP expression in ECs. (A) Shows a schematic of zebrafish vasculature labelled, (B) shows a representative F0 transgenic zebrafish expressing the humanSOX7:GFP transgene at 28hpf, and (C) at 48hpf. (D) shows a representative F0 transgenic zebrafish expressing the humanHLX:GFP transgene at 31hpf. Images taken by Dr Svanhild Nornes.

Abbreviations: CV: cardinal vein, DA: dorsal aorta, DLAV: dorsal longitudinal anastomosing vessel, GFP: green fluorescent protein, hpf: hours post fertilisation, ISV: intersegmental vessels, PCV: posterior cardinal vein, tg: transgenic

3.1.3.2 Functional analysis of the human SOX7-58 enhancer in transient transgenic murine lines

Whilst zebrafish enhancer:reporter assays are useful for initially investigating the functionality of putative enhancers, validation in F0 transgenic mice lines is necessary to confirm their activity in a mammalian genomic context.

The generation of F0 transgenic mouse embryos was outsourced to Cyagen Inc (https://www.cyagen.com/us/en/). In brief, the F0 mice expressed a transgene combining SOX7-58 with *LacZ*, linked by an hsp68 minimal promoter. The hsp68 minimal promoter functions in a very similar manner to the E1B minimal promoter, it is silent in the absence of an associated regulatory sequence.[236,248,249] This ensures that the *LacZ* expression depends entirely on SOX7-58 activity. The F0 mouse embryos were then genotyped by PCR and stained with X-Gal to identify *LacZ* expressing embryos.

The postnatal retinae of the F0 transgenic mice exhibited an X-Gal staining pattern which was highly specific to tip ECs (**Figure 12: Panel F and G**). A time course analysis between E9.5 and E14.5 also shows activity of the *SOX7-58:*lacZ transgene in regions undergoing angiogenesis. It was therefore concluded that this novel enhancer, SOX7-58, directs gene expression specifically to angiogenic ECs downstream of angiogenic cues.

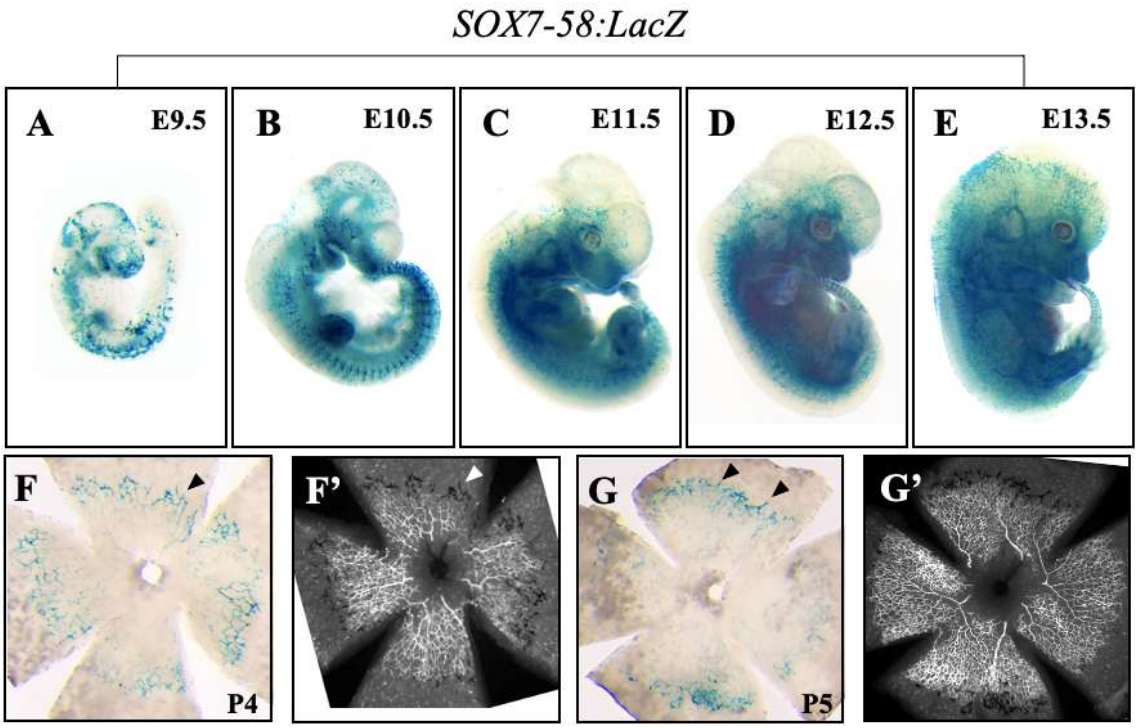

Figure 15: Time course analysis of transient (F0) transgenic *SOX7-58:LacZ* embryos show robust vascular transgene expression, seemingly highly specific to tip ECs. (A-E) shows a time course from E9.5 to E13.5, whilst (F) and (F') show a P4 retina, and (G) and (G') show a P5 retina. Images taken by Professor Sarah De Val. White and black arrows show examples of tip ECs.

3.2 Aims and Objectives

The hypothesis for this chapter states that by delineating the transcriptional regulation of SOX7-58, a novel tip endothelial-specific enhancer, important upstream and downstream signalling pathways in sprouting angiogenesis can be elucidated.

The aims of this chapter were to:

1. Analysis of angiogenic activity of SOX7-58 orthologues

2. Identification of transcription factors interacting with SOX7-58 using an *in silico* approach

3. Functional analysis of the role of putative transcription factor binding motifs within SOX7-58

4. Identification of putative transcription factor binding sites using TRANSFAC and FIMO (MEME SUITE) for SOX7-58 and two other angiogenic enhancers

3.2.1 *In silico* analysis of angiogenic enhancers using TRANSFAC and FIMO (MEME SUITE)

In **Section 3.1**, the De Val group have established that SOX7-58 is a functional enhancer, with activity specifically in tip ECs. Therefore, the first objective in my project was to define the TFs that govern its activation. Indeed, by gaining a greater understanding of the underlying TF network, I hoped to better discern the context-dependent and cell-type specific activation of SOX7-58. To achieve this, a range of experimental strategies can be employed; chromatin immunoprecipitation, reporter mutagenesis, and loss-of-function models. However, each of these methods is time-intensive and limited in throughput.

Therefore, I chose to start my project with *in silico* motif analysis; a computational approach that involves the systematic interrogation of SOX7-58 for enriched TF binding sites. This then produces a list of candidate regulators which can be probed experimentally. As such, *in silico* motif analysis offers a cost-effective and unbiased framework for defining putative TF networks that can subsequently be tested using targeted functional assays.

To this end, I first analysed the SOX7-58 enhancer sequence using the TRANScription FACtor database (TRANSFAC).[250] In this approach, the sequence is scanned against vertebrate position weight matrices (PWMs) using the Match™ tool.[251] Putative TF binding motifs are then identified using two scoring systems: the matrix similarity score (MSS) and the core similarity score (CSS). Whilst MSS reflects the match across the full motif, CSS instead evaluates conservation at the most critical positions.[251] To reduce the number of false positive and false negative motifs identified, the angiogenic enhancer sequences were assessed using the minSUM profile (Figure 16).

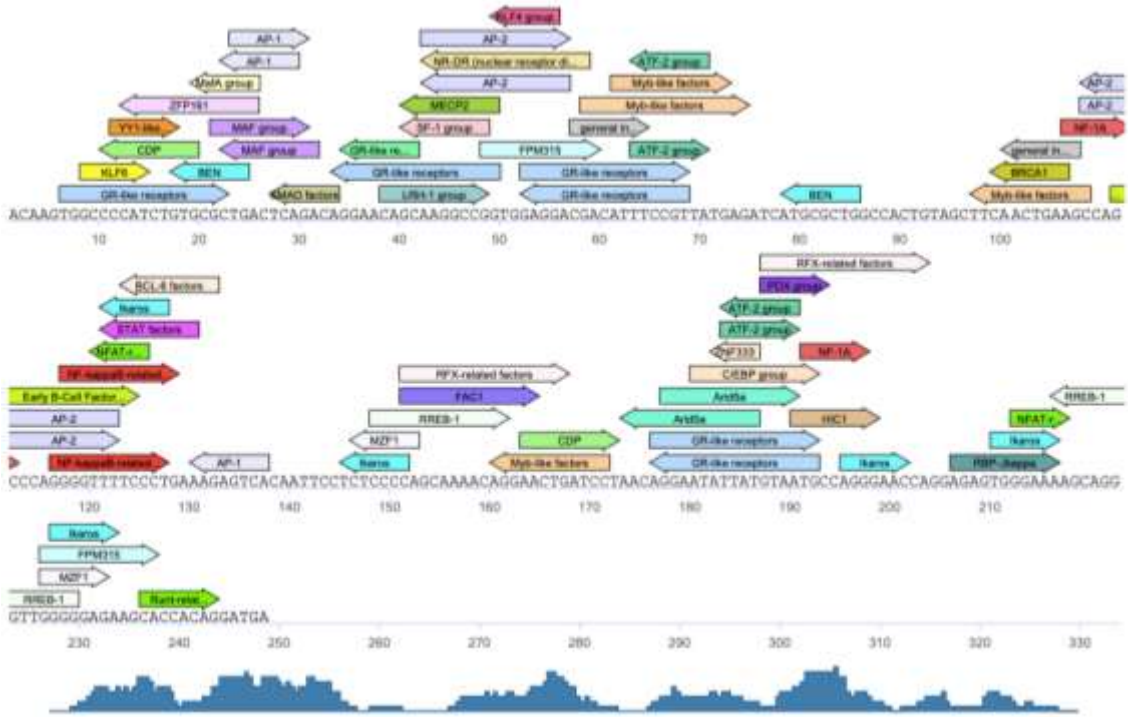

Figure 16: TRANSFAC minSUM profile analysis of the SOX7-58 enhancer sequence.

This approach identified a wide variety of putative TFs: ZNF, HOX, bHLH, bZIP, ETS, AP1, FOX, NR, SOX, SMAD, KLF, RFX, and E2F (Figure 16).

More than one computational methodology exists for motif searching, and so, in parallel, I analysed the SOX7-58 enhancer sequence using FIMO (Find Individual Motif Occurrences) from the MEME Suite (https://meme-suite.org/meme/doc/fimo.html).[252] Using position frequency matrices, which reflect the average binding preference for TFs, FIMO scans the sequence against a database of known motifs. To minimise bias, the JASPAR2024_vertebrate_non-redundant_pfms dataset was inputted (https://jaspar.elixir.no/downloads/). This dataset encompasses all vertebrate TF profiles derived from ChIP-seq and SELEX data, without duplication. This produced a table of identified motifs, along with their position, and p-value representing the likelihood the motif was a true positive (see Table 22). This approach also identified a wide variety of putative TFs: ZNF, HOX, bHLH, bZIP, ETS, AP1, FOX, NR, STAT and CTCF (Table 22).

Table 22: FIMO Motif Analysis of the SOX7-58 enhancer

Motif ID	Alt ID	Strand	Start	End	p-value
MA1579.2	ZBTB26	+	12	19	5.04E-05
MA1589.2	ZNF140	+	19	37	9.76E-05
MA0105.4	NFKB1	+	22	34	6.54E-05
MA0105.4	NFKB1	-	22	34	8.95E-05
MA0101.1	REL	+	23	32	4.69E-06
MA0107.1	RELA	+	23	32	1.56E-05
MA0778.2	NFKB2	-	23	33	3.75E-05
MA1117.2	RELB	-	23	29	5.35E-05
MA0778.2	NFKB2	+	23	33	8.25E-05
MA0515.1	Sox6	-	35	44	4.49E-05
MA0074.1	RXRA:VDR	-	42	56	8.25E-05
MA1561.2	SOX12	+	45	54	5.48E-05
MA1724.2	Rfx6	+	46	54	9.45E-05
MA0907.2	HOXC13	+	100	108	6.05E-05
MA1936.2	ERF::FOXO1	+	125	136	3.69E-05
MA1576.2	THRB	+	139	156	3.04E-05
MA0739.2	Hic1	+	140	147	9.26E-05
MA1559.2	SNAI3	-	143	151	4.13E-05
MA0499.3	MYOD1	+	144	152	1.15E-05
MA0745.3	SNAI2	+	144	151	3.88E-05
MA1620.2	Ptf1A	+	144	151	6.29E-05
MA1631.2	ASCL1	+	144	152	7.07E-05
MA1109.2	NEUROD1	-	144	151	9.54E-05
MA0525.2	TP63	-	145	162	8.49E-05
MA1558.2	SNAI1	-	145	151	9.74E-05
MA0861.2	TP73	-	146	161	5.37E-05
MA0861.2	TP73	+	146	161	9.34E-05
MA1969.2	THRA	+	148	165	5.12E-05
MA1646.2	OSR2	-	161	168	1.47E-05
MA1542.2	OSR1	+	161	168	8.53E-05
MA1625.2	Stat5b	-	163	171	6.17E-05
MA1470.2	BACH2	+	169	187	5.63E-05
MA0869.3	Sox11	-	185	192	4.72E-05
MA1594.1	ZNF382	+	203	226	4.02E-05
MA0659.4	Mafg	-	215	226	9.97E-05
MA0478.2	FOSL2	-	217	226	5.06E-05
MA1723.2	PRDM9	-	222	241	9.81E-06
MA0599.1	KLF5	+	225	234	4.49E-05
MA0685.2	SP4	-	226	234	3.34E-06
MA0079.5	SP1	-	226	234	3.34E-06

MA0516.3	SP2	-	226	234	1.03E-05
MA0742.2	KLF12	-	226	234	1.22E-05
MA0740.2	KLF14	-	226	234	1.33E-05
MA1511.2	KLF10	-	226	234	1.40E-05
MA1959.2	KLF7	-	226	233	3.11E-05
MA0493.3	KLF1	-	226	233	5.90E-05
MA2328.1	ZBED4	+	227	236	8.64E-05
MA1600.2	ZNF684	+	228	241	3.39E-05
MA1929.2	CTCF	+	228	258	7.91E-05
MA1981.2	ZNF530	-	229	242	3.94E-05
MA0599.1	KLF5	+	230	239	7.52E-07
MA1961.2	PATZ1	-	230	240	6.25E-06
MA0741.1	KLF16	+	230	240	1.08E-05
MA0746.3	SP3	+	230	240	2.69E-05
MA1107.3	KLF9	+	230	240	3.19E-05
MA1981.2	ZNF530	-	230	243	6.61E-05
MA1511.2	KLF10	-	231	239	5.17E-06
MA0039.5	KLF4	+	231	238	8.13E-06
MA0493.3	KLF1	-	231	238	1.48E-05
MA0740.2	KLF14	-	231	239	1.70E-05
MA1515.2	KLF2	+	231	238	3.28E-05
MA1959.2	KLF7	-	231	238	3.92E-05
MA1723.2	PRDM9	-	231	250	5.31E-05
MA0747.2	SP8	+	231	241	6.91E-05
MA1517.2	KLF6	+	231	239	7.81E-05
MA1512.2	KLF11	+	231	240	7.91E-05
MA1653.2	ZNF148	+	231	240	8.09E-05
MA0753.3	ZNF740	+	231	240	8.15E-05
MA1630.3	ZNF281	-	231	240	8.36E-05
MA0079.5	SP1	-	231	239	8.63E-05
MA0685.2	SP4	-	231	239	8.71E-05
MA1564.2	SP9	+	231	240	9.42E-05
MA1723.2	PRDM9	-	232	251	3.01E-05
MA1987.2	ZNF701	-	232	248	3.84E-05
MA1149.2	RARA::RXRG	-	233	249	2.10E-05
MA0730.1	RARA	-	233	249	8.21E-05
MA0159.1	RARA::RXRA	-	233	249	9.97E-05
MA1719.2	ZNF816	-	237	251	2.60E-05
MA0163.1	PLAG1	-	237	250	3.96E-05
MA0139.2	CTCF	-	243	257	4.04E-05
MA1929.2	CTCF	-	244	274	4.89E-05
MA0116.1	Znf423	-	244	258	7.93E-05
MA2002.2	Zfp335	+	309	315	9.74E-05

MA1117.2	RELB	-	332	338	5.35E-05
MA0809.3	TEAD4	-	333	340	8.69E-05
MA1121.2	TEAD2	-	334	340	6.51E-05
MA1102.3	CTCFL	+	363	370	8.02E-05
MA1123.3	TWIST1	+	369	376	7.13E-05
MA0646.2	GCM1	-	381	390	2.71E-05
MA1715.1	ZNF707	-	381	395	3.82E-05
MA1597.1	ZNF528	+	389	405	6.64E-05
MA1594.1	ZNF382	+	394	417	2.07E-05
MA0739.2	Hic1	+	410	417	9.26E-05
MA1956.2	FOXO1::FLI1	+	412	424	4.50E-05
MA1953.2	FOXO1::ELF1	+	412	424	8.69E-05
MA1950.2	FLI1::FOXI1	+	413	423	7.20E-05
MA1935.2	ERF::FOXI1	+	414	423	8.51E-05
MA1508.2	IKZF1	+	415	422	3.26E-05
MA0073.2	RREB1	+	461	479	2.01E-05
MA0073.2	RREB1	+	463	481	2.74E-06
MA1514.2	KLF17	+	465	478	6.94E-05
MA0039.5	KLF4	+	468	475	7.24E-05
MA1579.2	ZBTB26	-	518	525	6.25E-05
MA1581.2	ZBTB6	+	519	527	4.23E-05
MA0672.2	NKX2-3	-	534	541	9.45E-05
MA1615.2	Plagl1	-	539	546	9.90E-06
MA1529.2	NHLH2	+	540	555	2.80E-05
MA1981.2	ZNF530	-	540	553	9.40E-05
MA1618.2	Ptf1A	-	543	551	5.13E-05
MA1109.2	NEUROD1	-	544	551	1.47E-05
MA0668.3	Neurod2	-	544	551	1.47E-05
MA1642.2	NEUROG2	-	544	550	5.35E-05
MA1467.3	Atoh1	-	544	550	5.35E-05
MA0659.4	Mafg	-	553	564	1.94E-05
MA0591.2	Bach1::Mafk	-	553	564	3.52E-05
MA0501.2	MAF::NFE2	-	553	563	5.01E-05
MA0089.3	MAFG::NFE2L1	-	553	563	8.77E-05
MA0150.3	Nfe2l2	-	553	563	8.96E-05
MA0496.4	MAFK	-	554	563	3.15E-06
MA0659.4	Mafg	+	554	565	1.36E-05
MA0478.2	FOSL2	+	554	563	6.76E-05
MA0496.4	MAFK	+	555	564	1.01E-05
MA0477.3	FOSL1	+	555	563	5.70E-05
MA1132.2	JUN::JUNB	+	555	562	7.40E-05
MA0491.3	JUND	+	555	563	8.90E-05
MA0490.3	JUNB	+	555	563	9.39E-05

MA0489.3	Jun	+	556	563	4.72E-05
MA1988.2	Atf3	+	556	562	6.51E-05
MA1928.2	BNC2	-	556	562	6.51E-05
MA1634.2	BATF	+	556	562	6.51E-05
MA0835.3	BATF3	+	556	562	6.51E-05
MA0462.3	BATF::JUN	+	556	562	6.51E-05
MA2101.1	ZNF677	+	563	574	1.75E-05
MA1508.2	IKZF1	+	563	570	4.72E-05
MA1730.2	ZNF708	-	566	574	7.91E-05
MA1725.2	ZNF189	-	567	575	3.31E-06
MA1655.2	ZNF341	+	568	575	2.67E-05
MA1708.2	ETV7	-	593	601	5.94E-05
MA0762.2	ETV2	-	594	602	4.78E-05
MA0475.3	FLI1	-	594	602	7.28E-05
MA1544.2	OVOL1	+	595	604	4.17E-05
MA0492.2	JUND	+	602	612	6.35E-05
MA0488.2	JUN	-	603	612	4.17E-05
MA1632.2	ATF2	+	603	612	4.32E-05
MA0492.2	JUND	-	603	613	6.17E-05
MA1632.2	ATF2	-	603	612	8.42E-05
MA1929.2	CTCF	+	623	653	8.13E-05
MA1973.2	ZKSCAN3	+	635	648	3.08E-05
MA1637.2	EBF3	+	645	653	5.53E-05
MA1604.2	Ebf2	+	645	653	7.79E-05
MA0105.4	NFKB1	+	648	660	1.16E-05
MA0105.4	NFKB1	-	648	660	1.46E-05
MA0101.1	REL	+	649	658	5.43E-06
MA0778.2	NFKB2	-	649	659	6.73E-06
MA0778.2	NFKB2	+	649	659	9.18E-06
MA0107.1	RELA	+	649	658	1.80E-05
MA0518.2	Stat4	-	654	663	2.08E-05
MA0137.4	STAT1	-	655	663	4.91E-05
MA1625.2	Stat5b	+	655	663	5.34E-05
MA0144.3	STAT3	-	655	663	5.89E-05
MA0519.2	Stat5a::Stat5b	+	655	663	7.87E-05
MA1589.2	ZNF140	-	665	683	4.76E-05
MA1956.2	FOXO1::FLI1	+	687	699	6.17E-06
MA1954.2	FOXO1::ELK1	+	687	699	7.63E-06
MA1953.2	FOXO1::ELF1	+	687	699	9.23E-06
MA1955.2	FOXO1::ELK3	+	687	699	1.63E-05
MA1947.2	ETV5::FOXO1	+	687	696	7.68E-05
MA1950.2	FLI1::FOXI1	+	688	698	4.74E-05
MA1623.2	Stat2	+	688	697	5.09E-05

MA0081.3	SPIB	-	689	701	5.12E-06
MA0080.7	Spi1	+	689	701	8.12E-06
MA1952.2	FOXJ2::ELF1	+	689	699	1.04E-05
MA1935.2	ERF::FOXI1	+	689	698	2.19E-05
MA1942.2	ETV2::FOXI1	+	689	699	5.73E-05
MA1508.2	IKZF1	+	690	697	1.79E-05
MA0474.4	Erg	+	691	700	1.83E-05
MA0062.4	GABPA	-	691	700	2.01E-05
MA0761.3	ETV1	+	691	699	5.60E-05
MA2332.1	ZNF175	+	691	699	6.75E-05
MA1992.2	Ikzf3	+	692	700	4.28E-05
MA0473.4	ELF1	+	692	700	4.48E-05
MA0640.3	ELF3	-	692	700	7.55E-05
MA0598.4	EHF	-	692	700	9.28E-05
MA1508.2	IKZF1	+	706	713	1.79E-05
MA0752.2	ZNF410	-	711	726	8.77E-06
MA0843.2	TEF	-	715	724	1.21E-05
MA0639.2	DBP	-	715	724	2.00E-05
MA0639.2	DBP	+	715	724	2.36E-05
MA0843.2	TEF	+	715	724	2.96E-05
MA1636.2	CEBPG	+	715	724	4.25E-05
MA0102.5	CEBPA	-	715	724	6.96E-05
MA0840.2	Creb5	-	715	724	8.23E-05
MA0025.3	NFIL3	+	716	724	1.33E-05
MA0043.4	HLF	+	716	724	2.90E-05
MA1945.2	ETV5::FIGLA	+	727	740	7.63E-05
MA1715.1	ZNF707	-	731	745	5.68E-06
MA2097.1	ZNF75A	-	741	752	3.30E-07
MA1601.2	ZNF75D	+	742	753	4.07E-05
MA1725.2	ZNF189	-	745	753	5.89E-05
MA1987.2	ZNF701	+	749	765	3.42E-05
MA1981.2	ZNF530	+	751	764	2.62E-05
MA1154.2	ZNF282	-	753	767	6.06E-05
MA0155.1	INSM1	+	754	765	6.93E-05
MA1627.2	Wt1	-	757	766	5.82E-05
MA2097.1	ZNF75A	-	758	769	2.55E-05
MA1942.2	ETV2::FOXI1	+	771	781	8.93E-05
MA1731.2	ZNF768	-	785	793	5.04E-05
MA1589.2	ZNF140	+	791	809	8.27E-05
MA1726.2	ZNF331	+	802	811	1.53E-05
MA1731.2	ZNF768	+	808	816	9.39E-05
MA0138.3	REST	+	824	843	5.88E-05
MA1986.2	ZNF692	+	838	845	8.20E-05

MA1542.2	OSR1	-	842	849	6.07E-05
MA1514.2	KLF17	+	848	861	5.90E-05
MA1600.2	ZNF684	+	849	862	3.06E-05
MA1645.2	NKX2-2	+	849	856	3.88E-05
MA1599.2	ZNF682	+	850	860	9.04E-05
MA0155.1	INSM1	-	854	865	3.70E-05
MA1604.2	Ebf2	-	868	876	9.93E-05
MA1597.1	ZNF528	-	873	889	3.25E-05
MA0731.1	BCL6B	+	878	894	3.89E-05
MA0155.1	INSM1	+	882	893	3.11E-05
MA2002.2	Zfp335	+	905	911	5.35E-05
MA1985.1	ZNF669	-	908	922	6.55E-05
MA2002.2	Zfp335	+	909	915	9.74E-05
MA1930.2	CTCF	-	913	945	6.10E-05
MA1652.2	ZKSCAN5	-	915	923	9.34E-06
MA0081.3	SPIB	+	916	928	9.09E-05
MA0079.5	SP1	-	917	925	3.49E-05
MA0685.2	SP4	-	917	925	3.58E-05
MA1642.2	NEUROG2	-	924	930	5.35E-05
MA1467.3	Atoh1	-	924	930	5.35E-05
MA1589.2	ZNF140	+	930	948	1.31E-05
MA0081.3	SPIB	-	931	943	5.91E-06
MA0080.7	Spi1	+	931	943	1.24E-05
MA1725.2	ZNF189	-	936	944	8.04E-05
MA0495.4	MAFF	-	963	973	7.20E-05
MA1717.2	ZNF784	-	978	985	8.60E-05
MA1999.2	Prdm5	+	988	998	8.82E-05
MA2120.1	ZNF184	-	1006	1018	3.37E-05
MA1984.2	ZNF667	-	1007	1017	7.51E-05
MA0606.3	Nfat5	-	1012	1019	9.72E-05
MA0152.3	Nfatc2	-	1013	1020	5.75E-05
MA1930.2	CTCF	-	1013	1045	6.05E-05
MA1580.1	ZBTB32	+	1039	1048	4.10E-05
MA1607.2	Foxl2	+	1042	1051	6.04E-05
MA0593.2	FOXP2	+	1044	1052	2.67E-05
MA2118.1	FOXS1	+	1044	1051	4.35E-05
MA0047.4	FOXA2	+	1044	1051	4.35E-05
MA0030.2	FOXF2	+	1044	1052	7.55E-05
MA2117.1	FOXP4	+	1045	1051	7.93E-05
MA1683.2	FOXA3	+	1045	1051	7.93E-05
MA1606.2	Foxf1	+	1045	1051	7.93E-05
MA1103.3	FOXK2	+	1045	1051	7.93E-05
MA0852.3	FOXK1	+	1045	1051	7.93E-05

MA0850.1	FOXP3	+	1045	1051	7.93E-05
MA0849.1	FOXO6	+	1045	1051	7.93E-05
MA0848.1	FOXO4	+	1045	1051	7.93E-05
MA0481.4	FOXP1	+	1045	1051	7.93E-05
MA0480.3	Foxo1	+	1045	1051	7.93E-05
MA0157.4	Foxo3	+	1045	1051	7.93E-05
MA0148.5	FOXA1	+	1045	1052	7.93E-05
MA0042.2	FOXI1	+	1045	1051	7.93E-05
MA0033.2	FOXL1	+	1045	1051	7.93E-05
MA0031.2	FOXD1	+	1045	1051	7.93E-05
MA0613.1	FOXG1	+	1045	1052	8.79E-05
MA0122.4	Nkx3-2	+	1047	1056	3.30E-05
MA0857.1	Rarb	+	1054	1069	2.63E-05
MA0729.1	RARA	+	1055	1072	1.41E-05
MA0728.1	Nr2F6	+	1055	1069	6.14E-05
MA0859.2	Rarg	+	1055	1069	6.53E-05
MA1947.2	ETV5::FOXO1	+	1058	1067	2.83E-05
MA1950.2	FLI1::FOXI1	+	1059	1069	8.82E-05
MA2323.1	Pgr	-	1063	1079	1.96E-05
MA0727.2	NR3C2	-	1064	1078	2.89E-05
MA0113.4	NR3C1	-	1064	1078	4.69E-05
MA0727.2	NR3C2	+	1064	1078	5.24E-05
MA0113.4	NR3C1	+	1064	1078	6.71E-05
MA1155.1	ZSCAN4	+	1080	1094	8.76E-05
MA1629.2	Zic2	+	1126	1134	8.90E-05
MA0114.5	HNF4A	-	1134	1142	8.50E-05
MA0737.1	GLIS3	-	1138	1151	1.17E-05
MA1491.3	GLI3	-	1138	1152	1.30E-05
MA0736.1	GLIS2	-	1138	1151	8.47E-05
MA1960.2	MGA::EVX1	+	1144	1154	5.85E-05
MA0158.2	HOXA5	-	1149	1156	6.14E-05
MA1496.2	HOXA4	-	1150	1156	7.93E-05
MA0774.1	MEIS2	+	1152	1159	7.08E-05
MA0138.3	REST	+	1159	1178	1.95E-05
MA1981.2	ZNF530	+	1165	1178	3.35E-06
MA1976.2	ZNF320	-	1172	1191	9.35E-05
MA0770.1	HSF2	-	1174	1186	8.22E-06
MA0771.1	HSF4	-	1174	1186	1.90E-05
MA0486.2	HSF1	-	1174	1186	2.43E-05
MA1972.1	ZFP14	-	1177	1191	4.35E-05
MA0770.1	HSF2	+	1179	1191	3.47E-06
MA0486.2	HSF1	+	1179	1191	1.69E-05
MA0771.1	HSF4	+	1179	1191	3.52E-05

MA1652.2	ZKSCAN5	-	1191	1199	3.78E-05
MA1716.2	ZNF76	+	1216	1232	1.96E-05
MA0696.1	ZIC1	+	1217	1230	8.05E-05
MA0139.2	CTCF	+	1221	1235	5.10E-05
MA1629.2	Zic2	-	1222	1230	3.92E-05
MA1723.2	PRDM9	+	1227	1246	9.57E-05
MA0163.1	PLAG1	+	1228	1241	5.52E-05
MA0528.3	ZNF263	+	1236	1242	4.39E-05
MA1719.2	ZNF816	+	1238	1252	5.87E-05
MA2121.1	ZNF213	-	1243	1254	9.10E-05
MA0155.1	INSM1	+	1246	1257	2.08E-05
MA1569.2	TFAP2E	-	1247	1255	6.30E-06
MA0812.2	TFAP2B	-	1247	1255	6.30E-06
MA1569.2	TFAP2E	+	1247	1255	1.18E-05
MA0814.3	TFAP2C	+	1247	1255	1.67E-05
MA0003.5	TFAP2A	-	1247	1255	2.30E-05
MA0812.2	TFAP2B	+	1247	1255	3.05E-05

3.3 Examining the functional conservation of the SOX7-58 enhancer across species

Unfortunately, TRASNFAC and FIMO produced markedly different *in silico* predictions for SOX7-58. This reduces the certainty in either result and underscores the limitations of computational methodology that depend heavily on initial data input. Indeed, whilst *in silico* motif analysis provides a valuable first-pass method for identifying candidate TF binding sites, it cannot distinguish functional motifs from spurious sequence matches. Since functionally important motifs are often subject to purifying selection, and therefore often remain conserved across species, I next wanted to assess the evolutionary conservation of SOX7-58.

As demonstrated in **Section 3.1**, the SOX7-58 enhancer is active in angiogenic ECs. If the transcriptional mechanisms driving this activity are functionally important, they would be expected to show evolutionary conservation. I therefore sought to determine whether orthologues of SOX7-58 could recapitulate a similar GFP expression pattern in F0 zebrafish embryos. Demonstrating conservation of enhancer activity across species would support the idea that the underlying regulatory architecture – including critical TF binding motifs – is evolutionarily maintained.

Orthologous enhancers to SOX7-58 were identified using the Vertebrate Multiz Alignment and Conservation Track on the UCSC Genome Browser (https://genome.ucsc.edu). To test the functional conservation, the human, mouse and opossum orthologues of the SOX7-58 sequence were selected (sequences are in **Chapter 2**). Since humans and mice share a relatively recent common ancestor, the mouse genome sequence was chosen to provide a test of conservation in placental mammals.[253] The inclusion of opossum, a marsupial species, offers a more distant evolutionary perspective, allowing for the investigation of enhancer conservation across a broader phylogenetic span.

To assess the activity of the SOX7-58 orthologues, each sequence was cloned upstream of an E1B minimal promoter driving GFP, and inserted into a Tol2 destination vector. The resulting constructs were: pE1b-human*SOX7-58:*GFP, pE1b-mouse*SOX7-58:*GFP, and pE1b-opossum*SOX7-58:*GFP. Along with Tol2 transposase, these were injected into one-cell stage zebrafish embryos to generate three F0 zebrafish populations, each expressing a different SOX7-58 orthologue. All injections were performed on the same day, to limit variability.

In total, 90 embryos expressed the pE1b-human*SOX7-58:*GFP transgene; 81 embryos expressed the pE1b-mouse*SOX7-58:*GFP transgene; and 91 embryos expressed the pE1b-opossum*SOX7-58:*GFP transgene. At 30 hpf, the GFP expression was quantitively assessed as either being present or absent in ECs (Table 23).

Table 23: Summary table showing the percentange of F0 zebrafish expressing each orthologue of *SOX7-58:*GFP transgene analysed at 28 hpf, raw numbers are in brackets

SOX7-58 Orthologues	Percentage of F0 zebrafish with EC GFP expression (Raw Number)	Percentage of F0 zebrafish with no EC GFP Expression (Raw Number)
Mouse	11% (9)	89% (72)
Opossum	8% (7)	92% (84)
Human	42% (38)	58% (52)

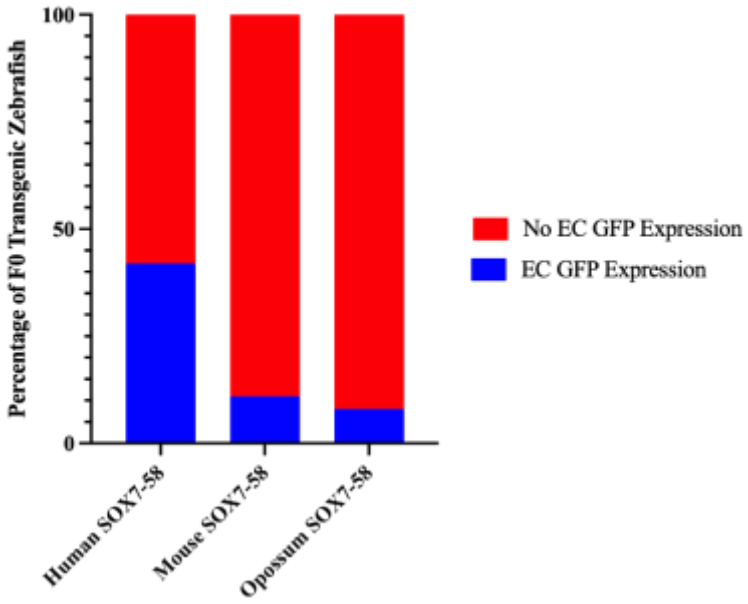

Figure 17: Bar graph depicts the percentage of F0 transgenic zebrafish embryos with GFP EC expression, driven by the human, mouse, and opossum orthologues of SOX7-58 at 28 hpf. The bar graph serves as a visual representation of the data in the table above.

Previously, enhancer expression has been defined as endothelial if more than 5% of injected F0 embryos express the enhancer:GFP transgene in ECs.[229] By this criterion, all three SOX7-58 orthologues tested had EC activity. However, the reproducibility of EC GFP expression varied considerably. Among the F0 zebrafish expressing the human*SOX7-58:*GFP transgene, 42% had GFP expression in ECs, compared with only 11% for the mouse orthologue and 8% for the opossum orthologue. Qualitatively, the human SOX7-58 enhancer also drove the most penetrant EC GFP expression, most notably in the ISVs. In comparison, GFP expression from the mouse and opossum orthologues was sparse, with very few ISVs labelled. Expression from the mouse orthologue was particularly limited, with only a few ECs expressing GFP. Whilst weaker than the human orthologue, the opossum orthologue had more pronounced GFP expression in the DLAV.

To assess whether GFP expression patterns changed over time, the same embryos were maintained until 48 hpf. Although GFP expression was not quantified at this timepoint, the overall proportions of F0 zebrafish embryos with EC GFP expression remained roughly the same. However, for each F0 population, the robustness of GFP expression pattern increased. This was particularly notable in F0 zebrafish expressing either the

human and mouse *SOX7-58:*GFP transgenes, both of which showed expanded expression in the ISVs. At 48 hpf, the human *SOX7-58:* GFP transgene also had increased activity in the DLAV and DA.

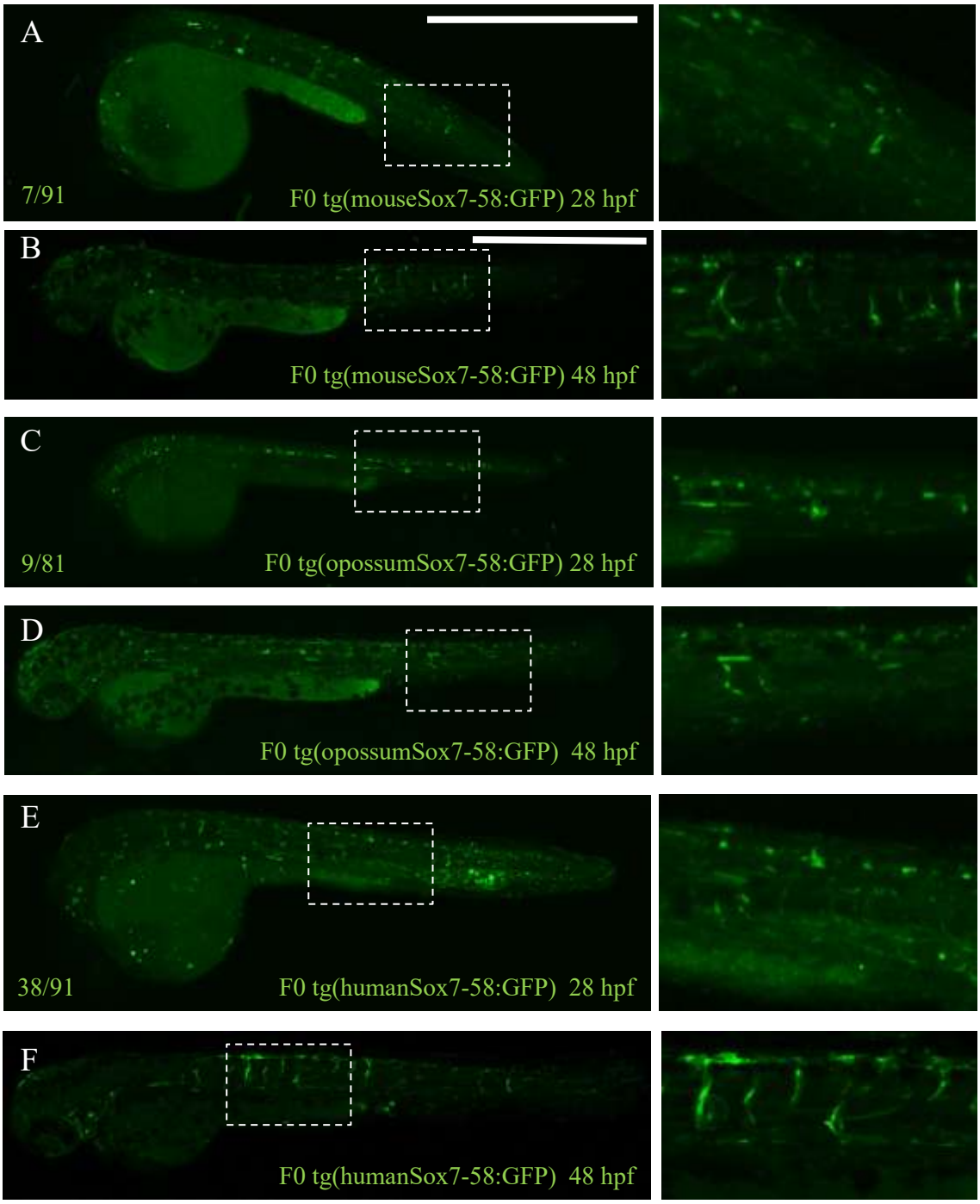

Figure 18: All three orthologues of *SOX7-58:*GFP were able to drive vascular GFP **expression** (A) shows a representative F0 zebrafish expressing the mouse*SOX7-58:*GFP at 28 hpf, with 7/91 having GFP expression in ECs, (B) shows a representative F0 zebrafish expressing the mouse*SOX7-58:*GFP at 48 hpf. (C) shows a representative F0 zebrafish expressing the opossum*SOX7-58:*GFP at 28 hpf, with 9/81 having GFP expression in ECs, (D) shows a representative F0 zebrafish expressing the opossum*SOX7-58:*GFP at 48 hpf. (E) shows a representative F0 zebrafish expressing the human*SOX7-58:*GFP at 28 hpf, with 38/91 having GFP expression in ECs, (F) shows a representative F0 zebrafish expressing the human*SOX7-58:*GFP at 48 hpf. Scale bar represents 1mm.

3.4 Phylogenetic foot-printing SOX7-58 to identify highly conserved regions

Since the human, mouse, and opossum SOX7-58 orthologues all drove EC GFP expression in the developing F0 zebrafish embryo, it is likely that these orthologues share conserved mechanisms of transcriptional regulation. This is regardless of the fact that the numbers of F0 zebrafish expressing GFP was different. To investigate this, I phylogenetically foot-printed SOX7-58 to identify highly conserved regions. This was done under the assumption that highly conserved regions are more likely to contain essential TF binding motifs.

The first step in phylogenetic foot-printing is to align the sequences from different species. This was achieved using ClustalW (https://www.genome.jp/tools-bin/clustalw). ClustalW is a multiple sequence alignment algorithm which computes pairwise similarities between all the input sequences, and then progressively aligns the sequences, with the most similar sequences aligned first.[254] In addition, ClustalW provides an alignment score. This reflects the sum-of-pairs score, normalised to the maximum possible score for that alignment.[255]

$$\text{SP\%} = \frac{\text{Observed SP score}}{\text{Maximum possible SP score}} \times 100$$

Equation 1: Normalised Sum-of-Pairs (SP%) Score for Multiple Sequence Alignment. The SP% score represents the quality of a multiple sequence alignment as a percentage where the *Observed SP score* is the sum of all pairwise alignment scores (including matches, mismatches, and gaps), and the *Maximum possible SP score* corresponds to an ideal alignment in which all sequences are perfectly conserved. Higher SP% values indicate better alignment quality, with 100% representing a perfectly conserved alignment.

As expected, the human and mouse sequences had the closest alignment (alignment score 67). The alignment score of the human and opossum orthologues (32) was very similar to that between the mouse and opossum orthologues (37), suggesting limited conservation across the marsupial-placental boundary. It is perhaps interesting that in the F0 transgenic zebrafish, at 30 hpf, the human and mouse SOX7-58 orthologues did not produce more similar patterns of EC GFP expression: the mouse and opossum SOX7-58 had very

similarly low rates of GFP expression in ECs compared with the human orthologue. This highlights that sequence conservation alone does not fully predict enhancer activity.

Across the human, mouse, and opossum orthologue sequences, I identified eight highly conserved regions (R1-R8). These were defined as regions of at least five nucleotides in length, with complete alignment across sequences. Although five nucleotides is an arbitrary length, it was chosen because five nucleotides is often considered the smallest number of nucleotides in a typical eukaryotic TF binding motif.[256] It should be noted that the number of highly conserved regions does not necessarily mean a high level of conservation, although in the case of the human and mouse this is also true. Of much more importance is the length of the conserved regions; whilst eukaryotic TF binding motifs can range in size from 5-31 nucleotides, the most evolutionarily stable distribution of TF binding motif lengths has an average of 9.9 nucleotides.[256] Therefore, conserved regions of at least 10 nucleotides are more likely to contain important TF binding motifs than smaller conserved regions with only five nucleotides.

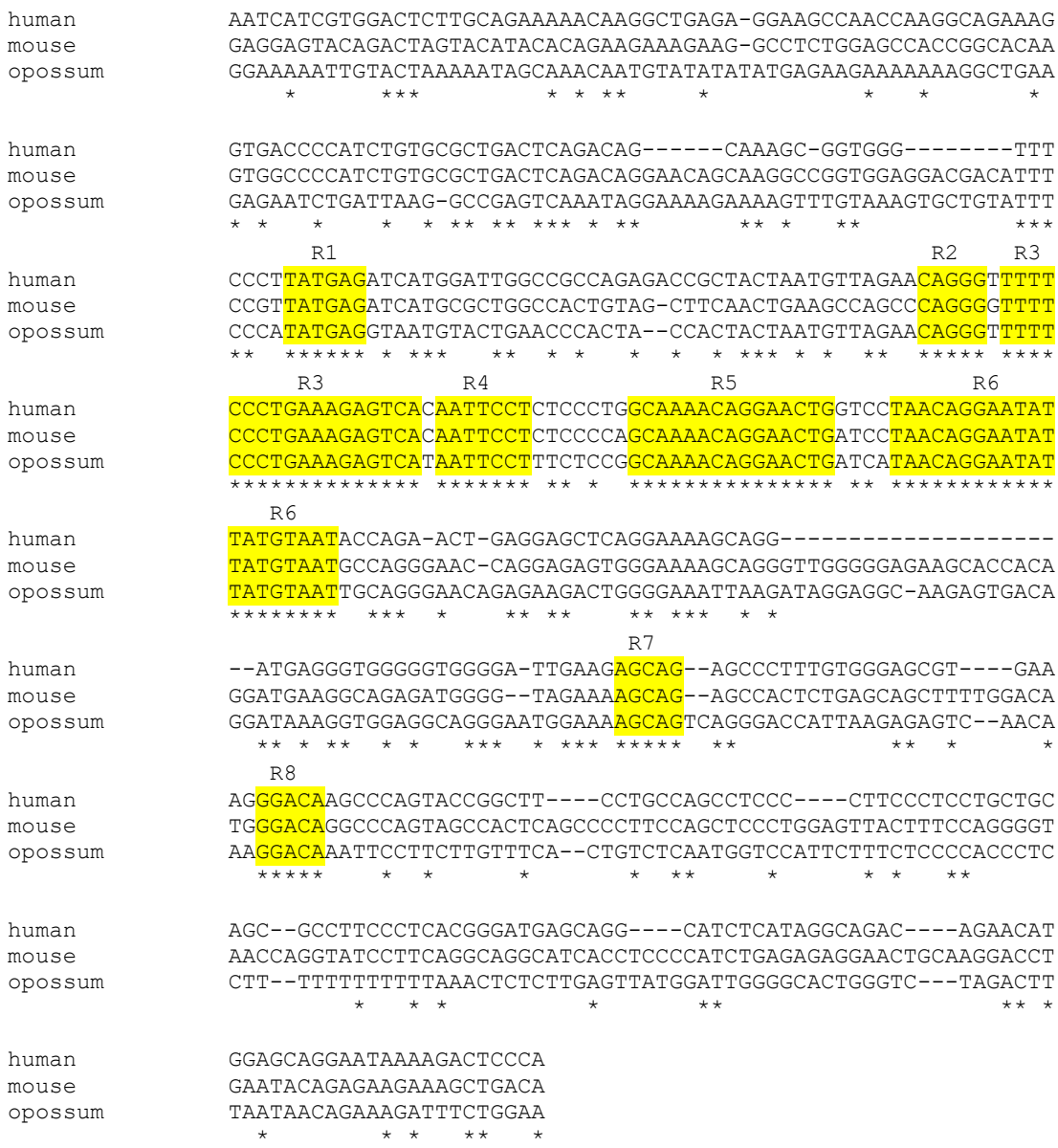

Figure 19: Eight highly conserved regions (labelled R1-R8) were identified upon alignment of the human, mouse and opossum orthologous sequences for SOX7-58. These have been highlighted in yellow.

* indicate alignment across all three species

3.5 Using sequence analysis to predict transcription factors binding to SOX7-58

Having identified eight highly conserved regions (R1-R8) between the human, mouse and opossum orthologous SOX7-58 sequences, I manually inspected these sequences for TF motifs for factors already implicated in EC regulation (Table 24).[24]

ETS factors motifs were identified in R3, R4, R5, and R6 (Figure 20). Given that SOX7-58 has EC activity, and ETS factors are thought to regulate all EC-specific enhancers, this was reassuring.[23,179,183] However, the ETS TF binding site has a relatively short and degenerate consensus binding motif, which occurs frequently by chance in the genome. As a result, the probability of false positives in ETS motif prediction is high. One potential indicator that a ETS TF binding motif may be functional is through the identification of a FOX:ETS motif: synergistic binding of FOX and ETS TFs to FOX:ETS motifs is alone sufficient to direct exclusive vascular expression, and FOX:ETS motifs are a common, although not ubiquitous, occurrence in endothelial enhancers.[23,177] In the SOX7-58 enhancer sequence, FOX:ETS TF binding motifs were identified in R5 and R6 (Figure 20).

R3 contains a possible FOS:JUN TF binding site, associated with the activator protein 1 (AP1) TF family, which has been previously associated with angiogenesis.[24,257] In particular, JunB has been shown to be upregulated in tip ECs as they form in the retinal and embryonic skin vasculature. Jun is thought to function as a transcriptional activator by forming a heterodimer with Fos.[258-260]

The R3 conserved sequence also contained a possible TCF/LEF motif. TCF/LEF TFs are the transcriptional effectors of canonical Wnt signalling pathway. This pathway has also been associated with angiogenesis, in particular, CNS angiogenesis.[199,209-211,261] Conditional inactivation of β-catenin in murine ECs results in aberrant vascular patterns, with the vessels becoming more fragile and permeable.[209]

Perhaps the most surprising find was the identification of a binding site for CCAAT/enhancer-binding protein (C/EBP) in R6. C/EBPδ has previously been linked with lymphangiogenesis, and in a tumour environment, C/EBPβ has been shown to

enhance VEGF2 expression and promote angiogenesis.[262,263] However, there is limited published data linking C/EBP to angiogenesis in physiological contexts.

Table 24: List of common TFs for EC-specific enhancers: Professor Sarah De Val

TF	Sequence Logo	Type	Source	TF	Sequence Logo	Type	Source
ETV2		HT-Selex	JASPAR 23332764	GATA/TAL1	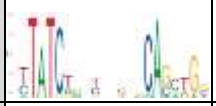	ChIP-seq	Primary publication 20566737
ETV2		ChIP-seq	Primary publication 25802403	TAL1		ChIP-seq	Primary publication 20566737
FLI1		ChIP-seq	JASPAR/ PAZAR 17916232	SMAD 4		ChIP-seq	JASPAR2018 / PAZAR 17916232
FLI1		HT-Selex	JASPAR 23332764	SMAD 4		ChIP-seq	Primary publication 21828274
FLI1		ChIP-seq	Primary publication 30500808	SMAD 1SMAD5		ChIP-seq	Primary publication 21764776
ERG		ChIP-seq	Primary publication 30500808	HIF1A		ChIP-seq	JASPAR/ ReMap2018
ERG		ChIP-seq	JASPAR/ PAZAR 17916232	HIF1A		ChIP-seq	Primary publication 22645302
ETS1		ChIP-seq	Primary publication 28851877	RBPJ		ChIP-seq	JASPAR/ ReMap2018
ETS1		ChIP-seq	JASPAR/ PAZAR 17916232	RBPJ		From notes	From SDV notes
ELK3		ChIP-seq	Primary publication 25401928	MEF2A		ChIP-seq	JASPAR/ ReMap2018
ELK3		HT-Selex	JASPAR 23332764	MEF2C		ChIP-seq	JASPAR/ ENCODE
FOXC1		HT-Selex	JASPAR 23332764	JUNB		ChIP-seq	JASPAR/ ENCODE
FOXC2		HT-Selex	JASPAR 23332764	MAFB		ChIP-seq	JASPAR
FOXC2		ChIP-chip	Primary publication 19398761	MAFF		ChIP-seq	JASPAR/ ENCODE
FOXO1		ChIP-seq	JASPAR/ PAZAR 17916232	TEAD1		ChIP-seq	JASPAR/ ReMap2022

FOXP1		ChIP-seq	JASPAR/ PAZAR 17916232	SOX7	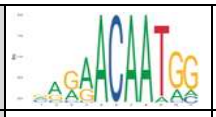	ChIP-seq	Primary publication 22645302
GATA2		ChIP-seq	JASPAR/ ENCODE	SOX17	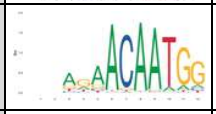	ChIP-seq	JASPAR/ ReMap2022
GATA2		ChIP-seq	Primary publication 21808000	SOX18	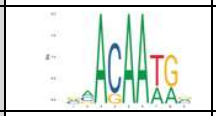	ChIP-seq	Primary publication 28137359
DACH1		CAST analysis/EMSA	20351289	POU3F2/BRN2		HT-Selex	JASPAR 23332764
TCF4		ChIP-seq	JASPAR/ Re-map	RUNX1		ChIP-seq	JASPAR 8413232
LEF1	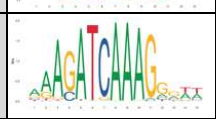	HT-Selex	JASPAR 23332764	KLF4	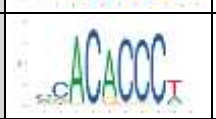	ChIP-seq	JASPAR 29126285
LEF1		HT-Selex	JASPAR 19443739	KLF6		HT-Selex	JASPAR 28473536
NFATC1		?	JASPAR 23332764	SRF		ChIP-seq	JASPAR/ ENCODE
NFATC1		ChIP-seq	Primary publication 25157100	SRF		HT-Selex	JASPAR 23332764
NFATC4		ChIP-seq	JASPAR/ PAZAR 17916232	NFKB1		ChIP-seq	JASPAR/ PAZAR
ISL1		ChIP-seq	JASPAR 18585359	RELA		SELEX	JASPAR
FOXO1/ELK1		HT-SELEX	JASPAR 26550823	C/EBP-related		ChIP-seq	JASPAR 9122243

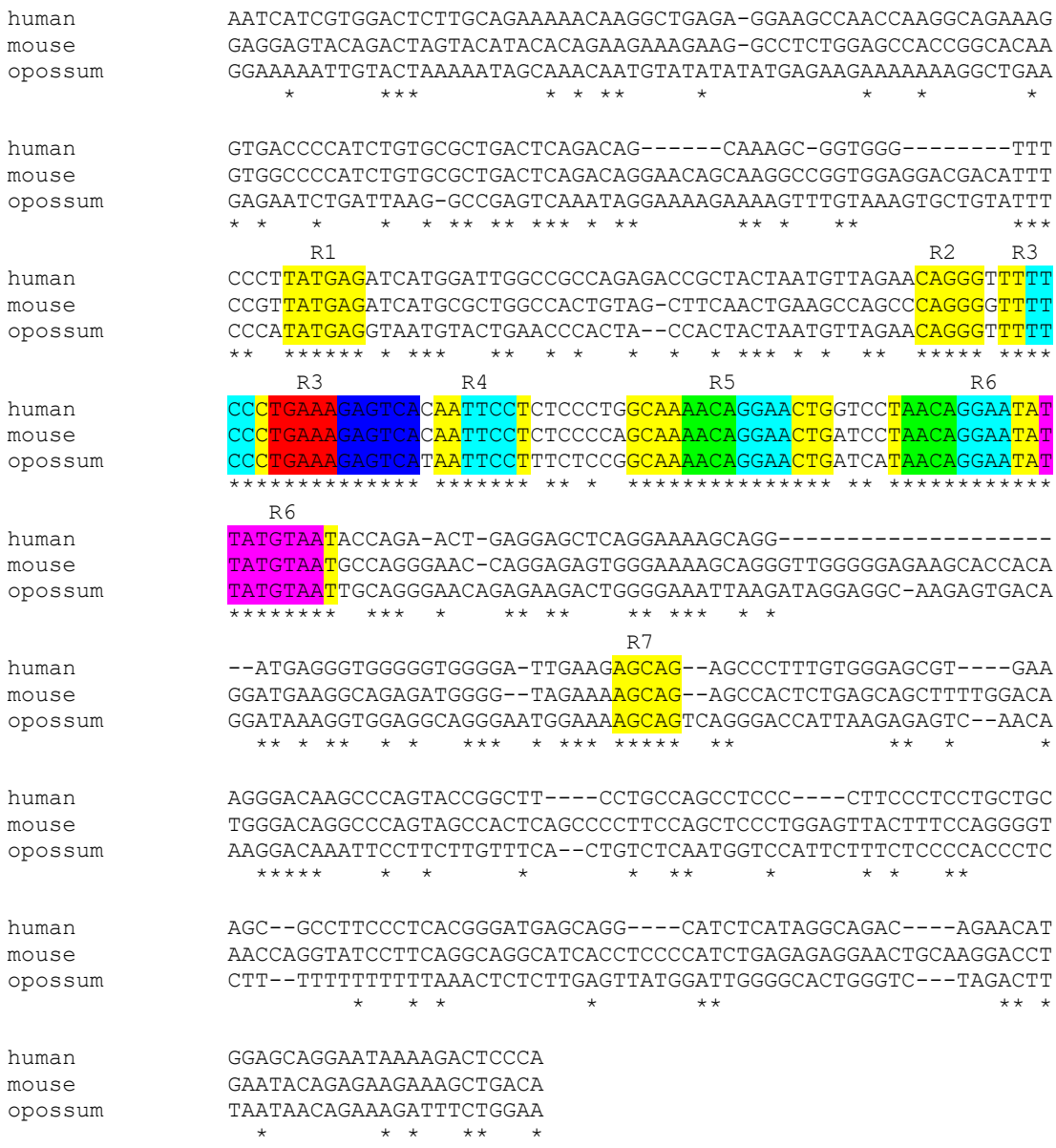

Figure 20: In the aligned SOX7-58 enhancer sequence, TF binding sites have been highlighted (colour): ETS (light blue), FOX:ETS (light green), FOS:JUN (dark blue) and SOXCEBP (pink), TCF/LEF (red).

3.6 Enhancer mutagenesis to identify key transcription factor motifs

After identifying putative TF binding motifs within the SOX-58 enhancer, I next wanted to examine their functionality *in vivo*. To do this, mutated versions of SOX7-58 were chemically synthesised as GeneArt®Strings™ from Thermo Fisher, each with a targeted disruption either in individual putative TF binding motifs, or in combinatorial TF binding motifs (Table 24). These mutant SOX7-58 sequences were then cloned upstream of pE1B and GFP, and inserted into a Tol2 destination vector. As before, these constructs were injected into one-cell stage zebrafish embryos, along with Tol2 transposase mRNA, to achieve genomic integration, and the subsequent GFP expression pattern was scored at 48 hpf. Alongside the injection of each mutated *SOX7-58:*GFP transgene, another clutch of embryos was injected with the original *SOX7-58:*GFP transgene. This allows the functional importance of each mutated TF binding motif to be systematically compared to both the original SOX7-58 sequence, and other mutated versions of SOX7-58, enabling the identification of essential, redundant, or combinatorial TF motifs.

Table 25: Five synthetic SOX7-58 sequences cloned into the transgene, four of which have targeted mutations in putative TF binding motifs (changes in red).

	Sequence
SOX7-58	AATCATCGTGGACTCTTGCAGAAAAACAAGGCTGAGAGGAAGCCAACCAAGGCAGAAAGGTG ACCCCATCTGTGCGCTGACTCAGACAGCAAAGCGGTGGGTTTCCCTTATGAGATCATGGATT GGCCGCCAGAGACCGCTACTAATGTTAGAACAGGGTTTTTCCCTGAAAGAGTCACAATTCCT CTCCCTGGCAAAACAGGAACTGGTCCTAACAGGAATATTATGTAATACCAGAACTGAGGAGC TCAGGAAAAGCAGGATGAGGGTGGGGGTGGGGATTGAAGAGCAGAGCCCTTTGTGGGAGCGT GAAAGGGACAAGCCCAGTACCGGCTTCCTGCCAGCCTCCCCTTCCCTCCTGCTGCAGCGCCT TCCCTCACGGGATGAGCAGGCATCTCATAGGCAGACAGAACATGGAGCAGGAATAAAAGACT CCCA
mutFOX:ETS SOX7-58	AATCATCGTGGACTCTTGCAGAAAAACAAGGCTGAGAGGAAGCCAACCAAGGCAGAAAGGTG ACCCCATCTGTGCGCTGACTCAGACAGCAAAGCGGTGGGTTTCCCTTATGAGATCATGGATT GGCCGCCAGAGACCGCTACTAATGTTAGAACAGGGTTTTTCCCTGAAAGAGTCACAATTCCT CTCCCTGGCAAA**tC**t**a**GAACTGGTCCTA**t**C**ta**GAATATTATGTAATACCAGAACTGAGGAGC TCAGGAAAAGCAGGATGAGGGTGGGGGTGGGGATTGAAGAGCAGAGCCCTTTGTGGGAGCGT GAAAGGGACAAGCCCAGTACCGGCTTCCTGCCAGCCTCCCCTTCCCTCCTGCTGCAGCGCCT TCCCTCACGGGATGAGCAGGCATCTCATAGGCAGACAGAACATGGAGCAGGAATAAAAGACT CCCA

mut[FOS:JUN, C/EBP, TCF/LEF] SOX7-58	AATCATCGTGGACTCTTGCAGAAAAACAAGGCTGAGAGGAAGCCAACCAAGGCAGAAAGGTG ACCCCATCTGTGCGCTGACTCAGACAGCAAAGCGGTGGGcTTCCCTTATGAGATCATGGATT GGCCGCCAGAGACCGCTACTAATGTTAGAACAGGGTTcTTCCCTGAtcccaaCACAATTCCT CTCCCTGGCAAAACAGGAACTGGTCCTAACAGGAATATTAgGgcATACCAGAACTGAGGAGC TCAGGAAAAGCAGGATGAGGGTGGGGGTGGGGATTGAAGAGCAGAGCCCTTTGTGGGAGCGT GAAAGGGACAAGCCCAGTACCGGCTTCCTGCCAGCCTCCCCTTCCCTCCTGCTGCAGCGCCT TCCCTCACGGGATGAGCAGGCATCTCATAGGCAGACAGAACATGGAGCAGGAATAAAAGACT CCCA
mutFOS:JUN SOX7-58	AATCATCGTGGACTCTTGCAGAAAAACAAGGCTGAGAGGAAGCCAACCAAGGCAGAAAGGTG ACCCCATCTGTGCGCTGACTCAGACAGCAAAGCGGTGGGTTTCCCTTATGAGATCATGGATT GGCCGCCAGAGACCGCTACTAATGTTAGAACAGGGTTTTTCCCTGAAcccaaCACAATTCCT CTCCCTGGCAAAACAGGAACTGGTCCTAACAGGAATATTATGTAATACCAGAACTGAGGAGC TCAGGAAAAGCAGGATGAGGGTGGGGGTGGGGATTGAAGAGCAGAGCCCTTTGTGGGAGCGT GAAAGGGACAAGCCCAGTACCGGCTTCCTGCCAGCCTCCCCTTCCCTCCTGCTGCAGCGCCT TCCCTCACGGGATGAGCAGGCATCTCATAGGCAGACAGAACATGGAGCAGGAATAAAAGACT CCCA
mutC/EBP SOX7-58	AATCATCGTGGACTCTTGCAGAAAAACAAGGCTGAGAGGAAGCCAACCAAGGCAGAAAGGTG ACCCCATCTGTGCGCTGACTCAGACAGCAAAGCGGTGGGTTTCCCTTATGAGATCATGGATT GGCCGCCAGAGACCGCTACTAATGTTAGAACAGGGTTTTTCCCTGAAAGAGTCACAATTCCT CTCCCTGGCAAAACAGGAACTGGTCCTAACAGGAATATTAgGgcATACCAGAACTGAGGAGC TCAGGAAAAGCAGGATGAGGGTGGGGGTGGGGATTGAAGAGCAGAGCCCTTTGTGGGAGCGT GAAAGGGACAAGCCCAGTACCGGCTTCCTGCCAGCCTCCCCTTCCCTCCTGCTGCAGCGCCT TCCCTCACGGGATGAGCAGGCATCTCATAGGCAGACAGAACATGGAGCAGGAATAAAAGACT CCCA
mutTCF/LEF SOX7-58	AATCATCGTGGACTCTTGCAGAAAAACAAGGCTGAGAGGAAGCCAACCAAGGCAGAAAGGTG ACCCCATCTGTGCGCTGACTCAGACAGCAAAGCGGTGGGTTTCCCTTATGAGATCATGGATT GGCCGCCAGAGACCGCTACTAATGTTAGAACAGGGTTTTTCCCTGAtcGGAGTCACAATTCC TCTCCCTGGCAAAACAGGAACTGGTCCTAACAGGAATATTAgGgcATACCAGAACTGAGGAG CTCAGGAAAAGCAGGATGAGGGTGGGGGTGGGGATTGAAGAGCAGAGCCCTTTGTGGGAGCG TGAAAGGGACAAGCCCAGTACCGGCTTCCTGCCAGCCTCCCCTTCCCTCCTGCTGCAGCGCC TTCCCTCACGGGATGAGCAGGCATCTCATAGGCAGACAGAACATGGAGCAGGAATAAAAGAC TCCCA

3.6.1 FOXETS

The first putative TF binding site I examined was the FOX:ETS site. My *in silico* analysis, identified two FOX:ETS motifs, one in R5 and one in R6 (Figure 20). To ablate both FOX and ETS binding together at these putative FOX:ETS TF binding motifs, base substitutions were made at the centre of the double motif, effectively mutating both the FOX and ETS motifs. The sequence was changed from **AACAG** to **AtCta**, by replacing adenine with thymine in position 2 and 4, and guanine with adenine in position 5.

86 zebrafish injected with the mutFOX:ETS *SOX7-58:*GFP transgene survived until analysis at 48 hpf, and were analysed alongside 124 zebrafish injected with the *SOX7-58:*GFP transgene that survived (Table 26). For both clutches, the EC-specific expression pattern of GFP was assessed as either being absent, weak, medium, or strong. This scoring system was designed to provide more quantitative information about the robustness of EC expression, as well as its reproducibility.

Embryos injected with the mutFOX:ETS *SOX7-58:*GFP transgene has no detectable GFP activity (0/86 with EC GFP expression). This result aligns with existing literature, suggesting that FOX:ETS motifs are very important for the activity EC-specific enhancers.[23] However, both of the putative FOX:ETS TF binding motifs were mutated in concert, and therefore it is not possible to discern if one is functional and the other not. Nonetheless, this experiment demonstrated that the FOX:ETS binding motifs are absolutely essential to the SOX7-58 enhancer activity.

Table 26: Summary table showing the percentange of F0 zebrafish (injected with either the *SOX7-58:*GFP transgene or the mutFOX:ETS *SOX7-58:*GFP transgene) with strong, medium, weak or no GFP expression in ECs at 48 hpf, raw numbers are in brackets

Transgene	Percentage of F0 zebrafish with strong EC GFP expression (Raw Number)	Percentage of F0 zebrafish with medium EC GFP expression (Raw Number)	Percentage of F0 zebrafish with weak EC GFP expression (Raw Number)	Percentage of F0 zebrafish with no EC GFP expression (Raw Number)
*SOX7-58:*GFP	24% (30)	36% (45)	14% (17)	26% (32)
mutFOX:ETS *SOX7-58:*GFP	0% (0)	0% (0)	0% (0)	100% (86)

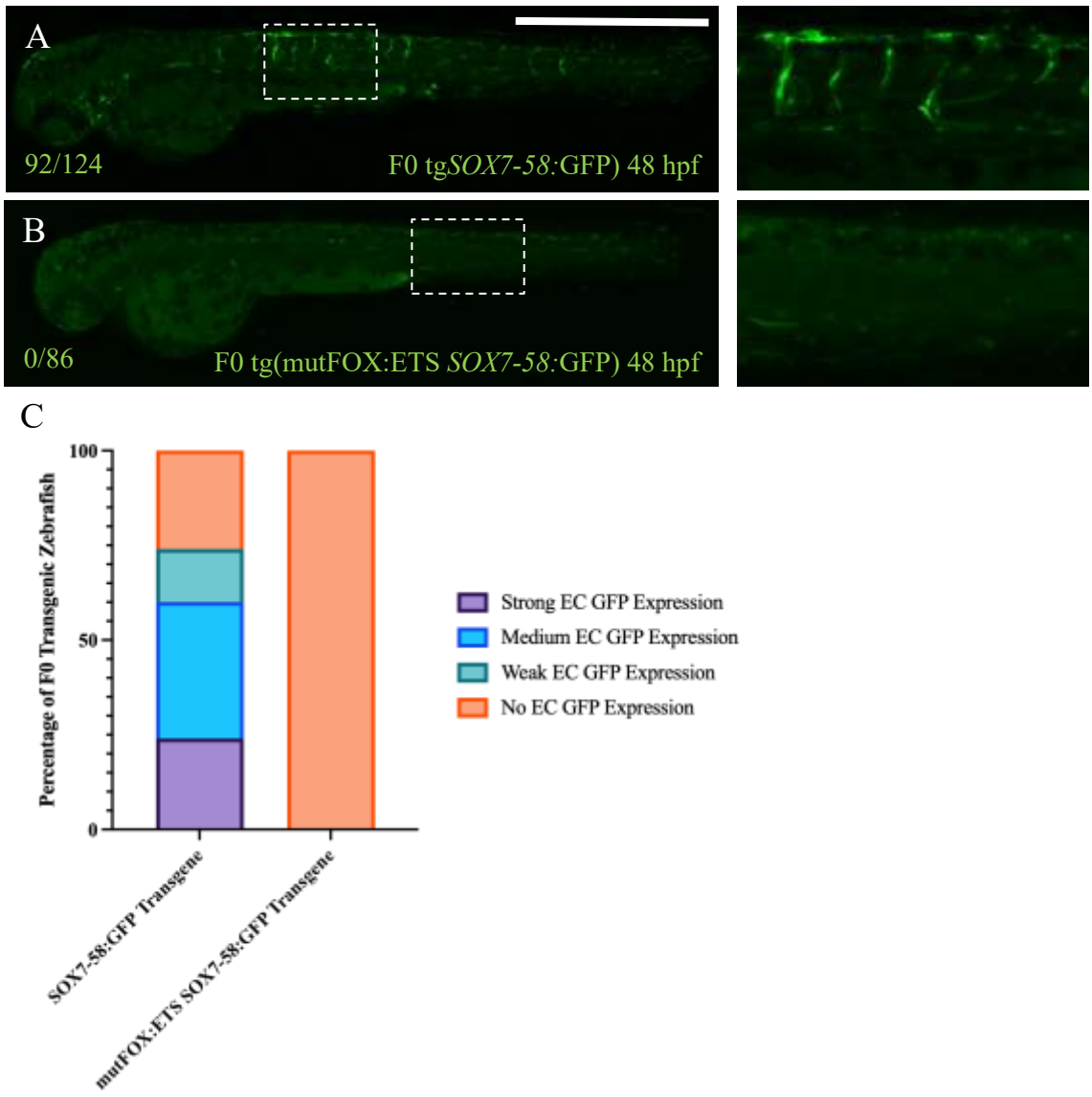

Figure 21: F0 transgenic zebrafish embryo expressing the mutFOX:ETS SOX7-58:GFP transgene had completely ablated EC GFP expression. (A) shows a representative F0 zebrafish injected with the SOX7-58:GFP transgene at 48 hpf, with (B) showing a representative F0 zebrafish injected with the mutFOX:ETS SOX7-58:GFP transgene at 48 hpf. (C) Bar graph to compare the percentage of F0 zebrafish embryos with either strong, medium, weak or no EC GFP expression. The bar graph serves as a visual representation of the data in the table above. Scale bar represents 1mm.

3.6.2 Testing the sufficiency of the putative ETS binding motifs

My analysis so far established that at least one of the FOX:ETS binding motif is both essential and functional for SOX7-58 enhancer activity. This raises the possibility that FOX and ETS motifs alone may be sufficient for angiogenic expression of SOX7-58. I therefore wanted to determine whether any non-ETS/FOX motifs were required for activity of this enhancer. To investigate this, I generated a mutant SOX7-58 enhancer (mut[FOS:JUN, C/EBP, TCF/LEF] SOX7-58) containing targeted mutations in all of the other putative TF binding motifs identified (TCF/LEF, FOS:JUN, and C/EBP). This deliberately left the putative ETS and FOX:ETS motifs intact.

121 zebrafish embryos injected with the mut[FOX, FOS:JUN, C/EBP, TCF/LEF] *SOX7-58:*GFP transgene survived until analysis at 48 hpf, alongside 130 embryos injected with the *SOX7-58:*GFP transgene (Table 27). At 48 hpf, F0 transgenic zebrafish expressing the mut[FOX, FOS:JUN, C/EBP, TCF/LEF] *SOX7-58:*GFP transgene showed significantly less GFP expression: fewer zebrafish showed any GFP expression in ECs, and those that showed EC expression had very limited expression (recorded here as "weak"). This reduction suggests that the TFs binding to the disrupted TF motifs contribute to the expression of SOX7-58 activity. However, despite this significant reduction in expression, GFP expression remained restricted to ECs. This suggests that the ETS alone may be sufficient to drive some activation of the enhancer to endothelial cells. This is not entirely concordant with previous work from my group, which found that although ETS is essential for angiogenic-specific enhancer activity patterns, it is not the primary regulator of gene expression pattern.[183] However, the mut[FOS:JUN, C/EBP, TCF/LEF] *SOX7-58:*GFP transgene drove such weak enhancer activity that definitive conclusions about spatial specificity can only be limited.

Table 27: Summary table showing the percentange of F0 zebrafish (injected with either the *SOX7-58:*GFP transgene or the mut[FOS:JUN, C/EBP, TCF/LEF] *SOX7-58:*GFP transgene) with strong, medium, weak or no GFP expression in ECs at 48 hpf, raw numbers are in brackets.

Transgene	Percentage of F0 zebrafish with strong EC GFP expression (Raw Number)	Percentage of F0 zebrafish with medium EC GFP expression (Raw Number)	Percentage of F0 zebrafish with weak EC GFP expression (Raw Number)	Percentage of F0 zebrafish with no EC GFP expression (Raw Number)
*SOX7-58:*GFP	8% (11)	70% (91)	0% (0)	22% (28)
mut[FOS:JUN, C/EBP, TCF/LEF] *SOX7-58:*GFP	0 (0)	1% (1)	12% (14)	88% (106)

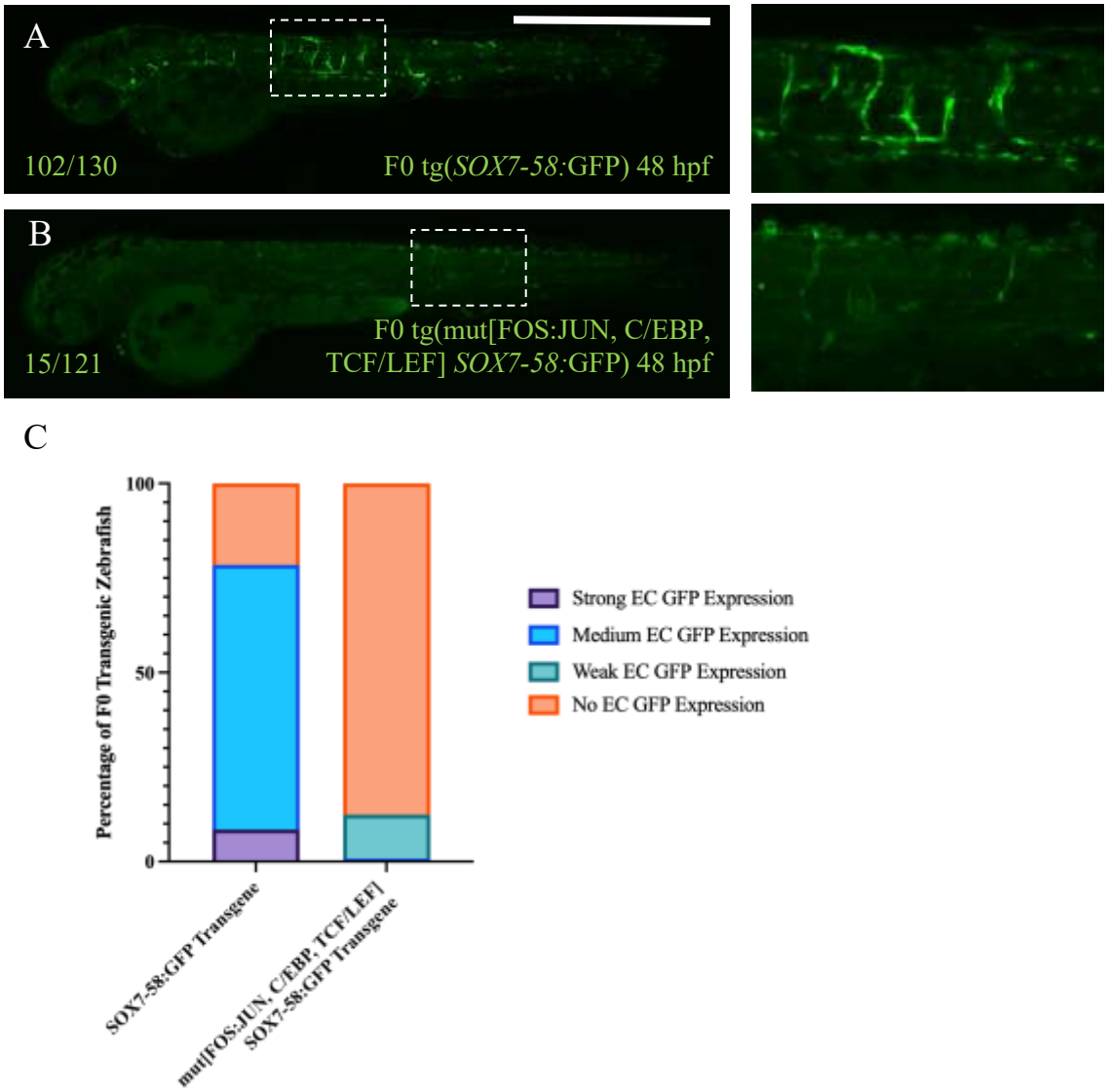

Figure 22: F0 transgenic zebrafish embryo expressing the mut[FOS:JUN, C/EBP, TCF/LEF] SOX7-58:GFP transgene had almost ablated EC GFP expression. (A) shows a representative F0 zebrafish injected with the SOX7-58:GFP transgene at 48 hpf, with (B) showing a representative F0 zebrafish injected with the mut[FOS:JUN, C/EBP, TCF/LEF] SOX7-58:GFP transgene at 48 hpf. (C) Bar graph to compare the percentage of F0 zebrafish embryos with either strong, medium, weak or no EC GFP expression. The bar graph serves as a visual representation of the data in the table above. Scale bar represents 1mm.

3.6.3 FOS:JUN

The first mutagenesis experiments revealed an important role for ETS and FOX:ETS motifs in SOX7-58 activity, whilst also demonstrating that these motifs were insufficient for full enhancer activity. Therefore, I hypothesised that other TFs also bind the SOX7-58 enhancer and contribute to the specific angiogenic EC pattern. My earlier analysis identified three other putative TF binding motifs, for FOS:JUN, C/EBP, and TCF/LEF. In order to dissect contribution of each of these motifs to enhancer activity, I next generated three different mutant SOX7-58 enhancer versions, each with a targeted mutation in a different putative TF binding motif (see Table 25).

To investigate the contribution of the putative FOS:JUN TF binding motif, I generated a mutFOS:JUN *SOX7-58:*GFP transgene, in which the putative FOS:JUN TF binding motif was altered from **GAGTCA** to **cccaaCA**, by replacing guanine, adenine, guanine in position 1, 2, and 3 respectively with cytosine, and then thymine and cytosine in positions 4 and 5 with adenine. 91 zebrafish embryos injected with the mutFOS:JUN *SOX7-58:*GFP transgene survived until analysis at 48 hpf, compared with 119 embryos injected with the *SOX7-58:*GFP transgene, and analysed as before (Table 28).

The majority of F0 transgenic zebrafish embryos injected with the mutFOS:JUN *SOX7-58:*GFP transgene had no detectable EC expression, although a small percentage of embryos exhibited weak EC expression (25/91 embryos). Although EC expression was not totally ablated, as seen in the mutFOXETS *SOX7-58:*GFP transgene, the proportions of embryos with EC expression remained statistically significant in comparison with embryos injected with the *SOX7-58:*GFP transgene ($P<0.0001$). This suggests that although the FOS:JUN binding motif is not absolutely essential in activating the enhancer, it is required for normal enhancer activity levels.

Interestingly, the F0 zebrafish injected with the mutFOS:JUN *SOX7-58:*GFP transgene only expressed GFP in the proximal ISVs, but not the distal tips. This is unlike the F0 transgenic injected with mutFOXETS *SOX7-58:*GFP transgene which had GFP throughout the entire length of the ISV. This raises the possibility that the mutFOS:JUN *SOX7-58:*GFP transgene lacks the regulatory elements necessary for full angiogenic expression.

Table 28: Summary table showing the percentange of F0 zebrafish (injected with either the *SOX7-58:*GFP transgene or the mutFOS:JUN *SOX7-58:*GFP transgene) with strong, medium, weak or no GFP expression in ECs at 48 hpf, raw numbers are in brackets

Transgene	Percentage of F0 zebrafish with strong EC GFP expression (Raw Number)	Percentage of F0 zebrafish with medium EC GFP expression (Raw Number)	Percentage of F0 zebrafish with weak EC GFP expression (Raw Number)	Percentage of F0 zebrafish with no EC GFP expression (Raw Number)
*SOX7-58:*GFP	25% (30)	38% (45)	12% (14)	25% (30)
mutFOS:JUN *SOX7-58:*GFP	0% (0)	0% (0)	27% (25)	73% (66)

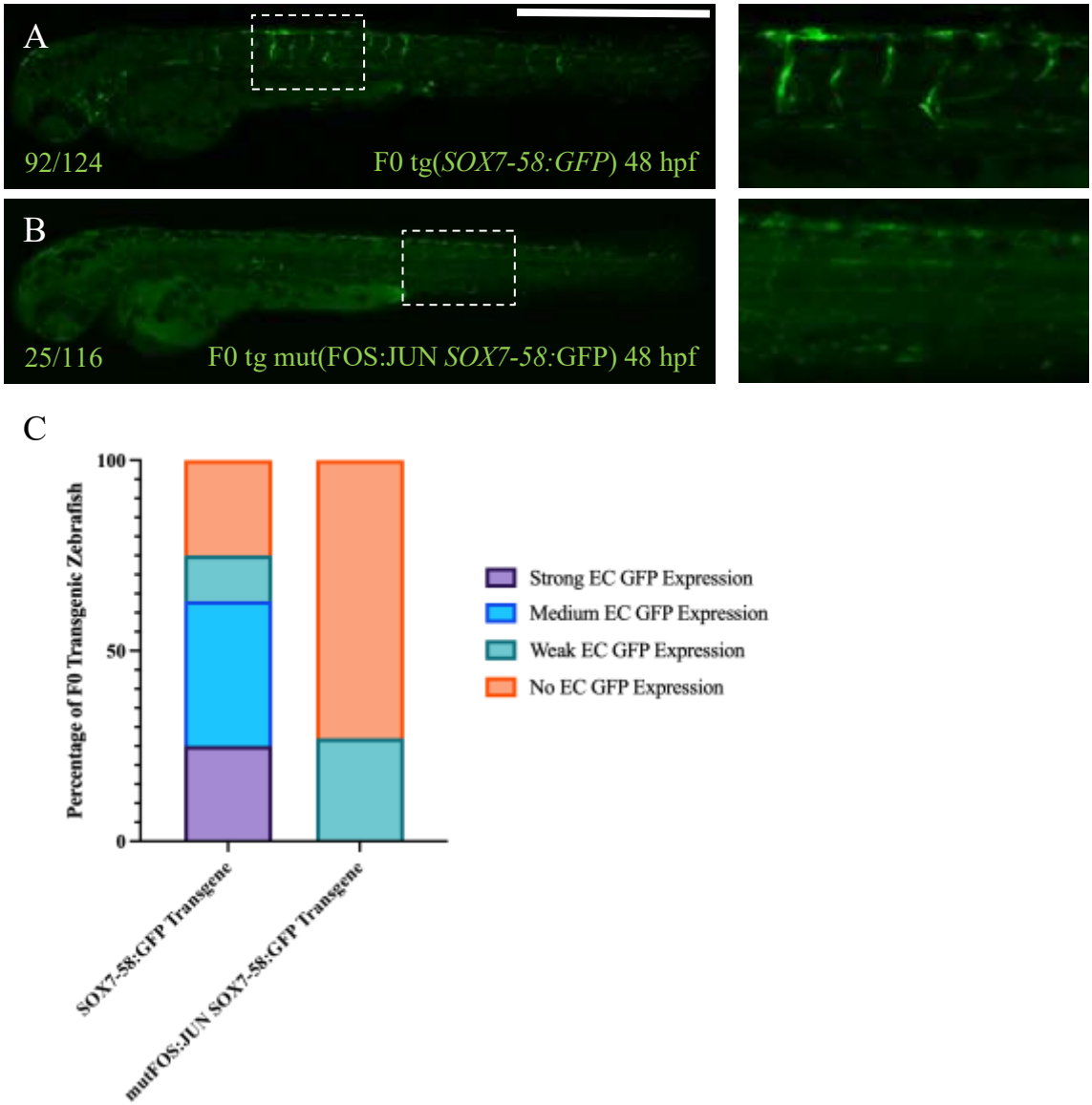

Figure 23: F0 transgenic zebrafish embryo expressing the mutFOS:JUN *SOX7-58:*GFP transgene had weaker EC GFP expression than F0 transgenic zebrafish embryo expressing the *SOX7-58:*GFP transgene. (A) shows a representative F0 zebrafish injected with the *SOX7-58:*GFP transgene at 48 hpf, with (B) showing a representative F0 zebrafish injected with the mutFOS:JUN *SOX7-58:*GFP transgene at 48 hpf. (C) Bar graph to compare the percentage of F0 zebrafish embryos with either strong, medium, weak or no EC GFP expression. The bar graph serves as a visual representation of the data in the table above. Scale bar represents 1mm.

3.6.4 C/EBP

To investigate the contribution of the putative C/EBP binding motif, base substitutions were made from **TTATGTAA** to **TTAgGgcA** within the SOX7-58 enhancer. This involved replacing the thymine position 4 and 6 with guanine, adenine in position 7 with cytosine. 101 zebrafish embryos injected with the mutC/EBP *SOX7-58:*GFP transgene survived until analysis at 48 hpf, alongside 130 embryos injected with the *SOX7-58:*GFP transgene (Table 29). The EC GFP expression pattern was analysed as before.

Whilst the majority of F0 transgenic zebrafish embryos injected with the mutC/EBP *SOX7-58:*GFP transgene also had no detectable EC expression, a greater proportion of embryos had some EC GFP expression (32/101) compared to the F0 zebrafish expressing the mutFOX:ETS *SOX7-58:*GFP, mut[FOX, FOS:JUN, C/EBP, TCF/LEF] *SOX7-58:*GFP or mutFOS:JUN *SOX7-58:*GFP transgenes. However, this expression was not especially localised, appearing in the all vascular structures, but with far less penetrance. Indeed, often only individual ECs were expressing GFP, whilst in the F0 transgenic zebrafish embryos expressing the *SOX7-58:*GFP transgene, whole ISVs were expressing GFP. This suggests that C/EBP, whilst not being entirely essential, is important in regulating the robustness of enhancer activity.

Table 29: Summary table showing the percentange of F0 zebrafish (injected with either the *SOX7-58:*GFP transgene or the mutC/EBP *SOX7-58:*GFP transgene) with strong, medium, weak or no GFP expression in ECs at 48 hpf, raw numbers are in brackets

Transgene	Percentage of F0 zebrafish with strong EC GFP expression (Raw Number)	Percentage of F0 zebrafish with medium EC GFP expression (Raw Number)	Percentage of F0 zebrafish with weak EC GFP expression (Raw Number)	Percentage of F0 zebrafish with no EC GFP expression (Raw Number)
*SOX7-58:*GFP	8% (11)	70% (91)	0% (0)	22% (28)
mutC/EBP *SOX7-58:*GFP	0% (0)	5% (5)	26% (26)	69% (70)

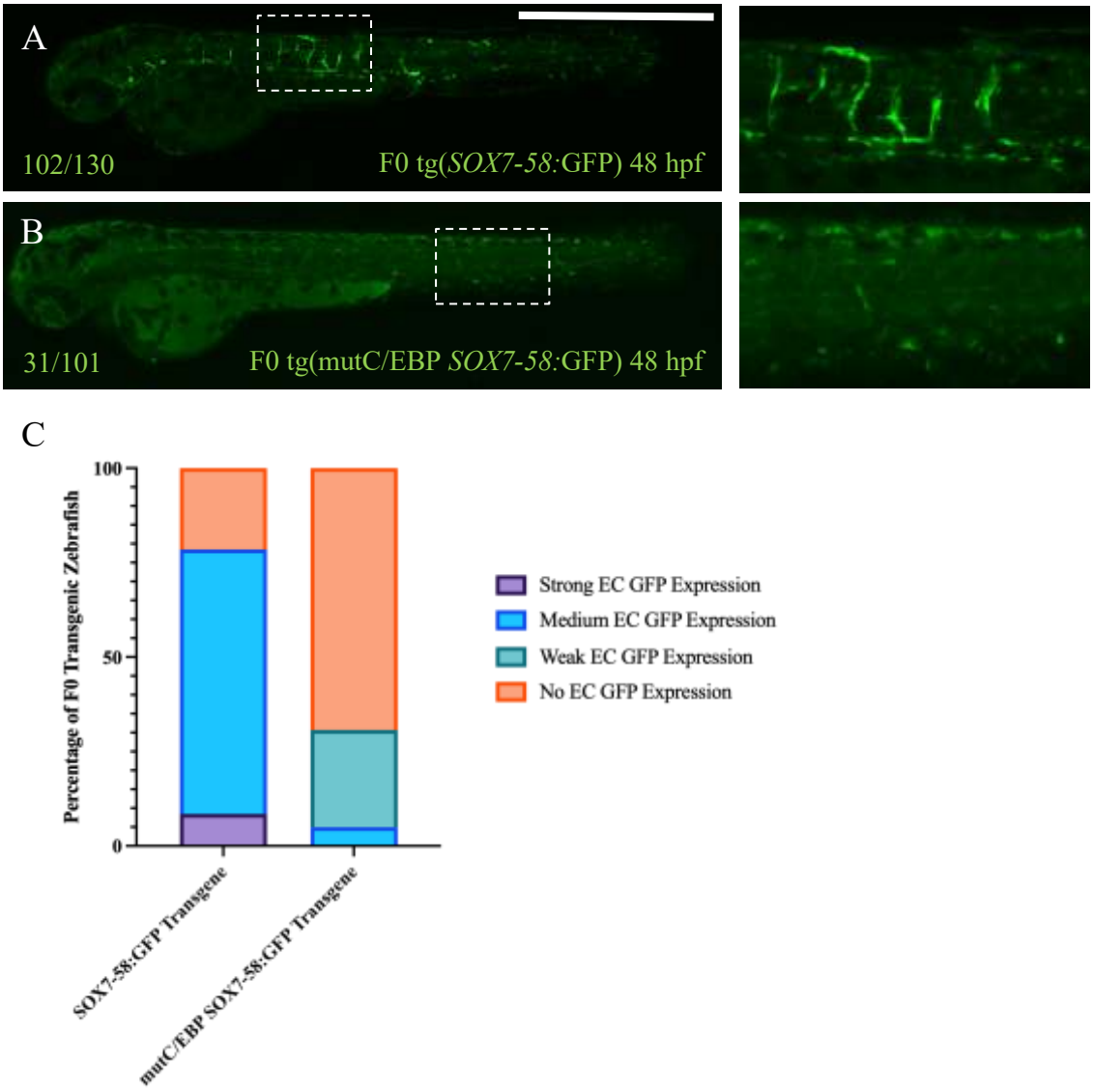

Figure 24: F0 transgenic zebrafish embryo expressing the mut C/EBP *SOX7-58:*GFP transgene had weaker EC GFP expression than F0 transgenic zebrafish embryo expressing the *SOX7-58:*GFP transgene. (A) shows a representative F0 zebrafish injected with the *SOX7-58:*GFP transgene at 48 hpf, with (B) showing a representative F0 zebrafish injected with the mutC/EBP *SOX7-58:*GFP transgene at 48 hpf. (C) Bar graph to compare the percentage of F0 zebrafish embryos with either strong, medium, weak or no EC GFP expression. The bar graph serves as a visual representation of the data in the table above. Scale bar represents 1mm.

3.6.5 TCF/LEF

To investigate whether the canonical Wnt signalling pathway was involved in the activity of SOX7-58, the putative TCF/LEF binding motif was changed from the **TGAAA** to **TGAtc**, with the adenines in position 4 and 5 replaced with thymine and cytosine, respectively. 39 zebrafish embryos injected with the mutTCF/LEF *SOX7-58:*GFP transgene survived until analysis at 48 hpf, alongside 100 embryos injected with the *SOX7-58:*GFP transgene (Table 30). The EC expression pattern was analysed as before.

Unlike my other mutant enhancers, the mutTCF/LEF SOX7-58 enhancer was still able to drive robust reporter gene expression in the zebrafish vasculature. In fact, the GFP expression pattern for the mutant transgene was comparatively stronger than the F0 zebrafish expressing the *SOX7-58:*GFP transgene. Of particular interest this expression appeared expanded to more of the vasculature, as seen in higher numbers of ISVs expressing GFP.

Table 30: Summary table showing the percentange of F0 zebrafish (injected with either the *SOX7-58:*GFP transgene or the mutTCF/LEF *SOX7-58:*GFP transgene) with strong, medium, weak or no GFP expression in ECs at 48 hpf, raw numbers are in brackets

Transgene	Percentage of F0 zebrafish with strong EC GFP expression (Raw Number)	Percentage of F0 zebrafish with medium EC GFP expression (Raw Number)	Percentage of F0 zebrafish with weak EC GFP expression (Raw Number)	Percentage of F0 zebrafish with no EC GFP expression (Raw Number)
*SOX7-58:*GFP	0% (0)	36% (36)	48% (48)	16% (16)
mutTCF/LEF *SOX7-58:*GFP	13% (5)	21% (8)	38% (15)	28% (11)

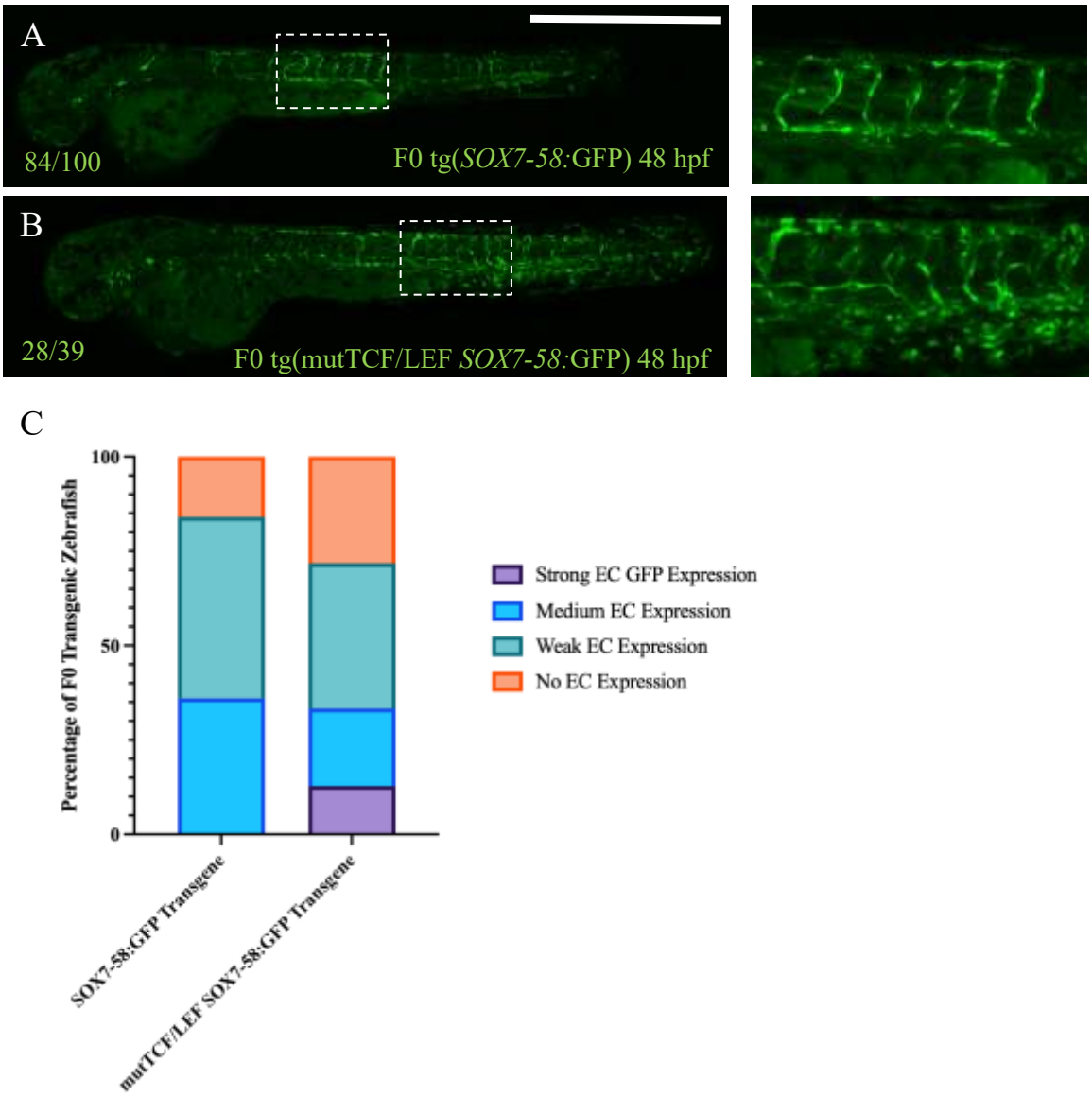

Figure 25: F0 transgenic zebrafish embryo expressing the mutTCF/LEF *SOX7-58:*GFP transgene had stronger EC GFP expression than F0 transgenic zebrafish embryo expressing the *SOX7-58:*GFP transgene. (A) shows a representative F0 zebrafish injected with the *SOX7-58:*GFP transgene at 48 hpf, with (B) showing a representative F0 zebrafish injected with the mutTCF/LEF *SOX7-58:*GFP transgene at 48 hpf. (C) Bar graph to compare the percentage of F0 zebrafish embryos with either strong, medium, weak or no EC GFP expression. The bar graph serves as a visual representation of the data in the table above. Scale bar represents 1mm.

Previous literature has already indicated a potential, although disputed, role for canonical Wnt signalling in arterial and venous specification.[210] Therefore, another cohort of embryos were injected, and rather than scoring the strength of EC GFP expression, the exact location of this expression was noted. This was categorised into arterial, venous, arterial and venous, and no EC GFP expression.

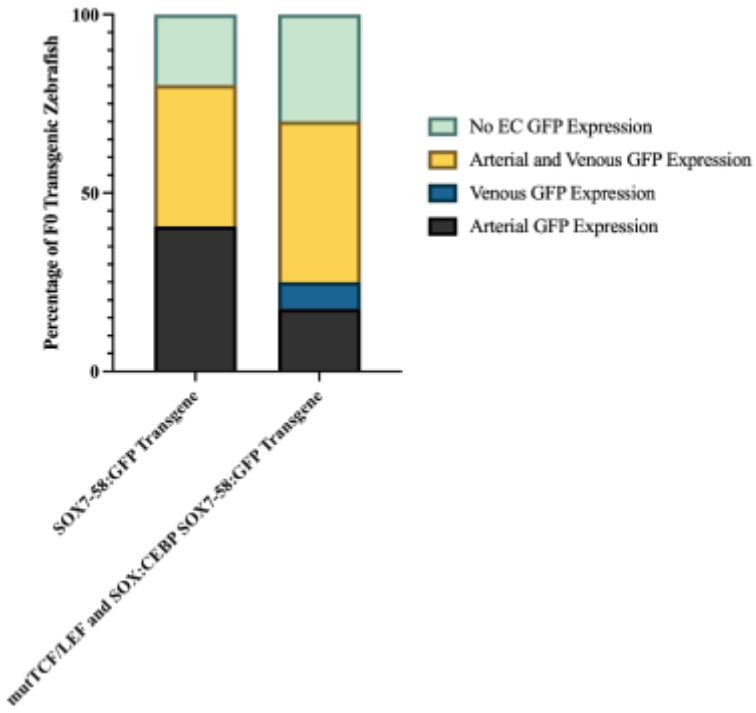

Figure 26: F0 transgenic zebrafish embryos expressing the mutTCF/LEF *SOX7-58:*GFP transgene had more GFP expression in venous ECs compared with F0 transgenic zebrafish embryos expressing the *SOX7-58:*GFP transgene.

Whilst none of the embryos injected with the *SOX7-58:*GFP transgene had GFP expression only in venous ECs (0/96), 3 embryos injected with the mutTCF/LEF *SOX7-58:*GFP transgene did (3/40). Although these numbers are low, this could indicate a change in enhancer activity location. Consistent with this, GFP expression restricted to the aorta was observed in nearly half of F0 zebrafish expressing the *SOX7-58:*GFP transgene (39/77), but in only a quarter of those carrying the mutTCF/LEF *SOX7-58:*GFP transgene (7/28).

3.7 Putative TCF/LEF binding motifs in other angiogenic enhancers

Identification of putative TCF/LEF binding motifs within SOX7-58, a validated tip EC enhancer, suggests that canonical Wnt/β-catenin signalling may directly regulate its activity. Given that enhancers regulating the same EC subpopulation often share key TF inputs, this finding raises the possibility that canonical Wnt/β-catenin signalling operates as a broader regulatory axis within the sprouting angiogenic programme. Systematically assessing additional angiogenic enhancers for TCF/LEF motifs therefore determines whether this reflects a recurrent, coordinated mechanism of transcriptional control rather than a locus-specific phenomenon. Evidence of motif enrichment or functional dependence across multiple enhancers would support a model in which TCF/LEF factors orchestrate a distributed enhancer network driving sprouting angiogenesis.

To this end, I next investigated other known angiogenic enhancers (HLX-3, ETS1+195 and DLL4in3) for putative TCF/LEF sites. HLX-3, ETS1+195 and DLL4in3 all have activity in angiogenic ECs, as observed in both F0 zebrafish and mice, with DLL4in3 also directing reporter gene expression in arterial ECs.[183,197,227] This analysis found consensus or near consensus TCF/LEF binding motifs in each of the three established angiogenic enhancers.

The HLX-3 enhancer contained four putative TCF/LEF binding motifs: two non-consensus LEF1 motifs in R1, a non-consensus LEF1 motif in R5, and a non-consensus TCF4 motif in R6 (Figure 27). The ETS1+195 enhancer had two putative TCF/LEF binding motifs: a consensus LEF1 motif in R13, and a non-consensus LEF1 motif in an unconserved region (Figure 28). The latter is unlikely to be a functional site. In the DLL4in3 enhancer, I identified four putative TCF/LEF binding motifs: a consensus LEF1 motif in R1, a non-consensus LEF1 motif in R2, a consensus TCF4 motif in R3, and a non-consensus LEF1 motif in R5 (Figure 29).

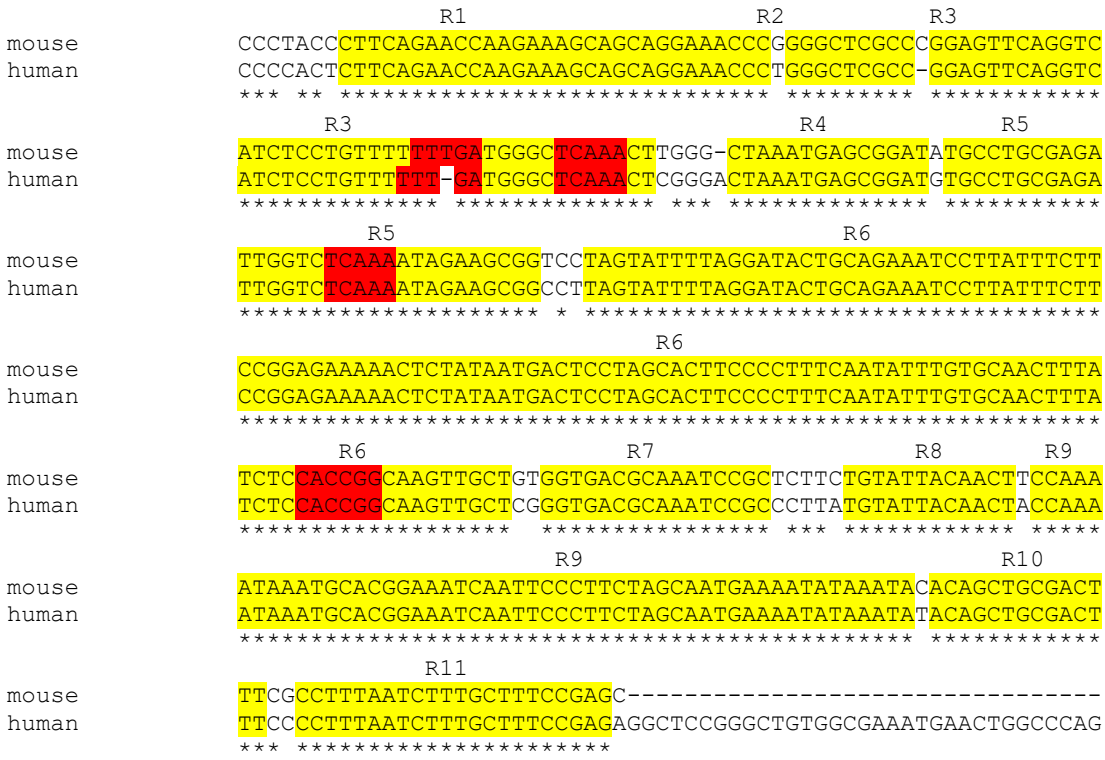

Figure 27: HLX-3 enhancer has 11 highly conserved regions (labelled R1-R11). TCF/LEF binding motifs are highlighted in red.

Figure 28: ETS1+195 enhancer has 24 highly conserved regions (labelled R1-R24). TCF/LEF binding motifs are highlighted in red.

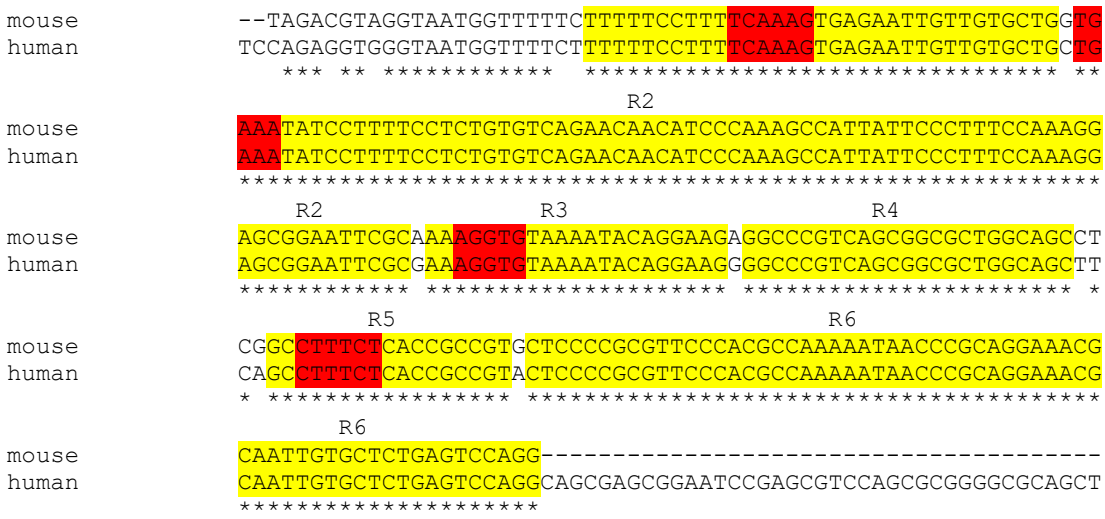

Figure 29: DLL4in3 enhancer has six highly conserved regions (labelled R1-R6). TCF/LEF binding motifs are highlighted in red.

3.7.1 Functional analysis of the putative TCF/LEF binding motifs in DLL4in3

To test whether the putative TCF/LEF binding motifs identified in DLL4in3 are functional, more F0 transgenic mosaic zebrafish embryos were created. This time, I tested a mutant Dll4in3 enhancer with targeted disruptions in the putative TCF/LEF binding motifs (sequence in **Chapter 2**), again cloned upstream of the E1b minimal promoter and GFP reporter gene, and inserted into a Tol2 destination vector.

In previous experiments, 48% of zebrafish embryos with the wildtype *DLL4in3:*GFP transgene express GFP in ECs at 24 hpf (533/1111).[197] In contrast, here I found 56% of embryos injected with the mutTCF/LEF *DLL4in3:*GFP transgene had GFP expression in ECs (63/112). This represents an increase, although the difference in sample size may be limit the statistical significance of this comparison. However, much like the F0 transgenic zebrafish expressing the mutTCF/LEF *SOX7-58:*GFP transgene, the F0 transgenic zebrafish expressing the mutTCF/LEF *DLL4in3:*GFP transgene had a GFP expression pattern that expanded beyond the normal EC pattern.

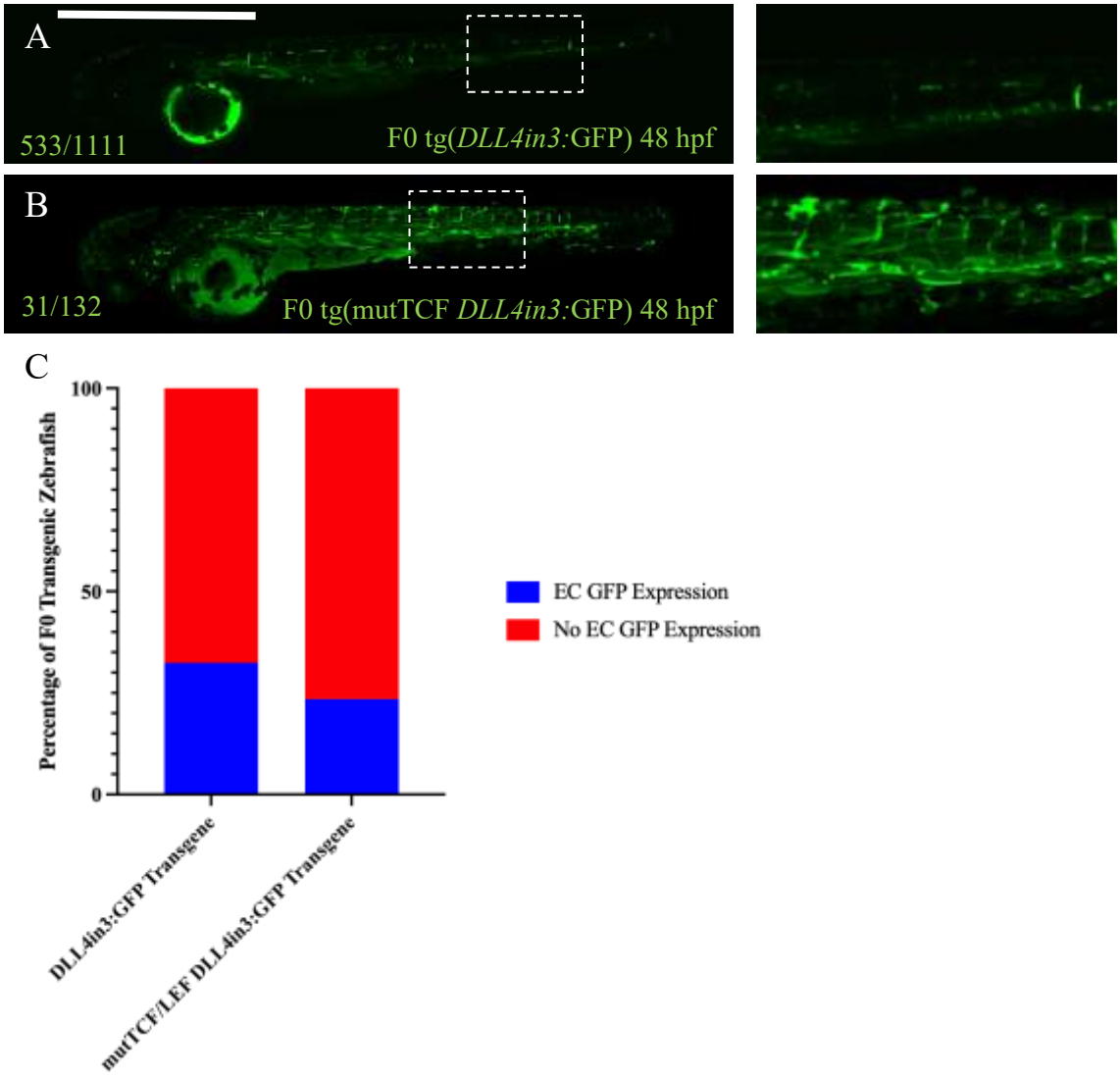

Figure 30: F0 transgenic zebrafish expressing the mutTCF/LEF DLL4in3 transgene had expanded EC GFP expression compared with embryos injected with wildtype DLL4in3 sequence. (A) shows a representative F0 zebrafish injected with the *DLL4in3:*GFP transgene at 48 hpf, with (B) showing a representative F0 zebrafish injected with the mutTCF/LEF *DLL4in3:*GFP transgene at 48 hpf. (C) Bar graph to compare the percentage of F0 zebrafish embryos with GFP expression in ECs versus no GFP expression in ECs. Scale bar represents 1mm.

3.8 Discussion

The discovery of a novel enhancer, SOX7-58, provided the initial framework for Chapter 3. Functional assays in F0 transgenic zebrafish and mice models demonstrated that the SOX7-58 enhancer was able to drive reporter gene expression specifically to angiogenic ECs. This activity was most clearly illustrated in the postnatal mouse retina, where X-Gal staining revealed robust *SOX7-58:LacZ* expression in tip ECs.

One of the major challenges in understanding angiogenic regulation has been the lack of well-characterised enhancers for key angiogenic genes. In published literature there are currently only three angiogenic EC enhancers - HLX-3, ETS1+195 and DLL4in3. However, the HLX-3 enhancers is not specific to tip cells in the postnatal retina, the activity of the ETS1+195 enhancer is not well characterised, and the Dll4in3 enhancer is also active in arterial ECs.[197,227] Whilst TF analysis of these enhancers has established a role for MEF2 TFs in the regulation of sprouting angiogenesis, it is hoped that with more angiogenic enhancers identified and characterised, other important regulatory pathways can be elucidated.[227]

3.8.1 Activity of the SOX7-58 enhancer requires FOX:ETS, FOS:JUN, C/EBP, and TCF/LEF motifs

All three orthologous *SOX7-58:*GFP transgenes (human*SOX7-58:*GFP, mouse*SOX7-58:*GFP and opossum*SOX7-58:*GFP) drove similar GFP expression patterns in F0 transgenic zebrafish. This conserved function indicates a degree of conserved regulation, and thus conserved TF binding motifs. When I compared the sequence within SOX7-58 across the human, mouse, and opossum genomes, I identified eight highly conserved regions. Each of the regions was then probed, via manual inspection, for putative TF binding motifs using a list of common TF binding sites in ECs. In addition, TRANSFAC and FIMO (MEME SUITE) were used to investigate putative TF binding motifs across the full length of the SOX7-58 enhancer sequence.

3.8.1.1 FOX:ETS binding motifs are essential for SOX7-58 activity, but FOX:ETS and ETS binding motifs alone are not sufficient for enhancer activity

All three *in silico* methodologies identified multiple ETS binding motifs in the SOX7-58 sequence. This was unsurprising, as the ETS TF family is involved in the regulation of all EC-expressed genes.[136,172,261] It has previously been noted that whilst EC enhancers contain multiple putative ETS binding motifs, only a few are functional, despite having similar sequences.[264] Different explanations have been given for this. One theory posits that EC enhancers have multiple ETS binding motifs to provide a degree of robustness against mutation. Alternatively, multiple ETS binding motif are present and have the capacity to become functional, but require the addition of specific co-factor binding.

Whilst four putative ETS binding motifs were identified, two were contained within putative FOX:ETS binding motifs. Previous studies have shown that FOX and ETS can bind synergistically at FOX:ETS motifs, and such motifs are effective predictors of EC-specific enhancers.[23,177] At 48 hpf, examination of F0 zebrafish expressing the mutFOX:ETS *SOX7-58:*GFP transgene found no GFP expression in their ECs. This strongly indicates that at least one of these binding motifs is essential, but since the two FOX:ETS motif were mutated in parallel, it is impossible to discern which. Indeed, they could also both be essential. To investigate this further, future studies could create two more mutated *SOX7-58:*GFP transgenes, each a different FOX:ETS motif disrupted.

Although EC enhancer activity has shown an essential requirement for ETS, it has also been demonstrated that ETS TFs alone are not sufficient to drive specific patterns of gene expression in EC subpopulations.[182,183,196,197,227,265] For example, mutations to RBPJ and SOXF motifs in arterial enhancers completely ablates activity, even though the ETS motifs remain functional.[182,183,196,197,265] Moreover, in HLX-3 and DLL4in3, two angiogenic enhancers, mutations to MEF2 motifs ablates transgene activity even though, again, ETS motifs within the enhancers remained functional.[227] Here, I observed similar results. Mutations to all conserved motifs except ETS (mut[FOX, FOS:JUN, C/EBP, TCF/LEF] SOX7-58):GFP also ablated enhancer activity. However, this experiment is potentially limited by the quality of *in silico* analysis: if functional TF binding motifs were not identified, then although the synthetic sequence has been designed to only allow ETS binding, in actual fact, other important TFs could also be present. Nonetheless, in

this experiment, only 25/121 embryos had any GFP expression in ECs. This agrees with previous work showing that ETS TFs are essential to EC enhancers, but they are not sufficient for normal enhancer activity.

3.8.1.2 FOS:JUN and CEBP binding motifs are essential for SOX7-58 activity

The FOS:JUN motif enables the co-operative binding of two AP1 subfamilies: Fos and Jun.[259] These two TFs have already been noted to act as a heterodimer, with high DNA affinity and transcriptional activity.[259] Whilst early *in vitro* studies suggested a role for AP-1 TFs in angiogenesis, more recent *in vivo* evidence highlights JunB as a key regulator of angiogenesis via two AP-1 TF binding motifs in the VEGF promoter.[259,266] Mutational analysis of the FOS:JUN motif revealed significantly reduced GFP EC expression in F0 zebrafish expressing the mutFOS:JUN *SOX7-58:*GFP transgene. This suggests that the FOS:JUN binding motif is essential to SOX7-58 activity. Given that SOX7-58 is thought to regulate tip EC gene expression, it is interesting to note two previous studies which reported upregulation of JunB expression in tip ECs.[258,260] This further supports the notion that AP-1 TFs are essential to tip EC regulation.

C/EBP is a member of the bZIP TF superfamily, which is one of the most diverse TFs in eukaryotes.[267] Although it has not been extensively studied in relation to physiological angiogenesis, it has been shown to regulate VEGF-A via a C/EBPβ-responsive element within the *Vegf-a* promoter.[268] In a disease context, loss of C/EBP-δ results in reduced tumour angiogenesis, with C/EBP-δ thought to directly regulate VEGFR2 transcription.[269] F0 zebrafish expressing the mutC/EBP:*SOX7-58:*GFP transgene had reduced GFP expression in their ECs. This suggests that the C/EBP motif is also functional.

Considering that C/EBP is not a classical TF involved in vascular development, I examined the TRANSFAC analysis to establish whether other putative TFs were predicted at this site. In addition to C/EBP, the analysis suggested AFT-2, Arid5a and GR-like receptors. Notably, the absence of glucocorticoid receptor (GR) has been reported to increase angiogenesis through activation of the canonical Wnt signalling pathway.[270] Given that a putative TCF binding motif was also identified in SOX7-58, this raises the possibility that GR may directly interact with TCF/LEF.[271]

3.8.1.3 SOX7-58 did not contain any putative MEF2 binding motifs

It is worth noting that the SOX7-58 enhancer did not contain any consensus or near-consensus MEF2 binding motifs. This was relatively surprising given that two previously identified angiogenic enhancers – HLX-3 and DLL4in3 – have functional MEF2 binding sites, and MEF2 TFs are key regulators of sprouting angiogenesis.[227] However, it is already well established that enhancers directing similar patterns of gene activation can share few TF binding motifs, a fact underscored by a recent analysis of arterial enhancers, which showed a range of transcriptional signatures.[229] This is, in part, what makes enhancer identification so challenging. The distinction between SOX7-58 and previously characterised angiogenic enhancers may reflect slightly different developmental trajectories.

3.8.1.4 TCF/LEF binding motifs regulate SOX7-58

TCF/LEF, the nuclear effectors of the canonical Wnt signalling pathway, have long been implicated in vascular development.[199] However, despite this, no currently characterised arterial, angiogenic or venous EC enhancers have defined TCF binding motifs.[24,62] It was therefore unexpected that both TRANSFAC and manual inspection analysis identified a putative TCF/LEF binding motif in the SOX7-58 enhancer sequence.

Due to the association of canonical Wnt signalling with physiological angiogenesis, I hypothesised that disrupting the putative TCF/LEF binding motif would abrogate SOX7-58 activity.[199] However, mutational analysis in F0 zebrafish found that mutating the TCF/LEF site in SOX7-58 instead potentially led to an expansion of enhancer activity. This raises the possibility that the TCF/LEF TFs are negatively regulating angiogenesis.

Mechanistically, the expanded enhancer activity may also reflect the dual role of TCF/LEF factors. Whilst in the presence of Wnt signalling, TCF/LEF TFs transcribe Wnt-responsive elements. However, in the absence of Wnt signalling they can recruit co-repressors, such as Groucho/TLE, to bind to Wnt-responsive elements.[200] Disruption of the TCF/LEF motif could therefore relieve this repression, resulting in de-repression of SOX7-58 activity.

Besides its role in angiogenesis, canonical Wnt signalling has also been implicated in arterial and venous specification.[210] Previous studies in mice have shown that constitutive

activation of β-catenin signalling causes the misexpression of arterial and venous makers: downregulation of *Ephb4* in veins alongside an upregulation of *Efnb2*.[210] In line with this, mutational analysis of the TCF/LEF binding motif resulted in an expansion of SOX7-58 activity into venous ECs. This could indicate that the TCF/LEF binding motif has a role in maintaining the angiogenic specificity of the *SOX7-58:*GFP transgene expression.

Although I have not demonstrated that SOX7-58 regulates SOX7, its close proximity to the gene could be indicative of this. Previous studies have reported a link between β-catenin and SOXF factors, and therefore it was interesting that a TCF/LEF binding motif was identified in the SOX7-58 enhancer sequence.[192,207,231] For example, in a murine model overexpressing Norrin (a non-Wnt ligand), Ye *et al* (2009) reported that *Sox17* was significantly upregulated, and in in ECs isolated from β-catenin gain-of-function mouse embryos, Corada *et al* (2013) also reported increased *Sox17* levels.[192,207] These two studies support the notion that *SOXF* factors lie downstream of β-Catenin signalling.

3.8.2 DLL4in3 enhancer activity requires TCF/LEF motifs

All three other angiogenic enhancers also contained TCF/LEF motifs, and mutational analysis of the TCF/LEF binding motifs in DLL4in3 resulted in expanded GFP expression in ECs. Interestingly, DLL4in3 has previously been linked mechanistically to arterial fate induction through convergent Notch and canonical Wnt signalling.[73,74,197] Indeed, Yamamizu *et al* (2010) found that dual activation of Notch and β-Catenin signalling induced formation of arterial ECs from an ES cell line, with NICD/β-Catenin/RBP-J protein complexes forming exclusively on arterial genes.[74] When the DLL4in3 enhancer sequence was previously analysed for putative TF binding motif, a RBP-J binding motif was identified.[74,197] Subsequently, Zhang *et al* (2011) reported that Ang1 recruits stabilised β-Catenin to form a complex with NIC/RBP-J on the DLL4in3 enhancer.[272] Therefore, whilst this project supports the notion that TCF/LEF are needed for the spatial specificity of DLL4in3, it is unclear if disrupting the canonical Wnt signalling pathway is affecting both the arterial and angiogenic functions equally.

3.9 Conclusion

The results of Chapter 3 strongly support a requirement for FOX:ETS, FOS:JUN, C/EBP, and TCF/LEF motifs in the regulation of SOX7-58. Whilst disruption to either the FOX:ETS, FOS:JUN or C/EBP motifs reduced SOX7-58 activity, mutating the TCF/LEF motif led to an expansion of *SOX7-58:*GFP transgene expression. This suggests that TCF/LEF is negatively regulating SOX7-58 and contributing to its spatial specificity. Investigating a role for TCF/LEF binding motifs in other angiogenic enhancers led to the identification of putative TCF/LEF sites in DLL4in3. Mutation of these TCF/LEF motifs led to an expansion of *DLL4in3:*GFP transgene expression in ECs.

Chapter 4: Investigating EC-specific *Ctnnb1* ablation in the developing murine vasculature

4.1 Rationale

In Chapter 3, I examined and characterised the novel SOX7-58 angiogenic EC enhancer. *In silico* analysis identified a putative TCF/LEF binding motif within this enhancer, and transgenic analysis of mutTCF/LEF *SOX7-58:*GFP in F0 transgenic zebrafish indicated an expansion in enhancer activity. TCF/LEF binding motifs were also identified in DLL4in3, another EC enhancer active during angiogenesis. As mentioned in Chapter 1, TCF/LEF are the nuclear effectors of the canonical Wnt signalling pathway.[199] Together, these observations suggest a potential role for canonical Wnt signalling may be directly involved in regulating angiogenesis.

In response to these results, here I investigated the role of canonical Wnt signalling pathway in vascular development. This used both constitutive and inducible Cre recombinase murine model systems to ablate canonical Wnt signalling in ECs. The consequence of this depletion to different EC subpopulations was then investigated using a combination of immunohistochemical analysis and expression of subtype-specific EC enhancer:*LacZ* transgenic lines.

4.2 Aims and Objectives

Considering the phenotypic variability previously reported in the literature, here I aim to re-examine the consequences of EC-specific perturbation of the canonical Wnt signalling pathway. This will be achieved with the *Tg(Tek-Cre)*^{12Flv} allele, which has consistently been shown to have high and stable expression in ECs, in combination with the *iSuRe-Cre* allele. The inclusion of a fluorescent Cre reporter will allow poorly recombined knockouts to be disregarded from future phenotypic analysis. Furthermore, to study the consequences of perturbed Wnt on transcriptional in different EC subpopulations, I will utilise a variety of EC subtype-specific enhancer:*LacZ* murine transgenic lines.

The hypothesis of this chapter is that canonical Wnt signalling is an important regulator of the developing vasculature, most specifically sprouting angiogenesis, via SOX7-58.

The aims of this chapter were to:

1. Investigate the gross morphological consequences of EC-specific *Ctnnb1* ablation in mouse embryos

2. Assess the impact of constitutive EC-specific *Ctnnb1* ablation on different EC subpopulations using EC subtype-specific enhancer:*LacZ* lines and immunohistochemistry for classical vascular markers

3. Using inducible EC-specific *Ctnnb1* ablation, investigate a role for canonical Wnt signalling in:

    a. VEGFC-driven angiogenesis in the coronary vasculature
    b. VEGFA-driven angiogenesis in the postnatal retinal vasculature

4.2.1 Achieving constitutive *Ctnnb1* ablation in the developing ECs

The first step in my investigation was to re-examine the gross morphological consequences of EC-specific perturbation of the canonical Wnt signalling. To achieve this, the Cre-Lox system was used to selectively ablate *Ctnnb1* from ECs. Since β-catenin is the central component in the signalling pathway, and many of the other signalling components can compensate for each other, EC-specific ablation of *Ctnnb1* is often considered the most direct method to disrupt canonical Wnt signalling.[201]

Briefly, the Cre-Lox system comprises a Cre recombinase enzyme, derived from bacteriophage P1, and two *loxP* recognition sites.[219,273,274] These *loxP* sites are positioned on either side of a critical exon or regulatory region of the target gene. The gene is thereby described as 'floxed'. When Cre binds to two *loxP* sites in the same orientation, it excises the intervening DNA, effectively inactivating the gene activity.[219] Tight spatial control of this excision is achieved by specific enhancer or promoter elements linked to the Cre, whilst temporal control is achieved via steroid-activated versions of Cre.[219,273]

To dissect out the contribution of EC-specific *Ctnnb1* expression during vascular development, I used an EC-specific Cre driver line with the Ctnnb1^{tm2Kem} allele.[220]. This allele has previously been discussed in the **Chapter 1**.

Within the vascular biology field, many different Cre recombinase alleles have been designed to examine EC-specific gene ablation. These have been engineered to either ablate genes in a pan-EC manner, or restrict the deletion to more specific EC subpopulations.[219] When investigating angiogenesis in a developmental context, it is important to select a Cre allele which is active from E8.5, and is expressed pan-endothelially. In addition, the pan-*Cre* driver should ideally not have any activity in non-EC tissue, since this could result in off-target effects and compound vascular phenotypes.[219]

As discussed, one potential explanation for the observational discrepancies in the literature could stem from the Cre driver selection. In previous studies, the two most common pan-EC drivers used are *Flk1-Cre* and *Tek-Cre* allele. Whilst both have pan-EC behaviour from E11.5, *Tek-Cre* is typically expressed earlier, with robust activity seen at E9.5.[219] In contrast, at E9.5, *Flk1-Cre* is only active in the head and vessels of the upper trunk.[219] This may account for phenotypes of selective dysregulation of only CNS angiogenesis.[211] Therefore, to ensure that there was *Ctnnb1* ablation in all developing vascular network, I have used the *Tek-Cre* driver (Figure 31).

However, there is not simply one *Tek-Cre* driver available, there are numerous options. These include *Tg(Tek-cre)^{1Ywa}*, *Tg(Tek-cre)^{12Flv}*, *Tg(Tek-cre)^{5326Sato}*, *Tg(Tek-cre)^{1Rwng}* and *Tg(Tek-cre)^{1Xyfu}*.[219] These have all been generated by separate research groups. The two most common *Tek-Cre* drivers are *Tg(Tek-cre)^{1Ywa}* and *Tg(Tek-cre)^{12Flv}*. Whilst both of these show Cre activity in the embryonic mesodermal yolk sac from E7.5, and pan-EC expression from E.95, at E8.5, their respective expression patterns diverge.[275-277] Indeed, whilst *Tg(Tek-cre)^{12Flv}* shows strong pan-EC activity across all embryonic vasculature, *Tg(Tek-cre)^{1Ywa}* instead has only sparse activity in the dorsal aorta and common atrial chamber.[275,277] Considering that angiogenesis initiates from E8.5 in the mouse, to fully capture vascular defects arising from EC-specific *Ctnnb1* ablation, the

Cre driver must be active pan-endothelially at this timepoint. Thus, the *Tg(Tek-Cre)*^{12Flv} allele was selected.

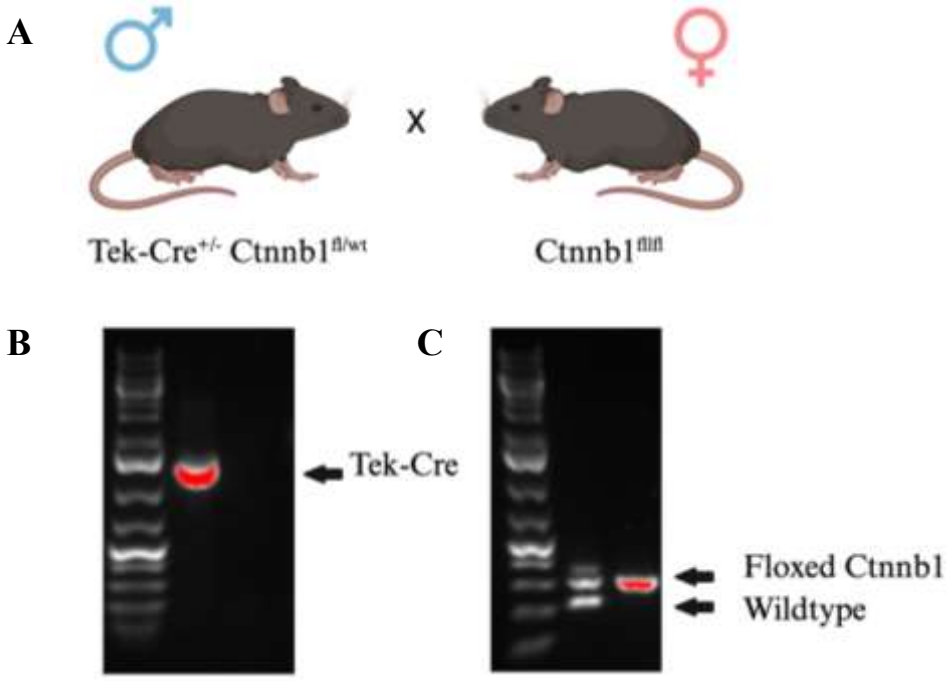

Figure 31: Generation and Genotyping of Constitutive *Ctnnb1* Knockout Mice using the Tek-Cre System. (A) A schematic depicting the breeding strategy where male mice heterozygous for Tek-Cre and carrying one floxed *Ctnnb1* allele (Tek-Cre$^{+/-}$ Ctnnb1$^{fl/wt}$) are crossed with female mice homozygous for floxed *Ctnnb1* alleles (Ctnnb1$^{fl/fl}$). (B) and (C) are gel electrophoresis images showing PCR genotyping results. (B) shows the detection of the Tek-Cre transgene indicated by the highlighted band. (C) shows the identification of floxed and wildtype Ctnnb1 alleles.

4.2.2 Constitutive ablation of *Ctnnb1* in ECs results in embryonic lethality by E10.5

4.2.2.1 Cross of Tek-Cre$^{+/-}$ Ctnnb1$^{fl/wt}$ males with Ctnnb1$^{fl/fl}$ females

One of the reported phenotypes of EC-specific *Ctnnb1* ablation is early embryonic lethality. Most notably, Cattelino *et al* (2003) reported that around 50% of *Ctnnb1* mutant embryos were dead at E11.5, and 100% of the embryos had died by E13.5,.[209] Since these experiments were done using the *Tg(Tek-cre)*^{1Ywa} allele, rather than the *Tg(Tek-cre)*^{12Flv} allele, I examined whether this phenotype could be recapitulated with this different EC-specific Cre driver. Since murine angiogenic begins around E8.5, which is when these two *Tek-Cre* alleles show the greatest disparity in expression pattern, I hypothesised that

a more severe vasculature defects may occur, potentially alongside earlier embryonic lethality.

To generate embryos, *Ctnnb1*$^{fl/wt}$ *Tek-Cre*$^{+/-}$ males were crossed with *Ctnnb1*$^{fl/fl}$ females (Figure 31). Embryos were collected between E10.5 and E11.5 and genotyped using the yolk sac, categorising them into one of four potential genotypes: *Ctnnb1*$^{fl/fl}$ *Tek-Cre*$^{+/-}$, *Ctnnb1*$^{fl/wt}$ *Tek-Cre*$^{+/-}$, *Ctnnb1*$^{fl/fl}$ *Tek-Cre*$^{-/-}$, and *Ctnnb1*$^{fl/wt}$ *Tek-Cre*$^{-/-}$. In the absence of early embryonic lethality, the proportion of embryos in each genotype category should follow Mendelian ratios (1:1:1:1).

Table 31: Genotype of embryos from cross with *Ctnnb1*$^{fl/wt}$ *Tek-Cre*$^{+/-}$ males with *Ctnnb1*^{flfl} females. Summary table showing the percentange of each genotype, raw numbers are in brackets.

	Ctnnb1$^{fl/fl}$ *Tek-Cre*$^{+/-}$	*Ctnnb1*$^{fl/wt}$ *Tek-Cre*$^{+/-}$	*Ctnnb1*$^{fl/fl}$ *Tek-Cre*$^{-/-}$	*Ctnnb1*$^{fl/wt}$ *Tek-Cre*$^{-/-}$	Total
Total	21% (15)	24% (17)	38% (27)	18% (13)	(72)
E10.5	19% (5)	27% (7)	27% (7)	27% (7)	(26)
E11.5	22% (10)	22% (10)	43% (20)	13% (6)	(46)

26 embryos were collected at E10.5 (Table 31). A Fisher's exact test was used to assess whether the observed genotype frequencies were statistically different from the expected Mendelian ratios. In this case, the Fisher's exact test was chosen instead of a Chi-square test because of the small sample size. However, although fewer *Tek-Cre*$^{+/-}$ *Ctnnb1*$^{fl/fl}$ embryos were collected than the other genotypes, this was not statistically significant, $p = 0.9478$.

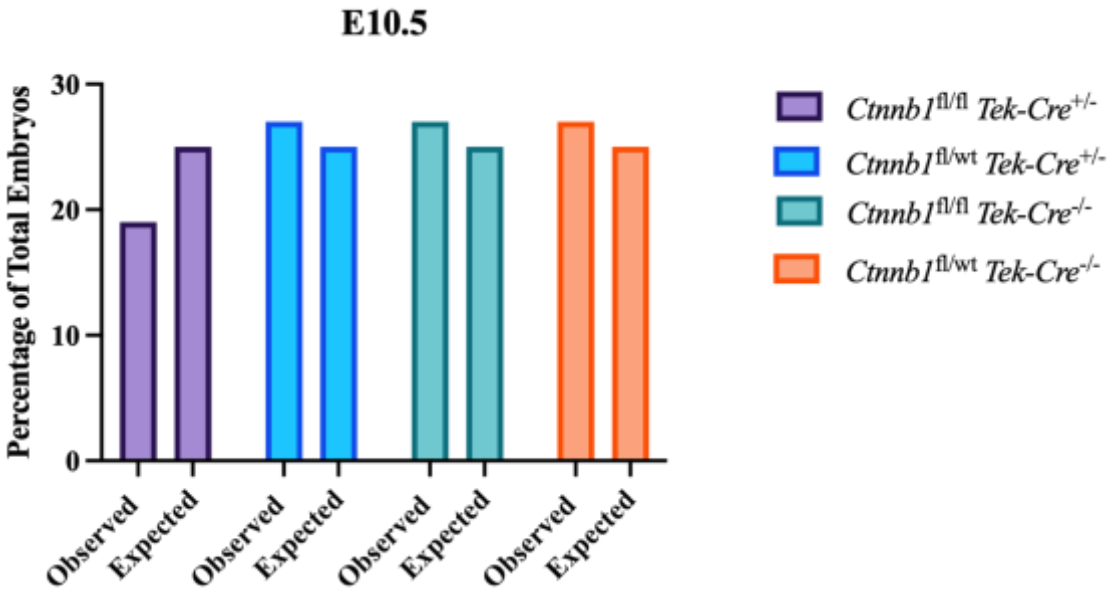

Figure 32: At E10.5, there were no statistically significant differences in the number of embryos collected in each genotype category from cross with *Ctnnb1*$^{fl/wt}$ *Tek-Cre*$^{+/-}$ males with *Ctnnb1*^{flfl} females. p = 0.9478. Data was assessed using the Fisher's exact test. Statistical significance was defined as $P < 0.05$ (*$P < 0.05$, **$P < 0.01$, ***$P < 0.001$, ****$P < 0.001$).

Next, I wanted to compare the genotype frequencies in my dataset with Cattelino *et al* (2003). This study formatted the genotype groups slightly differently, categorising them instead into three groups: +/+, indicating one floxed *Ctnnb1* allele and no Cre allele; +/, representing either the presence of two floxed *Ctnnb1* alleles with no Cre allele, or one floxed *Ctnnb1* allele and the presence of a Cre allele ; and -/-, indicating deletion of both floxed *Ctnnb1* alleles. When I re-organised my data into the three genotype groups used by Cattelino, I recorded 5 -/- embryos, 14 +/- embryos, and 7 +/+ embryos. When my genotypes proportions were compared with Cattelino, using a Fisher's exact test, there was no significant difference, p = 0.6279. This indicates that my E10.5 results recapitulate previous literature.

At E11.5, 46 embryos were collected (Table 31). Somewhat surprisingly, the genotype with the least collected was *Ctnnb1*$^{fl/wt}$ *Tek-Cre*$^{-/-}$. In this group, there is no recombination and therefore the *Ctnnb1* gene remains fully functional. However, it should be emphasised that these initial studies have low *n* numbers, and therefore more vulnerable to random variation. A Fisher's exact test found no statistical significance, p = 0.2401.

This suggests that embryonic lethality does not start until after this point. At E11.5, I observed 10 -/- embryos, 30 +/-, and 6 +/+. When compared with Cattelino, there was no significant difference, p = 0.0537.

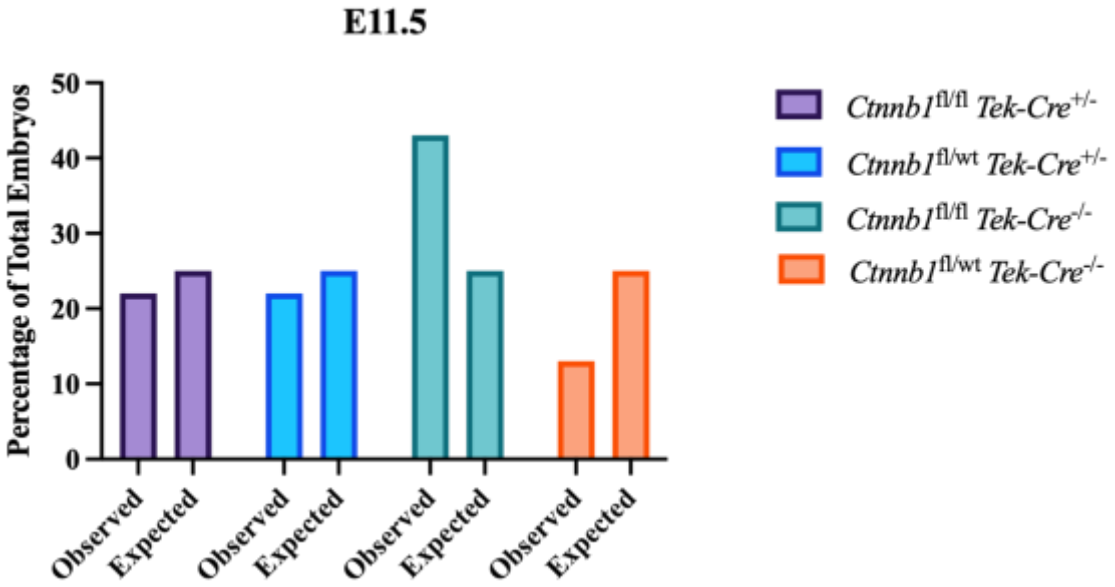

Figure 33: At E11.5, there were no statistically significant differences in the number of embryos collected in each genotype category from cross with *Ctnnb1*$^{fl/wt}$ *Tek-Cre*$^{+/-}$ males with *Ctnnb1*^{flfl} females. p = 0.2401. Data was assessed using the Fisher's exact test. Statistical significance was defined as P < 0.05 (*P < 0.05, **P < 0.01, ***P < 0.001, ****P < 0.001).

4.2.2.2 Cross of Tek-Cre$^{+/-}$ Ctnnb1$^{fl/wt}$ males with iSuRe-Cre$^{+/+}$Ctnnb1$^{fl/fl}$ females

These initial results indicated that whilst fewer *Ctnnb1*$^{fl/fl}$ *Tek-Cre*$^{+/-}$ embryos were collected between E10.5 - E11.5 than Mendelian ratios would predict, these differences were not statistically significant.

For the next set of experiments, I have also included the *iSuRe-Cre* allele in an aim to circumvent inter-litter recombination variability often reported with Cre drivers.[219,278] This allele, developed by Rui Benedito's group, enhances the efficiency of Cre-mediated gene recombination via a self-amplifying mechanism.[278] This is achieved through a strong Cre expression cassette which is permanently activated after recombination, thereby increasing the likelihood that the floxed gene is fully excised. Therefore, if inclusion of the *iSuRe-Cre* allele results in more complete EC-ablation of *Ctnnb1*, and

Ctnnb1 is found to be essential for normal vascular development, embryonic lethality may be earlier.[278] In addition, the *iSuRe-Cre* allele is coupled with a fluorescent reporter gene, *MbTomato*. This means that, upon successful recombination, recombined cells will be permanently *MbTomato*-positive (Figure 34). Therefore, any embryos which had either ectopic or no recombination could be removed from future analysis.

To assess whether inclusion of an *iSuRe-Cre* allele would affect embryonic lethality, the genotype frequencies in litters generated from *Ctnnb1*$^{fl/wt}$ *Tek-Cre*$^{+/-}$ males crossed with *Ctnnb1*^{flfl} *iSuRe-Cre*$^{+/+}$ females were analysed. Since the mothers were all *iSuRe-Cre*$^{+/+}$, all progeny were *iSuRe-Cre*$^{+/}$. This was confirmed with genotyping.

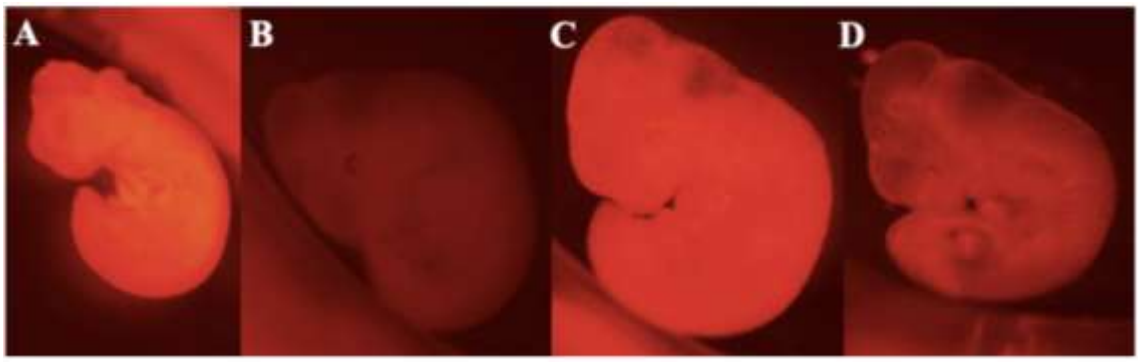

Figure 34: Embryos from the same litter show great variation in *MbTomato* expression. (A) shows non-EC specific Cre expression, whilst (B) shows no Cre expression. On the other hand, (C) and (D) both demonstrate EC specific recombination, but with the great variability in level.

Table 32: Genotype of embryos from cross with *Ctnnb1*$^{fl/wt}$ *Tek-Cre*$^{+/-}$ males with *Ctnnb1*^{flfl} *iSuRe-Cre*$^{+/-}$ females. Summary table showing the percentange of each genotype, raw numbers are in brackets.

	Ctnnb1$^{fl/fl}$ *Tek-Cre*$^{+/-}$ *iSuRe-Cre*$^{+/-}$	*Ctnnb1*$^{fl/wt}$ *Tek-Cre*$^{+/-}$ *iSuRe-Cre*$^{+/-}$	*Ctnnb1*$^{fl/fl}$ *Tek-Cre*$^{-/-}$ *iSuRe-Cre*$^{+/-}$	*Ctnnb1*$^{fl/wt}$ *Tek-Cre*$^{-/-}$ *iSuRe-Cre*$^{+/-}$	Total
Total	10% (61)	24% (140)	30% (177)	35% (203)	581
E9.5	7% (1)	47% (7)	13% (2)	33% (5)	15
E10.5	11% (24)	19% (44)	35% (79)	35% (80)	227
E11.5	12% (34)	25% (72)	27% (76)	36% (102)	284
E12.5	5% (2)	33% (14)	42% (18)	21% (9)	43
> E13.5	0% (0)	25% (3)	17% (2)	58% (7)	12

227 embryos were collected at E10.5 (Table 32). A Chi-square test revealed highly statistically significant differences in the genotype frequencies, p = <0.0001. This could suggest that the inclusion of an *iSuRe-Cre* allele generates a more penetrant knockout model with earlier embryonic lethality.

Nonetheless, there was no statistical significance between this dataset (Table 32), and my previous dataset without *iSuRe-Cre* allele (Table 31), p = 0.3796. One explanation for this might be that the strong deviation observed within the *iSuRe-Cre* allele dataset is balanced by a similarly skewed, but not statistically distinct, distribution in the non-*iSuRe-Cre* allele dataset. This implies that, even without the *iSuRe-Cre* allele, there may be some variability in viability that masks between-dataset differences.

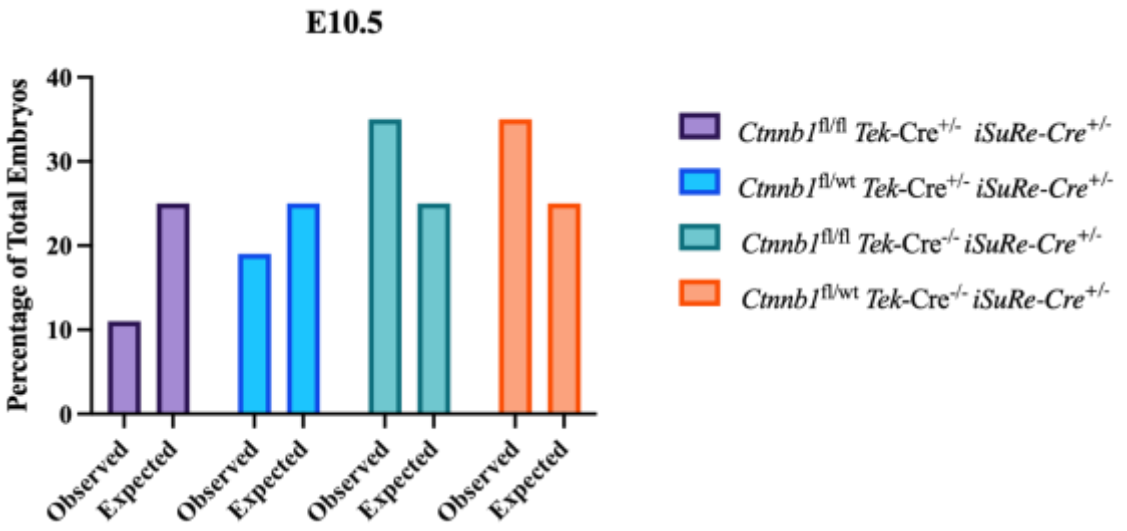

Figure 35: At E10.5, there were no statistically significant differences in the number of embryos collected in each genotype category from cross with *Ctnnb1*$^{fl/wt}$ *Tek-Cre*$^{+/-}$ males with *Ctnnb1*^{flfl} iSuRe-*Cre*$^{+/-}$ females. Data was assessed using the Fisher's exact test. $p < 0.0001$. Statistical significance was defined as $P < 0.05$ (*$P < 0.05$, **$P < 0.01$, ***$P < 0.001$, ****$P < 0.001$).

At E11.5, 284 embryos were collected (Table 32). A Chi-square test revealed highly statistically significant differences in the genotype frequencies, $p = 0.0003$. Considering that there was a highly statistically significant differences at E10.5, it is not surprising to observe significance again at E11.5. However, it is noteworthy that the level of significance is somewhat reduced compared to the earlier timepoint ($p < 0.0001$ at E10.5). This may potentially indicate that the *Ctnnb1* ablation affects the embryo most acutely at E10.5, triggering embryonic lethality. As these *Tek-Cre*$^{+/-}$ *Ctnnb1*$^{fl/fl}$ *iSuRe-Cre*$^{+/-}$ embryos die, their reabsorption could affect neighbouring embryos, regardless of their genotype, thereby normalising the genotype distribution by E11.5. Nonetheless, with a p value of 0.0003 at E11.5, the result still robustly exceeds the threshold for statistical significance. This effectively supports the notion that inclusion of the *iSuRe-Cre* allele is associated with altered genotype ratios, likely due to enhanced Cre-mediated recombination and increased embryonic lethality.

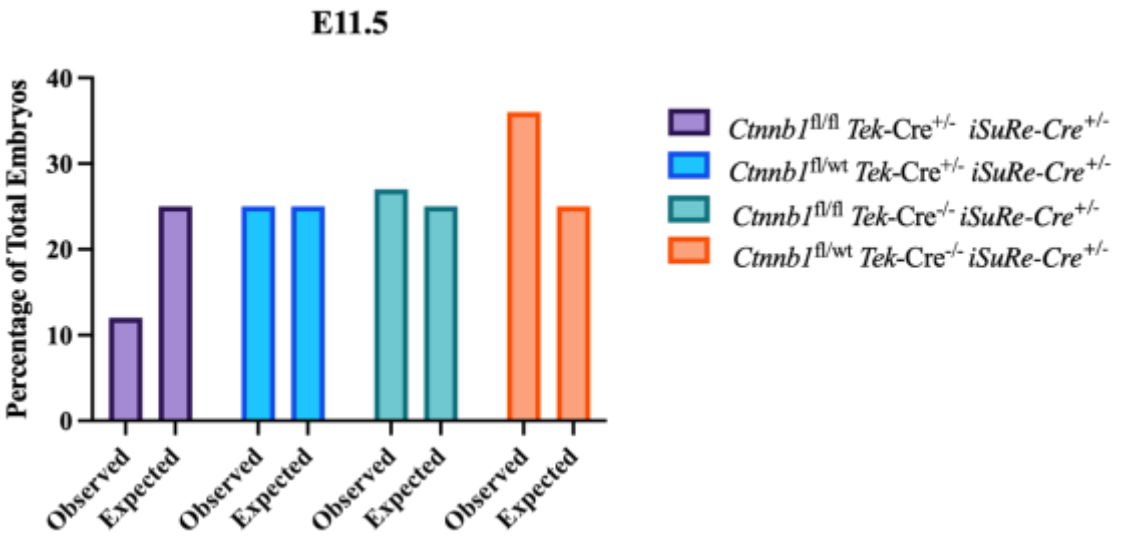

Figure 36: At E11.5, there were no statistically significant differences in the number of embryos collected in each genotype category from cross with Ctnnb1$^{fl/wt}$ *Tek-Cre*$^{+/-}$ males with Ctnnb1^{flfl} iSuRe-*Cre*$^{+/-}$ females. p = 0.0003. Data was assessed using the Fisher's exact test. p < 0.0001 **** Statistical significance was defined as P < 0.05 (*P < 0.05, **P < 0.01, ***P < 0.001, ****P < 0.001).

When compared with my previous data (Table 31), that there were statistically significant differences in the genotype proportions collected, p = 0.0043. This suggests that, by E11.5, the more robust recombination generated by *iSuRe-Cre* profoundly affects the embryos. When compared with the dataset from Cattelino *et al*, statistically significant differences were also observed, p value = 0.0004.

At E12.5, 43 embryos were collected (Table 32). A Fisher's exact test revealed statistically significant differences in the genotype frequencies, p = 0.0344. However, neither of the two embryos collected at E12.5 were viable. Additionally, litters taken from E13.5 onwards, had no *Tek-Cre*$^{+/-}$ *Ctnnb1*$^{fl/fl}$ *iSuRe-Cre*$^{+/-}$ embryos. This suggests that EC-specific ablation of *Ctnnb1* results in embryonic lethality from at least E10.5, to E12.5. Considering that key vasculogenic and angiogenic embryonic events occur in the

mouse embryo between E8.5 and E11.5 of gestation, it is therefore possible that the lethality is, at least in part, contributed to by irregular vasculature formation.[279]

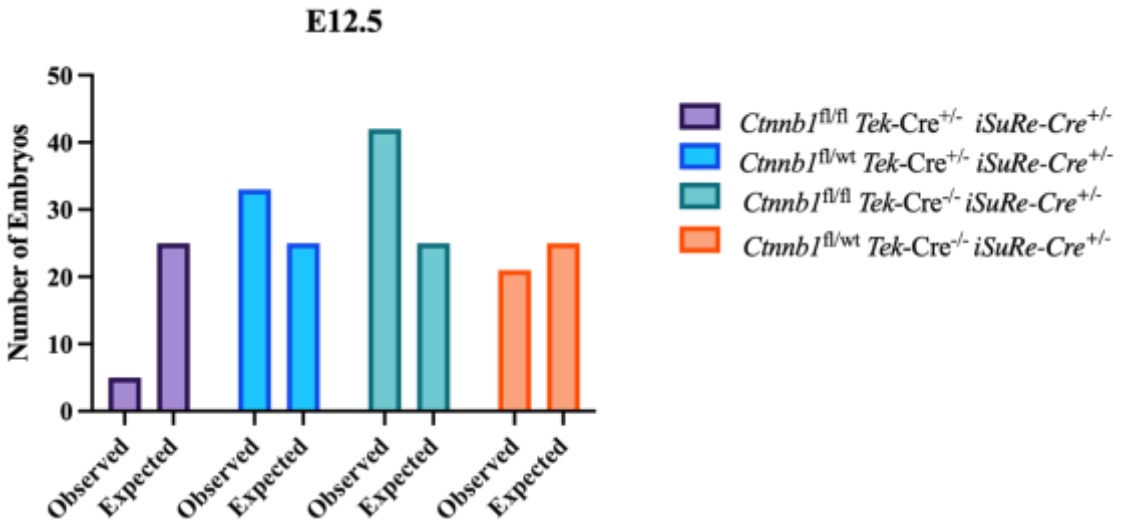

Figure 37: At E12.5, there were no statistically significant differences in the number of embryos collected in each genotype category from cross with *Tek-Cre*$^{+/-}$ *Ctnnb1*$^{fl/wt}$ males with *Ctnnb1*^{flfl} *iSuRe-Cre*$^{+/-}$ females. p = 0.0344. Data was assessed using the Fisher's exact test. p < 0.0001 **** Statistical significance was defined as P < 0.05 (*P < 0.05, **P < 0.01, ***P < 0.001, ****P < 0.001).

4.2.2.3 Cross of Etv2-Cre$^{+/-}$ Ctnnb1$^{fl/wt}$ males with iSuRe-Cre$^{+/+}$Ctnnb1$^{fl/fl}$ females

So far in this investigation, I used the *Tg(Tek-cre)*^{12Flv}allelle to ablate *Ctnnb1* specifically in ECs. Whilst not as widely used, I also wanted to ablate *Ctnnb1* in ECs using the *Tg(Etv2-Cre)1Blk* allele. This *Etv2-Cre* driver has also been shown to have pan-EC Cre activity by E8.5, with no expression in the myocardium.[216] However, considering that *Etv2* is one of the earliest lineage determinants of haematoendothelial cells, I hypothesised that *Etv2-Cre* would likely direct earlier Cre activity in a higher proportion of ECs than the *Tek-Cre* driver.[225] This would enable me to investigate the consequences of earlier and more complete ablation of EC *Ctnnb1* on vascular development and endothelial specification.

Table 33: Genotype of embryos from cross with *Etv2-Cre*$^{+/-}$ *Ctnnb1*$^{fl/wt}$ males with *Ctnnb1*^{flfl} *iSuRe-Cre*$^{+/-}$ females. Summary table showing the percentange of each genotype, raw numbers are in brackets.

	Ctnnb1$^{fl/fl}$ *Etv2-Cre*$^{+/-}$ *iSuRe-Cre*$^{+/-}$	*Ctnnb1*$^{fl/wt}$ *Etv2-Cre*$^{+/-}$ *iSuRe-Cre*$^{+/-}$	*Ctnnb1*$^{fl/fl}$ *Etv2-Cre*$^{-/-}$ *iSuRe-Cre*$^{+/-}$	*Ctnnb1*$^{fl/wt}$ *Etv2-Cre*$^{-/-}$ *iSuRe-Cre*$^{+/-}$	Total
Total	21% (28)	25% (33)	19% (25)	35% (46)	(132)
E10.5	21% (21)	24% (24)	20% (20)	34% (34)	(99)
E11.5	17% (5)	28% (8)	14% (4)	41% (12)	(29)
E12.5	50% (2)	25% (1)	25% (1)	0% (0)	(4)

At E10.5, 99 embryos were collected (Table 33). A Fisher's exact test revealed no statistically significant differences in the genotype frequencies, p = 0.5210. When the genotype frequencies are compared with the cross of *Ctnnb1*$^{fl/wt}$ *Tek-Cre*$^{+/-}$ males with *Ctnnb1*^{flfl} *iSuRe-Cre*$^{+/+}$ females (Table 32), there was no statistically significant difference, p = 0.2106.

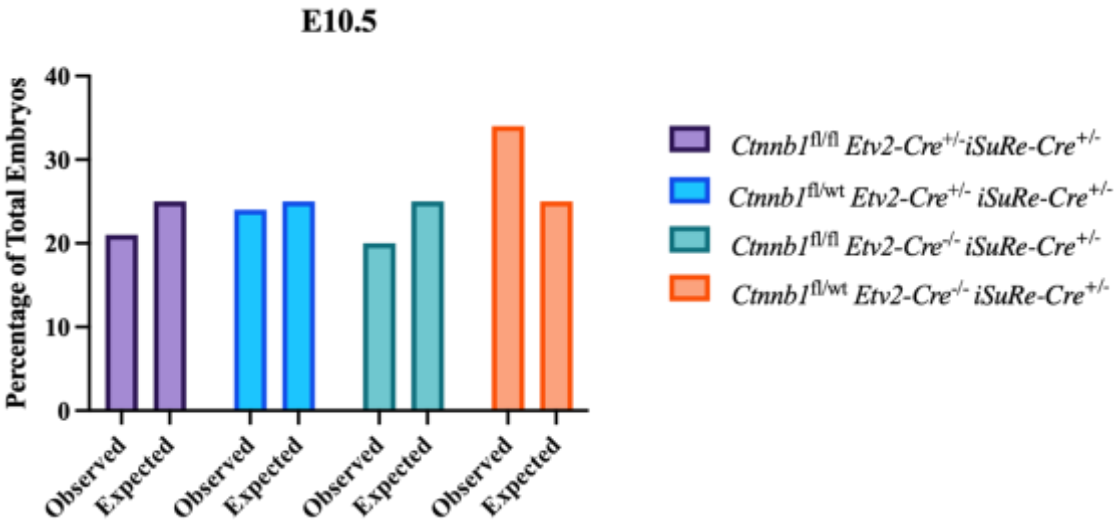

Figure 38: At E10.5, there were no statistically significant differences in the number of embryos collected in each genotype category from cross with *Etv2-Cre*$^{+/-}$ *Ctnnb1*$^{fl/wt}$ males with *iSuRe-Cre*$^{+/-}$ *Ctnnb1*^{flfl} females. p = 0.5210. Data was assessed using the Fisher's exact test. p < 0.0001 **** Statistical significance was defined as P < 0.05 (*P < 0.05, **P < 0.01, ***P < 0.001, ****P < 0.001).

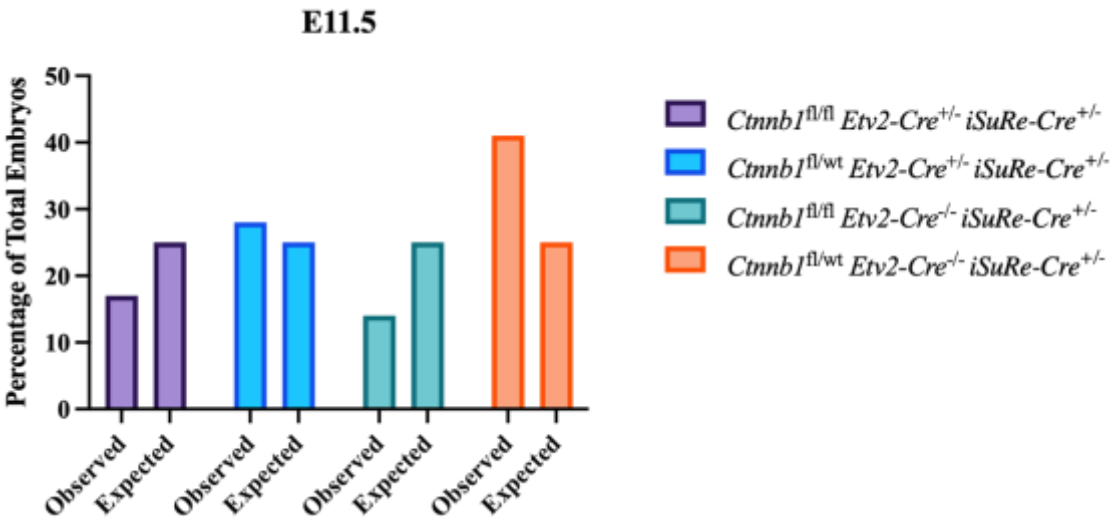

Figure 39: At E11.5, there were no statistically significant differences in the number of embryos collected in each genotype category from cross with *Etv2-Cre*$^{+/-}$ *Ctnnb1*$^{fl/wt}$ males with *iSuRe-Cre*$^{+/-}$ *Ctnnb1*^{flfl} females. p = 0.1008. Data was assessed using the Fisher's exact test. p < 0.0001 **** Statistical significance was defined as P < 0.05 (*P < 0.05, **P < 0.01, ***P < 0.001, ****P < 0.001).

At E11.5, 29 embryos were collected (Table 33). A Fisher's exact test revealed no statistically significant differences in the genotype frequencies, p = 0.1008. Once again, there was no statistically significant difference when compared with the cross of *Ctnnb1*$^{fl/wt}$ *Tek-Cre*$^{+/-}$ males with *Ctnnb1*^{flfl} *iSuRe-Cre*$^{+/+}$ females (Table 32), p = 0.4149. This suggest that even if the *Etv2-Cre* driver does lead to an earlier and more complete EC *Ctnnb1* ablation than the *Tek-Cre* driver, it does not result in statistically significant earlier embryonic lethality.

4.2.3 Crown-rump length analysis of Ctnnb1$^{E/EC}$ embryos

Embryos resulting from crosses between *Ctnnb1*$^{fl/wt}$ *Tek-Cre*$^{+/-}$ males and *Ctnnb1*^{flfl} *iSuRe-Cre*$^{+/+}$ females, when studied at E10-11.5, have genotype frequencies that significantly deviate from Mendelian ratios (p < 0.0001 and p = 0.0003, respectively) (Figure 38 and 39). To determine the cause of this, I next examined the embryos for gross morphological abnormalities.

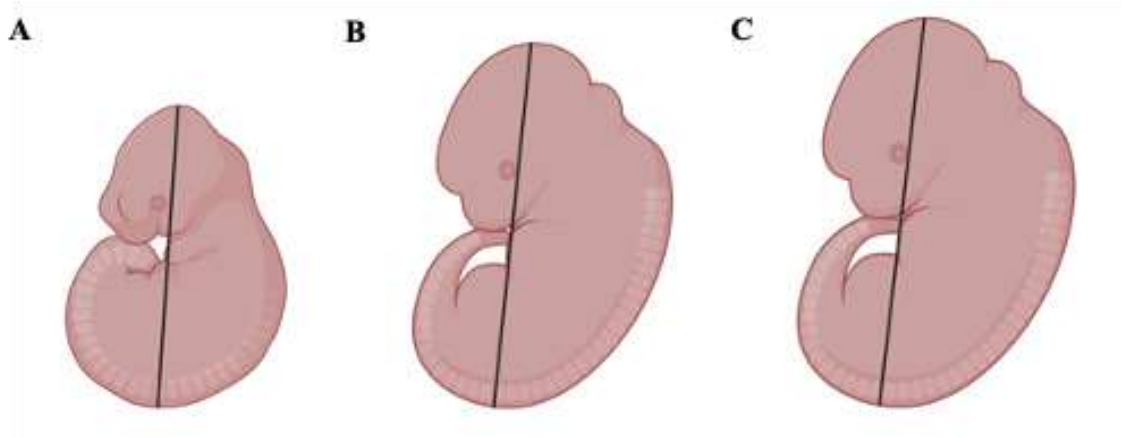

Figure 40: **Crown-Rump Length**. Crown-Rump length visually depicted in schematics of an (A) E10.5 embryo, (B) E11.5 embryo and (C) E12.5 embryo.

First, I examined the crown-rump length (CRL) of each embryo. CRL is a well-established metric used to assess embryonic growth, and is measured as the maximum distance from the cephalic pole to the caudal pole (Figure 40).[280] Embryos were imaged after dissection and fixation, and the images were analysed using FIJI/ImageJ software, with a line drawn from crown to rump to measure pixel distance. These measurements were then converted into micrometres (μm) to give the CRL (Table 36). At E10.5, I found no significant CRL differences between the *Ctnnb1*$^{fl/wt}$ *Tek-Cre*$^{-/-}$ *iSuRe-Cre*$^{+/-}$ embryos and the *Ctnnb1*$^{fl/fl}$ *Tek-Cre*$^{+/-}$ *iSuRe-Cre*$^{+/-}$ embryos, p = 0.3032. However, when examining descriptive statistics for each genotype category, it was evident that the *Ctnnb1*$^{fl/fl}$ *Tek-Cre*$^{+/-}$ *iSuRe-Cre*$^{+/-}$ embryos have a smaller mean CRL value, at 4370μm, compared to a mean of 4913μm for *Ctnnb1*$^{fl/wt}$ *Tek-Cre*$^{-/-}$ *iSuRe-Cre*$^{+/-}$ embryos. Moreover, *Ctnnb1*$^{fl/fl}$ *Tek-Cre*$^{+/-}$ *iSuRe-Cre*$^{+/-}$ embryos had less variability, with a range of 3433 μm and a standard deviation of 1031 μm.

At E11.5, I found statistically significant differences between the CRL in *Ctnnb1*$^{fl/wt}$ *Tek-Cre*$^{-/-}$ *iSuRe-Cre*$^{+/-}$ embryos compared with the *Ctnnb1*$^{fl/fl}$ *Tek-Cre*$^{+/-}$ *iSuRe-Cre*$^{+/-}$ embryos, p = 0.0001 ***. The mean CRL for *Ctnnb1*$^{fl/fl}$ *Tek-Cre*$^{+/-}$ *iSuRe-Cre*$^{+/-}$ embryos was 5234μm, compared to 6028μm for *Ctnnb1*$^{fl/wt}$ *Tek-Cre*$^{-/-}$ *iSuRe-Cre*$^{+/-}$ embryos. This

suggests that by E11.5, embryos with no *Ctnnb1* expression in their ECs are morphologically distinguishable from wildtype, and show general growth retardation.

Table 34: Descriptive statistics for E10.5 *Ctnnb1*$^{fl/wt}$ *Tek-Cre*$^{-/-}$ *iSuRe-Cre*$^{+/-}$ embryos and the *Ctnnb1*$^{fl/fl}$ *Tek-Cre*$^{+/-}$ *iSuRe-Cre*$^{+/-}$ embryos

	Ctnnb1$^{fl/fl}$ *Tek-Cre*$^{+/-}$ *iSuRe-Cre*$^{+/-}$	*Ctnnb1*$^{fl/wt}$ *Tek-Cre*$^{-/-}$ *iSuRe-Cre*$^{+/-}$
Number of Values	13	33
Minimum	3178	2406
Maximum	6611	9161
Range	3433	6755
Mean	4370	4913
Standard Deviation	1031	1754
Standard Error of Mean	286.1	305.3

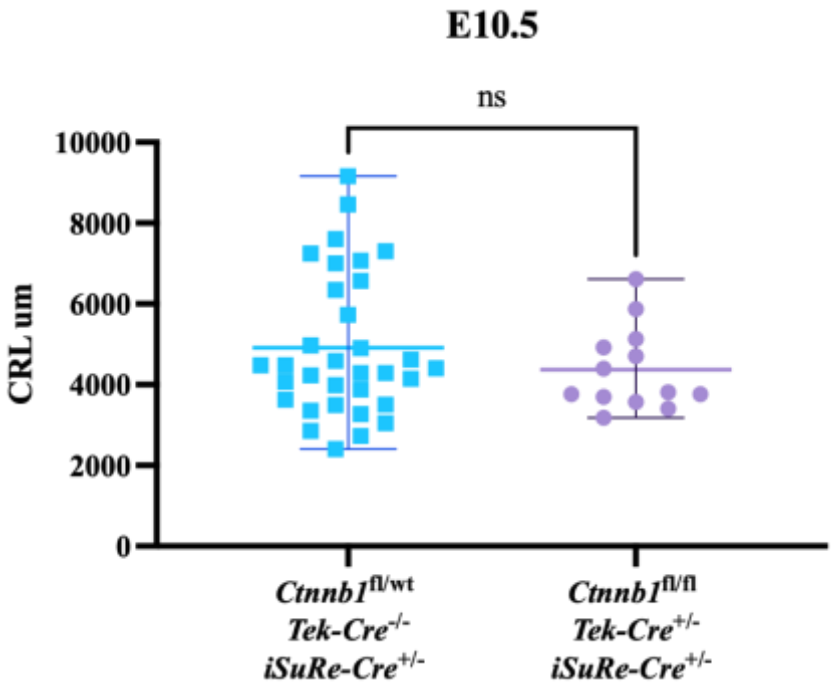

Figure 41: At E10.5, there was no statistically difference in CRL between *Ctnnb1*$^{fl/wt}$ *Tek-Cre*$^{-/-}$ *iSuRe-Cre*$^{+/-}$ embryos and the *Tek-Cre*$^{+/-}$ *Ctnnb1*$^{fl/fl}$ *iSuRe-Cre*$^{+/-}$ embryos, p = 0.3032**.** Data was first assessed for normality using the Shapiro-Wilks test, and then genotype groups were compared using an unpaired, two-tailed Student's t-test. Statistical significance was defined as $P < 0.05$ (*$P < 0.05$, **$P < 0.01$, ***$P < 0.001$, ****$P < 0.001$).

Table 35: Descriptive statistics for E11.5 *Tek-Cre*$^{-/-}$ *Ctnnb1*$^{fl/wt}$ *iSuRe-Cre*$^{+/-}$ embryos and the *Tek-Cre*$^{+/-}$ *Ctnnb1*$^{fl/fl}$ *iSuRe-Cre*$^{+/-}$ embryos

	Ctnnb1$^{fl/fl}$ *Tek-Cre*$^{+/-}$ *iSuRe-Cre*$^{+/-}$	*Ctnnb1*$^{fl/wt}$ *Tek-Cre*$^{-/-}$ *iSuRe-Cre*$^{+/-}$
Number of Values	30	81
Minimum	2882	3514
Maximum	6643	9161
Range	3761	5647
Mean	5234	6028
Standard Deviation	1128	848.4
Standard Error of Mean	205.9	94.26

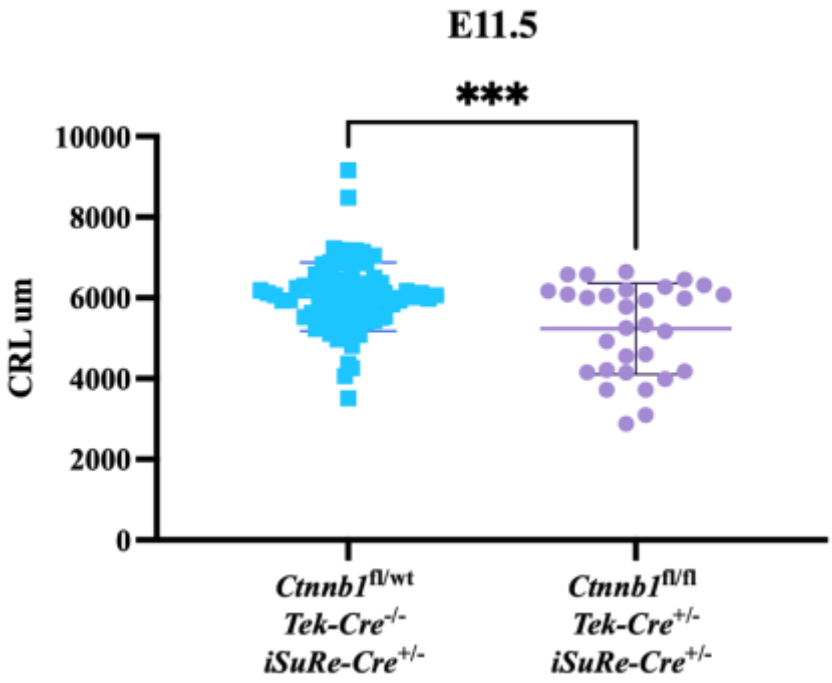

Figure 42: At E11.5, there was a statistically difference in CRL between *Tek-Cre*$^{-/-}$ *Ctnnb1*$^{fl/wt}$ *iSuRe-Cre*$^{+/-}$ embryos and the *Tek-Cre*$^{+/-}$ *Ctnnb1*$^{fl/fl}$ *iSuRe-Cre*$^{+/-}$ embryos, p = 0.0001. Data was first assessed for normality using the Shapiro-Wilks test, and then genotype groups were compared using an unpaired, two-tailed Student's t-test. Statistical significance was defined as $P < 0.05$ (*$P < 0.05$, **$P < 0.01$, ***$P < 0.001$, ****$P < 0.001$).

4.3 Using enhancer:reporter constructs to evaluate different EC subpopulations

Thus far, I have demonstrated a clear link between canonical Wnt signalling and embryonic lethality and growth retardation. Specifically, EC-ablation of *Ctnnb1* using the *Tek-Cre* driver in combination with *iSuRe-Cre* results in embryonic lethality by E10.5 ($p < 0.0001$), and a significantly reduced CRL by E11.5 ($p = 0.0001$). However, *Tek-Cre* is a pan-EC Cre driver, and therefore it is impossible to discern whether these gross phenotypes are being driven by all ECs, or a specific EC subpopulation. To answer this question, the consequences of *Ctnnb1* loss in distinct EC subtypes must be examined.

One approach to easily image different subtypes of ECs is to cross in enhancer:reporter genes specifically active in different types of ECs. As introduced in Chapter 3, enhancers can be used as a tool to study gene regulation in *in vivo* transgenic reporter assays. Consequently, here I used a variety of enhancer:*LacZ* lines to directly assess how canonical Wnt signalling influences the transcriptional regulation of these discrete EC subtypes and probe the regulation of distinct EC subpopulations. These include COUP-TFII:*LacZ* (active in venous and lymphatic ECs), *Dll4-12:LacZ* (active in mature arterial ECs), and *DLL4in3:LacZ* active in early and mature arterial ECs and angiogenic ECs).[197,230]

4.3.1 The *CoupTFII-965:LacZ* transgene shows a subtle expansion in activity in *Ctnnb1*$^{EC/EC}$ embryos

The first EC subpopulation I investigated was venous ECs. This EC subpopulation is often characterised by the expression of two distinct marker genes, *Nr2f2* (COUP-TFII) and *Ephb4*.[281-283] In addition to lining venous vessels, venous ECs are also now understood to contribute to the expansion of vascular networks through angiogenesis and lymphangiogenesis.[62,69,284] To study the consequences of *Ctnnb1* loss on venous ECs, I used the stable murine *CoupTFII-965:LacZ* transgenic line. The activity of this transgene has been extensively studied in both mice and zebrafish models, where it is mostly restricted to the venous endothelium.[183,230,285]

To examine the venous vasculature, I therefore crossed *CoupTFII-965:LacZ*$^{+/-}$ *Ctnnb1*$^{fl/wt}$ *Tek-Cre*$^{+/-}$ males with *Ctnnb1*^{flfl} *iSuRe-Cre*$^{+/+}$females. This means that, if Mendelian

ratios occur, 50% of embryos will carry the *LacZ* gene. In total, I collected 201 embryos between E9.5 and E12.5, 114 of which were positive for *CoupTFII-965:LacZ*. For simplicity, from hereon in, *Ctnnb1*$^{fl/fl}$ *Tek-Cre*$^{+/-}$ *iSuRe-Cre*$^{+/-}$ embryos will be shortened to *Ctnnb1*$^{EC/EC}$. The presence or absence of *LacZ* will be written as *LacZ*$^{+/-}$ or *LacZ*$^{-/-}$, respectively.

At E10.5, 126 embryos were collected, 12 of which were genotyped as *Ctnnb1*$^{EC/EC}$. From these 12 embryos, 6 had the *LacZ* gene present, although one of these embryos was significantly disintegrated **(**Figure 43, Panel E**)**, and one had been badly dissected **(**Figure 43, Panel H), resulting in the accidental removal of the bottom half of the embryo.

Table 36: Genotype of embryos from cross with *CoupTFII-965:LacZ*$^{+/-}$ *Ctnnb1*$^{fl/wt}$ *Tek-Cre*$^{+/-}$ males with *Ctnnb1*^{flfl} *iSuRe-Cre*$^{+/+}$ females. Summary table showing the percentange of each genotype, raw numbers are in brackets.

	Ctnnb1$^{fl/fl}$ *Tek-Cre*$^{+/-}$ *iSuRe-Cre*$^{+/-}$	*Ctnnb1*$^{fl/wt}$ *Tek-Cre*$^{+/-}$ iSuRe-*Cre*$^{+/-}$	*Ctnnb1*$^{fl/fl}$ *Tek-Cre*$^{-/-}$ iSuRe-*Cre*$^{+/-}$	*Ctnnb1*$^{fl/wt}$ *Tek-Cre*$^{-/-}$ iSuRe-*Cre*$^{+/-}$	Total
E9.5	0% (0)	83% (5)	0% (0)	17% (1)	6
E10.5	10% (12)	16% (20)	39% (49)	36% (45)	126
E11.5	9% (6)	32% (21)	21% (14)	38% (25)	66
E12.5	0% (0)	67% (2)	33% (1)	0% (0)	3

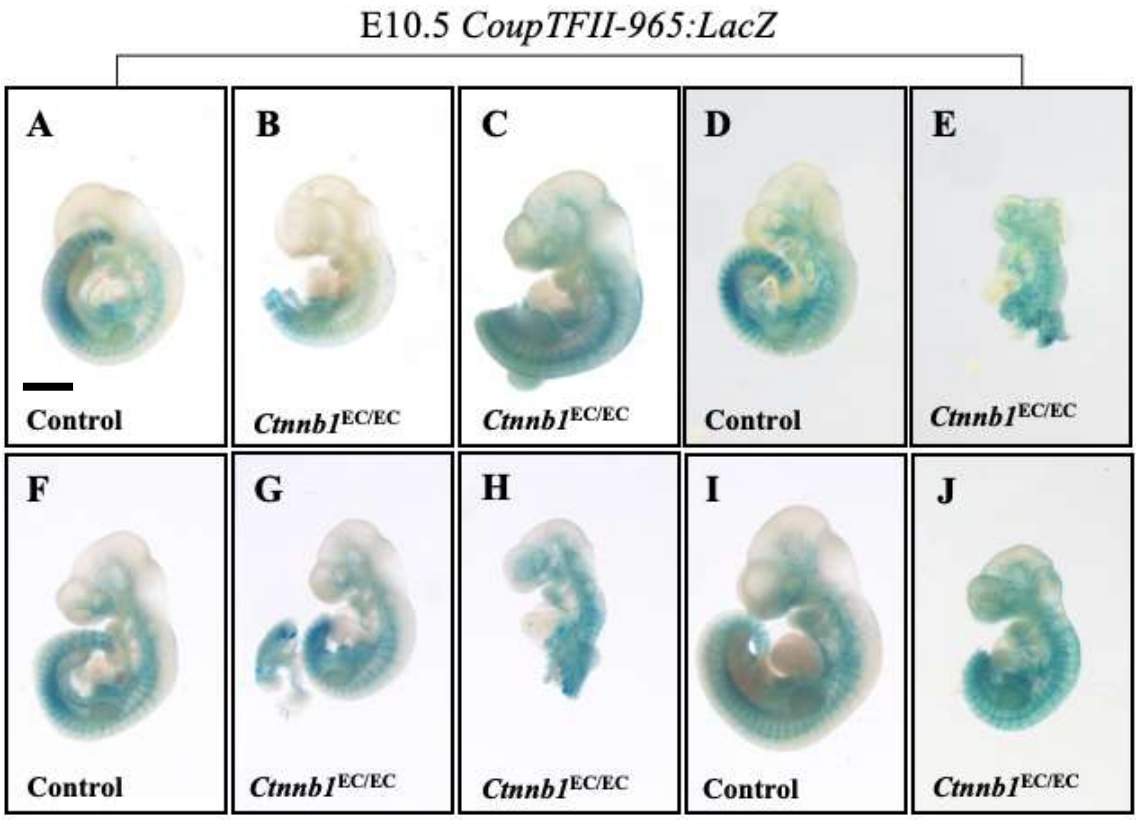

Figure 43: Of the 12 *Ctnnb1*$^{EC/EC}$ embryos collected at E10.5, six expressed the *CoupTFII-965:LacZ* gene. These came from four different litters. (A) represents a control E10.5 embryo expressing *CoupTFII-965:LacZ* gene, with (B) and (C) representing littermate *Ctnnb1*$^{EC/EC}$ embryos. Likewise (D) is the control embryo for (E); (F) the littermate control for (G) and (H); and, (I) the littermate control for (J). Scale bar represents 1mm.

The six *Ctnnb1*$^{EC/EC}$ *LacZ*$^{+/-}$ embryos came from four separate litters, and all have littermate controls positive for the *LacZ* gene (Figure 43). Although all the control embryos have a similar X-Gal staining pattern, as expected, there was considerable variability in the *Ctnnb1*$^{EC/EC}$ embryos. Despite two of the *Ctnnb1*$^{EC/EC}$ *LacZ*$^{+/-}$ embryos appearing smaller than their respective litter control embryos, their X-Gal staining pattern appears very similar (Figure 43: Panel B and G). This suggests that, even in the context of growth retardation, the vein EC enhancer regulation is not compromised. However, two of the *Ctnnb1*$^{EC/EC}$ *LacZ*$^{+/-}$ embryos instead had expanded X-Gal staining, most notably in the head and spinal region (Figure 43: Panel C and J). Two other *Ctnnb1*$^{EC/EC}$ *LacZ*$^{+/-}$ embryos, although not fully intact, also showed this expanded *LacZ* expression pattern (Figure 43: Panel E and H). Interestingly, whilst one viable *Ctnnb1*$^{EC/EC}$ embryo had significant growth retardation (Figure 43: Panel J), another *Ctnnb1*$^{EC/EC}$ embryo was larger than its littermate control (Figure 43: Panel C).

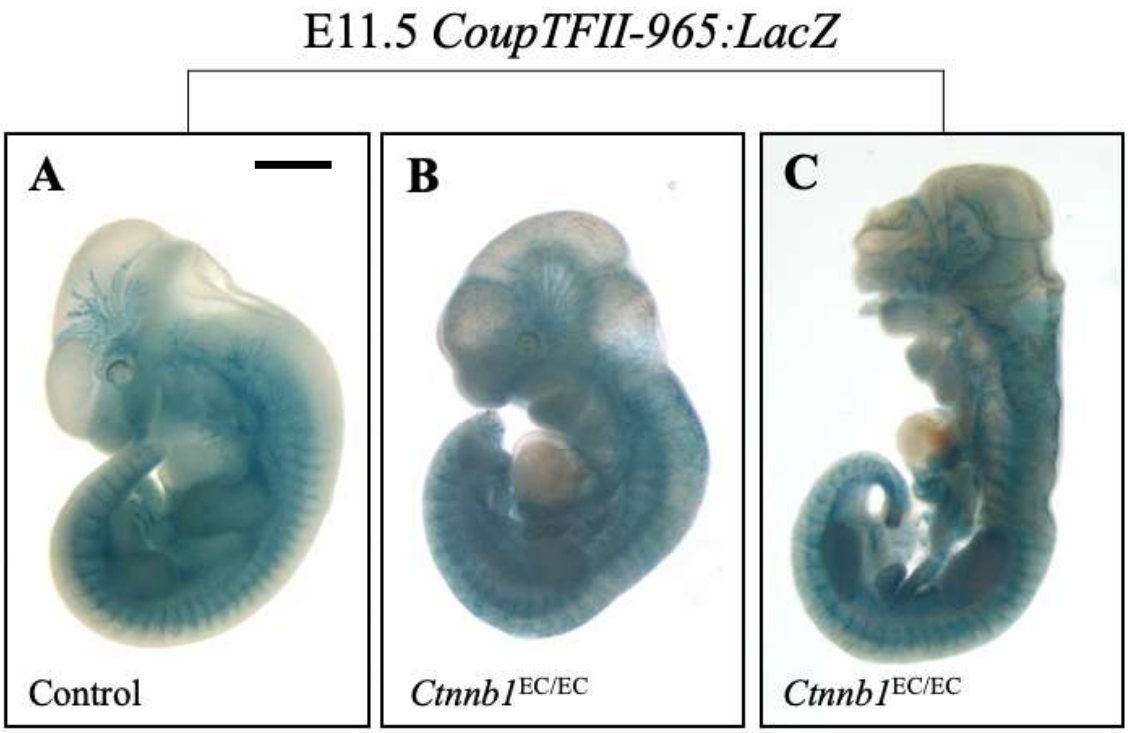

Figure 44: Of the six Ctnnb1$^{EC/EC}$ embryos collected at E11.5, only two expressed the COUP-TFII-965:*LacZ* gene. These came from two different litters. (A) represents a control E11.5 embryo expressing COUP-TFII-965:*LacZ* gene, with (B) representing the littermate Ctnnb1$^{EC/EC}$ *LacZ*$^{+/-}$ embryo. (C) shows a Ctnnb1$^{EC/EC}$ *LacZ*$^{+/-}$ embryo with no littermate control. All the embryos were imaged at the same magnification. Scale bar represents 1mm.

Despite collecting 66 embryos at E11.5, I only obtained six *Ctnnb1*$^{EC/EC}$, of which only two expressed LacZ. These two *LacZ*$^{+/-}$ *Ctnnb1*$^{EC/EC}$ embryos came from two different litters: frustratingly, one of which did not have a littermate control (Figure 44: Panel C). Although two embryos is a small sample, both appear to have an expanded X-Gal staining pattern in the head and spinal region compared to the control embryo. In addition, whilst the heart of the control embryo was had very faint X-Gal staining, the *LacZ*$^{+/-}$ *Ctnnb1*$^{EC/EC}$ hearts had no X-Gal staining at all. One of the *LacZ*$^{+/-}$ *Ctnnb1*$^{EC/EC}$ embryos has significant physical malformations, particularly in relation to its head which appears crumpled, and abnormally formed (Figure 44: Panel C).

In general, this slight expansion in *CoupTFII-965:LacZ* transgene activity, particularly in the head and spinal region, could reflect one of two things: either a loss of venous EC-specific spatial restriction for the COUPTFII enhancer, and thus transcriptional dysregulation, or an increase in venous vessels. In some ways this could be considered a similar outcome, since venous ECs are largely defined by expression of CoupTFII.

Additionally, considering that venous ECs are often the source of angiogenic sprouting, this could also reflect a general expansion in the vascular network.[69]

4.3.2 Arterial enhancer activity is unaffected in *Ctnnb1*$^{EC/EC}$ embryos relative to control

Having potentially identified an expanded venous EC identity phenotype in the *Ctnnb1*$^{EC/EC}$ embryos, I next investigated if there were any perturbations in arterial EC identity. Previous studies have reported that overexpression of the canonical Wnt signalling pathway in ECs causes defective arterial-venous specification, with arterial identity shown to expand beyond its usual territory and into venous compartments.[210] However, this analysis was restricted to analysis of a single arterial gene in a limited number of embryonic sections.[210] Here I wanted to further examine this potential phenotype.

One of the best characterised arterial EC enhancers is the Dll4-12 enhancer, located 12kb upstream of the Dll4 gene. The Dll4-12 enhancer can direct arterial EC-specific reporter gene expression both embryonically and postnatally.[197,227,229] To examine the effects of pan-EC *Ctnnb1* ablation on the arterial EC population, *Dll4-12:LacZ*$^{+/-}$ *Ctnnb1*$^{fl/wt}$ *Tek-Cre*$^{+/-}$ males were crossed with *Ctnnb1*^{flfl} *iSuRe-Cre*$^{+/+}$ females.

Table 37: Genotype of embryos from cross with *Dll4-12:LacZ*$^{+/-}$ *Ctnnb1*$^{fl/wt}$ *Tek-Cre*$^{+/-}$ males with *Ctnnb1*^{flfl} *iSuRe-Cre*$^{+/+}$ females. Summary table showing the percentange of each genotype, raw numbers are in brackets.

	Ctnnb1$^{fl/fl}$ *Tek-Cre*$^{+/-}$ *iSuRe-Cre*$^{+/-}$	*Ctnnb1*$^{fl/wt}$ *Tek-Cre*$^{+/-}$ *iSuRe-Cre*$^{+/-}$	*Ctnnb1*$^{fl/fl}$ *Tek-Cre*$^{-/-}$ *iSuRe-Cre*$^{+/-}$	*Ctnnb1*$^{fl/wt}$ *Tek-Cre*$^{-/-}$ *iSuRe-Cre*$^{+/-}$	Total
E11.5	11% (2)	6% (1)	44% (8)	39% (7)	18
E12.5	33% (1)	33% (1)	33% (1)	0% (0)	3

In total, 18 embryos, from three litters, were collected at E11.5. Two *Ctnnb1*$^{EC/EC}$ embryos were collected, both of which had the *LacZ* gene present, one of which was significantly growth retarded. In both cases, the *Ctnnb1*$^{EC/EC}$ embryos expressed *Dll4-12:LacZ* selectively in arteries, with no expansion or loss of *LacZ* expression (Figure 45). Previous studies in mice have suggested that canonical Wnt signalling is an important

regulator of arteriovenous identity acquisition. For instance, constitutive activation of β-catenin signalling causes veins to downregulate *Ephb4* whilst concomitantly upregulating *Efnb2*.[210] However, this experiment does not suggest a role for canonical Wnt signalling in regulating arterial expression.

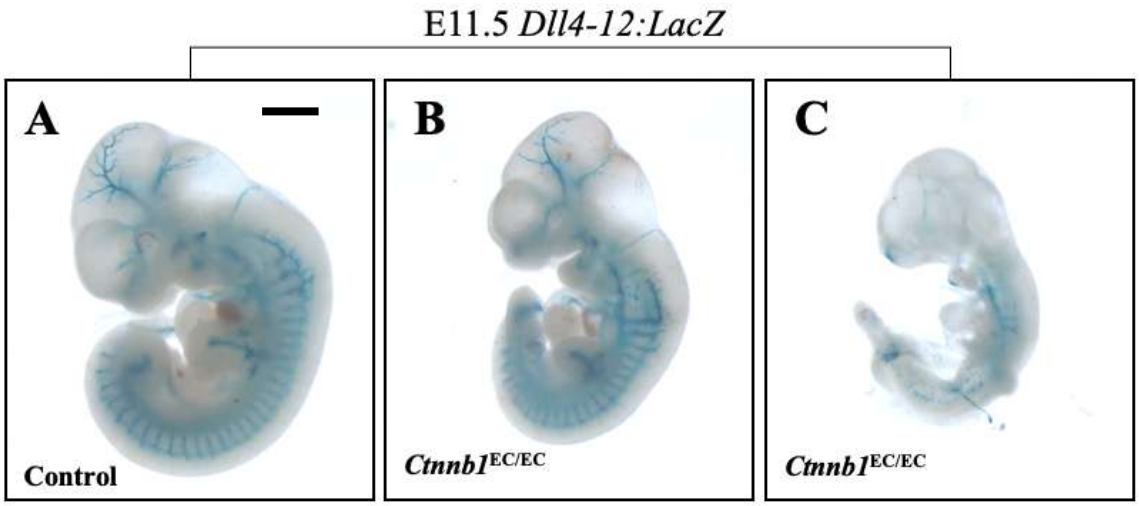

Figure 45: Both of the *Ctnnb1*$^{EC/EC}$ embryos collected at E11.5, expressed the *Dll4-12:LacZ* gene. These came from the same litter. (A) represents a control E11.5 embryo expressing *Dll4-12:LacZ* gene, with (B) and (C) representing the littermate *Ctnnb1*$^{EC/EC}$ embryos. All the embryos were imaged at the same magnification. Scale bar represents 1mm.

In total, only three embryos, from one litter, were collected at E12.5. One of these was a *Ctnnb1*$^{EC/EC}$ embryo, which had the *LacZ* gene present (Figure 46: Panel B). Whilst this embryo displayed no obvious phenotypic difference from the control embryo, this could be explained by lack of successful Cre recombination (Figure 46: Panel B').

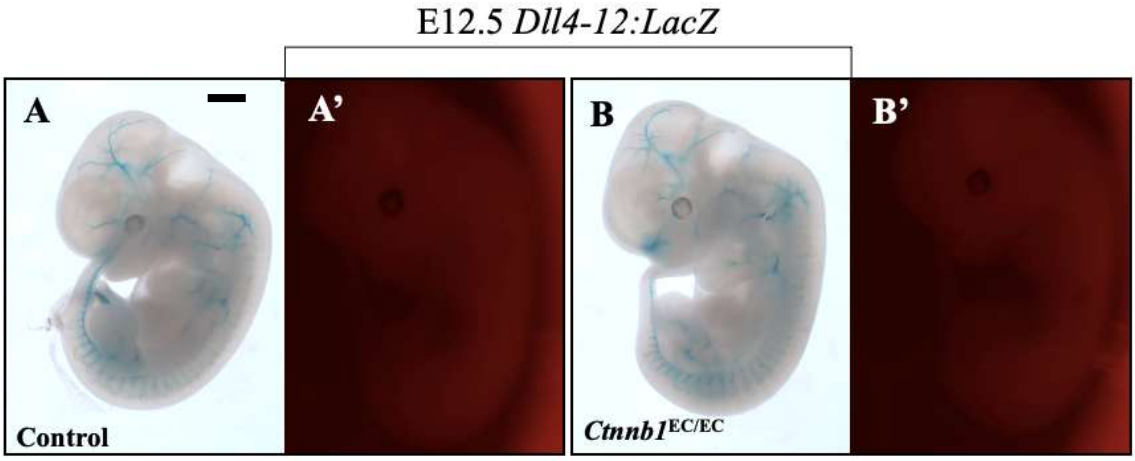

Figure 46: At E12.5, only one *Ctnnb1*$^{EC/EC}$ embryo was collected, which expressed the *Dll4-12:LacZ* gene. (A) represents a control E12.5 embryo expressing *Dll4-12:LacZ* gene, with (A') showing the lack of Cre recombination. (B) represents the *Ctnnb1*$^{EC/EC}$ embryo, with (B') showing the absence of successful Cre recombination despite having the *Tek-Cre* allele present. Therefore, although this embryo has the *Ctnnb1*$^{EC/EC}$ genotype, *Ctnnb1* has not been successfully ablated in ECs. All the embryos were imaged at the same magnification. Scale bar represents 1mm.

4.3.3 The *DLL4in3:LacZ* transgene activity subtly expands in E11.5 *Ctnnb1*$^{EC/EC}$ embryos

So far, I have found no significant differences in the arterial EC-specific enhancer activity patterns between *Ctnnb1*$^{EC/EC}$ and control embryos. However, there are multiple different arterial enhancers which have been characterised.[229] Whilst some have very specific activity restricted to arterial ECs, others are also active in other EC subpopulations. One such example is DLL4in3, which has been shown to direct reporter gene expression in both arterial ECs and angiogenic vessels.[197,227] Using a murine *DLL4in3:LacZ* transgenic line would therefore allow both arterial and angiogenic EC subpopulations to be investigated in parallel. When the regulation of the DLL4in3 enhancer was investigated in Chapter 3, TCF/LEF TFs emerged as potential determinants of spatial specificity. In total 125 embryos were collected ranging from E10.5 to E12.5 (Table 38).

Table 38: Genotype of embryos from cross with *DLL4in3:LacZ*$^{+/-}$ *Ctnnb1*$^{fl/wt}$ *Tek-Cre*$^{+/-}$ males with *Ctnnb1*^{flfl} *iSuRe-Cre*$^{+/+}$ females. Summary table showing the percentange of each genotype, raw numbers are in brackets.

	Ctnnb1$^{fl/fl}$ *Tek-Cre*$^{+/-}$ *iSuRe-Cre*$^{+/-}$	*Ctnnb1*$^{fl/wt}$ *Tek-Cre*$^{+/-}$ *iSuRe-Cre*$^{+/-}$	*Ctnnb1*$^{fl/fl}$ *Tek-Cre*$^{-/-}$ *iSuRe-Cre*$^{+/-}$	*Ctnnb1*$^{fl/wt}$ *Tek-Cre*$^{-/-}$ *iSuRe-Cre*$^{+/-}$	Total
E10.5	8% (1)	0% (0)	46% (6)	46% (6)	13
E11.5	16% (13)	25% (20)	25% (20)	33% (26)	79
E12.5	4% (1)	31% (8)	42% (11)	23% (6)	26

At E10.5, 13 embryos were collected, including one *Ctnnb1*$^{EC/EC}$ *LacZ*$^{+/-}$ embryo (Figure 47: Panel B). Unfortunately, this embryo did not remain completely intact. Although it is hard to be completely sure, there does not appear to be any growth retardation, and the X-Gal staining pattern is very similar.

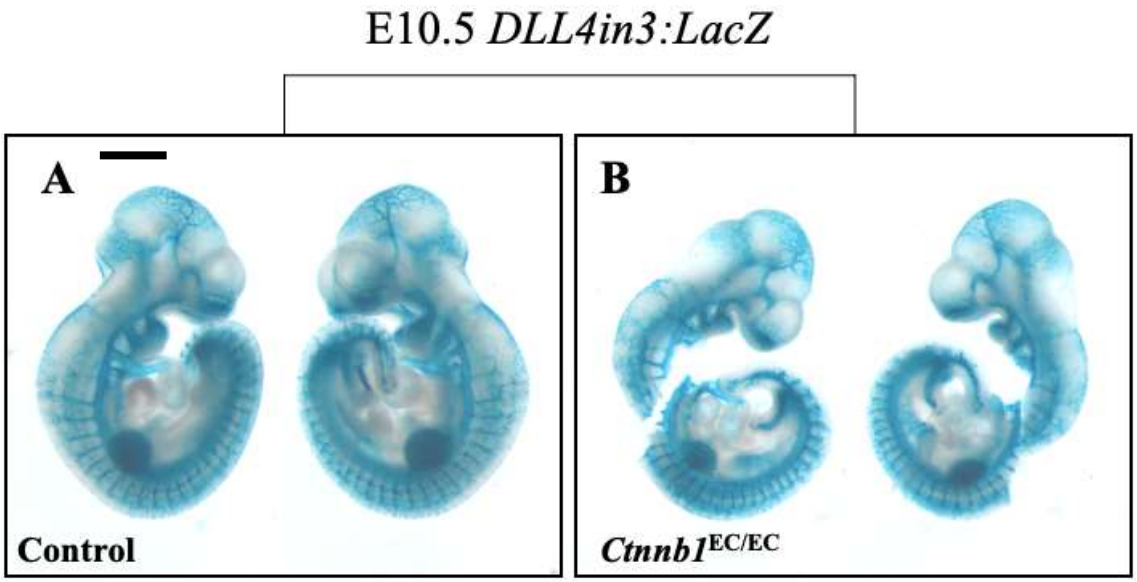

Figure 47: There was only one *Ctnnb1*$^{EC/EC}$ embryo collected at E10.5, which expressed the *DLL4in3:LacZ* gene. (A) represents a control E10.5 embryo expressing *DLL4in3:LacZ* gene, with (B) representing the littermate *Ctnnb1*$^{EC/EC}$ embryo. All the embryos were imaged at the same magnification. Scale bar represents 1mm.

At E11.5, 79 embryos were collected, including 13 *Ctnnb1*$^{EC/EC}$. Eight of these *Ctnnb1*$^{EC/EC}$ embryos had the *LacZ* gene. Of these 8 *LacZ*$^{+/-}$ *Ctnnb1*$^{EC/EC}$ embryos, three appeared dead (Figure 48: Panel D, G and M), and one embryo had such little tissue remaining that no conclusions can be drawn (Figure 48: Panel E). One *Ctnnb1*$^{EC/EC}$

LacZ$^{+/-}$ embryo had no recombination, as evidenced with no *MbTomato* expression (Figure 48: Panel J'). This was excluded from further analysis. Although obviously hard to ascertain, the LacZ expression pattern in Figure 48: Panel D and G seemed to be consistent with the control littermate embryos. Therefore, whilst they seem to have died *in utero*, they have probably only been dead relatively recently. Despite one *Ctnnb1*$^{EC/EC}$ embryos being genotyped as *LacZ*$^{+/-}$, there was no observable X-Gal staining (Figure 48: Panel M).

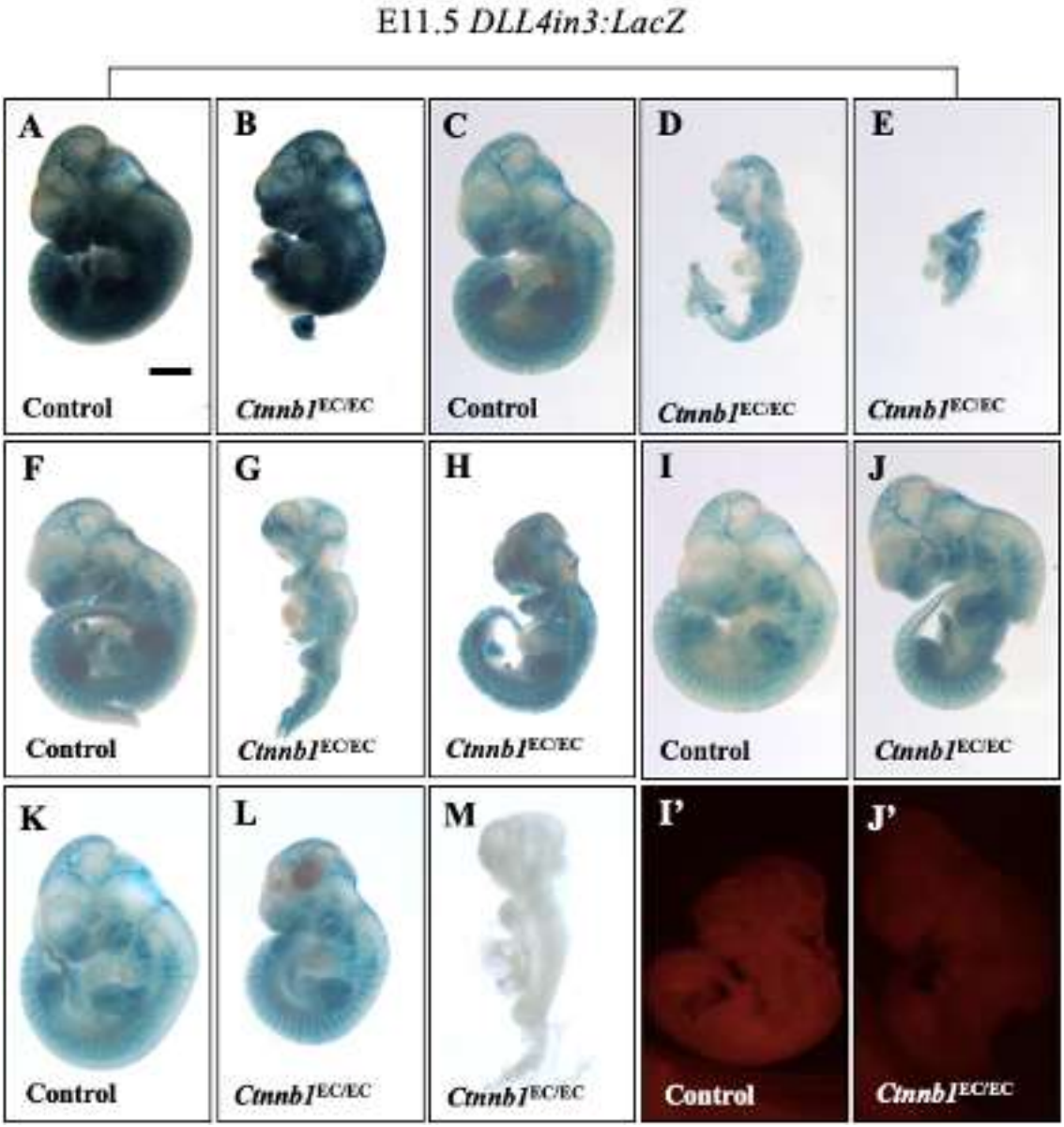

Figure 48: Of the 13 *Ctnnb1*$^{EC/EC}$ embryos collected at E11.5, eight expressed the *DLL4in3:LacZ* gene. These came from five different litters. (A) represents a control E10.5 embryo expressing *DLL4in3:LacZ* gene, with (B) representing littermate *Ctnnb1*$^{EC/EC}$ embryos. Likewise (C) is the control embryo for (D) and (E); (F) the littermate control for (G) and (H); (I) the littermate control for (J); and (K) the littermate control for (L) and (M). (J') shows the absence of successful Cre recombination. All the embryos were imaged at the same magnification.

Four of the *Ctnnb1*$^{EC/EC}$ *LacZ*$^{+/-}$ embryos appeared viable at the timepoint of analysis. Whilst one *Ctnnb1*$^{EC/EC}$ *LacZ*$^{+/-}$ embryo had very similar X-Gal staining patterns to its respective littermate controls (Figure 48: Panel K and L), another *Ctnnb1*$^{EC/EC}$ *LacZ*$^{+/-}$ embryos appeared to have an expansion in X-Gal staining compared to the littermate control (Figure 48: Panel A and B). Whilst it is harder to ascertain the X-Gal staining pattern in Figure 48: Panel H, considering the significant physical deformities, this *Ctnnb1*$^{EC/EC}$ *LacZ*$^{+/-}$ embryo also does seem to have an expansion in *LacZ* expression. This appears in accordance with my previous observations in transient mutTCF/LEF *DLL4in3:GFP* transgenic zebrafish. However, once again, this is a very small *n* number.

Of note, one *Ctnnb1*$^{EC/EC}$ *LacZ*$^{+/-}$ embryo, whilst still viable, had significantly different morphology from the control, with potential diffuse haemorrhaging (Figure 48: Panel H). These distinctive brown patches were also observed in another *Ctnnb1*$^{EC/EC}$ *LacZ*$^{+/-}$ embryo (Figure 48: Panel L).

A general growth retardation was noted in two of the *LacZ*$^{+/-}$ *Ctnnb1*$^{EC/EC}$ embryos (Figure 48: Panel L and H). Curiously, both of these embryos have proportionally smaller heads than their control littermates, (head length : CRL). Indeed, Figure 48: Panel L (0.38:1) compared to Figure 48: Panel K (0.48:1), and Figure 48: Panel H (0.38:1) to Figure 48: Panel F (0.43:1).

4.3.4 In a *Tek-Cre* background, the *SOX7-58:LacZ* transgene activity expands in E11.5 *Ctnnb1*$^{EC/EC}$ embryos

So far, my results suggest that the transcription regulation of arterial ECs is not compromised in *Ctnnb1*$^{EC/EC}$ embryos, whilst the spatial specificity of venous and angiogenic EC enhancers might be perturbed. In Chapter 3, SOX7-58 was shown to drive reporter gene expression specifically in angiogenic ECs, most obviously in the postnatal retina of transgenic mice expressing the *SOX7-58:LacZ* transgene. When the regulation of SOX7-58 was investigated, TCF/LEF TFs emerged as potential determinants of spatial specificity. Here, to assess the impact of EC-specific *Ctnnb1* on angiogenic ECs, I therefore now looked at the expression of the *SOX7-58:LacZ* transgene, using both *Tek-Cre* and *Etv2-Cre*.

In total, 247 embryos between E9.5 and E12.5 were collected from crosses with *SOX7-58:LacZ*$^{+/-}$ *Ctnnb1*$^{fl/wt}$ *Tek-Cre*$^{+/-}$ males with *Ctnnb1*^{flfl} *iSuRe-Cre*$^{+/+}$females (Table 39).

Table 39: Genotype of embryos from cross with *SOX7-58:LacZ*$^{+/-}$ *Ctnnb1*$^{fl/wt}$ *Tek-Cre*$^{+/-}$ males with *Ctnnb1*^{flfl} *iSuRe-Cre*$^{+/+}$ females. Summary table showing the percentange of each genotype, raw numbers are in brackets.

	Ctnnb1$^{fl/fl}$ *Tek-Cre*$^{+/-}$ *iSuRe-Cre*$^{+/-}$	*Ctnnb1*$^{fl/wt}$ *Tek-Cre*$^{+/-}$ *iSuRe-Cre*$^{+/-}$	*Ctnnb1*$^{fl/fl}$ *Tek-Cre*$^{-/-}$ *iSuRe-Cre*$^{+/-}$	*Ctnnb1*$^{fl/wt}$ *Tek-Cre*$^{-/-}$ *iSuRe-Cre*$^{+/-}$	Total
E9.5	11% (1)	22% (2)	22% (2)	44% (4)	9
E10.5	17% (11)	29% (19)	23% (15)	32% (21)	66
E11.5	12% (17)	20% (27)	27% (37)	29% (40)	137
E12.5	4% (1)	22% (5)	48% (11)	26% (6)	23
>E13.5	0% (0)	25% (3)	17% (2)	58% (7)	12

At E9.5, nine embryos were collected, including one *Ctnnb1*$^{EC/EC}$ embryo. However, this embryo did not carry the *SOX7-58:LacZ* transgene.

At E10.5, 66 embryos were collected, including 11 *Ctnnb1*$^{EC/EC}$ embryos. Six of these *Ctnnb1*$^{EC/EC}$ embryos had the *SOX7-58:LacZ* transgene, with only one embryo appearing dead (Figure 49: Panel B). In general, quite similar vascular X-Gal staining patterns were observed between the *Ctnnb1*$^{EC/EC}$ embryos and their littermate controls. Whilst undoubtedly subtle, there perhaps is an expansion in *SOX7-58:LacZ* transgene activity in the spinal region of one *LacZ*$^{+/-}$ *Ctnnb1*$^{EC/EC}$ embryo (Figure 49: Panel G), and in head region of another *LacZ*$^{+/-}$ *Ctnnb1*$^{EC/EC}$ embryo (Figure 49: Panel E). Growth retardation was observed in four *LacZ*$^{+/-}$ *Ctnnb1*$^{EC/EC}$ embryos, although in two of these embryos, this is not in conjunction with expansion in X-Gal staining (Figure 49: Panel D and J). This does not seem to support the notion that canonical Wnt signalling is required for the angiogenic EC specificity of SOX7-58 activity at E10.5.

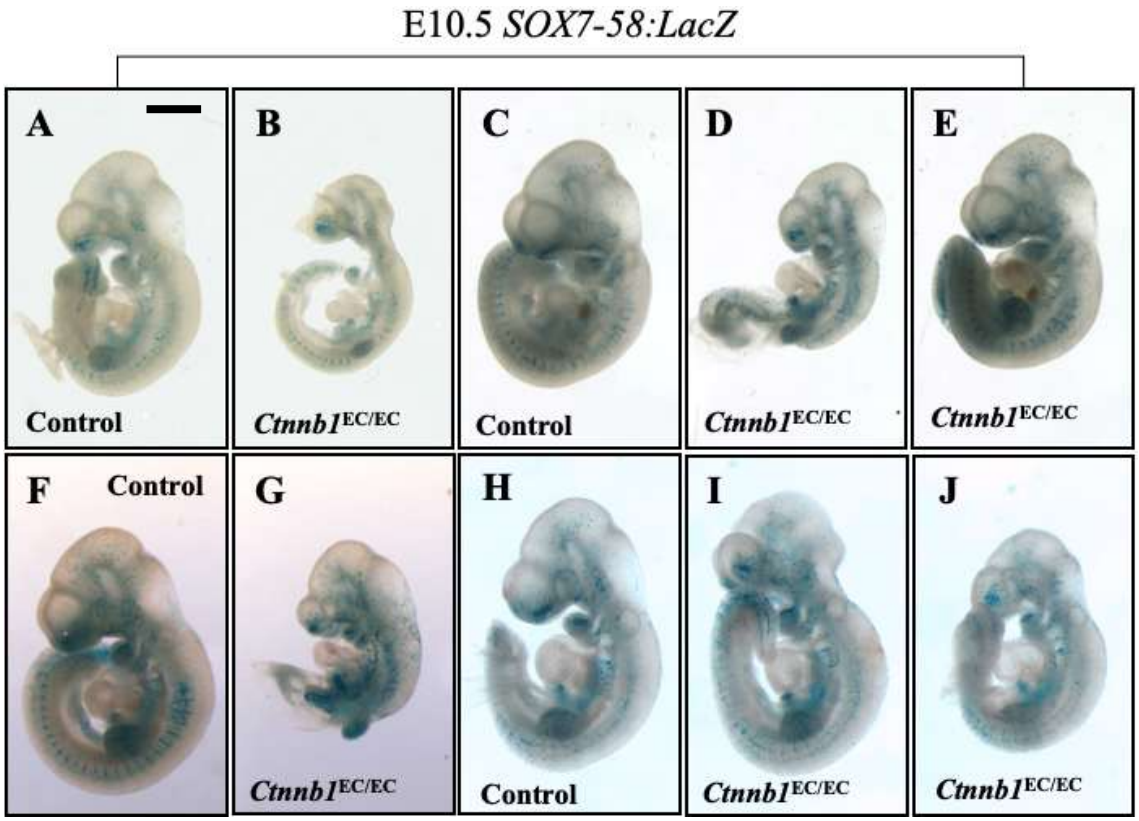

Figure 49: Of the 11 *Ctnnb1*$^{EC/EC}$ embryos collected at E10.5, six expressed the *SOX7-58:LacZ* gene. These came from four different litters. (A) represents a control E10.5 embryo expressing *SOX7-58:LacZ* gene, with (B) representing the littermate *Ctnnb1*$^{EC/EC}$ embryo. Likewise (C) is the control embryo for (D) and (E); (F) the littermate control for (G)); and (H) the littermate control for (I) and (J). All the embryos were imaged at the same magnification.

At E11.5, 137 embryos were collected, including 17 including *Ctnnb1*$^{EC/EC}$ embryos. At this timepoint, *Ctnnb1*$^{EC/EC}$ embryo collection was significantly hindered by embryonic lethality. However, from these 17 *Ctnnb1*$^{EC/EC}$ embryos, 12 expressed the *LacZ* gene. Compared to the *Ctnnb1*$^{EC/EC}$ embryos collected at E10.5, the *Ctnnb1*$^{EC/EC}$ E11.5 had drastic variability, both with regard to their overall morphology and their X-Gal staining pattern. Indeed, more of the embryos had clearly died, somewhat limiting analysis of SOX7-58 activity in an *in vivo* context (Figure 50: Panel L, O, P, Q, R, and T).

Nonetheless, it is clear that many of the *Ctnnb1*$^{EC/EC}$ embryos which remained viable still had significant growth and developmental delay (Figure 50: Panel B, C, E, G and H). Generally, the embryos exhibited an expansion in X-Gal staining, indicating more widespread SOX7-58 activity (Figure 50: Panel B, E and J, but also to a lesser extent Figure 50: Panel N). This increase in activity does not seem restricted to one specific region of the embryo, potentially reflecting a widespread change. This is different to the

expansion in X-Gal staining observed with the *DLL4in3:LacZ* transgene which was mostly restricted to the head and spinal region. For example, there appeared to be more vascular X-Gal staining in the limb buds in some *SOX7-58:LacZ*$^{+/-}$ embryos (Figure 50: Panel B, E, J and N). Whilst Figure 50: Panel B and E both had significant growth retardation, Figure 50: Panel J and D were comparative sizes with their littermate controls. This suggests that dysregulation of SOX7-58 enhancer activity is not just restricted to embryos with gross growth phenotypes. Analysis of Figure 50: Panel C and G does not seem to show an expansion in *LacZ* expression, although these embryos have been damaged during dissection, and therefore it is hard to truly ascertain the staining in the complete embryo.

In order to better interpret the potential expansion of *SOX7-58:LacZ* activity observed in whole-mount X-Gal staining, one *SOX7-58:LacZ*$^{+/-}$ control and one *SOX7-58:LacZ*$^{+/-}$ *Ctnnb1*$^{EC/EC}$ embryo were sectioned. This allowed me to assess whether the X-Gal staining expression was confined to the vasculature, or if there was ectopic enhancer activity in non-vascular structures. In the whole-mount X-Gal staining, the *LacZ*$^{+/-}$ *Ctnnb1*$^{EC/EC}$ embryo in Figure 50: Panel E was chosen for sectioning, as it appeared viable and exhibited some expansion in SOX7-58 activity. The embryo in Figure 50: Panel D was used as a control, as it was from same litter and therefore both embryos were stained and fixed under identical conditions.

Both the control and *Ctnnb1*$^{EC/EC}$ embryo had X-Gal staining restricted to ECs (Figure 51). The most notable differences were observed around the neural tube, with the *Ctnnb1*$^{EC/EC}$ embryo expressing *LacZ* in far more the small perineural and intraneural vessels. This was true throughout the entirety of the embryo. However, this expansion of EC+ vessels was seen beyond neural tissue, as the *Ctnnb1*$^{EC/EC}$ embryo also showed extensive expanded *LacZ* expression in the mid-trunk around the forming limb bud (Figure 51: Panel N), and the hepatic primordia (Figure 51: Panel O).

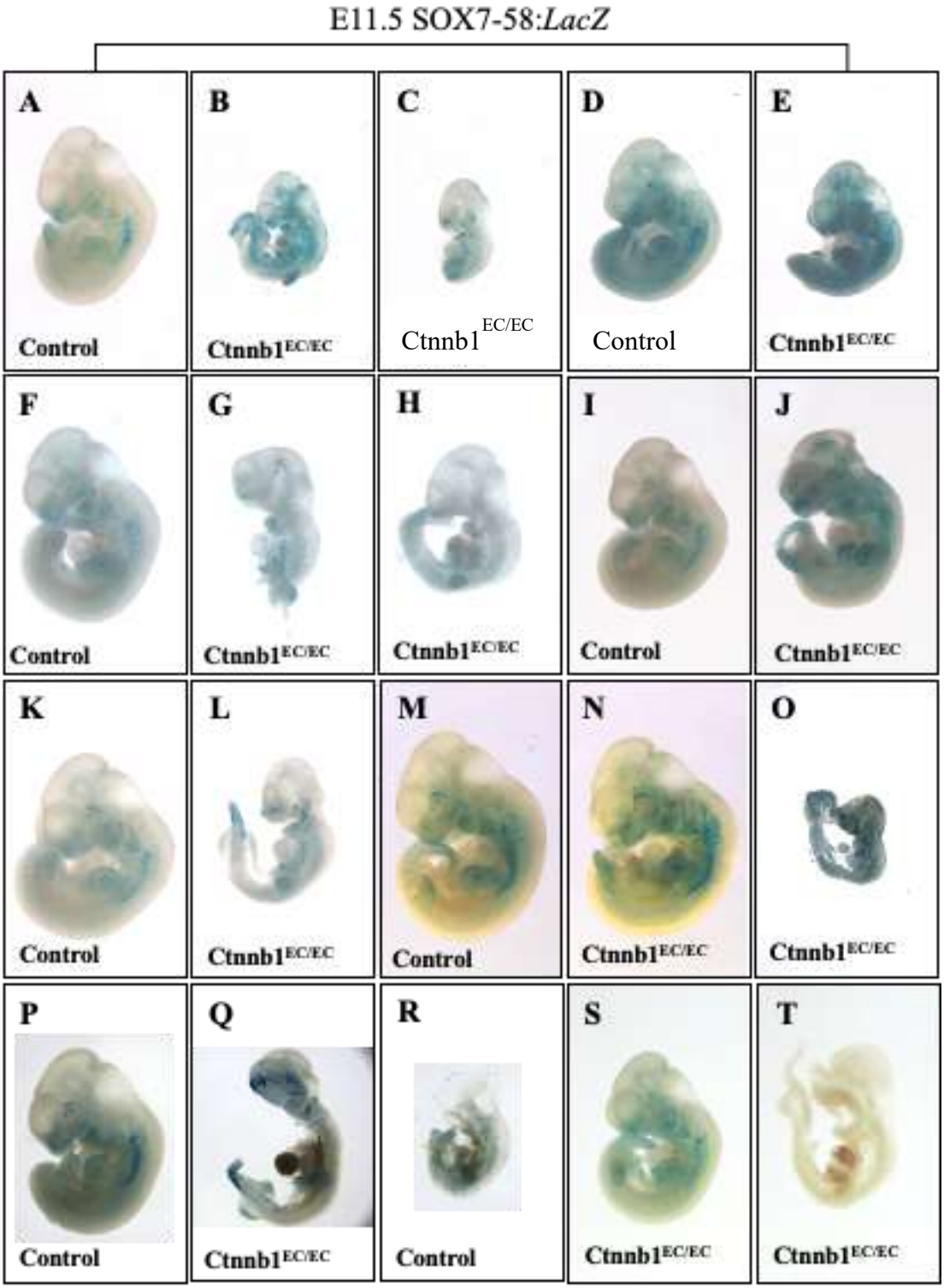

Figure 50: Of the 17 *Ctnnb1*$^{EC/EC}$ embryos collected at E11.5, 12 expressed the *SOX7-58:LacZ* gene. These came from nine different litters. (A) represents a control E10.5 embryo expressing *SOX7-58:LacZ* transgene, with (B) and (C) representing littermate *Ctnnb1*$^{EC/EC}$ embryos. Likewise (D) is the control embryo for (E); (F) the littermate control for (G) and (H); (I) the littermate control for (J); (K) the littermate control for (L); (M) the littermate control for (N); (O) a *Ctnnb1*$^{EC/EC}$ embryo with no littermate control; (P) the littermate control for (Q) and (R); and (S) the littermate control for (T).

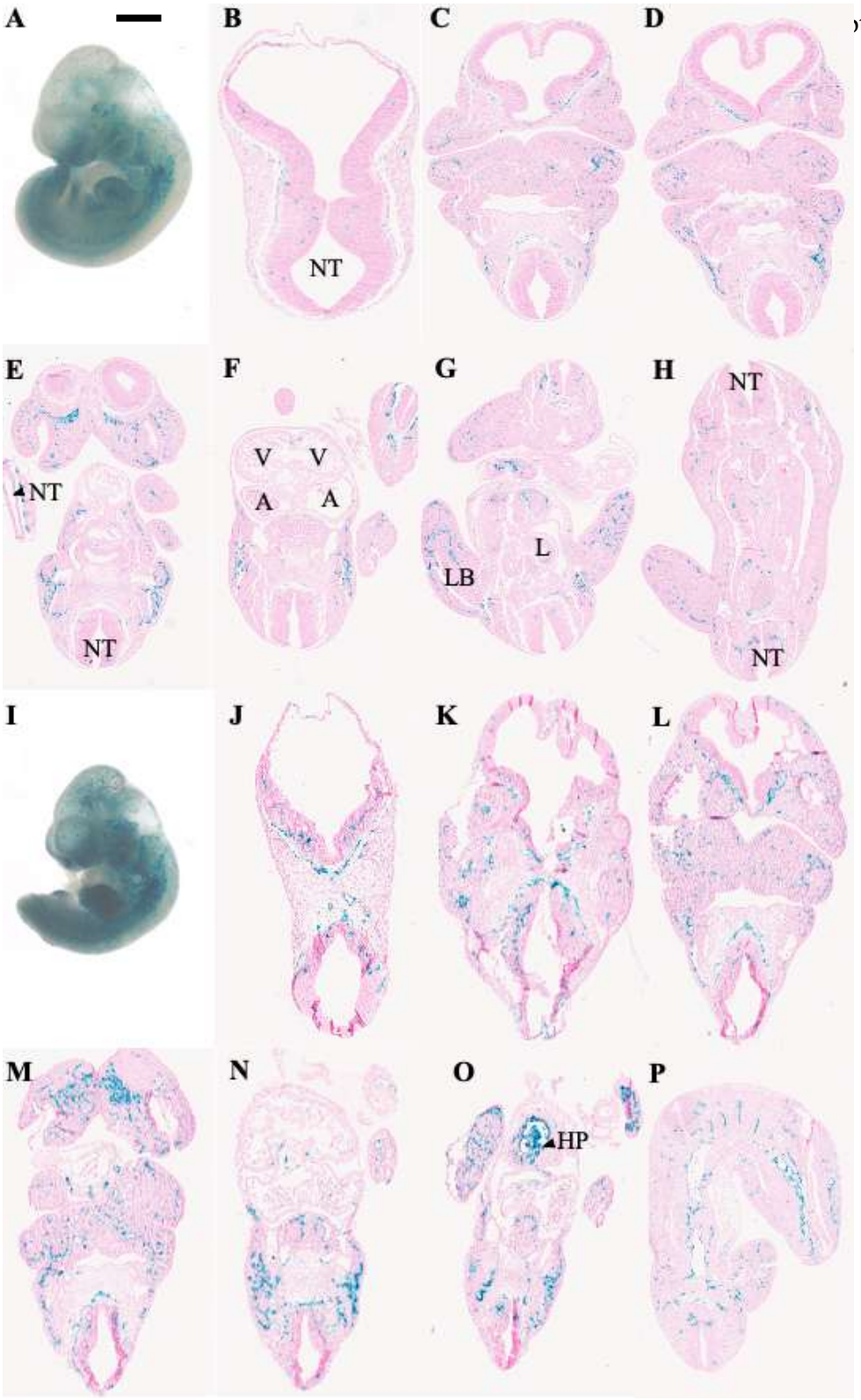

Figure 51: Expansion of X-Gal staining is seen throughout sections of an E11.5 *Ctnnb1*$^{EC/EC}$ (I) compared to a littermate control (A). X-Gal stained embryos were sectioned and counter-stained with Nuclear Fast Red. *Ctnnb1*$^{EC/EC}$ sections (J-P), littermate control sections (B-H). Scale bar represents 1mm.

Abbreviations: A = aorta; HP = hepatic primordia; L = lung; LB = limb bud; NT = neural tube; V = ventricle

At E12.5, only one *Ctnnb1*$^{EC/EC}$ embryo was collected, and although it did express the *LacZ* gene, it was not viable (Figure 52: Panel B).

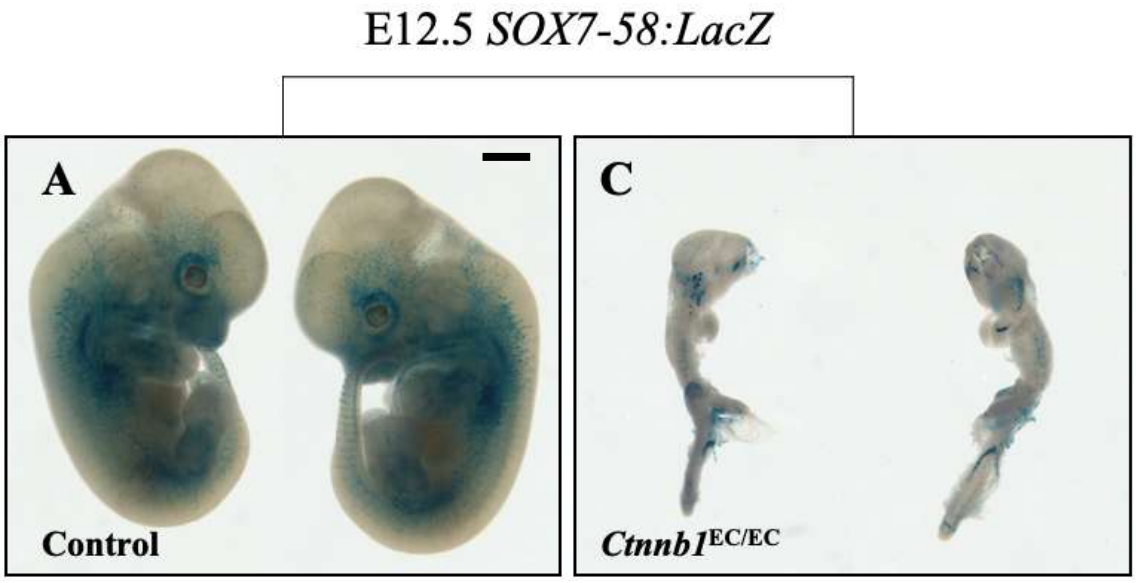

Figure 52: Only one *Ctnnb1*$^{EC/EC}$ embryos collected at E12.5, which although did express the *SOX7-58:LacZ* gene, was non-viable, with significant developmental retardation. (A) represents a control E12.5 embryo expressing *SOX7-58:LacZ* gene, with (B) representing the littermate *Ctnnb1*$^{EC/EC}$ embryo. All the embryos were imaged at the same magnification. Scale bar represents 1mm.

4.3.5 In an *Etv2-Cre* background, the *SOX7-58:LacZ* transgene activity potentially expands in E11.5 *Ctnnb1*$^{EC/EC}$ embryos, with no expansion observed at in E10.5 *Ctnnb1*$^{EC/EC}$ embryos

Having observed an expansion of SOX7-58 activity in E11.5 *Ctnnb1*$^{EC/EC}$ embryos generated using the *Tek-Cre* driver, I next investigated whether an expansion in X-Gal staining would be observed in *SOX7-58:LacZ*$^{+/-}$ *Ctnnb1*$^{EC/EC}$ embryos generated with the *Etv2-Cre* driver.

Table 40: Genotype of embryos from cross with *SOX7-58:LacZ*$^{+/-}$ *Etv2-Cre*$^{+/-}$ *Ctnnb1*$^{fl/wt}$ males with *Ctnnb1*^{flfl} *iSuRe-Cre*$^{+/+}$ females. Summary table showing the percentange of each genotype, raw numbers are in brackets.

	Ctnnb1$^{fl/fl}$ *Etv2-Cre*$^{+/-}$ *iSuRe-Cre*$^{+/-}$	*Ctnnb1*$^{fl/wt}$ *Etv2-Cre*$^{+/-}$ *iSuRe-Cre*$^{+/-}$	*Ctnnb1*$^{fl/fl}$ *Etv2-Cre*$^{-/-}$ *iSuRe-Cre*$^{+/-}$	*Ctnnb1*$^{fl/wt}$ *Etv2-Cre*$^{-/-}$ *iSuRe-Cre*$^{+/-}$	Total
E10.5	20% (8)	27% (11)	20% (8)	34% (14)	41
E11.5	17% (5)	28% (8)	14% (4)	42% (12)	29
E12.5	50% (2)	25% (1)	25% (1)	0% (0)	4

At E10.5, 41 embryos were collected, including eight *Ctnnb1*$^{EC/EC}$ embryo, four of which had the LacZ gene present (Figure 53). These embryos came from three different litters, with one litter having two *LacZ*$^{+/-}$ *Ctnnb1*$^{EC/EC}$ embryos. Frustratingly, the two of the *Ctnnb1*$^{EC/EC}$ embryos did not have littermate controls (Figure 53: Panel D and E). However, none of the four *LacZ*$^{+/-}$ *Ctnnb1*$^{EC/EC}$ embryos appear to have an expanded X-Gal staining compared with the control in Figure 53: Panel A.

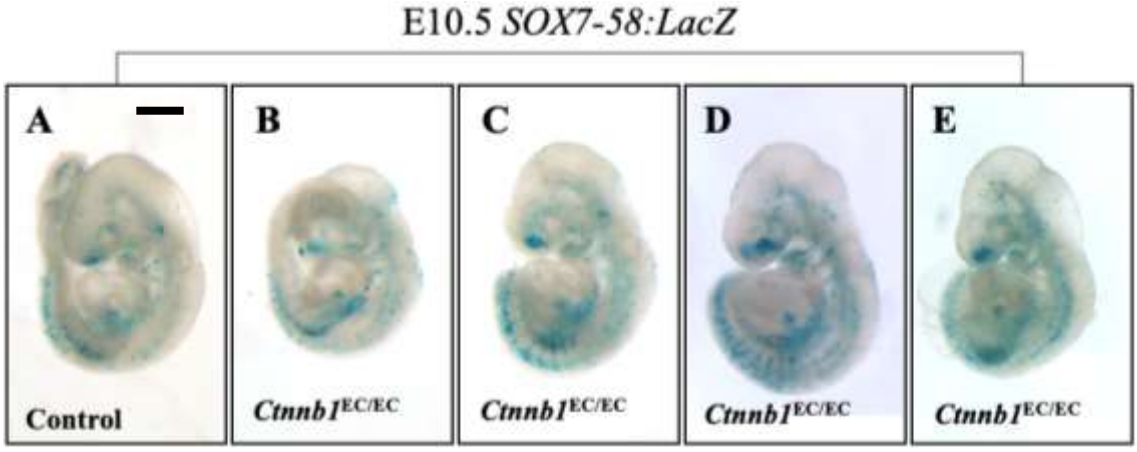

Figure 53: Of the eight *Ctnnb1*$^{EC/EC}$ embryos collected at E10.5, four expressed the *SOX7-58:LacZ* gene. These came from three different litters. (A) represents a control E10.5 embryo expressing *SOX7-58:LacZ* gene, with (B) and (C) representing littermate *Ctnnb1*$^{EC/EC}$ embryos. Both (D) and (E) are *LacZ*$^{+/-}$ *Ctnnb1*$^{EC/EC}$ embryos, but do not have littermate controls. All the embryos were imaged at the same magnification.

At E11.5, 29 embryos were collected, including five *Ctnnb1*$^{EC/EC}$ embryo, four of which had the *LacZ* gene present. These embryos came from three different litters, although one *Ctnnb1*$^{EC/EC}$ embryo did not have a littermate control (Figure 54: Panel F). Unfortunately, not all of the *Ctnnb1*$^{EC/EC}$ embryos collected were viable, with two appearing dead (Figure 54: Panel B and C). The *Ctnnb1*$^{EC/EC}$ embryo in Figure 54: Panel F had significant growth retardation, but interestingly, did not seem to have an expansion in X-Gal staining. However, it did not have a littermate control. Perhaps most informative is the *LacZ*$^{+/-}$ *Ctnnb1*$^{EC/EC}$ embryo in Figure 54: Panel E: there was slight growth retardation, a deformed head, and an increase in X-Gal staining. There also appeared to be haemorrhage, as evidenced by the brown patches.

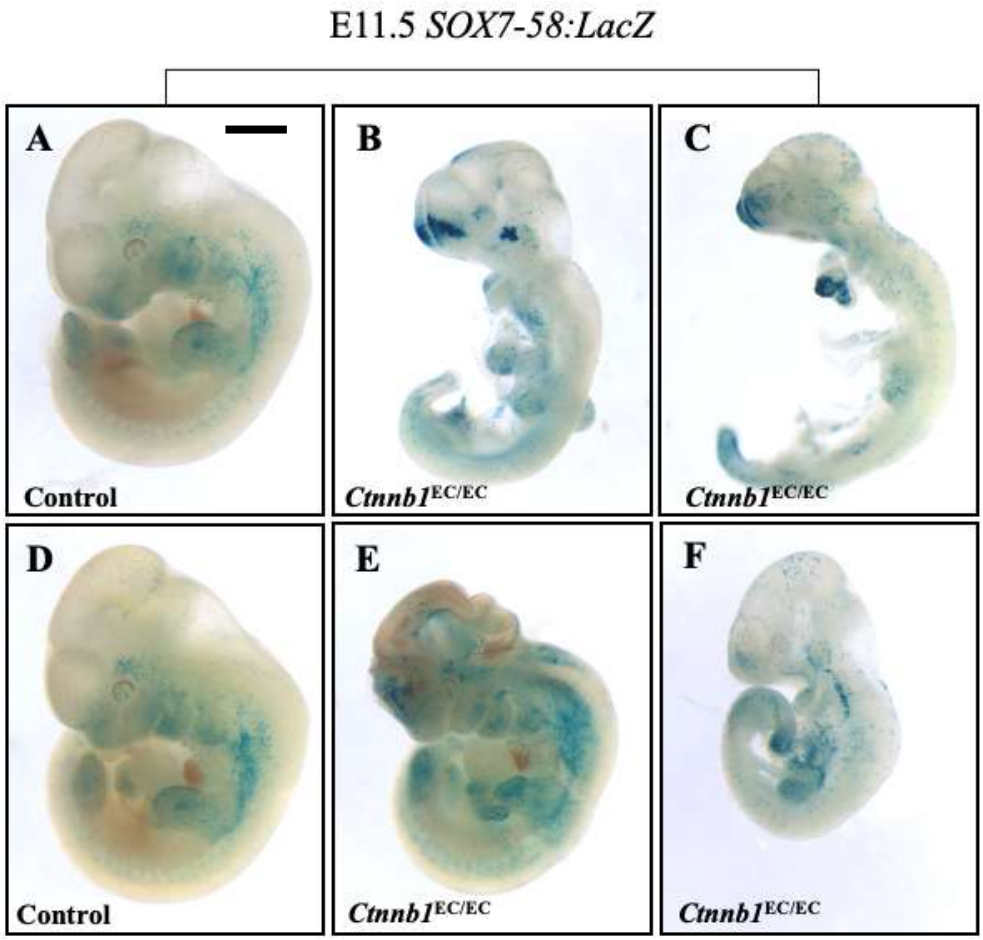

Figure 54: Of the five *Ctnnb1*$^{EC/EC}$ embryos collected at E11.5, four expressed the *SOX7-58:LacZ* gene. These came from three different litters. (A) represents a control E11.5 embryo expressing *SOX7-58:LacZ* gene, with (B) and (C) representing littermate *Ctnnb1*$^{EC/EC}$ embryos. Likewise (D) is the control embryo for (E); (F) is a *Ctnnb1*$^{EC/EC}$ embryo with no littermate control. All the embryos were imaged at the same magnification.

At E12.5, only four embryos were collected. From this litter, there were two *Ctnnb1*$^{EC/EC}$ embryos, both of which carried the *LacZ* gene. As expected, neither were viable, limiting analysis at this timepoint.

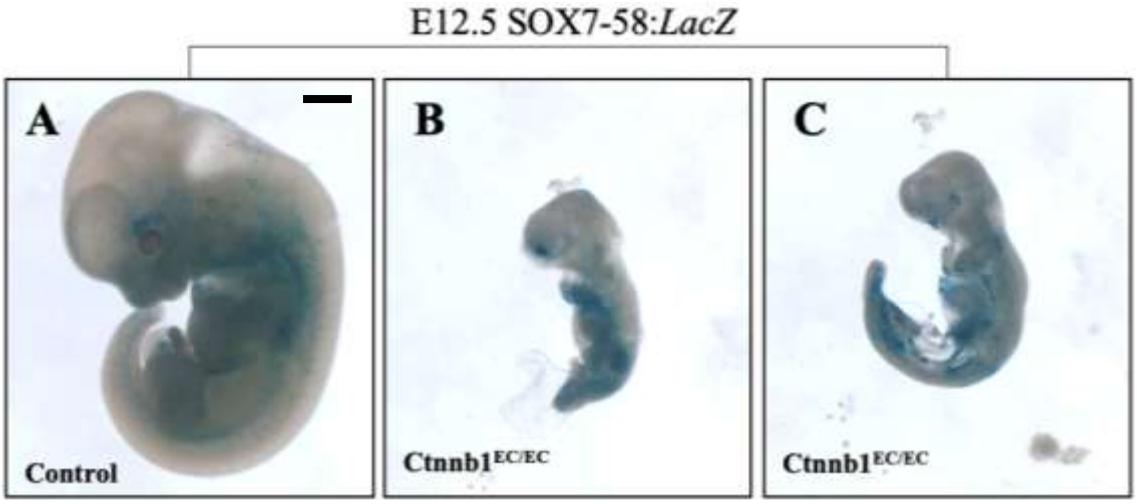

Figure 55: Of the two *Ctnnb1*$^{EC/EC}$ embryos collected at E12.5, both expressed the *SOX7-58:LacZ* gene. These came from the same litter. (A) represents a control E12.5 embryo expressing *SOX7-58:LacZ* gene, with (B) and (C) representing littermate *Ctnnb1*$^{EC/EC}$ embryos. All the embryos were imaged at the same magnification.

4.4 Immunofluorescence analysis reveals no overall differences in vessel density between *Ctnnb1*$^{EC/EC}$ and control embryos, although *Ctnnb1*$^{EC/EC}$ embryos had fewer intra- and perineural blood vessels

Analysis of the *SOX7-58:LacZ* and *DLL4in3:LacZ* transgenes indicated a potential expansion in angiogenic EC enhancer activity in *Ctnnb1*$^{EC/EC}$ embryos. This was most evident for the SOX7-58 enhancer. However, an expanded *SOX7-58:LacZ* transgene expression may not correlate with increased angiogenesis: for example, an increased X-Gal staining pattern could simply reflect an ectopic expansion of SOX7-58 activity into non-angiogenic ECs. Therefore, to assess if more blood vessels were forming in the *Ctnnb1*$^{EC/EC}$ embryos, I characterised the spatiotemporal distribution of the vasculature.

To this end, I sacrificed control and *Ctnnb1*$^{EC/EC}$ embryos at E10.5. These were cryo-sectioned and then I performed immunostaining against Endomucin, SOX17, and COUP-TFII. Whilst Endomucin is a well-established early marker of ECs, SOX17 marks arterial ECs, and COUP-TFII marks venous ECs.[192,286,287] Embryos were sectioned at a thickness 10 µm, with four sections loaded onto a single slide. Every third slide was then immuno-stained to ensure that the vasculature across the whole length of the embryo was assessed. QuPath Analysis was used to assess the presence of EMCN^{+}, SOX17^{+}, and COUP-TFII^{+} vessels.

Three *Ctnnb1*$^{EC/EC}$ embryos generated with the *Tek-Cre* allele were collected, alongside three littermate control embryos. In total, the *Ctnnb1*$^{EC/EC}$ embryos had 42.81% fewer EMCN^{+} blood vessels than the littermate controls. However, this may simply reflect that *Ctnnb1*$^{EC/EC}$ embryos are generally smaller. Assessment of SOX17 and COUP-TFII expression revealed no misexpression of markers in arterial or venous compartments. Although not quantified, there appeared to be an increase in COUP-TFII positive vessels in *Ctnnb1*$^{EC/EC}$ embryos. When the vascular density was assessed for the head region, *Ctnnb1*$^{EC/EC}$ embryos had no obvious change compared to the littermate control, although there did seem to be a trend towards fewer blood vessels both in and around the neural tube. Most noticeably, every littermate control had at least five blood vessels in the neural tube, whilst two *Ctnnb1*$^{EC/EC}$ embryos had fewer than three blood vessels present (Figure 56: Panel F and H). When examining the midsection of the embryo through the heart, these trends continued: there was a similar overall vasculature density between the littermate control embryo and the *Ctnnb1*$^{EC/EC}$ embryo, but the *Ctnnb1*$^{EC/EC}$ embryo had fewer blood vessels in and around the neural tube (Figure 57: Panel F and H). In the lower region of the embryo, two of the *Ctnnb1*$^{EC/EC}$ embryos had no blood vessels in the neural tubes, whilst all littermate control embryos had at least four blood vessels present (Figure 58: Panel F and H). The limb buds had a similar density of EMCN^{+} blood vessels (Figure 59).

Three *Ctnnb1*$^{EC/EC}$ embryos generated with the *Etv2-Cre* allele were collected, alongside three littermate control embryos. In total, the *Ctnnb1*$^{EC/EC}$ embryos had only 9.75% fewer blood vessels than the littermate controls. Once again, there was no inappropriate expression of SOX17 and COUP-TFII. Much like the previous experiment when the vascular density was assessed for the head region, *Ctnnb1*$^{EC/EC}$ embryos had no obvious change compared to the littermate control, but a reduction in intra and perineural vessels. Indeed, two *Ctnnb1*$^{EC/EC}$ embryos had no blood vessels in the neural tube (Figure 60: Panel F and H). Likewise, the littermate control embryos and the *Ctnnb1*$^{EC/EC}$ embryos had a similar vascular density in the cryo-sections through their mid region (Figure 61: Panel F and H). In the lower region of the embryo, two of the *Ctnnb1*$^{EC/EC}$ embryos had no blood vessels in the neural tubes, whilst all littermate control embryos had at least nine blood vessels present (Figure 62: Panel F and H). The limb buds also had a similar density of EMCN^{+} blood vessels (Figure 63).

These results suggest pose an interesting paradox: in the absence of EC *Ctnnb1* expression, SOX7-58 enhancer activity increases, despite no more angiogenesis occurring. Whilst this indicates that enhancer activity alone is insufficient to drive vessel formation, it does suggest a novel role for canonical Wnt signalling in constraining angiogenic EC enhancer activation.

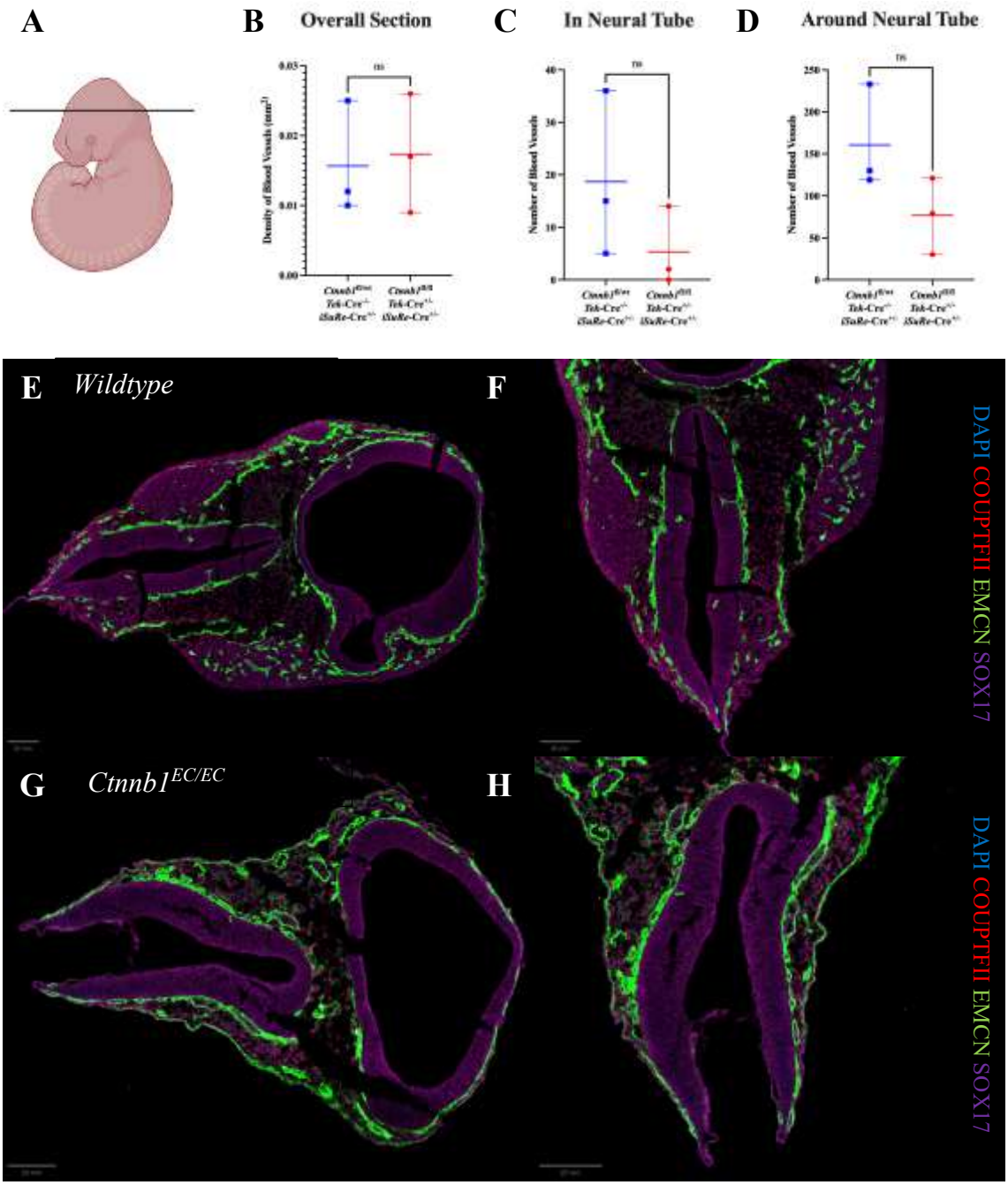

Figure 56: There are fewer EMCN^{+} vessels in and around the neural tube, but overall vascular density remains similar between control and Ctnnb1$^{EC/EC}$ embryos. (A) Schematic of an E10.5 embryo with the cross section clearly marked. (B) shows a comparison of blood vessel density across the section, with (C) showing a comparison of the number of blood vessels in the neural tube, and (D) showing the number of blood vessels around the neural tube. Statistical tests were performed for normality (Shapiro-Wilk) and comparisons between genotype groups (two-tailed Student's t-test). Immuno-stained cryosections taken from the littermate control embryos are found in (E) and (F). Immuno-stained cryosections taken from *Ctnnb1*$^{EC/EC}$ embryos are found in (G) and (H). DAPI (blue), COUPTFII (red), EMCN (green), SOX17 (magenta), and COUP-TFII (red). EC-specific *Ctnnb1* ablation was achieved with the *Tek-Cre* allele. Statistical significance was defined as $P < 0.05$ (*$P < 0.05$, **$P < 0.01$, ***$P < 0.001$, ****$P < 0.001$).

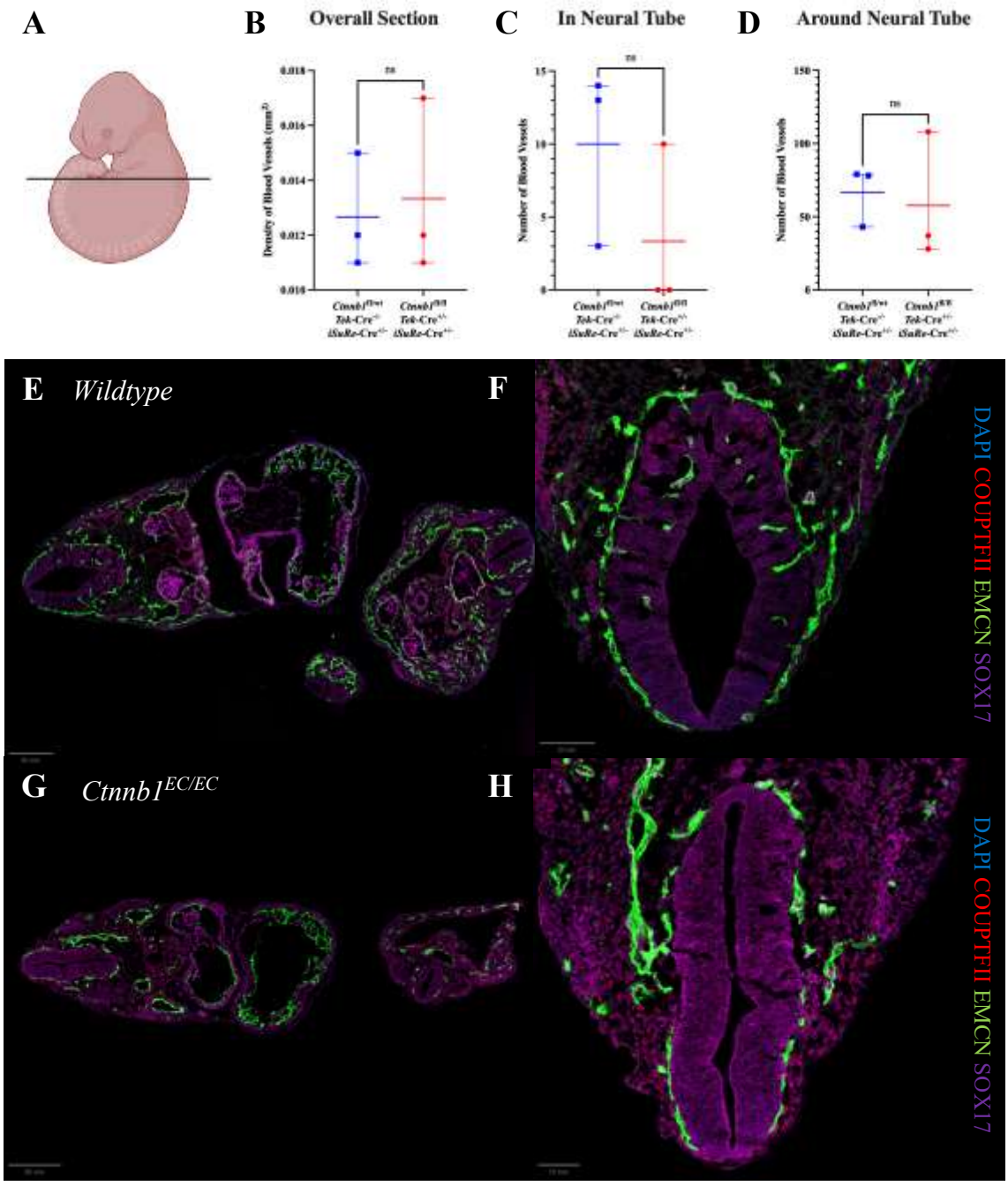

Figure 57: There are fewer EMCN^{+} vessels in and around the neural tube, but overall vascular density remains similar between control and Ctnnb1$^{EC/EC}$ embryos. (A) Schematic of an E10.5 embryo with the cross section clearly marked. (B) shows a comparison of blood vessel density across the section, with (C) showing a comparison of the number of blood vessels in the neural tube, and (D) showing the number of blood vessels around the neural tube. Statistical tests were performed for normality (Shapiro-Wilk) and comparisons between genotype groups (two-tailed Student's t-test). Immuno-stained cryosections taken from the littermate control embryos are found in (E) and (F). Immuno-stained cryosections taken from *Ctnnb1*$^{EC/EC}$ embryos are found in (G) and (H). DAPI (blue), COUPTFII (red), EMCN (green), SOX17 (magenta), and COUP-TFII (red). EC-specific *Ctnnb1* ablation was achieved with the *Tek-Cre* allele. Statistical significance was defined as $P < 0.05$ (*$P < 0.05$, **$P < 0.01$, ***$P < 0.001$, ****$P < 0.001$).

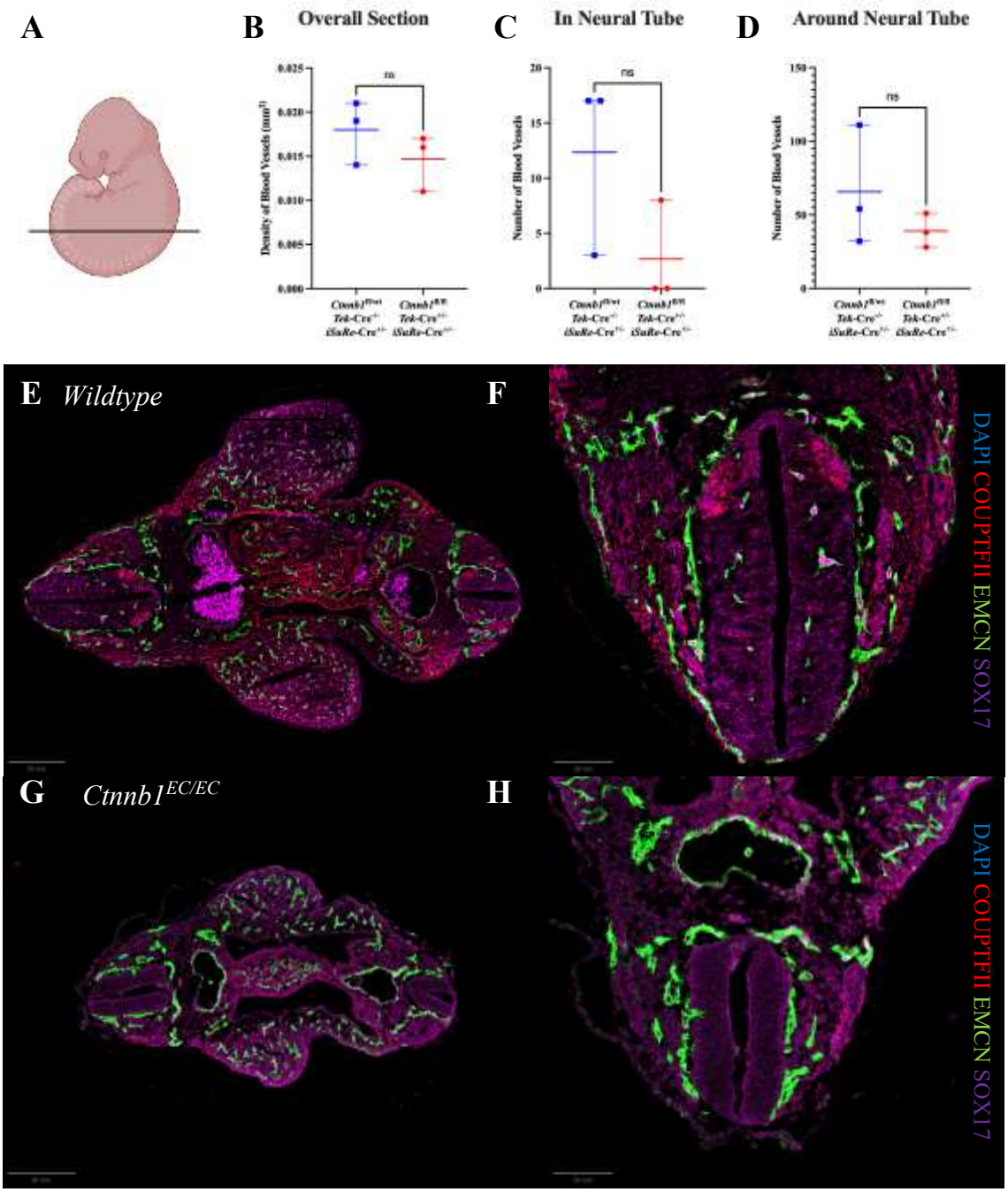

Figure 58: There are fewer EMCN$^+$ vessels in and around the neural tube, but overall vascular density remains similar between control and Ctnnb1$^{EC/EC}$ embryos. (A) Schematic of an E10.5 embryo with the cross section clearly marked. (B) shows a comparison of blood vessel density across the section, with (C) showing a comparison of the number of blood vessels in the neural tube, and (D) showing the number of blood vessels around the neural tube. Statistical tests were performed for normality (Shapiro-Wilk) and comparisons between genotype groups (two-tailed Student's t-test). Immuno-stained cryosections taken from the littermate control embryos are found in (E) and (F). Immuno-stained cryosections taken from *Ctnnb1*$^{EC/EC}$ embryos are found in (G) and (H). DAPI (blue), COUPTFII (red), EMCN (green), SOX17 (magenta), and COUP-TFII (red). EC-specific *Ctnnb1* ablation was achieved with the *Tek-Cre* allele. Statistical significance was defined as $P < 0.05$ (*$P < 0.05$, **$P < 0.01$, ***$P < 0.001$, ****$P < 0.001$).

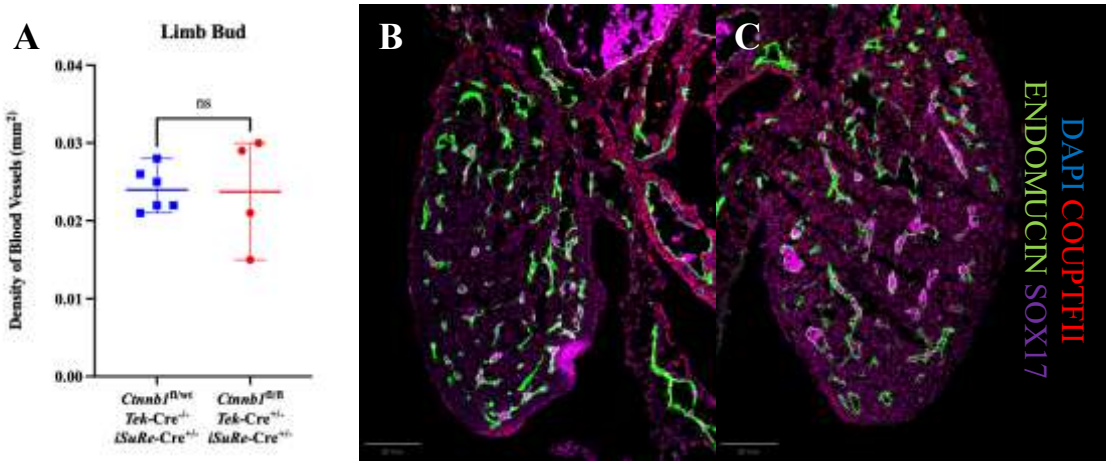

Figure 59: There are fewer EMCN^{+} vessels in and around the neural tube, but overall vascular density remains similar between control and Ctnnb1$^{EC/EC}$ embryos. (A) Schematic of an E10.5 embryo illustrating the region of Panels F-I. (B) Schematic of an E10.5 embryo illustrating the region of Panels J-M. (C) Schematic of an E10.5 embryo illustrating the region of Panels N-Q. (D) and (E) show the limb buds. Immuno-stained cryosections taken from *Ctnnb1*$^{EC/EC}$ embryos are found in Panels E, H, I, L, M, P, and Q. Immuno-stained cryosections taken from the littermate control embryos are found in Panels D, F, G, J, K, N, and O. DAPI (blue), COUP-TFII (red), EMCN (green), SOX17 (magenta), and COUPTFII (red). EC-specific *Ctnnb1* ablation was achieved with the *Tek2-Cre* allele. Statistical significance was defined as $P < 0.05$ (*$P < 0.05$, **$P < 0.01$, ***$P < 0.001$, ****$P < 0.001$).

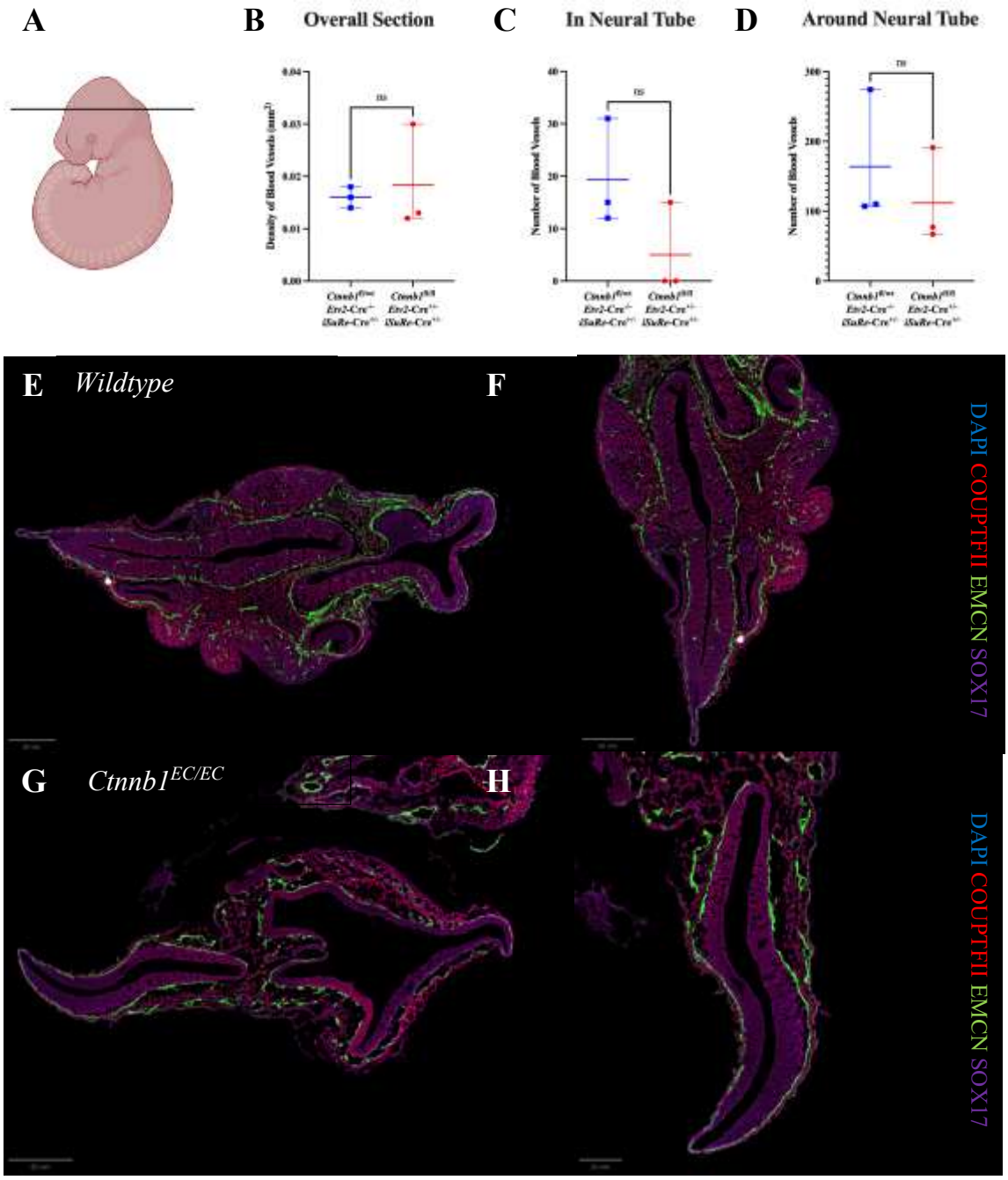

Figure 60: There are fewer EMCN^{+} vessels in and around the neural tube, but overall vascular density remains similar between control and Ctnnb1$^{EC/EC}$ embryos. (A) Schematic of an E10.5 embryo with the cross section clearly marked. (B) shows a comparison of blood vessel density across the section, with (C) showing a comparison of the number of blood vessels in the neural tube, and (D) showing the number of blood vessels around the neural tube. Statistical tests were performed for normality (Shapiro-Wilk) and comparisons between genotype groups (two-tailed Student's t-test). Immuno-stained cryosections taken from the littermate control embryos are found in (E) and (F). Immuno-stained cryosections taken from *Ctnnb1*$^{EC/EC}$ embryos are found in (G) and (H). DAPI (blue), COUPTFII (red), EMCN (green), SOX17 (magenta), and COUP-TFII (red). EC-specific *Ctnnb1* ablation was achieved with the *Etv2-Cre* allele. Statistical significance was defined as $P < 0.05$ (*$P < 0.05$, **$P < 0.01$, ***$P < 0.001$, ****$P < 0.001$).

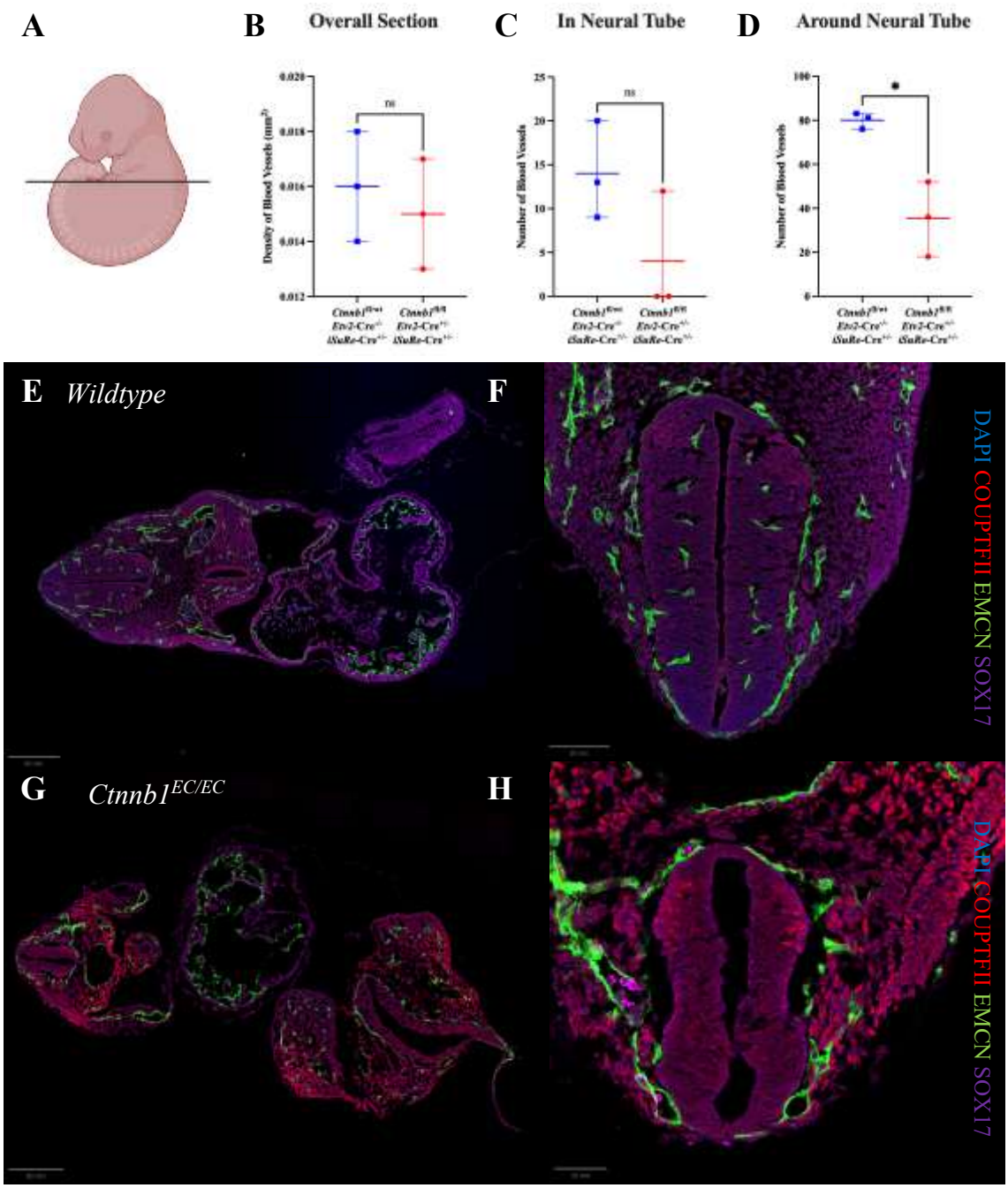

Figure 61: There are fewer EMCN^{+} vessels in and around the neural tube, but overall vascular density remains similar between control and Ctnnb1$^{EC/EC}$ embryos. (A) Schematic of an E10.5 embryo with the cross section clearly marked. (B) shows a comparison of blood vessel density across the section, with (C) showing a comparison of the number of blood vessels in the neural tube, and (D) showing the number of blood vessels around the neural tube. Statistical tests were performed for normality (Shapiro-Wilk) and comparisons between genotype groups (two-tailed Student's t-test). Immuno-stained cryosections taken from the littermate control embryos are found in (E) and (F). Immuno-stained cryosections taken from *Ctnnb1*$^{EC/EC}$ embryos are found in (G) and (H). DAPI (blue), COUPTFII (red), EMCN (green), SOX17 (magenta), and COUP-TFII (red). EC-specific *Ctnnb1* ablation was achieved with the *Etv2-Cre* allele. Statistical significance was defined as $P < 0.05$ (*$P < 0.05$, **$P < 0.01$, ***$P < 0.001$, ****$P < 0.001$).

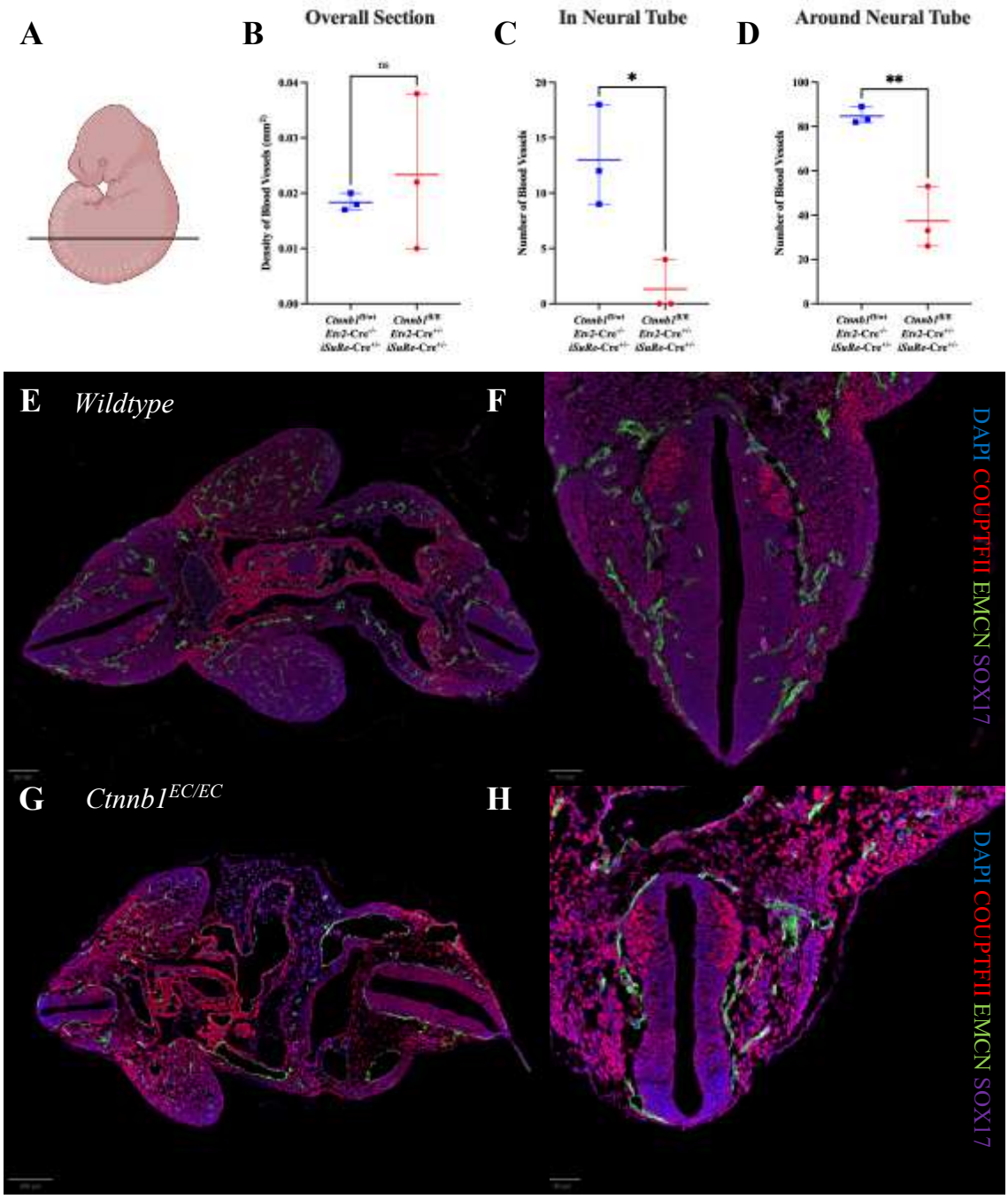

Figure 62: There are fewer EMCN^{+} vessels in and around the neural tube, but overall vascular density remains similar between control and Ctnnb1$^{EC/EC}$ embryos. (A) Schematic of an E10.5 embryo with the cross section clearly marked. (B) shows a comparison of blood vessel density across the section, with (C) showing a comparison of the number of blood vessels in the neural tube, and (D) showing the number of blood vessels around the neural tube. Statistical tests were performed for normality (Shapiro-Wilk) and comparisons between genotype groups (two-tailed Student's t-test). Immuno-stained cryosections taken from the littermate control embryos are found in (E) and (F). Immuno-stained cryosections taken from *Ctnnb1*$^{EC/EC}$ embryos are found in (G) and (H). DAPI (blue), COUPTFII (red), EMCN (green), SOX17 (magenta), and COUP-TFII (red). EC-specific *Ctnnb1* ablation was achieved with the *Etv2-Cre* allele. Statistical significance was defined as $P < 0.05$ (*$P < 0.05$, **$P < 0.01$, ***$P < 0.001$, ****$P < 0.001$).

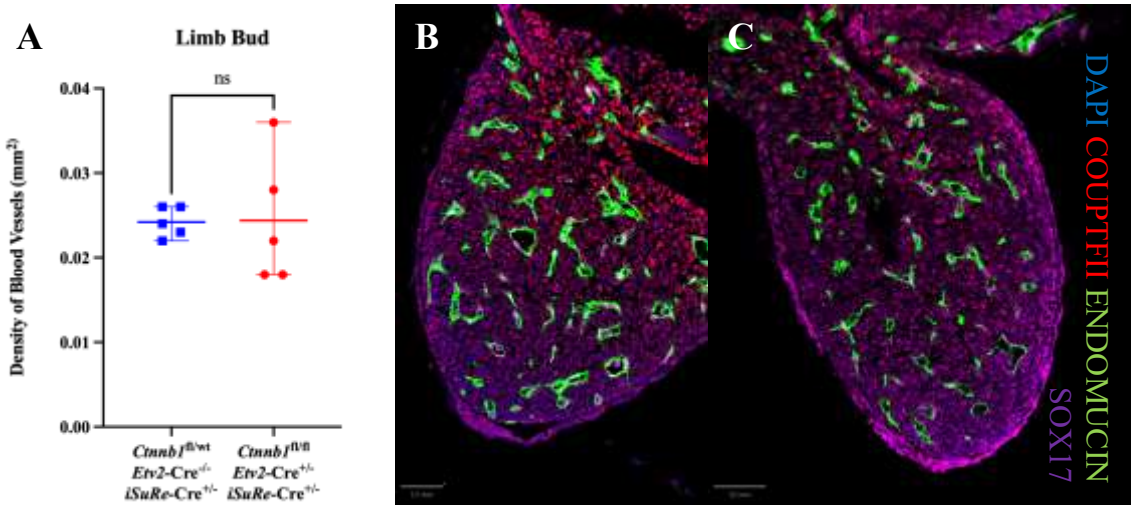

Figure 63: There are fewer EMCN^{+} vessels in and around the neural tube, but overall vascular density remains similar between control and Ctnnb1$^{EC/EC}$ embryos. (A) Schematic of an E10.5 embryo illustrating the region of Panels F-I. (B) Schematic of an E10.5 embryo illustrating the region of Panels J-M. (C) Schematic of an E10.5 embryo illustrating the region of Panels N-Q. (D) and (E) show the limb buds. Immuno-stained cryosections taken from *Ctnnb1*$^{EC/EC}$ embryos are found in Panels E, H, I, L, M, P, and Q. Immuno-stained cryosections taken from the littermate control embryos are found in Panels D, F, G, J, K, N, and O. DAPI (blue), COUP-TFII (red), EMCN (green), SOX17 (magenta), and COUPTFII (red). EC-specific *Ctnnb1* ablation was achieved with the *Etv2-Cre* allele. Statistical significance was defined as $P < 0.05$ (*$P < 0.05$, **$P < 0.01$, ***$P < 0.001$, ****$P < 0.001$).

4.5 Investigating a role for canonical Wnt signalling in the developing coronary vasculature

So far in Chapter 4, I have analysed the vascular consequences of constitutively ablating *Ctnnb1* in ECs in the early developing mouse embryo. Whilst this is informative about the overall importance of canonical Wnt signalling, removing *Ctnnb1* expression from all ECs during development can make it difficult to dissect the root cause of complex phenotypes. For example, it is challenging to determine whether defects in arterial and venous specification arise directly from disrupted canonical Wnt signalling, or whether they occur as a secondary consequence of impaired angiogenesis. In contrast, inducing *Ctnnb1* EC ablation at specific timepoints allows each stage of vascular development to be probed in isolation. This effectively maps which processes are directly perturbed by disrupted canonical Wnt signalling, and which processes are perturbed as a result of earlier defects.

One of the best described vascular network formations is that of the coronary vasculature.[85,86,88] Although this vasculature develops after the systemic vasculature, it recapitulates many of the same developmental processes whilst following a temporally precise and spatially compartmentalised pattern.[85,88] This has been previously described in **Chapter 1: Section 1.1.6**. Briefly, at E11.5, ECs start sprouting from the SV, initiating the formation of coronary vessels. This angiogenesis is driven by VEGFC-VEGFR3 signalling. Between E11.5 and E13.5, these SV-derived ECs migrate caudally over the dorsal face and eventually populate the outer ventricular wall.[85,86,88] Simultaneously, ECs start sprouting from the endocardium and contribute to vessels in the septum and inner ventricular walls.[85] This angiogenesis is instead driven by VEGFA-VEGF2 signalling. By E13.5, these two progenitor sources have established a primitive vascular plexus over the heart. From E13.5 to P28, this immature coronary plexus undergoes extensive remodelling and angiogenic expansion to form the mature coronary circulation.[85] During this period, the coronary plexus recruits pericytes and vascular smooth muscle cells, whilst acquiring arteriovenous identity through a well-defined vein-to-arterial EC differentiation pathway.[66,288]

Given that coronary vessel formation proceeds according to a defined temporal and spatial programme, it can be used to investigate the stage-specific roles of canonical Wnt

signalling. To this end, I used the tamoxifen inducible Cdh5-CreERT2 ^{1Rha} allele to ablate *Ctnnb1* in ECs.[219,289] To investigate the initial sprouting and formation of the coronary plexus, pregnant dams were administrated 100 µl of 10mg/ml tamoxifen via oral gavage on two consecutive days, corresponding to E9.5 and E10.5. Embryos were then collected at E12.5 and E13.5. To investigate the maturation and remodelling of the coronary plexus, the same tamoxifen regimen was administered at E11.5 and E12.5. Embryos were then collected from E14.5 to E16.5.

To probe the effects of EC-specific ablation of *Ctnnb1* on VEGFC driven angiogenesis, I used the stable murine *NOTCH1+16:LacZ* transgenic line.[285] Between E11.5 and E16.5, *NOTCH1+16:LacZ* has extensive activity in the heart.[285] This activity which has been shown to correlate with SV-derived vessels.[285] Embryonic hearts were obtained from matings of either *NOTCH1+16:LacZ*$^{+/-}$ *Ctnnb1*$^{fl/wt}$ *Cdh5-Cre*ERT2$^{+/-}$ males, or *NOTCH1+16:LacZ*$^{+/-}$ *Ctnnb1*$^{fl/fl}$ *Cdh5-Cre*ERT2$^{+/-}$ males, with *Ctnnb1*^{flfl} iSuRe-*Cre*$^{+/+}$ females.

4.5.1 Investigating a role for canonical Wnt signaling in coronary vasculature sprouting from the sinus venosus and endocardium

Between E11.5 and E13.5, EC contributions from both the SV and the endocardium form an immature coronary plexus. This plexus then expands across the heart until the heart is fully encompassed.[290] To investigate a requirement for canonical Wnt signalling in the initial sprouting and coronary plexus formation, *Ctnnb1* was ablated in ECs after exposure to tamoxifen at E9.5 and E10.5. Embryos were then taken between E12.5 and E13.5.

At E12.5, 13 *LacZ*$^{+/-}$ control hearts and six *LacZ*$^{+/-}$ *Ctnnb1*$^{iEC/iEC}$ hearts were collected. (Figure 64 and Figure 65). These came from four different litters. At E12.5, there was little X-Gal staining on either the dorsal or ventral side of the heart, reflective of the fact that the SV has only just started to sprout, with a similar *LacZ* expression pattern observed between *Ctnnb1*$^{iEC/iEC}$ and littermate control hearts. The lack of obvious difference in *LacZ* expression suggests that the SV sprouting process is unaffected, and therefore EC canonical Wnt signalling is not essential for the initial stages of coronary vessel development.

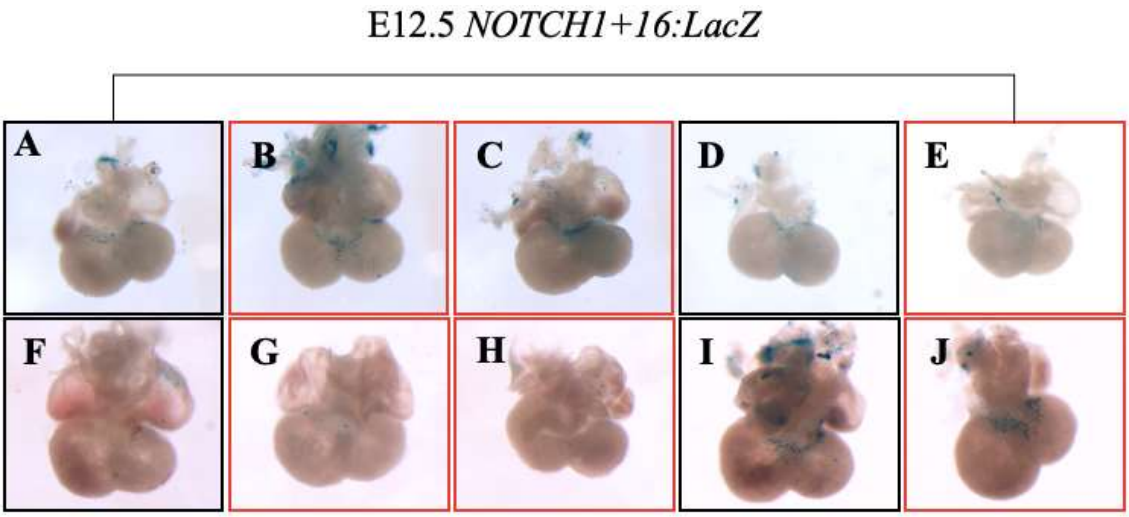

Figure 64: At E12.5, 13 *LacZ*$^{+/-}$ control hearts and six *LacZ*$^{+/-}$ *Ctnnb1*$^{iEC/iEC}$ hearts were collected. This figure shows the dorsal side of the heart. (A) represents a control E12.5 heart expressing *Notch1+16:LacZ* gene, with (B) and (C) representing littermate *Ctnnb1*$^{iEC/iEC}$ hearts. Likewise (D) is the control embryo for (E); (F) is a control littermate for (G) and (H); and (I) a control littermate for (J). Control hearts are in black boxes, *Ctnnb1*$^{iEC/iEC}$ hearts are in red boxes. All hearts were imaged at the same magnification.

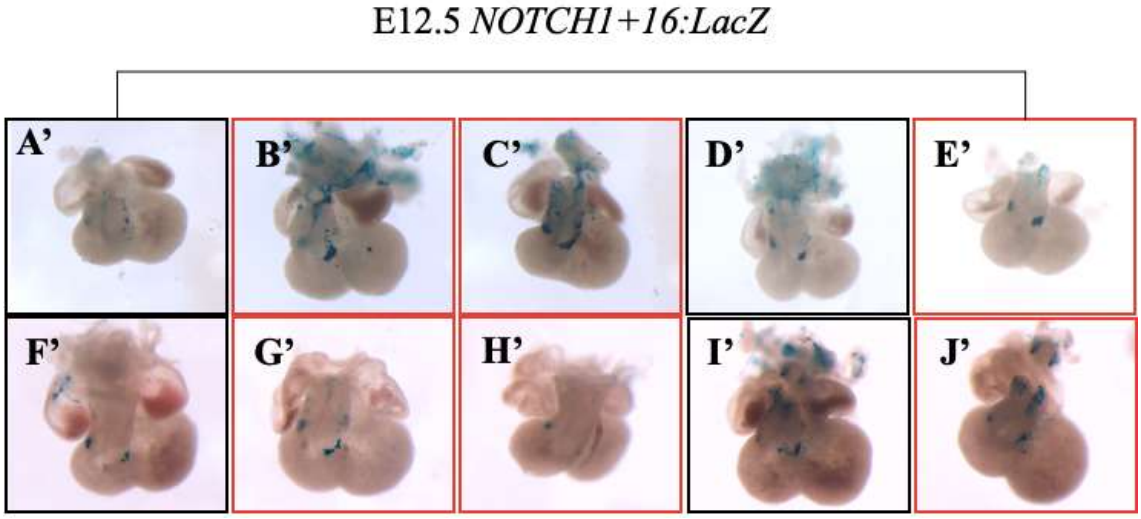

Figure 65: At E12.5, 13 *LacZ*$^{+/-}$ control hearts and six *LacZ*$^{+/-}$ *Ctnnb1*$^{iEC/iEC}$ hearts were collected. This figure shows the ventral side of the heart. (A') represents a control E12.5 heart expressing *Notch1+16:LacZ* gene, with (B') and (C') representing littermate *Ctnnb1*$^{iEC/iEC}$ hearts. Likewise (D') is the control embryo for (E'); (F) is a control littermate for (G') and (H'); and (I') a control littermate for (J'). Control hearts are in black boxes, *Ctnnb1*$^{iEC/iEC}$ hearts are in red boxes. All hearts were imaged at the same magnification.

At E13.5, seven *LacZ*$^{+/-}$ control hearts and four *LacZ*$^{+/-}$ *Ctnnb1*$^{iEC/iEC}$ hearts were collected. (Figure 66 and Figure 67). These came from two litters. In one litter, there was a clear difference in *LacZ* expression, with the *Ctnnb1*$^{iEC/iEC}$ hearts showing decreased X-Gal staining on the dorsal side. However, the three *Ctnnb1*$^{iEC/iEC}$ hearts all appeared smaller, potentially indicative of developmental retardation and delayed SV sprouting. The embryonic hearts in the other litter were more similarly developed, and although the *Ctnnb1*$^{iEC/iEC}$ heart did show a slight decrease in *LacZ* expression on the dorsal side, this was not as significant. When the percentage of the dorsal heart face stained with X-Gal was quantified using FIJI/ImageJ, there were a slight statistical difference, p = 0.0132 (Figure 68). This suggests that although the initial sprouting is not dependent on canonical Wnt signalling, there may a role for *Ctnnb1* expression in the expansion of the coronary plexus over the dorsal side of the heart.

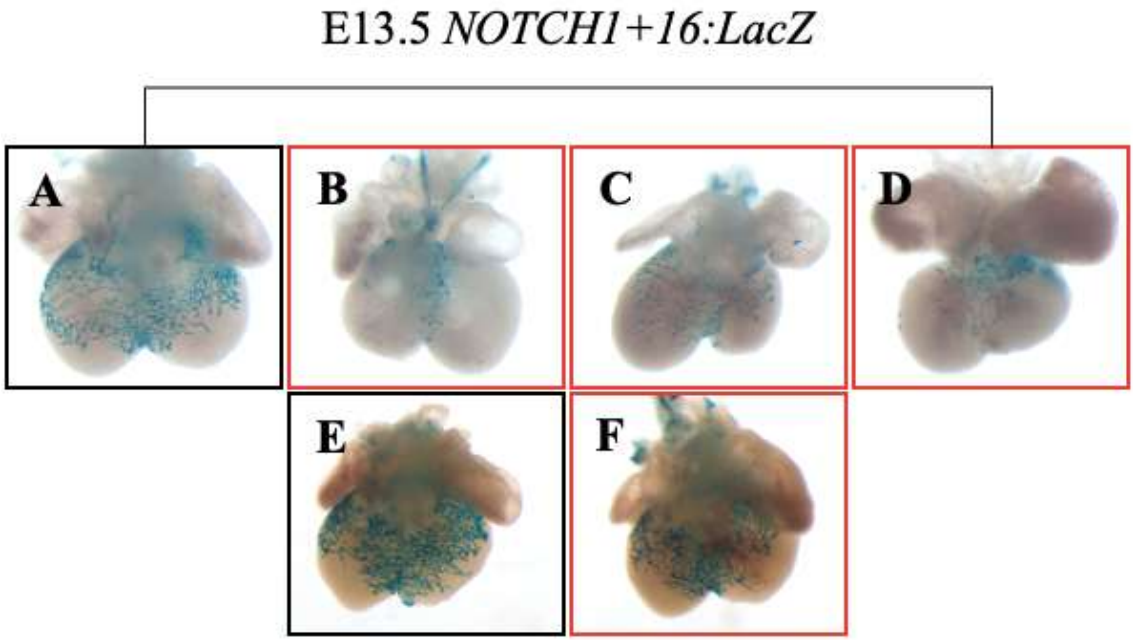

Figure 66: At E13.5, seven *LacZ*$^{+/-}$ control hearts and four *LacZ*$^{+/-}$ *Ctnnb1*$^{iEC/iEC}$ hearts were collected. This figure shows the dorsal side of the heart. (A) represents a control E13.5 heart expressing *Notch1+16:LacZ* gene, with (B), (C) and (D) representing littermate *Ctnnb1*$^{iEC/iEC}$ hearts. Likewise (E) is the control embryo for (F). Control hearts are in black boxes, *Ctnnb1*$^{iEC/iEC}$ hearts are in red boxes.

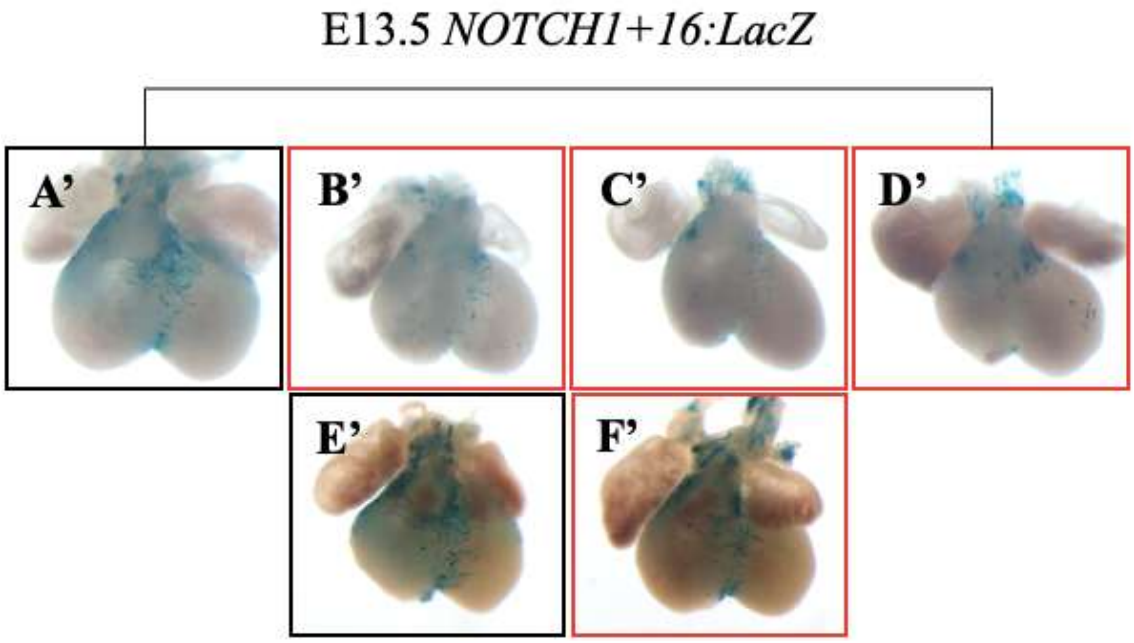

Figure 67: At E13.5, seven *LacZ*$^{+/-}$ control hearts and four *LacZ*$^{+/-}$ *Ctnnb1*$^{iEC/iEC}$ hearts were collected. This figure shows the ventral side of the heart. (A') represents a control E13.5 heart expressing *Notch1+16:LacZ* gene, with (B'), (C') and (D') representing littermate *Ctnnb1*$^{iEC/iEC}$ hearts. Likewise (E') is the control embryo for (F'). Control hearts are in black boxes, *Ctnnb1*$^{iEC/iEC}$ hearts are in red boxes.

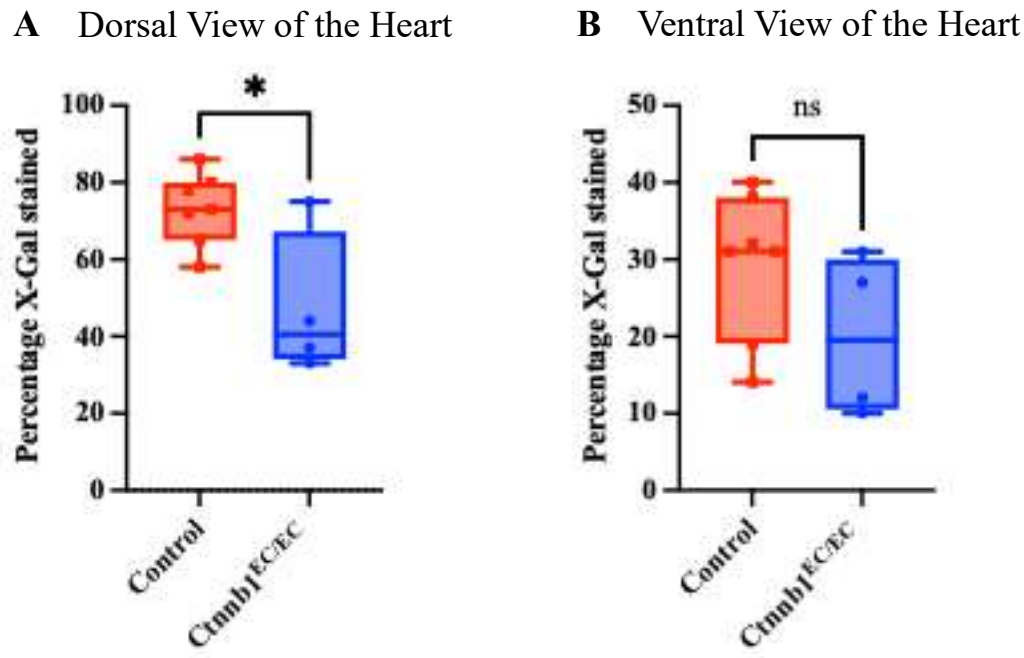

Figure 68: (A) shows a statistically significant difference in the percentage of X-gal staining between control and *Ctnnb1*$^{iEC/iEC}$ hearts on the dorsal side. p = 0.0132 *, whilst (B) shows no significant difference in percentage of X-gal staining on the ventral side. p = 0.1677. Data was first assessed for normality using the Shapiro-Wilks test, and then genotype groups were compared using an unpaired, two-tailed Student's t-test. Statistical significance was defined as $P < 0.05$ (*$P < 0.05$, **$P < 0.01$, ***$P < 0.001$, ****$P < 0.001$).

4.5.2 Investigating a role for canonical Wnt signalling in the maturation of the coronary vasculature

Once the initial immature coronary plexus has formed, it undergoes extensive remodelling from E12.5 and P28 to form the mature coronary vasculature.[85,86,88] Initially, between E12.5. and E14.5, the primitive coronary plexus invades the aorta and coronary sinus to complete the circuit.[85] To investigate a requirement for canonical Wnt signalling in these processes, *Ctnnb1* was ablated in ECs after exposure to tamoxifen at E11.5 and E12.5. Embryos were then analysed between E14.5 and E16.5.

At E14.5, seven *LacZ*$^{+/-}$ control hearts and eight *LacZ*$^{+/-}$ *Ctnnb1*$^{iEC/iEC}$ hearts were collected. (Figure 69 and Figure 70). These came from three litters. With the exception of a single *Ctnnb1*$^{iEC/iEC}$ heart with reduced *LacZ* expression, there was generally no obvious differences in the X-Gal staining pattern between *Ctnnb1*$^{iEC/iEC}$ hearts and littermate control hearts. In each case, the SV-derived vascular plexus covered the same area of the heart, indicating that SV-derived angiogenesis was unaffected by Ctnnb1 ablation. Moreover, unlike the E13.5 *Ctnnb1*$^{iEC/iEC}$ hearts, the E14.5 *Ctnnb1*$^{iEC/iEC}$ hearts were morphologically indistinguishable from their littermate controls.

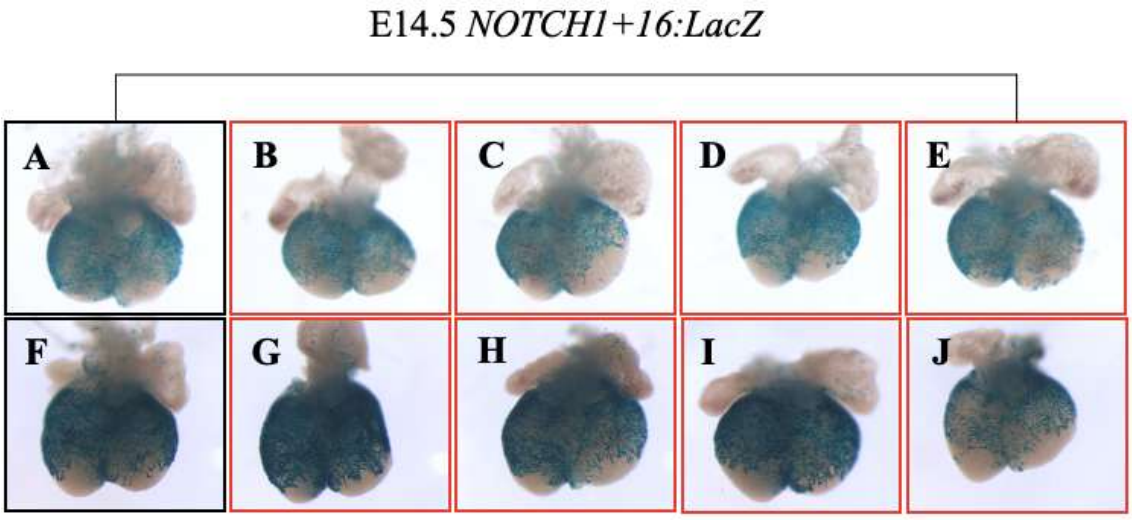

Figure 69: At E14.5, seven *LacZ*$^{+/-}$ control hearts and eight *LacZ*$^{+/-}$ *Ctnnb1*$^{iEC/iEC}$ hearts were collected. This figure shows the dorsal side of the heart. (A) represents a control E14.5 heart expressing *Notch1+16:LacZ* gene, with (B), (C), (D) and (E) representing littermate *Ctnnb1*$^{EC/EC}$ hearts. Likewise (F) is the control embryo for (G), (H), (I) and (J). Control hearts are in black boxes, *Ctnnb1*$^{EC/EC}$ hearts are in red boxes.

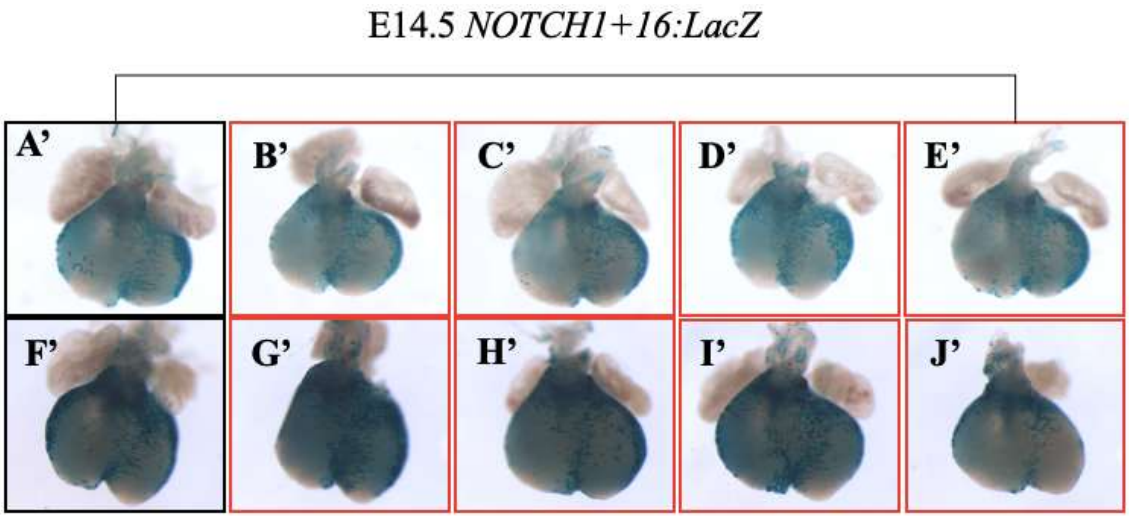

Figure 70: At E14.5, seven LacZ$^{+/-}$ control hearts and eight *LacZ*$^{+/-}$ *Ctnnb1*$^{iEC/iEC}$ hearts were collected. This figure shows the ventral side of the heart. (A') represents a control E14.5 heart expressing *Notch1+16:LacZ* gene, with (B'), (C'), (D') and (E') representing littermate Ctnnb1$^{iEC/iEC}$ hearts. Likewise (F') is the control embryo for (G'), (H'), (I') and (J'). Control hearts are in black boxes, *Ctnnb1*$^{iEC/iEC}$ hearts are in red boxes.

At E15.5, 11 *LacZ*$^{+/-}$ control hearts and six *LacZ*$^{+/-}$ *Ctnnb1*$^{iEC/iEC}$ hearts were collected. (Figure 71 and Figure 72). These came from three litters. Once again, there did not appear to be obvious differences in the lacZ+ SV-derived coronary plexus *Ctnnb1*$^{iEC/iEC}$ and control hearts. Moreover, the developing vascular network looked morphologically similar between *Ctnnb1*$^{iEC/iEC}$ and control hearts, except in one *Ctnnb1*$^{iEC/iEC}$ heart (Figure 71: Panel G) where it appeared disorganised and thickened. Although one heart was smaller and possibly deformed (Figure 71: Panel I), the X-Gal staining pattern and vascular plexus remained very similar. This suggests that canonical Wnt signalling is not required for coronary plexus remodelling and maturation.

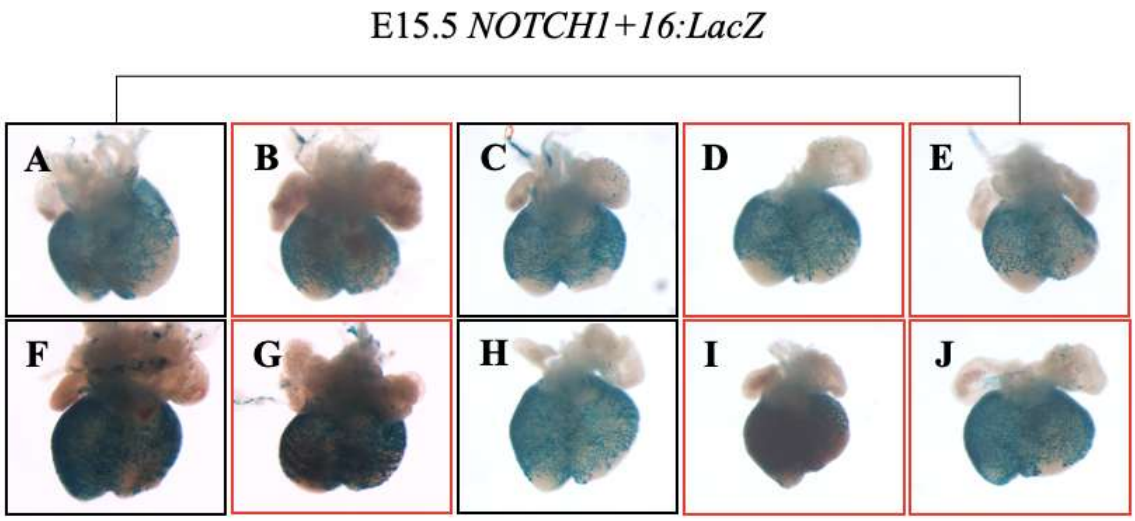

Figure 71: At E15.5, 11 *LacZ*$^{+/-}$ control hearts and six *LacZ*$^{+/-}$ *Ctnnb1*$^{iEC/iEC}$ hearts were collected. This figure shows the dorsal side of the heart. (A) represents a control E15.5 heart expressing *Notch1+16:LacZ* gene, with (B) representing littermate *Ctnnb1*$^{iEC/iEC}$ hearts. Likewise (C) and (H) are the control littermates for (D), (E), (I) and (J); and (F) is the control littermate for (G). Control hearts are in black boxes, *Ctnnb1*$^{EC/EC}$ hearts are in red boxes.

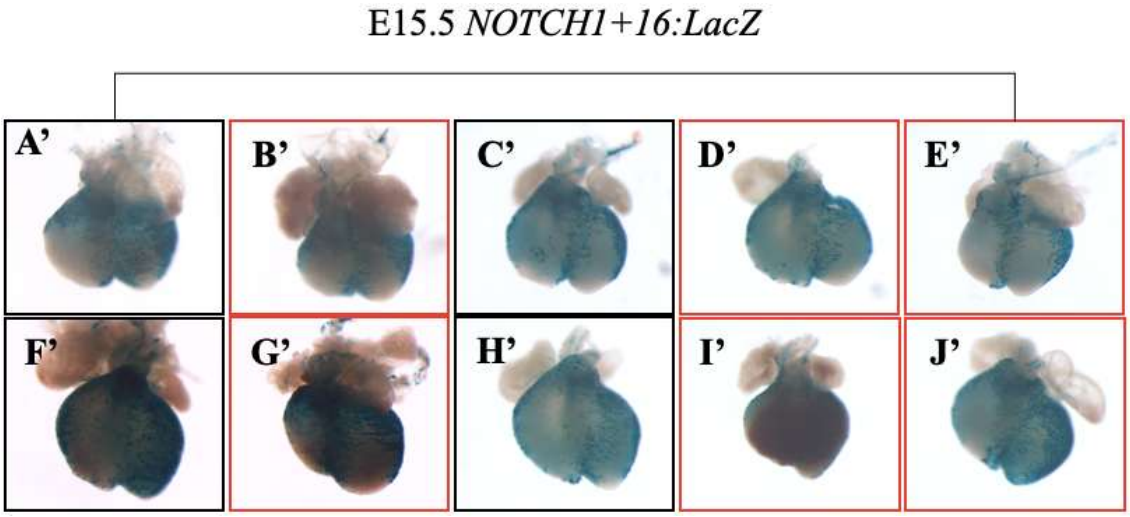

Figure 72: At E15.5, 11 *LacZ*$^{+/-}$ control hearts and six *LacZ*$^{+/-}$ *Ctnnb1*$^{iEC/iEC}$ hearts were collected. This figure shows the ventral side of the heart. (A') represents a control E12.5 heart expressing *Notch1+16:LacZ* gene, with (B') representing littermate Ctnnb1$^{EC/EC}$ hearts. Likewise (C') and (H') are the control littermates for (D'), (E'), (I') and (J'); and (F') is the control littermate for (G').

At E16.5, seven *LacZ*$^{+/-}$ control hearts and six *LacZ*$^{+/-}$ *Ctnnb1*$^{iEC/iEC}$ hearts were collected. (Figure 73 and Figure 74). These came from three litters. There were no obvious differences in X-Gal staining pattern or vascular plexus over the ventricles, both with regard to localisation and coverage, between the *Ctnnb1*$^{EC/EC}$ hearts and the littermate control hearts. Combining the results from the E14.5, E15.5 and E16.5 hearts, there does not appear to be much difference in *NOTCH1+16:LacZ* expression and SV-derived vascular plexus formation and maturation between the *Ctnnb1*$^{iEC/iEC}$ hearts and littermate control hearts. This suggests that the coronary vasculature, at least the vessels derived from the SV, are not dependent on canonical Wnt signalling for normal enhancer activity.

The SV-derived ECs rely on VEGFC dependent angiogenesis, rather than VEGFA dependent angiogenesis. This distinction may explain why in the absence of canonical Wnt signalling had little effect on SV-derived angiogenesis. Therefore, we next examined whether canonical Wnt signalling has a specific role in VEGFA-driven angiogenesis, by investigating angiogenesis in the postnatal retina.

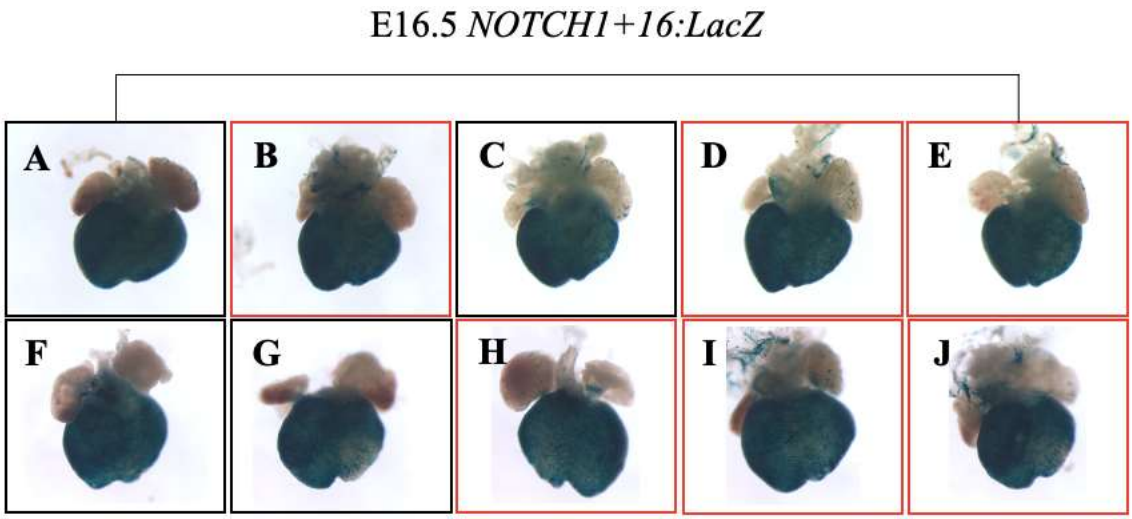

Figure 73: At E16.5, seven *LacZ*$^{+/-}$ control hearts and six *LacZ*$^{+/-}$ *Ctnnb1*$^{iEC/iEC}$ hearts were collected. These came from 3 different litters. This figure shows the dorsal side of the heart. (A) represents a control E12.5 heart expressing *Notch1+16:LacZ* gene, with (B) representing littermate *Ctnnb1*$^{iEC/iEC}$ hearts. Likewise (C) is the control embryo for (D) and (E); (F) and (G) are the control littermates for (H), (I) and (J). Control hearts are in black boxes, *Ctnnb1*$^{iEC/iEC}$ hearts are in red boxes.

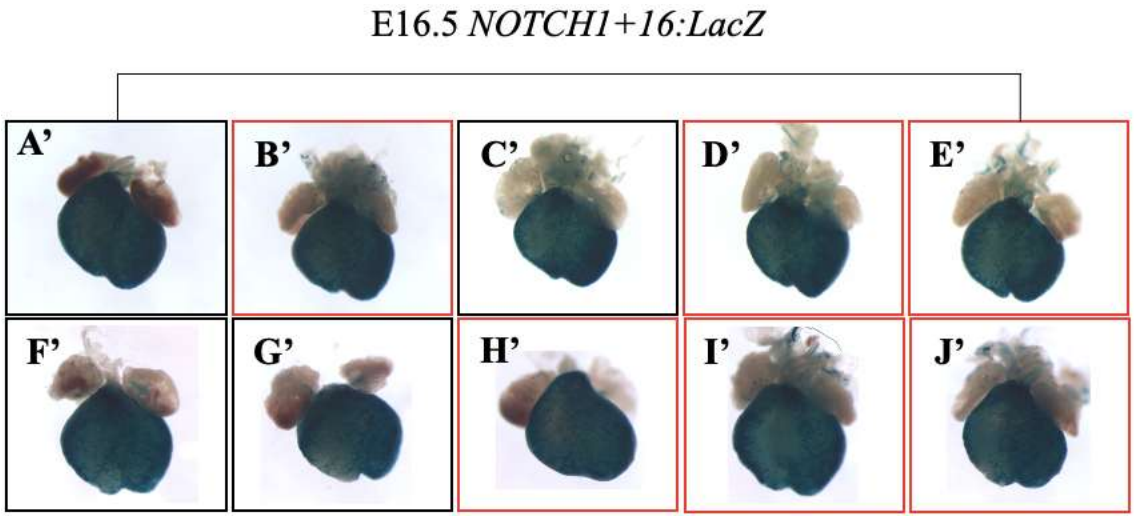

Figure 74: At E16.5, seven *LacZ*$^{+/-}$ control hearts and six *LacZ*$^{+/-}$ *Ctnnb1*$^{iEC/iEC}$ hearts were collected These came from 3 different litters. This figure shows the ventral side of the heart. (A') represents a control E12.5 heart expressing *Notch1+16:LacZ* gene, with (B') representing littermate *Ctnnb1*$^{iEC/iEC}$ hearts. Likewise (C') is the control embryo for (D') and (E'); (F') and (G') are the control littermates for (H), (I') and (J'). Control hearts are in black boxes, *Ctnnb1*$^{iEC/iEC}$ hearts are in red boxes.

4.6 Postnatal vascular development in the retina following EC-specific *Ctnnb1* ablation at P1

Having investigated stage-specific roles for canonical Wnt signalling in VEGFC-driven angiogenesis using the coronary vasculature, I now wanted to investigate VEGFA-driven angiogenesis. To achieve this, I used the postnatal mouse retina.[18,210,291-293] *In vivo*, the postnatal retina has proven an excellent model to study physiological angiogenesis: as vascular network forms, it follows a highly stereotypical developmental sequence; and since the vasculature develops as a planar vascular plexus, it can be prepared flat-mount for microscopy.[291] Moreover, much like studying the coronary vasculature formation, the use of the tamoxifen inducible *Cdh5-CreERT2* ^{1Rha} allele allows the development of the retinal vasculature (and thus the CNS vasculature) to be investigated at a timepoint when the embryo would otherwise be unviable.[219]

In contrast to humans, where retinal vasculature development is mostly complete before birth, the retinal vasculature in mice develops entirely postnatally.[291] From P0, retinal vessels sprout from the optic nerve head and expand radially across the retinal periphery to form the superficial vascular plexus. This process is driven by VEGFA. Once the superficial vascular plexus has reached the periphery of the retina, around P7, the angiogenic sprouts dive into the retina to form the deep vascular plexus.[71,294]

Postnatal retinae were obtained from matings of *SOX7-58:LacZ*$^{+/-}$ *Ctnnb1*$^{fl/fl}$ *Cdh5-Cre*ERT2$^{+/-}$ males with *Ctnnb1*$^{fl/fl}$ *iSuRe-Cre*$^{+/+}$ females. To induce strong recombination, 2 µl of 25 mg/ml tamoxifen in corn oil were fed to pups at P1 and P2. To characterise the spatial distribution and morphology of blood vessels, I performed wholemount staining for Isolectin B4 (IB4). IB4 is a well characterised marker of ECs.[295]

When comparing *Ctnnb1*$^{iEC/iEC}$ retinae with littermate control retinae, I found a reduced radial expansion and an increased incidence of arteriovenous cross-overs in *Ctnnb1*$^{iEC/iEC}$ retinae (Figure 75: Panel C and D). These were both statistically significant, $p = 0.0284$ and $p = 0.0045$, respectively. Moreover, the *Ctnnb1*$^{iEC/iEC}$ retinae were hypovascularized, with fewer branch points and a less dense capillary bed (Figure 75: Panel A and B). This agrees with a study by a previous group, who also reported reduced branch points and a higher incidence of arteriovenous crossover in postnatal *Ctnnb1*$^{iEC/iEC}$ retinae.[292]

In addition, Martowicz *et al* (2019) reported that *Ctnnb1*$^{iEC/iEC}$ retinae had reduced tip EC formation and sprouting.[292] To assess the tip EC population, I first used the *SOX7-58:LacZ* transgene, crossing this into the *SOX7-58:LacZ*; *Ctnnb1*$^{fl/fl}$; *Cdh5-Cre*ERT2$^{+/-}$ genetically modified mice (Figure 76). Upon X-Gal staining, the *Ctnnb1*$^{iEC/iEC}$ retinae had expanded *LacZ* expression compared to littermate controls. This expansion seemed more apparent in the stalk ECs and the capillary beds. Considering that the *Ctnnb1*$^{EC/EC}$ retinae have less vasculature, and therefore reduced angiogenesis, it was interesting that the activity of the SOX7-58 enhancer (an enhancer which is usually active in tip ECs) increased. This again suggests a de-coupling of SOX7-58 activity and functional angiogenesis. This loss of tip EC-specificity potentially mirrors what was observed in the systemic vasculature and may reflect a role for canonical Wnt signalling in maintaining tip EC specification in VEGFA driven angiogenesis.

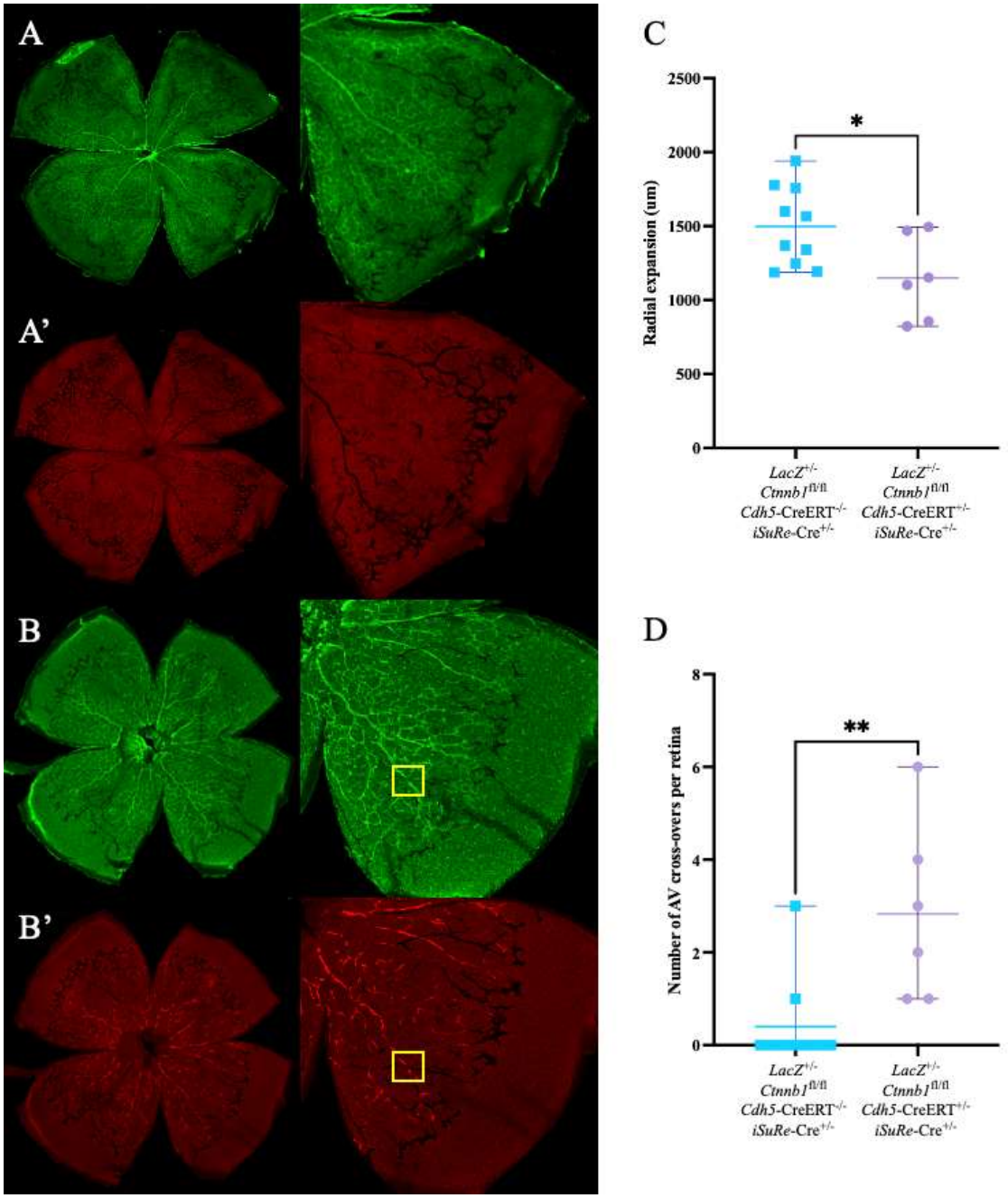

Figure 75: Vascular development in retinae with EC-specific ablation of *Ctnnb1*. (A) Wholemount retina from a control pup showing normal vascular organization. Green is IB4-488, marking ECs. (A') Shows the same retinae but the red marks EC expressing MbTomato, and thus have successfully (B and B′) Show a wholemount retina staining from a *LacZ*$^{+/-}$ *Ctnnb1*$^{EC/EC}$ pup. Higher magnification views for (A, A', B and B') are shown to the right. The yellow box is highlighting an arteriovenous cross-over (C) Quantification of mean radial expansion, n = 15 and (D) number of arteriovenous (AV) cross-overs per retina, n = 15. Data was first assessed for normality using the Shapiro-Wilks test, and then genotype groups were compared using an unpaired, two-tailed Student's t-test. Statistical significance was defined as $P < 0.05$ (*$P < 0.05$, **$P < 0.01$, ***$P < 0.001$, ****$P < 0.001$).

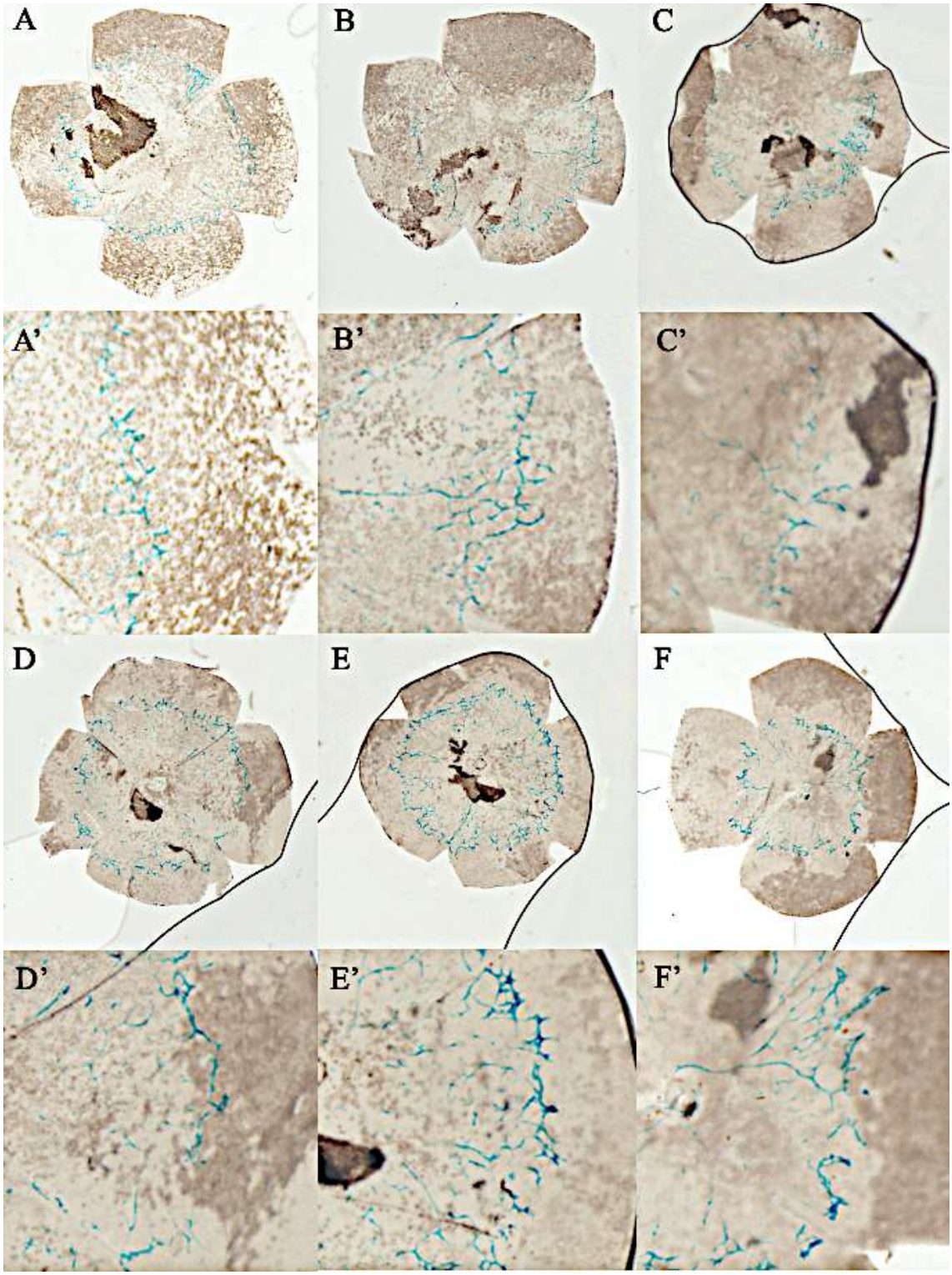

Figure 76: X-Gal staining in *Ctnnb1*$^{iEC/iEC}$ retinae appear more intense than control retinae. (A-C) show littermate control retinae, (A'-C') representing zoomed images of a retina leaflet. (D-F) show *SOX7-58:LacZ*$^{+/-}$ *Ctnnb1*$^{iEC/iEC}$ retinae, (D'-F') representing images of a retina leaflet.

4.7 Loss of Wnt in individual ECs did not prevent the acquisition of any one EC subtype

When *Ctnnb1* was ablated from all ECs in the postnatal retina, I noted a decrease in the radial expansion of the vascular plexus, potentially indicative of reduced angiogenesis. This links with previous work by Martowicz *et al* (2019), who identified a reduced number of tip ECs in *Ctnnb1*$^{iEC/iEC}$ retinae. However, by ablating *Ctnnb1* in all ECs, I could not determine whether the absence of *Ctnnb1* predisposes the ECs to become particular EC subtypes. This is because all the ECs are similarly lacking *Ctnnb1*, and therefore they are not competing against physiologically normal ECs. One way to circumvent this problem, and introduce competition between mutant and wildtype ECs in the same vascular bed, is to only induce recombination in a subset of ECs. This can be achieved by feeding pups a lower dose of tamoxifen.

To investigate whether canonical Wnt signalling affects the ability of ECs to form different EC subtypes, I bred *Ctnnb1*$^{fl/fl}$ *Cdh5-Cre*ERT2$^{+/-}$ *iSuRe-Cre*$^{+/-}$ pups, and at P1, fed them 2 µl of 2.5 mg of tamoxifen. This was designed to recombine <5% of ECs in the developing retinal vasculature.[296] Consequently, *Ctnnb1*-ablated ECs develop in an environment of wildtype ECs. At P5 the pups were sacrificed, and their retinae were wholemount stained with IB4 (conjugated to Alexa Fluor 488), and then mounted in fluorescent mounting medium on slides. Since *iSuRe-Cre* allele is coupled to the *MbTomato* gene, recombined ECs could be visualised on the Zeiss LSM 710 confocal microscope, and using QuPath Analysis, I quantitively recorded their EC subtype as either arterial, venous, capillary, tip, or sprout (Table 41). In parallel, I bred *Ctnnb1*$^{fl/wt}$ *Cdh5-Cre*ERT2$^{+/-}$ *iSuRe-Cre*$^{+/-}$ pups, subjected them to the same tamoxifen regimen, and culled them at P5. Since these pups retained one functional *Ctnnb1* allele in their recombined ECs, they served as a control population. Breeding pairs were designed in such a way that the same litter had both *Ctnnb1*$^{fl/fl}$ *Cdh5-Cre*ERT2$^{+/-}$ *iSuRe-Cre*$^{+/-}$ pups and *Ctnnb1*$^{fl/wt}$ *Cdh5-Cre*ERT2$^{+/-}$ *iSuRe-Cre*$^{+/-}$ pups. By quantifying the distribution of *Ctnnb1*$^{fl/fl}$ ECs relative to *Ctnnb1*$^{fl/wt}$ ECs, I could effectively investigate the role of canonical Wnt signalling in EC subtype identity acquisition.

Table 41: The localisation of recombined ECs (average percentage in each position per retina), *Ctnnb1*$^{fl/wt}$ *Cdh5-CreERT2*$^{+/-}$ *iSuRe-Cre*$^{+/-}$ $n = 12$, *Ctnnb1*$^{fl/fl}$ *Cdh5-CreERT2*$^{+/-}$ *iSuRe-Cre*$^{+/-}$ $n = 9$

	Ctnnb1$^{fl/wt}$ *Cdh5-Cre*ERT2$^{+/-}$ *iSuRe-Cre*$^{+/-}$	*Ctnnb1*$^{fl/fl}$ *Cdh5-Cre*ERT2$^{+/-}$ *iSuRe-Cre*$^{+/-}$
Arterial EC	14%	14%
Venous EC	14%	16%
Capillary EC	38%	33%
Tip EC	16%	17%
Stalk EC	18%	21%

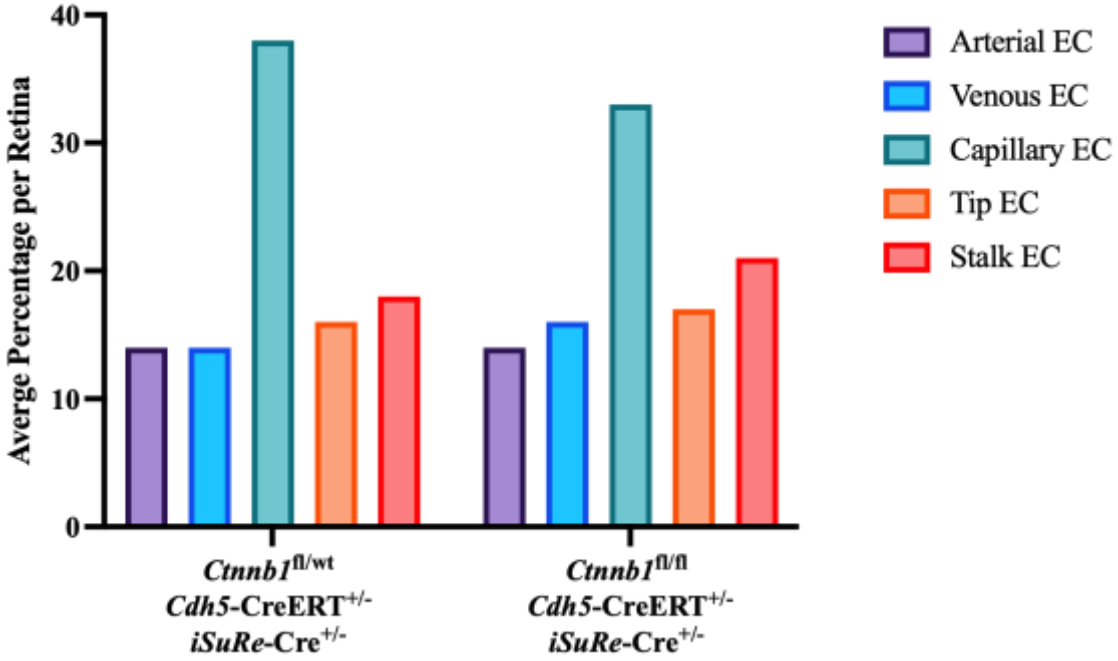

Figure 77: Bar graph showing comparing the localisation of recombined ECs (average percentage in each position per retina), p = 0.5992. Data was assessed using the Fisher's exact test. Statistical significance was defined as $P < 0.05$ (*$P < 0.05$, **$P < 0.01$, ***$P < 0.001$, ****$P < 0.001$).

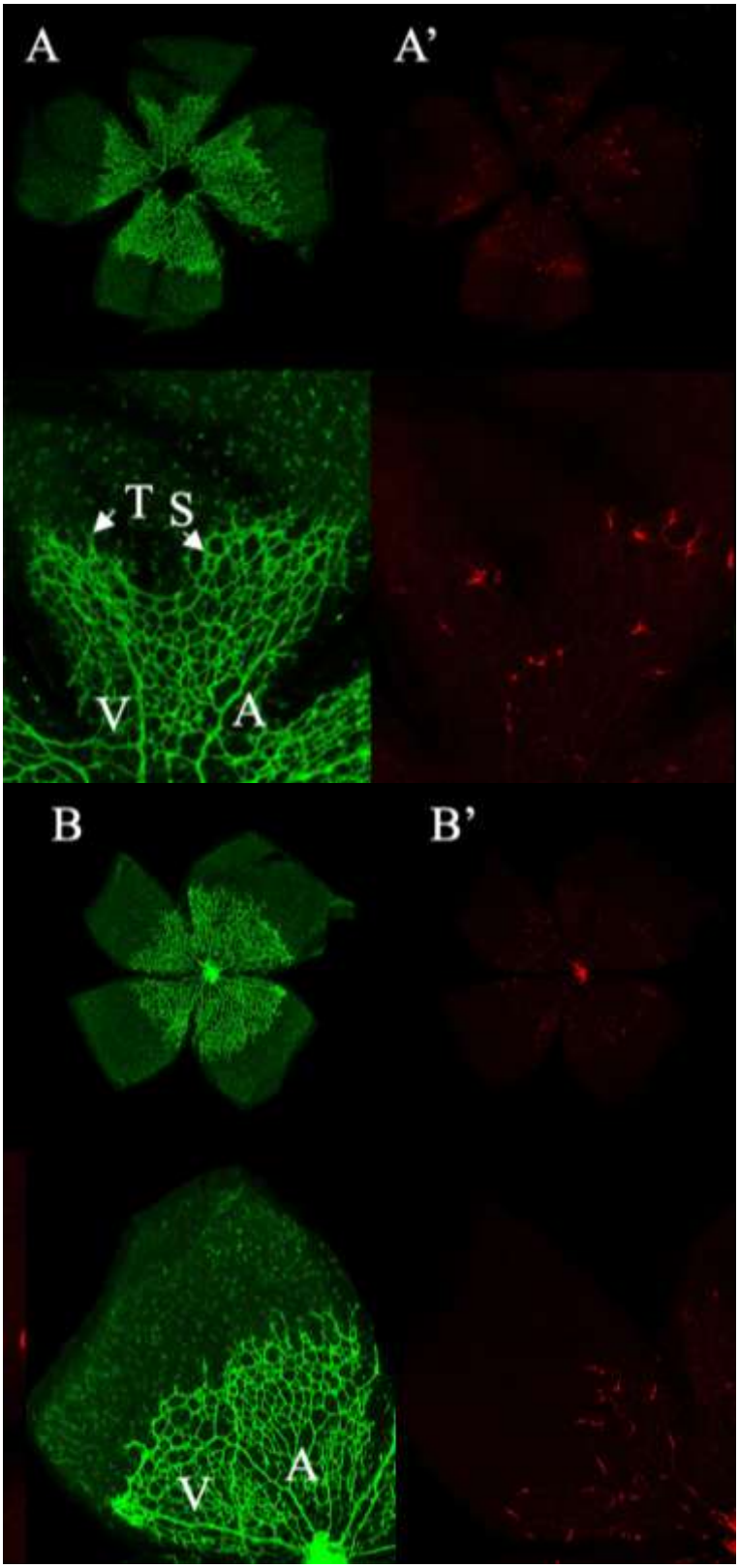

Figure 78: No significant difference in the location of recombined ECs with ablated canonical Wnt signalling. (A) A control retina from a P5 pup. The vasculature is marked in green, as stained by isolectin-488. (A') shows the recombination rate in the same control retina. Recombined ECs express MbTomato, and therefore are red. (B) A *Ctnnb1*$^{EC/EC}$ retina from a P5 pup, with recombination shown in (B').

Abbreviations: A = arterial; S = stalk; T = tip; V = venous

In total, 12 *Ctnnb1*$^{fl/wt}$ *Cdh5-Cre*ERT2$^{+/}$ *iSuRe-Cre*$^{+/-}$ retinae were collected from six different pups. On average, the *Ctnnb1*$^{fl/wt}$ *Cdh5-Cre*ERT2$^{+/}$ *iSuRe-Cre*$^{+/-}$ retinae had 47.5 recombined ECs, with a range between 29 and 77. To avoid bias from retinae with a higher number of recombined ECs, the number of recombined ECs in each location was expressed as a percentage of the total recombined ECs within that retina. For each location, these percentages were then totalled across each retina and divided by the total number of retinae. This yielded the average percentage of recombined ECs per location. The most common vascular subtype of recombined ECs in *Ctnnb1*$^{fl/wt}$ *Cdh5-Cre*ERT2$^{+/}$ *iSuRe-Cre*$^{+/-}$ retinae were the capillaries (38%), followed by stalk and tip (18% and 16%, respectively). There appeared to be no preference for an arterial versus venous EC subtype (14% versus 14%) (**Table 41**).

In contrast, nine *Ctnnb1*$^{fl/fl}$ *Cdh5-Cre*ERT2$^{+/}$ *iSuRe-Cre*$^{+/-}$ retinae were collected from six different pups. None of the pups were born without two retinae, but as the dissections were technically challenging, not all retinae were usable. On average, the *Ctnnb1*$^{fl/fl}$ *Cdh5-Cre*ERT2$^{+/}$ *iSuRe-Cre*$^{+/-}$ retinae had 45 recombined ECs, with a range between 13 and 74. This was a slightly larger range than with the *Ctnnb1*$^{fl/wt}$ *Cdh5-Cre*ERT2$^{+/}$ *iSuRe-Cre*$^{+/-}$ retinae, but the mean average was similar. This suggests that there was no significant difference in the number of recombined ECs between the two groups. Once again, the most common subtypes within the vasculature for recombined ECs were the capillaries (32.54%), and then stalk and tip (20.58% and 16.90%, respectively). There also did not appear to be preference for arterial versus vein position (14.48% versus 15.60%). When the Fisher's exact test was used to assess if the proportions of recombined ECs in each location varied between the two genotypes, the difference was not statistically significant, $p = 0.5992$ (Figure 77).

4.8 Discussion

The overall aim of Chapter 4 was to investigate the role of canonical Wnt signalling in the developing vasculature. To achieve this, both constitutive and inducible Cre murine models were used to ablate *Ctnnb1* from ECs. Analysis of blood vessel number, density and location was assessed in transverse embryonic cross sections using IF. To assess the effects on the regulation of different EC subpopulations, stable EC enhancer:*LacZ* murine transgenic lines were used to observe perturbations in enhancer activity. The key findings from these experiments are discussed below.

4.8.1 Constitutive EC-specific *Ctnnb1* ablation results in embryonic lethality and growth retardation by E11.5

Throughout the embryonic analysis, fewer *Ctnnb1*$^{EC/EC}$ embryos were collected than would be expected according to Mendelian ratios: by E10.5, this was statistically significant, $p < 0.0001$. This observation is earlier than previous studies, which report early embryonic lethality at E12.5.[209] One likely explanation for this disparity is the inclusion of the *iSuRe-Cre* allele. Indeed, when *Ctnnb1* was ablated with just the *Tg(Tek-Cre)*^{12Flv} allele, there were no statistically significant differences at E10.5 or E11.5 ($p = 0.9478$ and $p = 0.2401$, respectively). Given that constitutive Cre murine models using the *Tg(Tek-Cre)*^{12Flv} allele have notoriously inconsistent recombination efficiency, the inclusion of the *iSuRe-Cre* allele could have generated a more faithful loss-of-function model system.[219] Whilst Cre-toxicity from the *iSuRe-Cre* allele must be considered, published data has already shown that viable and fertile mice are produced with germline recombination of the *Gt(ROSA)26Sor-iSuRe-Cre* allele.[278,297] Moreover, my project did not report a reduction in the proportion of *Ctnnb1*$^{fl/wt}$ *Tek-Cre*$^{+/-}$*iSuRe-Cre*$^{+/-}$ embryos collected. This suggests that the phenotypes are arising directly from a more penetrant EC *Ctnnb1* ablation, rather than confounding Cre toxicity effects.

One potential explanation for this earlier embryonic lethality is the formation of defective or fragile vessels. Indeed, diffuse haemorrhaging in up to 50% of *Ctnnb1*$^{EC/EC}$ embryos has been reported before.[209] This vascular fragility was thought to arise from changes in EC morphology, with mutant ECs displaying more fenestrae.[209] In this project, I also observed haemorrhaging in *Ctnnb1*$^{EC/EC}$ embryos. One major limitation of the previous literature, and indeed my own project, is the use of a floxed *Ctnnb1* allele which does not

distinguish between the cell adhesive and transcriptional functions of β-Catenin. To overcome this limitation, the β-Catenin^{DM} allele could have been used instead, however it was not available to the De Val group at the inception of my project.[298,299]

In addition to reduced numbers, *Ctnnb1*$^{EC/EC}$ embryos were also consistently smaller than litter mates. This agrees with Cattelino *et al* (2003), which found that the hearts of mutant embryos were significantly smaller than wildtype hearts.[209] They also reported aberrant placentae, with poorly organised and fragile foetal vessels which failed to properly interdigitate with maternal blood spaces.[209] It is well established that the placenta is highly sensitive to perturbations in vascular patterning, and these vascular defects can severely impair the maternal foetal exchange capacity.[300] This raises the question of whether the overall reduction in embryonic size reflects a direct developmental consequence of EC-specific *Ctnnb1* ablation, or whether it arises secondarily from placental defects. Whilst this project has found evidence for vascular defects in the *Ctnnb1*$^{EC/EC}$ embryos, we cannot rule out an effect from the placenta. However, Cattelino *et al* concluded that placental insufficiency was unlikely to be the primary cause of their aberrant phenotypes since these were distinct from embryos with comparable placental insufficiency. Therefore, whilst placental defects could be compounding any of my observed phenotypes, it is highly likely that aberrant embryonic vasculature is majorly contributing to the overall changes in embryonic lethality and CRL.

4.8.2 Constitutive EC-specific *Ctnnb1* ablation does not result in clear arterial or venous defects

In a murine model overexpressing *Ctnnb1* in ECs, Corada *et al* (2010) had previously reported misexpression of arterial and venous markers, including aberrant expression of arterial *Efnb2* in the anterior cardinal vein.[210] However, my analysis using *Dll4-12:LacZ* and *DLL4in3:LacZ* to assess changes in arterial EC enhancer activity did not find the same phenotype. X-Gal staining of *Dll4-12:LacZ*$^{+/-}$ *Ctnnb1*$^{fl/fl}$ embryos revealed *LacZ* expression confined to arterial ECs, much as is seen in littermate controls. Moreover, IF staining for Sox17 (a classical arterial marker) saw no difference in localisation between control and *Ctnnb1*$^{EC/EC}$ embryos. This suggested that canonical Wnt signalling is not required for the proper acquisition of arterial EC identity.

Nevertheless, some researchers have reported active canonical Wnt signalling in arterial ECs as early as E9.5, based on Wnt reporter activity, and β-catenin stabilisation has been associated with arteriovenous malformation.[210] In this project, I observed an expansion in DLL4in3 activity - an enhancer active in both arterial and angiogenic EC subpopulations. However, because Dll4-12 activity remained unaltered, I did not interpret this ectopic DLL4in3 activity as a defect in arterial EC regulation.

4.8.3 Constitutive EC-specific *Ctnnb1* ablation results in increased activity of venous and angiogenic enhancers

Whilst arterial EC identity did not appear expanded, *LacZ*$^{+/-}$ *Ctnnb1*$^{EC/EC}$ embryos showed a noticeable, though not always consistent, expansion in the expression of venous and angiogenic EC identity. This was assessed using the *CoupTFII-965:LacZ* transgene (active in venous ECs) and the *DLL4in3:LacZ,* and *SOX7-58:LacZ* transgenes (active in angiogenic ECs). Evidence has recently emerged that venous ECs are the principal EC subtype driving angiogenic vascular expansion.[69] Accordingly, the combined increase in angiogenic and venous enhancer activity initially led me to hypothesis that *Ctnnb1* ablation might promote angiogenesis. Unexpectedly, however, despite the broader SOX7-58 activity observed in *SOX7-58:LacZ*$^{+/-}$ *Ctnnb1*$^{EC/EC}$ embryos, overall vascular density remained unchanged. This suggests a disconnect between SOX7-58 activation and the execution of downstream angiogenic programmes in the absence of EC-specific *Ctnnb1*.

4.8.4 EC-specific *Ctnnb1* ablation potentially affected the formation of the coronary plexus, but not its subsequent remodelling

Evidence has recently emerged linking canonical Wnt signalling with the development of adult cardiac diseases.[301] For example, in one patient study, a family with autosomal dominant early coronary artery disease were found to have a missense mutation in *LRP6*.[302] Developmentally, canonical Wnt signalling has also been implicated in proper coronary artery formation.[290,303]

In this project I did not observe significant differences in initial sprouting from the SV at E12.5, or coronary vessel maturation and remodelling from E14.5. The one process that could potentially be dependent on canonical Wnt signalling is the formation of the primary plexus and its initial migration across the dorsal face of the heart at E13.5.

However, as these *Ctnnb1*$^{iEC/EC}$ hearts only came from two litters, it would be important to ascertain if this trend continued in a larger sample size. Using the *NOTCH1+16:LacZ* transgene, I was able to dissect specific effects on VEGFC-driven angiogenesis. Given that the *SOX7-58:LacZ* transgene showed clear expansion in the postnatal retinal vasculature, this could indicate that canonical Wnt signalling is only important for VEGFA-driven angiogenesis.

4.8.5 EC-specific *Ctnnb1* ablation results in BBB defects

In agreement with previous studies, I found that the blood-brain barrier (BBB) was particularly affected by the ablation of *Ctnnb1*. Using IF, I demonstrated that both *Tek-Cre*- and *Etv2-Cre*-mediated deletion of *Ctnnb1* reduced vascular density within and around the neural tube, despite overall vascular density across the section being preserved. Interestingly, when examining the expansion of COUP-TFII:*LacZ*, *DLL4in3:LacZ,* and *SOX7-58:LacZ* expression in *Ctnnb1*$^{EC/EC}$ embryonic vasculature, most of the ectopic activity was observed in the head and spinal regions. This could indicate that the ECs forming the BBB are transcriptionally compromised, with enhancer activity becoming ectopic.

These BBB-specific observations resonate with prior studies implicating canonical Wnt signalling in CNS-specific angiogenesis.[18,211,212,304] Indeed, multiple studies have demonstrated that β-catenin is essential for CNS-specific vessel formation and the regulation of angiogenic invasion.[18,209,211,212,304] Whilst the use of *Flk1-Cre* in some studies could account for this discrepancy, other studies also used the *Tg(Tek-Cre)*^{12Flv} allele and still only reported CNS vascular defects.[211] When ablating different components of the canonical Wnt signalling pathway, Zhou *et al* (2014) reported a plethora of vascular phenotypes with varying severity, most of which were related to suppression of normal vascular development in the neural tube or retina.[18] Moreover, when Tran *et al* (2016) ablated *Ctnnb1* in adult mice ECs using the *SCL-Cre*ER, they reported that *Ctnnb1*$^{EC/EC}$ mice developed severe seizures, brain petechial haemorrhages, CNS inflammation, and, ultimately, postictal death.[305] More recently, having identified USP9X as an EC regulator of canonical Wnt activity in the CNS, Lei *et al* (2025) reported that EC-specific deletion of *Usp9x* resulted in impaired blood-brain and blood-retina barrier formation, widespread leakage, and an inability to establish or maintain vascular integrity during development.[306] These studies, combined with my project, all highlight

the indispensable role of canonical Wnt signalling in CNS-specific vascular morphogenesis.

4.8.6 EC-specific *Ctnnb1* ablation in the postnatal retinal vasculature results in reduced radial angiogenesis and a higher incidence of arteriovenous crossovers

Genetic retinal diseases, such as Norrie disease, have implicated defective canonical Wnt signalling in retinal hypovascularisation.[207,307-310] This has been observed in patients with partial mutations in *Ndp*, or complete loss-of-function mutations in *Lrp5*.[207] This finding has also been recapitulated in *Ndp, Fz4,* or *Lrp5* loss-of-function mouse models.[207,311-314] Two major phenotypes have been described upon EC-specific *Ctnnb1* ablation: an increased number of arteriovenous cross-overs and a reduction in vascular density (or branch points).[292]

In this project, I report a reduced radial expansion and an increased incidence of arteriovenous cross-overs in *Ctnnb1*$^{EC/EC}$ retinae. Whilst Martowicz *et al* (2019) also reported a significant increase in arteriovenous cross-overs, they did not neither find any significant difference in radial expansion.[210,292] This difference could reflect the day of tamoxifen given, whilst I gave the tamoxifen at P1, Martowicz gave it at P3. In concordance, when Lei *et al* (2025) ablated *Usp9x* (a crucial regulator of Wnt signalling) from ECs at P1*,* they also observed a reduction in vascular area, branching, and radial outgrowth.[306] This suggests that although canonical Wnt signalling is crucial for early retinal vascular development, if it is initially present, the radial expansion is not affected.

Interestingly, when Corada *et al* examined their gain-of-function model, they found a significant reduction in radial extension, but no differences in the number of tip cells.[210] Normal sprouting has also been reported by Phng *et al* (2009), who used a *Pdgfb*-iCreER driver to ablate *Ctnnb1* in ECs.[293] This was despite there being a significant reduction in vascular density, with excessive vessel regression.[293] Using the *SOX7-58:LacZ* transgene to mark tip ECs in the retinal vasculature, I observed expanded *LacZ* expression compared to littermate controls. However, this may not reflect increased numbers of tip ECs, instead perhaps indicating a loss of SOX7-58 tip EC-specificity. To assess this further, I should quantify the number of tip ECs in each *Ctnnb1*$^{iEC/iEC}$ retina compared to littermate control retina.

4.8.7 Differential EC *Ctnnb1* expression does not regulate EC subtype identity acquisition within the developing postnatal retina vasculature

Martowicz *et al* (2019) has previously used mosaic genetic studies to show that ECs lacking β-catenin were less likely to occupy the tip cell position.[292] Following tamoxifen induction at P1, only 35% of tip cell positions in the P5 mosaic *Ctnnb1*$^{iEC/iEC}$ retinae were occupied by recombined ECs.[292] In contrast, I did not observe any differences in the ability of recombined *Ctnnb1*-ablated ECs to acquire any EC subtype identity (arterial, vein, capillary, tip or stalk) compared with recombined control ECs, $p = 0.5992$. This instead suggests that canonical Wnt signalling is not critical for tip EC specification.

A key difference between these studies lies in tamoxifen dosage and route of administration. Whilst I administrated 5µg of tamoxifen orally in corn oil, Martowicz *et al* used 3.75µg of tamoxifen administrated subcutaneously.[292] In both studies, recombination was induced at P1. Although my higher dosage would be expected to yield greater recombination, their retinae appeared to show a substantially higher degree of recombination. Unfortunately, Martowicz *et al* did not report recombination efficiency, but their confocal images indicate frequent clustering of recombined ECs. By contrast, in my model system, recombined ECs were always interspersed with wildtype EC neighbours. Thus, whilst mutant ECs in my project are directly competing with adjacent non-recombined ECs, in the Martowicz *et al* study, clusters of recombined ECs could have amplified cell-autonomous defects. This could account for the discrepancy in findings.

4.9 Conclusions

The results of Chapter 4 support the notion that EC canonical Wnt signalling is essential to normal CNS vascular development, but may not be absolutely necessary for the formation of non-CNS vasculature. Indeed, whilst the overall vasculature remained comparable between control and *Ctnnb1*$^{EC/EC}$ embryos, the number of blood vessels in and around the neural tube differed significantly. Nonetheless, the characterisation of enhancer:*LacZ* transgenes in this genetic *Ctnnb1* perturbation model has revealed aberrant COUP-TFII, DLL4in3 and SOX7-58 enhancer activity. This activity seems un-coupled from genuine vascular expansion. In the coronary vasculature, the *NOTCH1+16:LacZ* transgene has revealed a potential role for canonical Wnt signalling

in the regulation of SV-derived coronary vessels. In a postnatal setting, canonical Wnt signalling continues to have an important function in the CNS vasculature, with *Ctnnb1* ablation resulting in a reduced radial expansion and increased incidence of arteriovenous cross-overs. However, individual ECs with ablated *Ctnnb1* do not appear to change their position within the developing vascular network.

Chapter 5: Conclusions

5.1 Overall conclusions

In this thesis, I initially set out to identify the TFs regulating the expression pattern of a novel angiogenic enhancer. This enhancer, situated 58 kilobases downstream of the *SOX7* gene, was termed SOX7-58. Mutation of a putative TCF/LEF binding motif within the SOX7-58 enhancer altered enhancer activity, leading me to examine the consequences of ablated canonical Wnt signalling on developmental angiogenesis and arteriovenous specification.

In Chapter 3, I demonstrated that orthologues of SOX7-58 were all able to drive EC-specific expression although at different penetrance. Phylogenetic foot-printing identified eight highly conserved regions between the human, mouse, and opossum genomes. Manual inspection for TF binding motifs identified potential binding sites for ETS, FOS:ETS, FOS:JUN, C/EBP and TCF/LEF TFs. The function of these motifs was tested via mutagenesis in a F0 transgenic zebrafish screen. This analysis suggested an essential role for the FOX:ETS, FOS:JUN and C/EBP motifs, with the ETS motifs shown to be essential but not sufficient to recapitulate the enhancer's expression pattern. The most notable finding from this Chapter was the expansion in GFP activity driven by the mutTCF/LEF *SOX7-58:*GFP transgene. This indicated a potential role for canonical Wnt signalling in restricting the activity of SOX7-58 to angiogenic ECs. Analysis of other angiogenic enhancers also identified potential TCF/LEF binding motifs in multiple other angiogenic enhancers, including the well-studied arterial and angiogenic DLL4in3 enhancer. Overall, these results suggested that canonical Wnt signalling may be a potential negative regulator of angiogenesis.

In Chapter 4, I sought to examine the effects of canonical Wnt signalling in vascular development using *in vivo* mouse models. Three different vascular beds were probed: constitutive Cre models were used to investigate the systemic vasculature, with inducible Cre models used to investigate both the coronary vasculature and the retinal vasculature. Using endothelial subtype-specific enhancer:*LacZ* lines, I found that angiogenic enhancers – DLL4in3 and SOX7-58 – have potentially expanded activity in the absence of EC *Ctnnb1* expression. In contrast, Dll4-12, an enhancer specifically active in arterial

ECs, did not alter expression. Moreover, when using IF to assess the distribution of Sox17 (a classical arterial marker) and CoupTFII (a classical vein marker), I found no inappropriate expression, i.e., Sox17 expression in venous compartments or CoupTFII expression in arterial compartments. This suggests that whilst arterial and venous specification is not affected by canonical Wnt signalling, this pathway may have a role in regulating some aspects of angiogenesis. However, analysis of the overall vasculature density and blood vessel number revealed that expanded angiogenic enhancer activity was not correlating with more blood vessels. This suggests a de-coupling of the angiogenic enhancer activity and function.

To better investigate the requirement for canonical Wnt signalling in distinct steps of angiogenesis, inducible Cre models were used to delete *Ctnnb1* in ECs at strict timepoints. VEGFC-driven angiogenesis was examined in the coronary vasculature, using the *NOTCH1+16:LacZ* transgene, whilst VEGFA-driven angiogenesis was probed in the postnatal retinal vasculature. To this end, I found that the absence of canonical Wnt signalling only affected VEGFA driven angiogenesis. When a reduced tamoxifen dosage was used to induce recombination only in >5% of ECs, there appeared to be no requirement for canonical Wnt signalling in the acquisition of any EC subtype identity.

In conclusion, these results demonstrate the complexity of angiogenic gene regulation, with a role for canonical Wnt signalling in the spatial specificity of angiogenic enhancer activity. In the absence of canonical Wnt signalling, this spatial specificity is lost, and aberrant angiogenic enhancer activity is observed. However, this aberrant activity is not correlated with an upregulation of angiogenesis.

5.2 Limitations

5.2.1 F0 transgenic zebrafish assays

F0 transgenic zebrafish screens were used extensively in Chapter 3 to test the functionality of putative TFs motifs within the SOX7-58 enhancer sequence.

One major limitation with this methodology is the assignment of EC *GFP* expression categories. For F0 transgenic zebrafish expressing a mutated version of the *SOX7*-

58:GFP transgene, *GFP* expression patterns were assigned as either 'strong', 'medium', 'weak' or 'absent'. Whilst this was initially performed in consultation with Dr Svanhild Nornes, this was mostly subject to my own opinion. Undoubtedly, this introduces a great degree of bias: a far more rigorous approach would have been to use a computational methods, such as ZFTool, ZF-Mapper, or commercial AI-based platforms like *Athena Zebrafish* (https://idea-bio.com/products/zebrafish-image-analysis/), which apply objective segmentation and fluorescence quantification algorithms.[315,316] In the absence of these platforms, another strategy would have been to have more than one experimenter score the fish. This would have highlighted any unintentional bias in the scoring system.

Another limitation with the F0 transgenic zebrafish screens was the lack of blinding: I knew exactly which population of fish were being screened at the time of analysis. One way to circumvent this bias would have been to inject the embryos with anonymised transgenes. Another issue with this lack of blinding was the selection of representative fish for imaging on the confocal microscope. Given that only between five and ten were chosen, any subjectivity would mask the true expression patterns of the enhancer. In part, such a small sample size was selected because imaging a zebrafish on the confocal is relatively time inefficient. To circumvent this limitation and image a greater number of zebrafish, I could have had instead used a Light-Sheet Flow Imaging System (LS-FIS). Indeed, this approach can image a zebrafish embryo in four seconds.[317] Whilst the LS-FIS approach produces lower-resolution images, these should still be sufficient quality to characterise the zebrafish by EC *GFP* expression and, unlike confocal microscopy, LS-FIS keeps photobleaching and phototoxicity to a minimum.[318]

5.2.2 Transgenic mouse studies

Transgenic mouse models were used to investigate a role for canonical Wnt signalling in vascular development. This was achieved with either the *Tg(Tek-cre)*^{12Flv} allele or the *Tg(Etv2-Cre)1Blk* allele, in combination with the *iSuRe*-Cre allele and the Ctnnb1^{tm2Kem} allele. Since the inception of this project, a new dual Cre-reporter allele has been created: *iSuRe*-HADCre.[319] Amongst other improvements, this allele has been designed to only be transiently expressed, thereby limiting Cre-related toxicity.[319] Moreover, this new allele has a greater sensitivity to induction by CreERT2, which would have been particularly beneficial in my experiments examining the development of both the coronary and retinal vasculature.

However, perhaps the biggest limitation in either my *Ctnnb1*$^{EC/EC}$ or *Ctnnb1*$^{iEC/iEC}$ models was the inclusion of the Ctnnb1^{tm2Kem} allele. Although, this allele has been extensively used in previous studies investigating the role of canonical Wnt signalling in vascular development, it does not distinguish between the cell adhesive and transcriptional functions of β-Catenin.[298,320] it does not distinguish between the transcriptional and cell-adhesion roles of β-catenin. This is incredibly problematic: any arising vascular defects cannot be accredited purely to the canonical Wnt signalling pathway without confounding contributions from defective cell adhesion. To circumvent this limitation, the β-Catenin^{DM} allele could have been used instead.[298,299] This allele, with a single amino acid mutation in the first armadillo repeat and a C-terminal truncation, produces a β-catenin protein which lacks any transcriptional activity, whilst retaining the intact cell adhesive function.

One frustrating limitation in this thesis was the lack of *Ctnnb1*$^{EC/EC}$ embryos used to analyse changes in vasculature density and localisation. Originally, I had planned to section *Ctnnb1*$^{EC/EC}$ embryos, along with littermate controls, previously stained whole-mount in X-Gal. However, the X-Gal stain blocked the binding of antibodies, concealing vasculature that co-localised with enhancer:*LacZ* transgene activity. Therefore, additional embryos had to be collected and cryo-sectioned for IF analysis. Given the early embryonic lethality associated with the *Ctnnb1*$^{EC/EC}$ genotype, and the time constraints of this thesis, I struggled to dissect enough *Ctnnb1*$^{EC/EC}$ embryos for meaningful statistical analysis.

5.2.3 *In silico* TF site predictions

When manually inspecting the SOX7-58 enhancer sequence for putative TF sites against a list of TFs already known to regulate EC enhancers, I was acutely aware of introducing bias to my search. To mitigate this, I also used computational methodologies to identify putative TF motifs. However, these are not without bias, and often result in a significant degree of false positives.[321] Indeed, *in silico* analysis relies on good quality data being inputted into the TF databases, but at present, this is not always the case. As a result, *in silico* motif prediction has been coined *futility theorem*, reflecting the reality that most predicted TF binding sites lack functionality *in vivo*.[322]

5.3 Future work

Moving forward, it will be crucial to definitively demonstrate that TCF/LEF binds to the SOX7-58 enhancer sequence. Although not mentioned in this thesis, I attempted to do so using CUT&RUN, however this effort was in vain, even when using the specialised CUT&RUN-LoV-U protocol.[323] Whilst trouble shooting could eventually yield results, it would be wise to also consider other methodologies. For example, an electrophoretic mobility shift assay (EMSA) could be used to test the ability of the putative TCF/LEF binding site to interact with TCF/LEF *in vitro*.[324] Another approach could be a ChIP-seq experiment, using the same antibodies I tested using the CUT&RUN methodology. Whilst this approach undoubtedly is not devoid of its own limitations – it requires more cells, and can produce higher background – many of the TCF/LEF/β-catenin antibodies have already been successfully tested in this context.[325]

In generating the F0 transgenic zebrafish for my enhancer mutagenesis screens, the Tol2 destination vector I used only contained a single enhancer:GFP construct. This meant that the activity of different enhancer:reporter transgenes was compared using different clutches of zebrafish embryos, each expressing a different enhancer:reporter transgene. Future experiments should instead use the Quantitative Spatial and Temporal Assessment of Regulatory element activity in Zebrafish (QSTARZ) system.[238] Crucially, this system enables the activity of two enhancer:reporter transgenes to be analysed in the same zebrafish embryo via two different fluorescent reporters (such as GFP and mCherry).[326] Furthermore, as both reporter cassettes are integrated into an identical genomic location, expression differences can be attributed to the enhancer sequences themselves rather than positional effects arising from random integration. Thus, the activity of SOX7-58:GFP transgene could have been directly tested against mutated versions of the SOX7-58:GFP transgene. From an ethics perspective, this would also have been preferable, as fewer zebrafish would have been required.

In addition, to complement the initial mutagenesis experiments in F0 transgenic zebrafish, F0 transgenic murine embryos will be generated which express a mutTCF/LEF *SOX7-58:LacZ* transgene. This transgene will have identical disruptions in the putative TCF/LEF binding motif as the mutTCF/LEF *SOX7-58:GFP* transgene expressed in F0 transgenic zebrafish embryos. This would indicate whether the original observation of

expanded SOX7-58 activity in F0 transgenic zebrafish is recapitulated in a mammalian setting.

Finally, although in **Section 3.1** I have shown that SOX7-58 is a functional enhancer in tip ECs, I have not directly demonstrated that it regulates the endogenous Sox7 gene. This is because whilst reporter assays confirm enhancer activity, they do not establish physical or functional links to the native promoter. As this was not the biological question I was investigating, I did not pursue this research question further, but it may be useful for future studies to establish whether this is indeed the case. Future work could combine chromatin conformation and functional assays to test this relationship. Techniques such as Hi-C, 3C, or Capture-C would reveal whether SOX7-58 physically interacts with the Sox7 promoter in its native chromatin context. CRISPR-based perturbations—activation (CRISPRa) or inhibition (CRISPRi) of the enhancer—followed by measurement of Sox7 mRNA or protein levels, would determine whether the enhancer is necessary or sufficient for gene expression. Moreover, complementary luciferase reporter assays, pairing SOX7-58 with the Sox7 promoter, could test enhancer-promoter specificity and the contribution of individual transcription factor motifs, such as TCF/LEF sites. Together, these experiments would provide direct mechanistic evidence linking SOX7-58 to Sox7 regulation, clarifying its role within the transcriptional network controlling tip EC identity and sprouting angiogenesis.

References

1 Aird, W. C. Endothelial cell heterogeneity. *Cold Spring Harb Perspect Med* **2**, a006429, doi:10.1101/cshperspect.a006429 (2012).

2 Augustin, H. G. & Koh, G. Y. A systems view of the vascular endothelium in health and disease. *Cell* **187**, 4833-4858, doi:10.1016/j.cell.2024.07.012 (2024).

3 Eelen, G., Treps, L., Li, X. & Carmeliet, P. Basic and Therapeutic Aspects of Angiogenesis Updated. *Circ Res* **127**, 310-329, doi:10.1161/CIRCRESAHA.120.316851 (2020).

4 Trimm, E. & Red-Horse, K. Vascular endothelial cell development and diversity. *Nat Rev Cardiol* **20**, 197-210, doi:10.1038/s41569-022-00770-1 (2023).

5 Udan, R. S., Culver, J. C. & Dickinson, M. E. Understanding vascular development. *Wiley Interdiscip Rev Dev Biol* **2**, 327-346, doi:10.1002/wdev.91 (2013).

6 Pugsley, M. K. & Tabrizchi, R. The vascular system. An overview of structure and function. *J Pharmacol Toxicol Methods* **44**, 333-340, doi:10.1016/s1056-8719(00)00125-8 (2000).

7 Ribatti, D. Aberrant tumor vasculature. Facts and pitfalls. *Front Pharmacol* **15**, 1384721, doi:10.3389/fphar.2024.1384721 (2024).

8 Taylor, A. M. & Bordoni, B. in *StatPearls* (2025).

9 Patan, S. Vasculogenesis and angiogenesis. *Cancer Treat Res* **117**, 3-32, doi:10.1007/978-1-4419-8871-3_1 (2004).

10 Potente, M., Gerhardt, H. & Carmeliet, P. Basic and therapeutic aspects of angiogenesis. *Cell* **146**, 873-887, doi:10.1016/j.cell.2011.08.039 (2011).

11 Patel-Hett, S. & D'Amore, P. A. Signal transduction in vasculogenesis and developmental angiogenesis. *Int J Dev Biol* **55**, 353-363, doi:10.1387/ijdb.103213sp (2011).

12 Sadler, T. W. *Langman's Medical Embryology*. 14th edn, (Wolters Kluwer, 2019).

13 Culver, J. C. & Dickinson, M. E. The effects of hemodynamic force on embryonic development. *Microcirculation* **17**, 164-178, doi:10.1111/j.1549-8719.2010.00025.x (2010).

14 Garcia, M. D. & Larina, I. V. Vascular development and hemodynamic force in the mouse yolk sac. *Front Physiol* **5**, 308, doi:10.3389/fphys.2014.00308 (2014).

15 Xiong, J. W. Molecular and developmental biology of the hemangioblast. *Dev Dyn* **237**, 1218-1231, doi:10.1002/dvdy.21542 (2008).

16 DeSesso, J. M. Vascular ontogeny within selected thoracoabdominal organs and the limbs. *Reprod Toxicol* **70**, 3-20, doi:10.1016/j.reprotox.2016.10.007 (2017).

17 Cool, T. & Forsberg, E. C. Chasing Mavericks: The quest for defining developmental waves of hematopoiesis. *Curr Top Dev Biol* **132**, 1-29, doi:10.1016/bs.ctdb.2019.01.001 (2019).

18 Zhou, Y. *et al.* Canonical WNT signaling components in vascular development and barrier formation. *J Clin Invest* **124**, 3825-3846, doi:10.1172/JCI76431 (2014).

19 Flamme, I., Frolich, T. & Risau, W. Molecular mechanisms of vasculogenesis and embryonic angiogenesis. *J Cell Physiol* **173**, 206-210, doi:10.1002/(SICI)1097-4652(199711)173:2<206::AID-JCP22>3.0.CO;2-C (1997).

20 Gritz, E. & Hirschi, K. K. Specification and function of hemogenic endothelium during embryogenesis. *Cell Mol Life Sci* **73**, 1547-1567, doi:10.1007/s00018-016-2134-0 (2016).
21 Scarfo, R. *et al.* CD32 captures committed haemogenic endothelial cells during human embryonic development. *Nat Cell Biol* **26**, 719-730, doi:10.1038/s41556-024-01403-0 (2024).
22 Fish, J. E. & Wythe, J. D. The molecular regulation of arteriovenous specification and maintenance. *Dev Dyn* **244**, 391-409, doi:10.1002/dvdy.24252 (2015).
23 De Val, S. *et al.* Combinatorial regulation of endothelial gene expression by ets and forkhead transcription factors. *Cell* **135**, 1053-1064, doi:10.1016/j.cell.2008.10.049 (2008).
24 Payne, S., Neal, A. & De Val, S. Transcription factors regulating vasculogenesis and angiogenesis. *Dev Dyn* **253**, 28-58, doi:10.1002/dvdy.575 (2024).
25 Risau, W. & Flamme, I. Vasculogenesis. *Annu Rev Cell Dev Biol* **11**, 73-91, doi:10.1146/annurev.cb.11.110195.000445 (1995).
26 Grunewald, M. *et al.* VEGF-induced adult neovascularization: recruitment, retention, and role of accessory cells. *Cell* **124**, 175-189, doi:10.1016/j.cell.2005.10.036 (2006).
27 Singhal, M. *et al.* Endothelial cell fitness dictates the source of regenerating liver vasculature. *J Exp Med* **215**, 2497-2508, doi:10.1084/jem.20180008 (2018).
28 Lenzi, P., Bocci, G. & Natale, G. John Hunter and the origin of the term "angiogenesis". *Angiogenesis* **19**, 255-256, doi:10.1007/s10456-016-9496-7 (2016).
29 Lugano, R., Ramachandran, M. & Dimberg, A. Tumor angiogenesis: causes, consequences, challenges and opportunities. *Cell Mol Life Sci* **77**, 1745-1770, doi:10.1007/s00018-019-03351-7 (2020).
30 Loizzi, V. *et al.* Biological Pathways Involved in Tumor Angiogenesis and Bevacizumab Based Anti-Angiogenic Therapy with Special References to Ovarian Cancer. *Int J Mol Sci* **18**, doi:10.3390/ijms18091967 (2017).
31 Makanya, A. N., Hlushchuk, R. & Djonov, V. G. Intussusceptive angiogenesis and its role in vascular morphogenesis, patterning, and remodeling. *Angiogenesis* **12**, 113-123, doi:10.1007/s10456-009-9129-5 (2009).
32 De Spiegelaere, W. *et al.* Intussusceptive angiogenesis: a biologically relevant form of angiogenesis. *J Vasc Res* **49**, 390-404, doi:10.1159/000338278 (2012).
33 Djonov, V., Baum, O. & Burri, P. H. Vascular remodeling by intussusceptive angiogenesis. *Cell Tissue Res* **314**, 107-117, doi:10.1007/s00441-003-0784-3 (2003).
34 Gerhardt, H. *et al.* VEGF guides angiogenic sprouting utilizing endothelial tip cell filopodia. *J Cell Biol* **161**, 1163-1177, doi:10.1083/jcb.200302047 (2003).
35 Luttun, A., Dewerchin, M., Collen, D. & Carmeliet, P. The role of proteinases in angiogenesis, heart development, restenosis, atherosclerosis, myocardial ischemia, and stroke: insights from genetic studies. *Curr Atheroscler Rep* **2**, 407-416, doi:10.1007/s11883-000-0079-z (2000).
36 Pepper, M. S. Extracellular proteolysis and angiogenesis. *Thromb Haemost* **86**, 346-355 (2001).
37 Hillen, F. & Griffioen, A. W. Tumour vascularization: sprouting angiogenesis and beyond. *Cancer Metastasis Rev* **26**, 489-502, doi:10.1007/s10555-007-9094-7 (2007).

38 Blanco, R. & Gerhardt, H. VEGF and Notch in tip and stalk cell selection. *Cold Spring Harb Perspect Med* **3**, a006569, doi:10.1101/cshperspect.a006569 (2013).
39 Eilken, H. M. & Adams, R. H. Dynamics of endothelial cell behavior in sprouting angiogenesis. *Curr Opin Cell Biol* **22**, 617-625, doi:10.1016/j.ceb.2010.08.010 (2010).
40 Guo, Y., Zhang, S., Wang, D., Heng, B. C. & Deng, X. Role of cell rearrangement and related signaling pathways in the dynamic process of tip cell selection. *Cell Commun Signal* **22**, 24, doi:10.1186/s12964-023-01364-1 (2024).
41 Hellstrom, M. *et al.* Dll4 signalling through Notch1 regulates formation of tip cells during angiogenesis. *Nature* **445**, 776-780, doi:10.1038/nature05571 (2007).
42 Harrington, L. S. *et al.* Regulation of multiple angiogenic pathways by Dll4 and Notch in human umbilical vein endothelial cells. *Microvasc Res* **75**, 144-154, doi:10.1016/j.mvr.2007.06.006 (2008).
43 Suchting, S. *et al.* The Notch ligand Delta-like 4 negatively regulates endothelial tip cell formation and vessel branching. *Proc Natl Acad Sci U S A* **104**, 3225-3230, doi:10.1073/pnas.0611177104 (2007).
44 Siekmann, A. F. & Lawson, N. D. Notch signalling limits angiogenic cell behaviour in developing zebrafish arteries. *Nature* **445**, 781-784, doi:10.1038/nature05577 (2007).
45 Funahashi, Y. *et al.* Notch regulates the angiogenic response via induction of VEGFR-1. *J Angiogenes Res* **2**, 3, doi:10.1186/2040-2384-2-3 (2010).
46 Benedito, R. *et al.* The notch ligands Dll4 and Jagged1 have opposing effects on angiogenesis. *Cell* **137**, 1124-1135, doi:10.1016/j.cell.2009.03.025 (2009).
47 Ruhrberg, C. *et al.* Spatially restricted patterning cues provided by heparin-binding VEGF-A control blood vessel branching morphogenesis. *Genes Dev* **16**, 2684-2698, doi:10.1101/gad.242002 (2002).
48 Fong, G. H., Rossant, J., Gertsenstein, M. & Breitman, M. L. Role of the Flt-1 receptor tyrosine kinase in regulating the assembly of vascular endothelium. *Nature* **376**, 66-70, doi:10.1038/376066a0 (1995).
49 Kearney, J. B. *et al.* Vascular endothelial growth factor receptor Flt-1 negatively regulates developmental blood vessel formation by modulating endothelial cell division. *Blood* **99**, 2397-2407, doi:10.1182/blood.v99.7.2397 (2002).
50 De Smet, F., Segura, I., De Bock, K., Hohensinner, P. J. & Carmeliet, P. Mechanisms of vessel branching: filopodia on endothelial tip cells lead the way. *Arterioscler Thromb Vasc Biol* **29**, 639-649, doi:10.1161/ATVBAHA.109.185165 (2009).
51 Vimalraj, S., Saravanan, S., Anuradha, D. & Chatterjee, S. Models to investigate intussusceptive angiogenesis: A special note on CRISPR/Cas9 based system in zebrafish. *Int J Biol Macromol* **123**, 1229-1240, doi:10.1016/j.ijbiomac.2018.11.164 (2019).
52 Jones, E. A., Baron, M. H., Fraser, S. E. & Dickinson, M. E. Dynamic in vivo imaging of mammalian hematovascular development using whole embryo culture. *Methods Mol Med* **105**, 381-394, doi:10.1385/1-59259-826-9:381 (2005).
53 Lucitti, J. L. *et al.* Vascular remodeling of the mouse yolk sac requires hemodynamic force. *Development* **134**, 3317-3326, doi:10.1242/dev.02883 (2007).

54 Chapman, W. B. The effect of the heart-beat upon the development of the vascular system in the chick. *Am. J. Anat* **23**, 175-203, doi:10.1002/aja.1000230107 (1918).

55 Papaioannou, I. *et al.* NKX2-5 regulates vessel remodeling in scleroderma-associated pulmonary arterial hypertension. *JCI Insight* **9**, doi:10.1172/jci.insight.164191 (2024).

56 Fang, Y., Wu, D. & Birukov, K. G. Mechanosensing and Mechanoregulation of Endothelial Cell Functions. *Compr Physiol* **9**, 873-904, doi:10.1002/cphy.c180020 (2019).

57 Zhou, Y., Williams, J., Smallwood, P. M. & Nathans, J. Sox7, Sox17, and Sox18 Cooperatively Regulate Vascular Development in the Mouse Retina. *PLoS One* **10**, e0143650, doi:10.1371/journal.pone.0143650 (2015).

58 Uyttendaele, H., Ho, J., Rossant, J. & Kitajewski, J. Vascular patterning defects associated with expression of activated Notch4 in embryonic endothelium. *Proc Natl Acad Sci U S A* **98**, 5643-5648, doi:10.1073/pnas.091584598 (2001).

59 Potente, M. & Makinen, T. Vascular heterogeneity and specialization in development and disease. *Nat Rev Mol Cell Biol* **18**, 477-494, doi:10.1038/nrm.2017.36 (2017).

60 Red-Horse, K. & Siekmann, A. F. Veins and Arteries Build Hierarchical Branching Patterns Differently: Bottom-Up versus Top-Down. *Bioessays* **41**, e1800198, doi:10.1002/bies.201800198 (2019).

61 Chong, D. C., Koo, Y., Xu, K., Fu, S. & Cleaver, O. Stepwise arteriovenous fate acquisition during mammalian vasculogenesis. *Dev Dyn* **240**, 2153-2165, doi:10.1002/dvdy.22706 (2011).

62 McCracken, I. R., Baker, A. H., Smart, N. & De Val, S. Transcriptional regulators of arterial and venous identity in the developing mammalian embryo. *Curr Opin Physiol* **35**, None, doi:10.1016/j.cophys.2023.100691 (2023).

63 Chen, D., Schwartz, M. A. & Simons, M. Developmental Perspectives on Arterial Fate Specification. *Front Cell Dev Biol* **9**, 691335, doi:10.3389/fcell.2021.691335 (2021).

64 Hwa, J. J. *et al.* Abnormal arterial-venous fusions and fate specification in mouse embryos lacking blood flow. *Sci Rep* **7**, 11965, doi:10.1038/s41598-017-12353-z (2017).

65 Fang, J. S. *et al.* Shear-induced Notch-Cx37-p27 axis arrests endothelial cell cycle to enable arterial specification. *Nat Commun* **8**, 2149, doi:10.1038/s41467-017-01742-7 (2017).

66 Su, T. *et al.* Single-cell analysis of early progenitor cells that build coronary arteries. *Nature* **559**, 356-362, doi:10.1038/s41586-018-0288-7 (2018).

67 Luo, W. *et al.* Arterialization requires the timely suppression of cell growth. *Nature* **589**, 437-441, doi:10.1038/s41586-020-3018-x (2021).

68 Sissaoui, S. *et al.* Genomic Characterization of Endothelial Enhancers Reveals a Multifunctional Role for NR2F2 in Regulation of Arteriovenous Gene Expression. *Circ Res* **126**, 875-888, doi:10.1161/CIRCRESAHA.119.316075 (2020).

69 Lee, H. W. *et al.* Role of Venous Endothelial Cells in Developmental and Pathologic Angiogenesis. *Circulation* **144**, 1308-1322, doi:10.1161/CIRCULATIONAHA.121.054071 (2021).

70 Park, H. *et al.* Defective Flow-Migration Coupling Causes Arteriovenous Malformations in Hereditary Hemorrhagic Telangiectasia. *Circulation* **144**, 805-822, doi:10.1161/CIRCULATIONAHA.120.053047 (2021).

71 Zarkada, G. *et al.* Specialized endothelial tip cells guide neuroretina vascularization and blood-retina-barrier formation. *Dev Cell* **56**, 2237-2251 e2236, doi:10.1016/j.devcel.2021.06.021 (2021).
72 Lawson, N. D., Vogel, A. M. & Weinstein, B. M. sonic hedgehog and vascular endothelial growth factor act upstream of the Notch pathway during arterial endothelial differentiation. *Dev Cell* **3**, 127-136, doi:10.1016/s1534-5807(02)00198-3 (2002).
73 Wythe, J. D. *et al.* ETS factors regulate Vegf-dependent arterial specification. *Dev Cell* **26**, 45-58, doi:10.1016/j.devcel.2013.06.007 (2013).
74 Yamamizu, K. *et al.* Convergence of Notch and beta-catenin signaling induces arterial fate in vascular progenitors. *J Cell Biol* **189**, 325-338, doi:10.1083/jcb.200904114 (2010).
75 Xu, J. & Shi, G. P. Vascular wall extracellular matrix proteins and vascular diseases. *Biochim Biophys Acta* **1842**, 2106-2119, doi:10.1016/j.bbadis.2014.07.008 (2014).
76 Rossant, J. & Howard, L. Signaling pathways in vascular development. *Annu Rev Cell Dev Biol* **18**, 541-573, doi:10.1146/annurev.cellbio.18.012502.105825 (2002).
77 Sato, T. N. *et al.* Distinct roles of the receptor tyrosine kinases Tie-1 and Tie-2 in blood vessel formation. *Nature* **376**, 70-74, doi:10.1038/376070a0 (1995).
78 Suri, C. *et al.* Requisite role of angiopoietin-1, a ligand for the TIE2 receptor, during embryonic angiogenesis. *Cell* **87**, 1171-1180, doi:10.1016/s0092-8674(00)81813-9 (1996).
79 Lindahl, P., Johansson, B. R., Leveen, P. & Betsholtz, C. Pericyte loss and microaneurysm formation in PDGF-B-deficient mice. *Science* **277**, 242-245, doi:10.1126/science.277.5323.242 (1997).
80 Hirschi, K. K. *et al.* Transforming growth factor-beta induction of smooth muscle cell phenotpye requires transcriptional and post-transcriptional control of serum response factor. *J Biol Chem* **277**, 6287-6295, doi:10.1074/jbc.M106649200 (2002).
81 Hirai, M. *et al.* Latent TGF-beta-binding protein 2 binds to DANCE/fibulin-5 and regulates elastic fiber assembly. *EMBO J* **26**, 3283-3295, doi:10.1038/sj.emboj.7601768 (2007).
82 Marigo, V., Volpin, D., Vitale, G. & Bressan, G. M. Identification of a TGF-beta responsive element in the human elastin promoter. *Biochem Biophys Res Commun* **199**, 1049-1056, doi:10.1006/bbrc.1994.1335 (1994).
83 Sauvage, M. *et al.* Localization of elastin mRNA and TGF-beta1 in rat aorta and caudal artery as a function of age. *Cell Tissue Res* **291**, 305-314, doi:10.1007/s004410051000 (1998).
84 Saharinen, P. *et al.* Angiopoietins assemble distinct Tie2 signalling complexes in endothelial cell-cell and cell-matrix contacts. *Nat Cell Biol* **10**, 527-537, doi:10.1038/ncb1715 (2008).
85 Lupu, I. E., De Val, S. & Smart, N. Coronary vessel formation in development and disease: mechanisms and insights for therapy. *Nat Rev Cardiol* **17**, 790-806, doi:10.1038/s41569-020-0400-1 (2020).
86 McCracken, I. R. & Smart, N. Control of coronary vascular cell fate in development and regeneration. *Semin Cell Dev Biol* **155**, 50-61, doi:10.1016/j.semcdb.2023.08.005 (2024).

87 Kapuria, S., Yoshida, T. & Lien, C. L. Coronary Vasculature in Cardiac Development and Regeneration. *J Cardiovasc Dev Dis* **5**, doi:10.3390/jcdd5040059 (2018).
88 Tian, X. & Zhou, B. Coronary vessel formation in development and regeneration: origins and mechanisms. *J Mol Cell Cardiol* **167**, 67-82, doi:10.1016/j.yjmcc.2022.03.009 (2022).
89 Reese, D. E., Mikawa, T. & Bader, D. M. Development of the coronary vessel system. *Circ Res* **91**, 761-768, doi:10.1161/01.res.0000038961.53759.3c (2002).
90 Boden, W. E. *et al.* Myocardial ischaemic syndromes: a new nomenclature to harmonize evolving international clinical practice guidelines. *Eur Heart J* **45**, 3701-3706, doi:10.1093/eurheartj/ehae278 (2024).
91 Bogers, A. J., Gittenberger-de Groot, A. C., Poelmann, R. E., Peault, B. M. & Huysmans, H. A. Development of the origin of the coronary arteries, a matter of ingrowth or outgrowth? *Anat Embryol (Berl)* **180**, 437-441, doi:10.1007/BF00305118 (1989).
92 Tian, X. *et al.* Vessel formation. De novo formation of a distinct coronary vascular population in neonatal heart. *Science* **345**, 90-94, doi:10.1126/science.1251487 (2014).
93 Red-Horse, K., Ueno, H., Weissman, I. L. & Krasnow, M. A. Coronary arteries form by developmental reprogramming of venous cells. *Nature* **464**, 549-553, doi:10.1038/nature08873 (2010).
94 Wu, B. *et al.* Endocardial cells form the coronary arteries by angiogenesis through myocardial-endocardial VEGF signaling. *Cell* **151**, 1083-1096, doi:10.1016/j.cell.2012.10.023 (2012).
95 Chen, H. I. *et al.* The sinus venosus contributes to coronary vasculature through VEGFC-stimulated angiogenesis. *Development* **141**, 4500-4512, doi:10.1242/dev.113639 (2014).
96 Zhang, H. *et al.* Endocardium Minimally Contributes to Coronary Endothelium in the Embryonic Ventricular Free Walls. *Circ Res* **118**, 1880-1893, doi:10.1161/CIRCRESAHA.116.308749 (2016).
97 Sharma, B. *et al.* Alternative Progenitor Cells Compensate to Rebuild the Coronary Vasculature in Elabela- and Apj-Deficient Hearts. *Dev Cell* **42**, 655-666 e653, doi:10.1016/j.devcel.2017.08.008 (2017).
98 Tian, X. *et al.* Subepicardial endothelial cells invade the embryonic ventricle wall to form coronary arteries. *Cell Res* **23**, 1075-1090, doi:10.1038/cr.2013.83 (2013).
99 Sedmera, D., Pexieder, T., Vuillemin, M., Thompson, R. P. & Anderson, R. H. Developmental patterning of the myocardium. *Anat Rec* **258**, 319-337, doi:10.1002/(SICI)1097-0185(20000401)258:4<319::AID-AR1>3.0.CO;2-O (2000).
100 Tang, J. *et al.* Extension of Endocardium-Derived Vessels Generate Coronary Arteries in Neonates. *Circ Res* **130**, 352-365, doi:10.1161/CIRCRESAHA.121.320335 (2022).
101 Amaral, P. *et al.* The status of the human gene catalogue. *Nature* **622**, 41-47, doi:10.1038/s41586-023-06490-x (2023).
102 Jackson, M., Marks, L., May, G. H. W. & Wilson, J. B. The genetic basis of disease. *Essays Biochem* **62**, 643-723, doi:10.1042/EBC20170053 (2018).
103 Alberts, B. *et al. Molecular Biology of the Cell*. (Garland Science, 2014).
104 Jacob, F. & Monod, J. Genetic regulatory mechanisms in the synthesis of proteins. *J Mol Biol* **3**, 318-356, doi:10.1016/s0022-2836(61)80072-7 (1961).

105 Lwoff, A. Lysogeny. *Bacteriological Reviews* **17**, 269-337 (1953).
106 Lwoff, A. in *Nobel Lectures, Physiology or Medicine 1963-1970* (ed Elsevier Nobel Foundation) 1-22 (1965).
107 Borsari, B. *et al.* Enhancers with tissue-specific activity are enriched in intronic regions. *Genome Res* **31**, 1325-1336, doi:10.1101/gr.270371.120 (2021).
108 Crick, F. H. On protein synthesis. *Symp Soc Exp Biol* **12**, 138-163 (1958).
109 Makalowski, W. The human genome structure and organization. *Acta Biochim Pol* **48**, 587-598 (2001).
110 van Steensel, B. Chromatin: constructing the big picture. *EMBO J* **30**, 1885-1895, doi:10.1038/emboj.2011.135 (2011).
111 Morrison, O. & Thakur, J. Molecular Complexes at Euchromatin, Heterochromatin and Centromeric Chromatin. *Int J Mol Sci* **22**, doi:10.3390/ijms22136922 (2021).
112 Misteli, T. The Self-Organizing Genome: Principles of Genome Architecture and Function. *Cell* **183**, 28-45, doi:10.1016/j.cell.2020.09.014 (2020).
113 McGinty, R. K. & Tan, S. Nucleosome structure and function. *Chem Rev* **115**, 2255-2273, doi:10.1021/cr500373h (2015).
114 Simpson, B., Tupper, C. & Al Aboud, N. M. in *StatPearls* (2025).
115 Sato, S., Dacher, M. & Kurumizaka, H. Nucleosome Structures Built from Highly Divergent Histones: Parasites and Giant DNA Viruses. *Epigenomes* **6**, doi:10.3390/epigenomes6030022 (2022).
116 Luger, K., Mader, A. W., Richmond, R. K., Sargent, D. F. & Richmond, T. J. Crystal structure of the nucleosome core particle at 2.8 A resolution. *Nature* **389**, 251-260, doi:10.1038/38444 (1997).
117 Arents, G., Burlingame, R. W., Wang, B. C., Love, W. E. & Moudrianakis, E. N. The nucleosomal core histone octamer at 3.1 A resolution: a tripartite protein assembly and a left-handed superhelix. *Proc Natl Acad Sci U S A* **88**, 10148-10152, doi:10.1073/pnas.88.22.10148 (1991).
118 Kornberg, R. D. Chromatin structure: a repeating unit of histones and DNA. *Science* **184**, 868-871, doi:10.1126/science.184.4139.868 (1974).
119 Bednar, J. *et al.* Nucleosomes, linker DNA, and linker histone form a unique structural motif that directs the higher-order folding and compaction of chromatin. *Proc Natl Acad Sci U S A* **95**, 14173-14178, doi:10.1073/pnas.95.24.14173 (1998).
120 Bell, O., Burton, A., Dean, C., Gasser, S. M. & Torres-Padilla, M. E. Heterochromatin definition and function. *Nat Rev Mol Cell Biol* **24**, 691-694, doi:10.1038/s41580-023-00599-7 (2023).
121 Penagos-Puig, A. & Furlan-Magaril, M. Heterochromatin as an Important Driver of Genome Organization. *Front Cell Dev Biol* **8**, 579137, doi:10.3389/fcell.2020.579137 (2020).
122 Tessarz, P. & Kouzarides, T. Histone core modifications regulating nucleosome structure and dynamics. *Nat Rev Mol Cell Biol* **15**, 703-708, doi:10.1038/nrm3890 (2014).
123 Bannister, A. J. & Kouzarides, T. Regulation of chromatin by histone modifications. *Cell Res* **21**, 381-395, doi:10.1038/cr.2011.22 (2011).
124 Pinel, C., Prainsack, B. & McKevitt, C. Markers as mediators: A review and synthesis of epigenetics literature. *Biosocieties* **13**, 276-303, doi:10.1057/s41292-017-0068-x (2019).
125 Deichmann, U. Epigenetics: The origins and evolution of a fashionable topic. *Dev Biol* **416**, 249-254, doi:10.1016/j.ydbio.2016.06.005 (2016).

126 Peserico, A. & Simone, C. Physical and functional HAT/HDAC interplay regulates protein acetylation balance. *J Biomed Biotechnol* **2011**, 371832, doi:10.1155/2011/371832 (2011).
127 Beacon, T. H. *et al.* The dynamic broad epigenetic (H3K4me3, H3K27ac) domain as a mark of essential genes. *Clin Epigenetics* **13**, 138, doi:10.1186/s13148-021-01126-1 (2021).
128 Wang, H. & Helin, K. Roles of H3K4 methylation in biology and disease. *Trends Cell Biol* **35**, 115-128, doi:10.1016/j.tcb.2024.06.001 (2025).
129 Creyghton, M. P. *et al.* Histone H3K27ac separates active from poised enhancers and predicts developmental state. *Proc Natl Acad Sci U S A* **107**, 21931-21936, doi:10.1073/pnas.1016071107 (2010).
130 Lam, U. T. F., Tan, B. K. Y., Poh, J. J. X. & Chen, E. S. Structural and functional specificity of H3K36 methylation. *Epigenetics Chromatin* **15**, 17, doi:10.1186/s13072-022-00446-7 (2022).
131 Moore, L. D., Le, T. & Fan, G. DNA methylation and its basic function. *Neuropsychopharmacology* **38**, 23-38, doi:10.1038/npp.2012.112 (2013).
132 Jin, B., Li, Y. & Robertson, K. D. DNA methylation: superior or subordinate in the epigenetic hierarchy? *Genes Cancer* **2**, 607-617, doi:10.1177/1947601910393957 (2011).
133 Ma, S. & Zhang, Y. Profiling chromatin regulatory landscape: insights into the development of ChIP-seq and ATAC-seq. *Mol Biomed* **1**, 9, doi:10.1186/s43556-020-00009-w (2020).
134 Kaya-Okur, H. S. *et al.* CUT&Tag for efficient epigenomic profiling of small samples and single cells. *Nat Commun* **10**, 1930, doi:10.1038/s41467-019-09982-5 (2019).
135 De Val, S. Key transcriptional regulators of early vascular development. *Arterioscler Thromb Vasc Biol* **31**, 1469-1475, doi:10.1161/ATVBAHA.110.221168 (2011).
136 De Val, S. & Black, B. L. Transcriptional control of endothelial cell development. *Dev Cell* **16**, 180-195, doi:10.1016/j.devcel.2009.01.014 (2009).
137 Shlyueva, D., Stampfel, G. & Stark, A. Transcriptional enhancers: from properties to genome-wide predictions. *Nat Rev Genet* **15**, 272-286, doi:10.1038/nrg3682 (2014).
138 Haberle, V. & Stark, A. Eukaryotic core promoters and the functional basis of transcription initiation. *Nat Rev Mol Cell Biol* **19**, 621-637, doi:10.1038/s41580-018-0028-8 (2018).
139 Roy, A. L. & Singer, D. S. Core promoters in transcription: old problem, new insights. *Trends Biochem Sci* **40**, 165-171, doi:10.1016/j.tibs.2015.01.007 (2015).
140 Sloutskin, A., Shir-Shapira, H., Freiman, R. N. & Juven-Gershon, T. The Core Promoter Is a Regulatory Hub for Developmental Gene Expression. *Front Cell Dev Biol* **9**, 666508, doi:10.3389/fcell.2021.666508 (2021).
141 Rach, E. A. *et al.* Transcription initiation patterns indicate divergent strategies for gene regulation at the chromatin level. *PLoS Genet* **7**, e1001274, doi:10.1371/journal.pgen.1001274 (2011).
142 Hoskins, R. A. *et al.* Genome-wide analysis of promoter architecture in Drosophila melanogaster. *Genome Res* **21**, 182-192, doi:10.1101/gr.112466.110 (2011).

143 Andersson, R. & Sandelin, A. Determinants of enhancer and promoter activities of regulatory elements. *Nat Rev Genet* **21**, 71-87, doi:10.1038/s41576-019-0173-8 (2020).
144 Carninci, P. *et al.* Genome-wide analysis of mammalian promoter architecture and evolution. *Nat Genet* **38**, 626-635, doi:10.1038/ng1789 (2006).
145 Verrijzer, C. P., Chen, J. L., Yokomori, K. & Tjian, R. Binding of TAFs to core elements directs promoter selectivity by RNA polymerase II. *Cell* **81**, 1115-1125, doi:10.1016/s0092-8674(05)80016-9 (1995).
146 FitzGerald, P. C., Sturgill, D., Shyakhtenko, A., Oliver, B. & Vinson, C. Comparative genomics of Drosophila and human core promoters. *Genome Biol* **7**, R53, doi:10.1186/gb-2006-7-7-r53 (2006).
147 Vo Ngoc, L., Cassidy, C. J., Huang, C. Y., Duttke, S. H. & Kadonaga, J. T. The human initiator is a distinct and abundant element that is precisely positioned in focused core promoters. *Genes Dev* **31**, 6-11, doi:10.1101/gad.293837.116 (2017).
148 Gardiner-Garden, M. & Frommer, M. CpG islands in vertebrate genomes. *J Mol Biol* **196**, 261-282, doi:10.1016/0022-2836(87)90689-9 (1987).
149 Panigrahi, A. & O'Malley, B. W. Mechanisms of enhancer action: the known and the unknown. *Genome Biol* **22**, 108, doi:10.1186/s13059-021-02322-1 (2021).
150 Sakabe, N. J., Savic, D. & Nobrega, M. A. Transcriptional enhancers in development and disease. *Genome Biol* **13**, 238, doi:10.1186/gb-2012-13-1-238 (2012).
151 Zabidi, M. A. & Stark, A. Regulatory Enhancer-Core-Promoter Communication via Transcription Factors and Cofactors. *Trends Genet* **32**, 801-814, doi:10.1016/j.tig.2016.10.003 (2016).
152 Kawasaki, K. & Fukaya, T. Regulatory landscape of enhancer-mediated transcriptional activation. *Trends Cell Biol*, doi:10.1016/j.tcb.2024.01.008 (2024).
153 Yang, J. H. & Hansen, A. S. Enhancer selectivity in space and time: from enhancer-promoter interactions to promoter activation. *Nat Rev Mol Cell Biol* **25**, 574-591, doi:10.1038/s41580-024-00710-6 (2024).
154 Bower, G. & Kvon, E. Z. Genetic factors mediating long-range enhancer-promoter communication in mammalian development. *Curr Opin Genet Dev* **90**, 102282, doi:10.1016/j.gde.2024.102282 (2025).
155 Pott, S. & Lieb, J. D. What are super-enhancers? *Nat Genet* **47**, 8-12, doi:10.1038/ng.3167 (2015).
156 Kim, Y. J., Xie, P., Cao, L., Zhang, M. Q. & Kim, T. H. Global transcriptional activity dynamics reveal functional enhancer RNAs. *Genome Res* **28**, 1799-1811, doi:10.1101/gr.233486.117 (2018).
157 Zhang, J. *et al.* Active enhancers: recent research advances and insights into disease. *Biol Direct* **19**, 112, doi:10.1186/s13062-024-00559-x (2024).
158 Gasperini, M., Tome, J. M. & Shendure, J. Towards a comprehensive catalogue of validated and target-linked human enhancers. *Nat Rev Genet* **21**, 292-310, doi:10.1038/s41576-019-0209-0 (2020).
159 Karr, J. P., Ferrie, J. J., Tjian, R. & Darzacq, X. The transcription factor activity gradient (TAG) model: contemplating a contact-independent mechanism for enhancer-promoter communication. *Genes Dev* **36**, 7-16, doi:10.1101/gad.349160.121 (2022).

160 Kent, S. *et al.* Phase-Separated Transcriptional Condensates Accelerate Target-Search Process Revealed by Live-Cell Single-Molecule Imaging. *Cell Rep* **33**, 108248, doi:10.1016/j.celrep.2020.108248 (2020).
161 Balasubramanian, D. *et al.* Enhancer-promoter interactions can form independently of genomic distance and be functional across TAD boundaries. *Nucleic Acids Res* **52**, 1702-1719, doi:10.1093/nar/gkad1183 (2024).
162 Xu, J. *et al.* A comprehensive benchmarking with interpretation and operational guidance for the hierarchy of topologically associating domains. *Nat Commun* **15**, 4376, doi:10.1038/s41467-024-48593-7 (2024).
163 Rajderkar, S. *et al.* Topologically associating domain boundaries are required for normal genome function. *Commun Biol* **6**, 435, doi:10.1038/s42003-023-04819-w (2023).
164 Boija, A. *et al.* Transcription Factors Activate Genes through the Phase-Separation Capacity of Their Activation Domains. *Cell* **175**, 1842-1855 e1816, doi:10.1016/j.cell.2018.10.042 (2018).
165 Lovering, R. C. *et al.* A GO catalogue of human DNA-binding transcription factors. *Biochim Biophys Acta Gene Regul Mech* **1864**, 194765, doi:10.1016/j.bbagrm.2021.194765 (2021).
166 Spitz, F. & Furlong, E. E. Transcription factors: from enhancer binding to developmental control. *Nat Rev Genet* **13**, 613-626, doi:10.1038/nrg3207 (2012).
167 Merika, M. & Thanos, D. Enhanceosomes. *Curr Opin Genet Dev* **11**, 205-208, doi:10.1016/s0959-437x(00)00180-5 (2001).
168 Vockley, C. M., McDowell, I. C., D'Ippolito, A. M. & Reddy, T. E. A long-range flexible billboard model of gene activation. *Transcription* **8**, 261-267, doi:10.1080/21541264.2017.1317694 (2017).
169 Junion, G. *et al.* A transcription factor collective defines cardiac cell fate and reflects lineage history. *Cell* **148**, 473-486, doi:10.1016/j.cell.2012.01.030 (2012).
170 Majesky, M. W. Vascular Development. *Arterioscler Thromb Vasc Biol* **38**, e17-e24, doi:10.1161/ATVBAHA.118.310223 (2018).
171 Oh, S. Y., Kim, J. Y. & Park, C. The ETS Factor, ETV2: a Master Regulator for Vascular Endothelial Cell Development. *Mol Cells* **38**, 1029-1036, doi:10.14348/molcells.2015.0331 (2015).
172 Randi, A. M., Sperone, A., Dryden, N. H. & Birdsey, G. M. Regulation of angiogenesis by ETS transcription factors. *Biochem Soc Trans* **37**, 1248-1253, doi:10.1042/BST0371248 (2009).
173 Birdsey, G. M. *et al.* Transcription factor Erg regulates angiogenesis and endothelial apoptosis through VE-cadherin. *Blood* **111**, 3498-3506, doi:10.1182/blood-2007-08-105346 (2008).
174 Pham, V. N. *et al.* Combinatorial function of ETS transcription factors in the developing vasculature. *Dev Biol* **303**, 772-783, doi:10.1016/j.ydbio.2006.10.030 (2007).
175 Hollenhorst, P. C., Jones, D. A. & Graves, B. J. Expression profiles frame the promoter specificity dilemma of the ETS family of transcription factors. *Nucleic Acids Res* **32**, 5693-5702, doi:10.1093/nar/gkh906 (2004).
176 Craig, M. P. & Sumanas, S. ETS transcription factors in embryonic vascular development. *Angiogenesis* **19**, 275-285, doi:10.1007/s10456-016-9511-z (2016).

177 Dejana, E., Taddei, A. & Randi, A. M. Foxs and Ets in the transcriptional regulation of endothelial cell differentiation and angiogenesis. *Biochim Biophys Acta* **1775**, 298-312, doi:10.1016/j.bbcan.2007.05.003 (2007).
178 Craig, M. P. *et al.* Etv2 and fli1b function together as key regulators of vasculogenesis and angiogenesis. *Arterioscler Thromb Vasc Biol* **35**, 865-876, doi:10.1161/ATVBAHA.114.304768 (2015).
179 Meadows, S. M., Myers, C. T. & Krieg, P. A. Regulation of endothelial cell development by ETS transcription factors. *Semin Cell Dev Biol* **22**, 976-984, doi:10.1016/j.semcdb.2011.09.009 (2011).
180 Gong, W. *et al.* ETV2 functions as a pioneer factor to regulate and reprogram the endothelial lineage. *Nat Cell Biol* **24**, 672-684, doi:10.1038/s41556-022-00901-3 (2022).
181 Ferdous, A. *et al.* Nkx2-5 transactivates the Ets-related protein 71 gene and specifies an endothelial/endocardial fate in the developing embryo. *Proc Natl Acad Sci U S A* **106**, 814-819, doi:10.1073/pnas.0807583106 (2009).
182 Becker, P. W. *et al.* An Intronic Flk1 Enhancer Directs Arterial-Specific Expression via RBPJ-Mediated Venous Repression. *Arterioscler Thromb Vasc Biol* **36**, 1209-1219, doi:10.1161/ATVBAHA.116.307517 (2016).
183 Neal, A. *et al.* ETS factors are required but not sufficient for specific patterns of enhancer activity in different endothelial subtypes. *Dev Biol* **473**, 1-14, doi:10.1016/j.ydbio.2021.01.002 (2021).
184 Golson, M. L. & Kaestner, K. H. Fox transcription factors: from development to disease. *Development* **143**, 4558-4570, doi:10.1242/dev.112672 (2016).
185 Wilhelm, K. *et al.* FOXO1 couples metabolic activity and growth state in the vascular endothelium. *Nature* **529**, 216-220, doi:10.1038/nature16498 (2016).
186 Furuyama, T. *et al.* Abnormal angiogenesis in Foxo1 (Fkhr)-deficient mice. *J Biol Chem* **279**, 34741-34749, doi:10.1074/jbc.M314214200 (2004).
187 Hosaka, T. *et al.* Disruption of forkhead transcription factor (FOXO) family members in mice reveals their functional diversification. *Proc Natl Acad Sci U S A* **101**, 2975-2980, doi:10.1073/pnas.0400093101 (2004).
188 Pijuan-Sala, B. *et al.* A single-cell molecular map of mouse gastrulation and early organogenesis. *Nature* **566**, 490-495, doi:10.1038/s41586-019-0933-9 (2019).
189 Kume, T. *et al.* The forkhead/winged helix gene Mf1 is disrupted in the pleiotropic mouse mutation congenital hydrocephalus. *Cell* **93**, 985-996, doi:10.1016/s0092-8674(00)81204-0 (1998).
190 Kume, T., Jiang, H., Topczewska, J. M. & Hogan, B. L. The murine winged helix transcription factors, Foxc1 and Foxc2, are both required for cardiovascular development and somitogenesis. *Genes Dev* **15**, 2470-2482, doi:10.1101/gad.907301 (2001).
191 Seo, S. *et al.* The forkhead transcription factors, Foxc1 and Foxc2, are required for arterial specification and lymphatic sprouting during vascular development. *Dev Biol* **294**, 458-470, doi:10.1016/j.ydbio.2006.03.035 (2006).
192 Corada, M. *et al.* Sox17 is indispensable for acquisition and maintenance of arterial identity. *Nat Commun* **4**, 2609, doi:10.1038/ncomms3609 (2013).
193 Francois, M. *et al.* Sox18 induces development of the lymphatic vasculature in mice. *Nature* **456**, 643-647, doi:10.1038/nature07391 (2008).
194 Lilly, A. J., Mazan, A., Scott, D. A., Lacaud, G. & Kouskoff, V. SOX7 expression is critically required in FLK1-expressing cells for vasculogenesis and

angiogenesis during mouse embryonic development. *Mech Dev* **146**, 31-41, doi:10.1016/j.mod.2017.05.004 (2017).

195 Lee, S. H. *et al.* Notch pathway targets proangiogenic regulator Sox17 to restrict angiogenesis. *Circ Res* **115**, 215-226, doi:10.1161/CIRCRESAHA.115.303142 (2014).

196 Chiang, I. K. *et al.* SoxF factors induce Notch1 expression via direct transcriptional regulation during early arterial development. *Development* **144**, 2629-2639, doi:10.1242/dev.146241 (2017).

197 Sacilotto, N. *et al.* Analysis of Dll4 regulation reveals a combinatorial role for Sox and Notch in arterial development. *Proc Natl Acad Sci U S A* **110**, 11893-11898, doi:10.1073/pnas.1300805110 (2013).

198 Reis, M. & Liebner, S. Wnt signaling in the vasculature. *Exp Cell Res* **319**, 1317-1323, doi:10.1016/j.yexcr.2012.12.023 (2013).

199 Dejana, E. The role of wnt signaling in physiological and pathological angiogenesis. *Circ Res* **107**, 943-952, doi:10.1161/CIRCRESAHA.110.223750 (2010).

200 Cadigan, K. M. & Waterman, M. L. TCF/LEFs and Wnt signaling in the nucleus. *Cold Spring Harb Perspect Biol* **4**, doi:10.1101/cshperspect.a007906 (2012).

201 Liu, J. *et al.* Wnt/beta-catenin signalling: function, biological mechanisms, and therapeutic opportunities. *Signal Transduct Target Ther* **7**, 3, doi:10.1038/s41392-021-00762-6 (2022).

202 Mege, R. M. & Ishiyama, N. Integration of Cadherin Adhesion and Cytoskeleton at Adherens Junctions. *Cold Spring Harb Perspect Biol* **9**, doi:10.1101/cshperspect.a028738 (2017).

203 Schunk, S. J., Floege, J., Fliser, D. & Speer, T. WNT-beta-catenin signalling - a versatile player in kidney injury and repair. *Nat Rev Nephrol* **17**, 172-184, doi:10.1038/s41581-020-00343-w (2021).

204 Franco, C. A., Liebner, S. & Gerhardt, H. Vascular morphogenesis: a Wnt for every vessel? *Curr Opin Genet Dev* **19**, 476-483, doi:10.1016/j.gde.2009.09.004 (2009).

205 Ishikawa, T. *et al.* Mouse Wnt receptor gene Fzd5 is essential for yolk sac and placental angiogenesis. *Development* **128**, 25-33, doi:10.1242/dev.128.1.25 (2001).

206 Monkley, S. J., Delaney, S. J., Pennisi, D. J., Christiansen, J. H. & Wainwright, B. J. Targeted disruption of the Wnt2 gene results in placentation defects. *Development* **122**, 3343-3353, doi:10.1242/dev.122.11.3343 (1996).

207 Ye, X. *et al.* Norrin, frizzled-4, and Lrp5 signaling in endothelial cells controls a genetic program for retinal vascularization. *Cell* **139**, 285-298, doi:10.1016/j.cell.2009.07.047 (2009).

208 Kazanskaya, O. *et al.* The Wnt signaling regulator R-spondin 3 promotes angioblast and vascular development. *Development* **135**, 3655-3664, doi:10.1242/dev.027284 (2008).

209 Cattelino, A. *et al.* The conditional inactivation of the beta-catenin gene in endothelial cells causes a defective vascular pattern and increased vascular fragility. *J Cell Biol* **162**, 1111-1122, doi:10.1083/jcb.200212157 (2003).

210 Corada, M. *et al.* The Wnt/beta-catenin pathway modulates vascular remodeling and specification by upregulating Dll4/Notch signaling. *Dev Cell* **18**, 938-949, doi:10.1016/j.devcel.2010.05.006 (2010).

211 Daneman, R. *et al.* Wnt/beta-catenin signaling is required for CNS, but not non-CNS, angiogenesis. *Proc Natl Acad Sci U S A* **106**, 641-646, doi:10.1073/pnas.0805165106 (2009).
212 Stenman, J. M. *et al.* Canonical Wnt signaling regulates organ-specific assembly and differentiation of CNS vasculature. *Science* **322**, 1247-1250, doi:10.1126/science.1164594 (2008).
213 Molenaar, M. *et al.* XTcf-3 transcription factor mediates beta-catenin-induced axis formation in Xenopus embryos. *Cell* **86**, 391-399, doi:10.1016/s0092-8674(00)80112-9 (1996).
214 Peifer, M., McCrea, P. D., Green, K. J., Wieschaus, E. & Gumbiner, B. M. The vertebrate adhesive junction proteins beta-catenin and plakoglobin and the Drosophila segment polarity gene armadillo form a multigene family with similar properties. *J Cell Biol* **118**, 681-691, doi:10.1083/jcb.118.3.681 (1992).
215 McCauley, B. S., Akyar, E., Saad, H. R. & Hinman, V. F. Dose-dependent nuclear beta-catenin response segregates endomesoderm along the sea star primary axis. *Development* **142**, 207-217, doi:10.1242/dev.113043 (2015).
216 Kelly, C., Chin, A. J., Leatherman, J. L., Kozlowski, D. J. & Weinberg, E. S. Maternally controlled (beta)-catenin-mediated signaling is required for organizer formation in the zebrafish. *Development* **127**, 3899-3911, doi:10.1242/dev.127.18.3899 (2000).
217 Dickinson, D. J., Nelson, W. J. & Weis, W. I. A polarized epithelium organized by beta- and alpha-catenin predates cadherin and metazoan origins. *Science* **331**, 1336-1339, doi:10.1126/science.1199633 (2011).
218 Haegel, H. *et al.* Lack of beta-catenin affects mouse development at gastrulation. *Development* **121**, 3529-3537, doi:10.1242/dev.121.11.3529 (1995).
219 Payne, S., De Val, S. & Neal, A. Endothelial-Specific Cre Mouse Models. *Arterioscler Thromb Vasc Biol* **38**, 2550-2561, doi:10.1161/ATVBAHA.118.309669 (2018).
220 Lainscek, D., Forstneric, V. & Mirosevic, S. CTNNB1 syndrome mouse models. *Mamm Genome* **36**, 390-402, doi:10.1007/s00335-025-10105-3 (2025).
221 Brault, V. *et al.* Inactivation of the beta-catenin gene by Wnt1-Cre-mediated deletion results in dramatic brain malformation and failure of craniofacial development. *Development* **128**, 1253-1264, doi:10.1242/dev.128.8.1253 (2001).
222 Olsen, J. J. *et al.* The Role of Wnt Signalling in Angiogenesis. *Clin Biochem Rev* **38**, 131-142 (2017).
223 Goodwin, A. M., Sullivan, K. M. & D'Amore, P. A. Cultured endothelial cells display endogenous activation of the canonical Wnt signaling pathway and express multiple ligands, receptors, and secreted modulators of Wnt signaling. *Dev Dyn* **235**, 3110-3120, doi:10.1002/dvdy.20939 (2006).
224 Harada, N. *et al.* Intestinal polyposis in mice with a dominant stable mutation of the beta-catenin gene. *EMBO J* **18**, 5931-5942, doi:10.1093/emboj/18.21.5931 (1999).
225 Materna, S. C., Sinha, T., Barnes, R. M., Lammerts van Bueren, K. & Black, B. L. Cardiovascular development and survival require Mef2c function in the myocardial but not the endothelial lineage. *Dev Biol* **445**, 170-177, doi:10.1016/j.ydbio.2018.12.002 (2019).
226 Neal, A., Rodriguez-Caro, H. & De Val, S. Finding and Verifying Enhancers for Endothelial-Expressed Genes. *Methods Mol Biol* **2441**, 351-368, doi:10.1007/978-1-0716-2059-5_28 (2022).

227 Sacilotto, N. *et al.* MEF2 transcription factors are key regulators of sprouting angiogenesis. *Genes Dev* **30**, 2297-2309, doi:10.1101/gad.290619.116 (2016).
228 Martinez-Ara, M., Comoglio, F. & van Steensel, B. Large-scale analysis of the integration of enhancer-enhancer signals by promoters. *Elife* **12**, doi:10.7554/eLife.91994 (2024).
229 Nornes, S., Bruche, S., Adak, N., McCracken, I. R. & De Val, S. Evaluating the transcriptional regulators of arterial gene expression via a catalogue of characterized arterial enhancers. *Elife* **14**, doi:10.7554/eLife.102440 (2025).
230 Neal, A. *et al.* Venous identity requires BMP signalling through ALK3. *Nat Commun* **10**, 453, doi:10.1038/s41467-019-08315-w (2019).
231 Wat, J. J. & Wat, M. J. Sox7 in vascular development: review, insights and potential mechanisms. *Int J Dev Biol* **58**, 1-8, doi:10.1387/ijdb.130323mw (2014).
232 Hermkens, D. M. *et al.* Sox7 controls arterial specification in conjunction with hey2 and efnb2 function. *Development* **142**, 1695-1704, doi:10.1242/dev.117275 (2015).
233 Andersson, R. *et al.* An atlas of active enhancers across human cell types and tissues. *Nature* **507**, 455-461, doi:10.1038/nature12787 (2014).
234 Zhou, P. *et al.* Mapping cell type-specific transcriptional enhancers using high affinity, lineage-specific Ep300 bioChIP-seq. *Elife* **6**, doi:10.7554/eLife.22039 (2017).
235 Consortium, E. P. An integrated encyclopedia of DNA elements in the human genome. *Nature* **489**, 57-74, doi:10.1038/nature11247 (2012).
236 Begeman, I. J., Emery, B., Kurth, A. & Kang, J. Regeneration and developmental enhancers are differentially compatible with minimal promoters. *Dev Biol* **492**, 47-58, doi:10.1016/j.ydbio.2022.09.007 (2022).
237 Kawakami, K. Transposon tools and methods in zebrafish. *Dev Dyn* **234**, 244-254, doi:10.1002/dvdy.20516 (2005).
238 Bhatia, S. *et al.* Quantitative spatial and temporal assessment of regulatory element activity in zebrafish. *Elife* **10**, doi:10.7554/eLife.65601 (2021).
239 Choi, T. Y., Choi, T. I., Lee, Y. R., Choe, S. K. & Kim, C. H. Zebrafish as an animal model for biomedical research. *Exp Mol Med* **53**, 310-317, doi:10.1038/s12276-021-00571-5 (2021).
240 Heller, I. S., Guenther, C. A., Meireles, A. M., Talbot, W. S. & Kingsley, D. M. Characterization of mouse Bmp5 regulatory injury element in zebrafish wound models. *Bone* **155**, 116263, doi:10.1016/j.bone.2021.116263 (2022).
241 Perez-Rico, Y. A. *et al.* Comparative analyses of super-enhancers reveal conserved elements in vertebrate genomes. *Genome Res* **27**, 259-268, doi:10.1101/gr.203679.115 (2017).
242 Yuan, X. *et al.* Heart enhancers with deeply conserved regulatory activity are established early in zebrafish development. *Nat Commun* **9**, 4977, doi:10.1038/s41467-018-07451-z (2018).
243 Kawakami, K. Tol2: a versatile gene transfer vector in vertebrates. *Genome Biol* **8 Suppl 1**, S7, doi:10.1186/gb-2007-8-s1-s7 (2007).
244 Kawakami, K., Asakawa, K., Muto, A. & Wada, H. Tol2-mediated transgenesis, gene trapping, enhancer trapping, and Gal4-UAS system. *Methods Cell Biol* **135**, 19-37, doi:10.1016/bs.mcb.2016.01.011 (2016).
245 Urasaki, A., Morvan, G. & Kawakami, K. Functional dissection of the Tol2 transposable element identified the minimal cis-sequence and a highly repetitive

sequence in the subterminal region essential for transposition. *Genetics* **174**, 639-649, doi:10.1534/genetics.106.060244 (2006).

246 Vrljicak, P. *et al.* Genome-Wide Analysis of Transposon and Retroviral Insertions Reveals Preferential Integrations in Regions of DNA Flexibility. *G3 (Bethesda)* **6**, 805-817, doi:10.1534/g3.115.026849 (2016).

247 Chouliaras, K. M. *Transcriptional regulation at the angiogenic sprout*, University of Oxford, (2019).

248 Kothary, R. *et al.* Inducible expression of an hsp68-lacZ hybrid gene in transgenic mice. *Development* **105**, 707-714, doi:10.1242/dev.105.4.707 (1989).

249 Kang, J. *et al.* Modulation of tissue repair by regeneration enhancer elements. *Nature* **532**, 201-206, doi:10.1038/nature17644 (2016).

250 Wingender, E. *et al.* TRANSFAC: an integrated system for gene expression regulation. *Nucleic Acids Res* **28**, 316-319, doi:10.1093/nar/28.1.316 (2000).

251 Kel, A. E. *et al.* MATCH: A tool for searching transcription factor binding sites in DNA sequences. *Nucleic Acids Res* **31**, 3576-3579, doi:10.1093/nar/gkg585 (2003).

252 Grant, C. E., Bailey, T. L. & Noble, W. S. FIMO: scanning for occurrences of a given motif. *Bioinformatics* **27**, 1017-1018, doi:10.1093/bioinformatics/btr064 (2011).

253 Ernst, P. B. & Carvunis, A. R. Of mice, men and immunity: a case for evolutionary systems biology. *Nat Immunol* **19**, 421-425, doi:10.1038/s41590-018-0084-4 (2018).

254 Thompson, J. D., Higgins, D. G. & Gibson, T. J. CLUSTAL W: improving the sensitivity of progressive multiple sequence alignment through sequence weighting, position-specific gap penalties and weight matrix choice. *Nucleic Acids Res* **22**, 4673-4680, doi:10.1093/nar/22.22.4673 (1994).

255 Wheeler, T. J. & Kececioglu, J. D. Multiple alignment by aligning alignments. *Bioinformatics* **23**, i559-568, doi:10.1093/bioinformatics/btm226 (2007).

256 Stewart, A. J., Hannenhalli, S. & Plotkin, J. B. Why transcription factor binding sites are ten nucleotides long. *Genetics* **192**, 973-985, doi:10.1534/genetics.112.143370 (2012).

257 Jeong, H. W. *et al.* Transcriptional regulation of endothelial cell behavior during sprouting angiogenesis. *Nat Commun* **8**, 726, doi:10.1038/s41467-017-00738-7 (2017).

258 Yoshitomi, Y. *et al.* JunB regulates angiogenesis and neurovascular parallel alignment in mouse embryonic skin. *J Cell Sci* **130**, 916-926, doi:10.1242/jcs.196303 (2017).

259 Yoshitomi, Y., Ikeda, T., Saito-Takatsuji, H. & Yonekura, H. Emerging Role of AP-1 Transcription Factor JunB in Angiogenesis and Vascular Development. *Int J Mol Sci* **22**, doi:10.3390/ijms22062804 (2021).

260 Yanagida, K. *et al.* Sphingosine 1-Phosphate Receptor Signaling Establishes AP-1 Gradients to Allow for Retinal Endothelial Cell Specialization. *Dev Cell* **52**, 779-793 e777, doi:10.1016/j.devcel.2020.01.016 (2020).

261 Birdsey, G. M. *et al.* The endothelial transcription factor ERG promotes vascular stability and growth through Wnt/beta-catenin signaling. *Dev Cell* **32**, 82-96, doi:10.1016/j.devcel.2014.11.016 (2015).

262 Liu, X. *et al.* C/EBPbeta promotes angiogenesis through secretion of IL-6, which is inhibited by genistein, in EGFRvIII-positive glioblastoma. *Int J Cancer* **136**, 2524-2534, doi:10.1002/ijc.29319 (2015).

263 Min, Y. *et al.* C/EBP-delta regulates VEGF-C autocrine signaling in lymphangiogenesis and metastasis of lung cancer through HIF-1alpha. *Oncogene* **30**, 4901-4909, doi:10.1038/onc.2011.187 (2011).
264 Fleisinger, L. *Transcriptional regulation of endothelial KLF2 in vascular development* DPhil thesis thesis, University of Oxford, (2022).
265 Robinson, A. S. *et al.* An arterial-specific enhancer of the human endothelin converting enzyme 1 (ECE1) gene is synergistically activated by Sox17, FoxC2, and Etv2. *Dev Biol* **395**, 379-389, doi:10.1016/j.ydbio.2014.08.027 (2014).
266 Hamik, A., Wang, B. & Jain, M. K. Transcriptional regulators of angiogenesis. *Arterioscler Thromb Vasc Biol* **26**, 1936-1947, doi:10.1161/01.ATV.0000232542.42968.e3 (2006).
267 Liang, Y. *et al.* Genome-Wide Identification and Analysis of bZIP Gene Family and Resistance of TaABI5 (TabZIP96) under Freezing Stress in Wheat (Triticum aestivum). *Int J Mol Sci* **23**, doi:10.3390/ijms23042351 (2022).
268 Li, Y., Schor, J., Bartko, J., Albert, G. & Halterman, M. W. The transcription factor C/EBPbeta promotes vascular endothelial growth factor A expression and neural stem cell expansion. *FEBS Lett* **596**, 1661-1671, doi:10.1002/1873-3468.14405 (2022).
269 Min, Y., Li, J., Qu, P. & Lin, P. C. C/EBP-delta positively regulates MDSC expansion and endothelial VEGFR2 expression in tumor development. *Oncotarget* **8**, 50582-50593, doi:10.18632/oncotarget.16410 (2017).
270 Liu, B. *et al.* Loss of endothelial glucocorticoid receptor promotes angiogenesis via upregulation of Wnt/beta-catenin pathway. *Angiogenesis* **24**, 631-645, doi:10.1007/s10456-021-09773-x (2021).
271 Zhou, H. *et al.* Endothelial cell-glucocorticoid receptor interactions and regulation of Wnt signaling. *JCI Insight* **5**, doi:10.1172/jci.insight.131384 (2020).
272 Zhang, J. *et al.* Angiopoietin-1/Tie2 signal augments basal Notch signal controlling vascular quiescence by inducing delta-like 4 expression through AKT-mediated activation of beta-catenin. *J Biol Chem* **286**, 8055-8066, doi:10.1074/jbc.M110.192641 (2011).
273 Kim, H., Kim, M., Im, S. K. & Fang, S. Mouse Cre-LoxP system: general principles to determine tissue-specific roles of target genes. *Lab Anim Res* **34**, 147-159, doi:10.5625/lar.2018.34.4.147 (2018).
274 Skarnes, W. C. *et al.* A conditional knockout resource for the genome-wide study of mouse gene function. *Nature* **474**, 337-342, doi:10.1038/nature10163 (2011).
275 Kisanuki, Y. Y. *et al.* Tie2-Cre transgenic mice: a new model for endothelial cell-lineage analysis in vivo. *Dev Biol* **230**, 230-242, doi:10.1006/dbio.2000.0106 (2001).
276 Koni, P. A. *et al.* Conditional vascular cell adhesion molecule 1 deletion in mice: impaired lymphocyte migration to bone marrow. *J Exp Med* **193**, 741-754, doi:10.1084/jem.193.6.741 (2001).
277 Gerety, S. S. & Anderson, D. J. Cardiovascular ephrinB2 function is essential for embryonic angiogenesis. *Development* **129**, 1397-1410, doi:10.1242/dev.129.6.1397 (2002).
278 Fernandez-Chacon, M. *et al.* iSuRe-Cre is a genetic tool to reliably induce and report Cre-dependent genetic modifications. *Nat Commun* **10**, 2262, doi:10.1038/s41467-019-10239-4 (2019).

279 Walls, J. R., Coultas, L., Rossant, J. & Henkelman, R. M. Three-dimensional analysis of vascular development in the mouse embryo. *PLoS One* **3**, e2853, doi:10.1371/journal.pone.0002853 (2008).
280 Mu, J., Slevin, J. C., Qu, D., McCormick, S. & Adamson, S. L. In vivo quantification of embryonic and placental growth during gestation in mice using micro-ultrasound. *Reprod Biol Endocrinol* **6**, 34, doi:10.1186/1477-7827-6-34 (2008).
281 Wang, H. U., Chen, Z. F. & Anderson, D. J. Molecular distinction and angiogenic interaction between embryonic arteries and veins revealed by ephrin-B2 and its receptor Eph-B4. *Cell* **93**, 741-753, doi:10.1016/s0092-8674(00)81436-1 (1998).
282 Wolf, K., Hu, H., Isaji, T. & Dardik, A. Molecular identity of arteries, veins, and lymphatics. *J Vasc Surg* **69**, 253-262, doi:10.1016/j.jvs.2018.06.195 (2019).
283 Adams, R. H. *et al.* Roles of ephrinB ligands and EphB receptors in cardiovascular development: demarcation of arterial/venous domains, vascular morphogenesis, and sprouting angiogenesis. *Genes Dev* **13**, 295-306, doi:10.1101/gad.13.3.295 (1999).
284 Ulvmar, M. H. & Makinen, T. Heterogeneity in the lymphatic vascular system and its origin. *Cardiovasc Res* **111**, 310-321, doi:10.1093/cvr/cvw175 (2016).
285 Payne, S. *et al.* Regulatory pathways governing murine coronary vessel formation are dysregulated in the injured adult heart. *Nat Commun* **10**, 3276, doi:10.1038/s41467-019-10710-2 (2019).
286 Brachtendorf, G. *et al.* Early expression of endomucin on endothelium of the mouse embryo and on putative hematopoietic clusters in the dorsal aorta. *Dev Dyn* **222**, 410-419, doi:10.1002/dvdy.1199 (2001).
287 You, L. R. *et al.* Suppression of Notch signalling by the COUP-TFII transcription factor regulates vein identity. *Nature* **435**, 98-104, doi:10.1038/nature03511 (2005).
288 D'Amato, G. *et al.* Endocardium-to-coronary artery differentiation during heart development and regeneration involves sequential roles of Bmp2 and Cxcl12/Cxcr4. *Dev Cell* **57**, 2517-2532 e2516, doi:10.1016/j.devcel.2022.10.007 (2022).
289 Wang, Y. *et al.* Ephrin-B2 controls VEGF-induced angiogenesis and lymphangiogenesis. *Nature* **465**, 483-486, doi:10.1038/nature09002 (2010).
290 Da Silva, F. *et al.* Coronary Artery Formation Is Driven by Localized Expression of R-spondin3. *Cell Rep* **20**, 1745-1754, doi:10.1016/j.celrep.2017.08.004 (2017).
291 Fantin, A. Quantifying and Characterizing Angiogenesis Using the Postnatal Mouse Retina. *Methods Mol Biol* **2441**, 63-73, doi:10.1007/978-1-0716-2059-5_5 (2022).
292 Martowicz, A. *et al.* Endothelial beta-Catenin Signaling Supports Postnatal Brain and Retinal Angiogenesis by Promoting Sprouting, Tip Cell Formation, and VEGFR (Vascular Endothelial Growth Factor Receptor) 2 Expression. *Arterioscler Thromb Vasc Biol* **39**, 2273-2288, doi:10.1161/ATVBAHA.119.312749 (2019).
293 Phng, L. K. *et al.* Nrarp coordinates endothelial Notch and Wnt signaling to control vessel density in angiogenesis. *Dev Cell* **16**, 70-82, doi:10.1016/j.devcel.2008.12.009 (2009).

294 Zarkada, G., Heinolainen, K., Makinen, T., Kubota, Y. & Alitalo, K. VEGFR3 does not sustain retinal angiogenesis without VEGFR2. *Proc Natl Acad Sci U S A* **112**, 761-766, doi:10.1073/pnas.1423278112 (2015).
295 Tisi, A., Parete, G., Flati, V. & Maccarone, R. Up-regulation of pro-angiogenic pathways and induction of neovascularization by an acute retinal light damage. *Sci Rep* **10**, 6376, doi:10.1038/s41598-020-63449-y (2020).
296 Pitulescu, M. E., Schmidt, I., Benedito, R. & Adams, R. H. Inducible gene targeting in the neonatal vasculature and analysis of retinal angiogenesis in mice. *Nat Protoc* **5**, 1518-1534, doi:10.1038/nprot.2010.113 (2010).
297 Rashbrook, V. S., Brash, J. T. & Ruhrberg, C. Cre toxicity in mouse models of cardiovascular physiology and disease. *Nat Cardiovasc Res* **1**, 806-816, doi:10.1038/s44161-022-00125-6 (2022).
298 Valenta, T. *et al.* Probing transcription-specific outputs of beta-catenin in vivo. *Genes Dev* **25**, 2631-2643, doi:10.1101/gad.181289.111 (2011).
299 Liu, H. *et al.* beta-Catenin regulates endocardial cushion growth by suppressing p21. *Life Sci Alliance* **6**, doi:10.26508/lsa.202302163 (2023).
300 Kalisch-Smith, J. I. Feto-placental blood vessel development. *Development* **152**, doi:10.1242/dev.204838 (2025).
301 Weerackoon, N., Gunawardhana, K. L. & Mani, A. Wnt Signaling Cascades and Their Role in Coronary Artery Health and Disease. *J Cell Signal* **2**, 52-62, doi:10.33696/Signaling.2.035 (2021).
302 Mani, A. *et al.* LRP6 mutation in a family with early coronary disease and metabolic risk factors. *Science* **315**, 1278-1282, doi:10.1126/science.1136370 (2007).
303 Zamora, M., Manner, J. & Ruiz-Lozano, P. Epicardium-derived progenitor cells require beta-catenin for coronary artery formation. *Proc Natl Acad Sci U S A* **104**, 18109-18114, doi:10.1073/pnas.0702415104 (2007).
304 Liebner, S. *et al.* Wnt/beta-catenin signaling controls development of the blood-brain barrier. *J Cell Biol* **183**, 409-417, doi:10.1083/jcb.200806024 (2008).
305 Tran, K. A. *et al.* Endothelial beta-Catenin Signaling Is Required for Maintaining Adult Blood-Brain Barrier Integrity and Central Nervous System Homeostasis. *Circulation* **133**, 177-186, doi:10.1161/CIRCULATIONAHA.115.015982 (2016).
306 Lei, Y. *et al.* Deubiquitinase USP9X controls Wnt signaling for CNS vascular formation and barrier maintenance. *Dev Cell* **60**, 1618-1635 e1617, doi:10.1016/j.devcel.2025.01.009 (2025).
307 Robitaille, J. *et al.* Mutant frizzled-4 disrupts retinal angiogenesis in familial exudative vitreoretinopathy. *Nat Genet* **32**, 326-330, doi:10.1038/ng957 (2002).
308 Jiao, X., Ventruto, V., Trese, M. T., Shastry, B. S. & Hejtmancik, J. F. Autosomal recessive familial exudative vitreoretinopathy is associated with mutations in LRP5. *Am J Hum Genet* **75**, 878-884, doi:10.1086/425080 (2004).
309 Toomes, C. *et al.* Mutations in LRP5 or FZD4 underlie the common familial exudative vitreoretinopathy locus on chromosome 11q. *Am J Hum Genet* **74**, 721-730, doi:10.1086/383202 (2004).
310 Ai, M., Heeger, S., Bartels, C. F., Schelling, D. K. & Osteoporosis-Pseudoglioma Collaborative, G. Clinical and molecular findings in osteoporosis-pseudoglioma syndrome. *Am J Hum Genet* **77**, 741-753, doi:10.1086/497706 (2005).
311 Kato, M. *et al.* Cbfa1-independent decrease in osteoblast proliferation, osteopenia, and persistent embryonic eye vascularization in mice deficient in

Lrp5, a Wnt coreceptor. *J Cell Biol* **157**, 303-314, doi:10.1083/jcb.200201089 (2002).

312 Xu, Q. *et al.* Vascular development in the retina and inner ear: control by Norrin and Frizzled-4, a high-affinity ligand-receptor pair. *Cell* **116**, 883-895, doi:10.1016/s0092-8674(04)00216-8 (2004).

313 Luhmann, U. F. *et al.* Role of the Norrie disease pseudoglioma gene in sprouting angiogenesis during development of the retinal vasculature. *Invest Ophthalmol Vis Sci* **46**, 3372-3382, doi:10.1167/iovs.05-0174 (2005).

314 Xia, C. H. *et al.* A model for familial exudative vitreoretinopathy caused by LPR5 mutations. *Hum Mol Genet* **17**, 1605-1612, doi:10.1093/hmg/ddn047 (2008).

315 Cabezas-Sainz, P. *et al.* Improving zebrafish embryo xenotransplantation conditions by increasing incubation temperature and establishing a proliferation index with ZFtool. *BMC Cancer* **18**, 3, doi:10.1186/s12885-017-3919-8 (2018).

316 Yamamoto, D., Sato, D., Nakayama, H., Nakagawa, Y. & Shimada, Y. ZF-Mapper: Simple and Complete Freeware for Fluorescence Quantification in Zebrafish Images. *Zebrafish* **16**, 233-239, doi:10.1089/zeb.2018.1683 (2019).

317 Yang, G. *et al.* Heterogeneities of zebrafish vasculature development studied by a high throughput light-sheet flow imaging system. *Biomed Opt Express* **13**, 5344-5357, doi:10.1364/BOE.470058 (2022).

318 Petersen, R. A. & Morris, A. C. Visualizing Ocular Morphogenesis by Lightsheet Microscopy Using rx3:GFP Transgenic Zebrafish. *J Vis Exp*, doi:10.3791/62296 (2021).

319 Garcia-Gonzalez, I. *et al.* iSuRe-HadCre is an essential tool for effective conditional genetics. *Nucleic Acids Res* **52**, e56, doi:10.1093/nar/gkae472 (2024).

320 Heuberger, J. & Birchmeier, W. Interplay of cadherin-mediated cell adhesion and canonical Wnt signaling. *Cold Spring Harb Perspect Biol* **2**, a002915, doi:10.1101/cshperspect.a002915 (2010).

321 Defrance, M. & Touzet, H. Predicting transcription factor binding sites using local over-representation and comparative genomics. *BMC Bioinformatics* **7**, 396, doi:10.1186/1471-2105-7-396 (2006).

322 Wasserman, W. W. & Sandelin, A. Applied bioinformatics for the identification of regulatory elements. *Nat Rev Genet* **5**, 276-287, doi:10.1038/nrg1315 (2004).

323 Zambanini, G., Nordin, A., Jonasson, M., Pagella, P. & Cantu, C. A new CUT&RUN low volume-urea (LoV-U) protocol optimized for transcriptional co-factors uncovers Wnt/beta-catenin tissue-specific genomic targets. *Development* **149**, doi:10.1242/dev.201124 (2022).

324 Zhurinsky, J., Shtutman, M. & Ben-Ze'ev, A. Differential mechanisms of LEF/TCF family-dependent transcriptional activation by beta-catenin and plakoglobin. *Mol Cell Biol* **20**, 4238-4252, doi:10.1128/MCB.20.12.4238-4252.2000 (2000).

325 Schuijers, J., Mokry, M., Hatzis, P., Cuppen, E. & Clevers, H. Wnt-induced transcriptional activation is exclusively mediated by TCF/LEF. *EMBO J* **33**, 146-156, doi:10.1002/embj.201385358 (2014).

326 Uttley, K. *et al.* Unique activities of two overlapping PAX6 retinal enhancers. *Life Sci Alliance* **6**, doi:10.26508/lsa.202302126 (2023).